

July, 2017

Lionel Camus, Project Manager, Akvaplan-niva

UNIQUE ARCTIC COMMUNITIES AND OIL SPILL
RESPONSE CONSEQUENCES: "OIL BIODEGRADATION
& PERSISTENCE" AND "OIL SPILL RESPONSE
CONSEQUENCES RESILIENCE AND SENSITIVITY"



EXECUTIVE SUMMARY

This report provides an overview of the research activities performed and the results obtained from the phase 2 activities of the Environmental Effects project "Unique Arctic Communities and Oil Spill Response Consequences" executed within the framework of the Arctic Oil Spill Response Technology - Joint Industry Programme. The research project included field and laboratory experiments, to better understand the oil weathering process, natural biodegradation and the sensitivity and resiliency of sea ice communities.

The field program included a first of its kind in-ice semi open mesocosm experiment using eight 1.6 meter diameter, 3 meter long mesocosms installed in the sea ice of Van Mijen Fjord, Svea, Svalbard, Norway (77.9°N). The use of these semi-open systems to study effects of contaminants in open water marine systems is well established, but this technique had never been deployed in Arctic ice environments. These systems were installed in January 2015 and remained in place until ice melt out in July 2015. Two mesocosms contained oil only to follow the effects of natural attenuation (no response); two mesocosms contained oil mixed with dispersant at a standard dose rate of 1:20 ratio that could remain on the surface following an ineffective dispersant application – i.e. oil that never dispersed; two contained burned residues of oil, and the two remaining mesocosms served as controls (no oil). The field experiments spanned a single winter and spring season including the period of peak biological activity until the ice melted. During the five-month study period researchers sampled and analysed the following parameters in the water column, through the ice layer and within the water-ice interface: chemical composition of the oil, total bacterial populations and oil degrading microorganisms, microbial activity and biodegradation activity, zooplankton – survival, feeding and reproduction (under ice), and ice algae primary production. In parallel to the mesocosm experiment, microcosms were deployed in situ during springtime to study the impact of the exact same treatments on the sea surface micro layer (SSML). In order to address the sensitivity and resiliency of wild polar cod exposed to mechanically dispersed crude oil or chemically dispersed or to residues of burnt oil a laboratory experiment was performed in Tromsø (Norway). Finally, calibrated rock tiles were smeared with oil and placed in situ submerged in the water of Van Mijen Fjord during 5 months to measure the oil weathering and biodegradation processes.

Section 1 focuses on the assessment of the persistence and biodegradation of oil frozen into ice using the in situ mesocosms following different oil spill response options with the aim at answering questions such as: how does the oil interact with the sea ice? How long does the oil persist? Does the oil biodegrade over time in the ice? Are arctic microbial communities which are naturally present able to biodegrade oil compounds? How long is this process expected to take?

In the mesocosms, for all treatments, the oil was found to be encapsulated in the sea ice. We observed that the lightest oil compounds diffused through the ice cores due to dissolution kinetics, and thus, explaining the presence of dissolved polycyclic aromatic hydrocarbons measured in the water column under the ice. This process was enhanced when oil was mixed with a chemical dispersant before it was allowed to freeze in. In addition, we observed a biodegradation process of light alkanes for oil alone and oil mixed with dispersant.

The microbial communities were found to be different at different ice-layer depths and significant changes between communities from ice and seawater were found. Also, Arctic microbial communities were found to shift in response to oil within the first month of exposure. Microbial communities that are able to biodegrade oil compounds were present and active in the sea-ice layers, even during the winter months. Hydrocarbon degradation incubation experiments showed

that bacteria present in sea ice were able to respond to and degrade petroleum hydrocarbons and started degrading them within weeks. This microbial activity showed a strong seasonal influence. For instance, during incubations executed in April, the observed microbial growth and degradation rates were less pronounced than in May, due to algal bloom.

The bacterial community structure in the seawater column shifted noticeably towards high numbers of *Colwellia* organisms as well as a higher activity of the *Oleispira* genus in the mesocosms with oil mixed with chemical dispersant treatment compared to the other treatments. Several species of these genera are known for actively degrading crude oil. These results indicated that oil may have leaked through from the ice layer to the seawater, where it was actively degraded by microorganisms. The higher activity of the bacterial community and greater shift of the microbial community towards oil degrading organisms in the mesocosms with oil mixed with dispersant indicate that this treatment enhances the bioavailability of the petroleum compounds, likely resulting in a faster biodegradation process. The biodegradation potential of bacteria present in seawater was also observed in this experiment.

The experiment with the oiled tiles, demonstrated a much denser bacterial biofilm on the oiled tiles compared to control, and a high fraction of potentially oil degrading organisms. This could be observed within the first month of the oil application and immersion of the tile in the water of the fjord. This is indicative of a biofilm constituted for a large part of oil degrading organisms forming on the surfaces, established due to the presence of the oil. The chemical analyses indicated that a relatively strong oil biodegradation was taking place. Two months after exposure the concentration of oil compounds had diminished on the tile surface, and bacteria including oil degrading bacteria were less densely populating the rock surfaces. Overall, the tile experiment showed that biofilms are formed by microorganisms on rock surfaces submerged in arctic seawater directly in the field. The microbial community identified on oil contaminated surfaces is dominant in metabolically active oil degrading microorganisms implying that these are also likely able to biodegrade at least some of the oil components from the environment.

Section two reports activities and results focusing on "Resilience and Sensitivity". There were three main research questions: What are the potential impacts of oil alone or oil mixed with dispersant or residues of burnt oil that get encapsulated into ice, on the sensitivity and resilience of plankton (phyto and zoo plankton) communities living in association with the pack ice (mesocosm study) and the sea surface microlayer (microcosm study). What are the potential impacts of mechanically dispersed oil or oil chemically dispersed or residues of burnt oil that get mixed in the water, on the sensitivity and resilience the polar cod (laboratory study).

In the mesocosms, the different oil spill response treatments had no discernible effect on sea ice growth and thickness. The oil alone or with dispersant added, prevented light penetration through the ice while residues of burnt oil let some a small amount of light to penetrate the sea ice. The controls with only added oil, exhibited a very low penetration of light, which is presumably due to the absorption of light by the opaque walls of the mesocosms which may have implication on primary production. None of the oil spill response treatments had any discernible impact on the exchange of nutrients between the brine channels of sea ice and the underlying water. Most taxonomic groups of sea ice protists exhibited low species richness with the exception of pennate diatoms, which had the highest number of species, followed by dinoflagellates and choanoflagellates. Overall the residues of burnt oil treatment had a lesser ecological impact on ice algae than natural attenuation or dispersant application. There were some significant effects on the composition of the microplankton community, but the potential

indirect effects on the higher trophic levels was not investigated. Zooplankton were not affected by the levels of exposure in this study, although some post-exposure effects were observed on nauplii malformation and development. No significant difference in microbial abundance between sea surface layer and underlying water as well as between various treatments was observed in the microcosms. In contrast, differences between the surface layer and the underlying water was observed on a microbial community level and these differences were less apparent amongst treatments.

No long-term effects on polar cod survival, growth or reproductive investment were revealed in polar cod exposed to mechanically dispersed oil, chemically dispersed oil and residues of burnt oil, in the laboratory exposure. Burnt oil residue did however lead to a significant increase in female fish interrupting the yolk formation in the eggs. This effect of the burnt oil residue needs further investigation including further validation of the selected exposure setup for burnt oil residues.

Results from the studies have improved the understanding of what happens to oil once frozen into ice, how microbiology is reacting to oil in ice and what the exposure potential is of the ecology associated with the ice. This information will help the response community in selecting a combination of response strategies that minimizes the effects to people and the environment.

TABLE OF CONTENTS

EXECUTIVE SUMMARY.....	2
SECTION 1 UNIQUE ARCTIC COMMUNITIES AND OIL SPILL RESPONSE CONSEQUENCES- OIL BIODEGRADATION & PERSISTENCE.....	14
1 INTRODUCTION.....	15
2 MATERIAL AND METHODS.....	16
2.1 Location of field site.....	16
2.2 Deployed experimental equipment.....	16
2.3 Oil and dispersant used for treatments	19
2.4 Treatments applied and sampling schedule.....	21
2.5 Sample collection and handling.....	22
2.6 Oil on tiles.....	24
2.7 Analytical methods.....	25
3 RESULTS AND DISCUSSION - MESOCOSM EXPERIMENT.....	31
3.1 Visual observations.....	31
3.2 Chemical analysis in the mesocosm experiment.....	32
3.3 Screening of general shifts in microbial populations in the mesocosm experiment.....	39
3.4 Microbial biomass in the mesocosm experiment - Quantification of bacteria, archaea and small eukaryotes	43
3.5 Bacterial community analysis in the mesocosm experiment.....	51
4 RESULTS AND DISCUSSION ON SHORT-TERM INCUBATION EXPERIMENTS	57
4.1 Microbial Abundance in ice and water samples.....	57
4.2 Microbial growth and oxygen consumption.....	58
4.3 Naphthalene degradation rates in short-term incubation experiments.....	60
5 RESULTS AND DISCUSSION ON BIOFILM ON TILES EXPERIMENT.....	62
5.1 Results and discussion from the chemical analysis from tiles	62
5.2 Results and discussion from the microbial analysis from tiles.....	64
6 CONCLUSIONS	68
6.1 Fate of oil and biodegradation through the sea-ice layer	68
6.2 Leakage of oil and biodegradation in the seawater below the ice layer.....	68
6.3 Fate of oil and biodegradation of oil on rock tiles	69
7 REFERENCES	70
SECTION 2 UNIQUE ARCTIC COMMUNITIES AND OIL SPILL RESPONSE CONSEQUENCES - RESILIENCE AND SENSITIVITY.....	71
1 INTRODUCTION.....	72
1.1 Background and research objectives	72
2 MATERIAL & METHODS	75
2.1 Location of field site.....	75
2.2 Deployed experimental equipment.....	75
2.3 Oil and dispersant used for treatments	77
2.4 Treatments applied and sampling schedule.....	79
2.5 Plankton	81
2.6 Light penetration, nutrients and ice-algal growth	92
2.7 Sea Surface Layer Microbial Community	93
2.8 Polar cod.....	96
3 RESULTS	100
3.1 Plankton	100
3.2 Light penetration, nutrients and ice-algal growth	114
3.3 Sea Surface Layer Microbial Community	122

3.4	Polar cod.....	129
4	DISCUSSION.....	136
4.1	Effects of oil compounds from OSR technologies on plankton.....	136
4.2	Light penetration, nutrients and ice-algal growth.....	143
4.3	Sea Surface Layer Microbial Community.....	145
4.4	Polar cod.....	146
5	CONCLUSIONS.....	150
5.1	Microplankton.....	150
5.2	Copepods.....	150
5.3	Light penetration, nutrients and ice-algal growth.....	150
5.4	Sea Surface Layer Microbial Community.....	150
5.5	Polar cod.....	151
6	REFERENCES.....	153
7	APPENDIX.....	160
7.1	1-A List of analysed chemical compounds.....	160
7.2	1-B Tiles experiment.....	161
7.3	1-C Mesocosm experiment.....	162
7.4	1-D Microbial community analysis.....	168
7.5	1-F Bacterial community composition – Silva NGS analysis.....	173
7.6	2-A Mean concentrations of PAHs and total hydrocarbon concentration in polar cod experiment	185

LIST OF FIGURES

Figure 1	a) Map of Svalbard archipelago. The red line illustrates the distance between Longyearbyen (airport location) and Svea, b) Svea mining town with the location of the living and working barracks marked with a blue point, and the field and sampling location marked with a red point. The red cross represents the location of the mesocosm set-ups (located 800 m from shore).	16
Figure 2	Industrial drawing of the mesocosms applied in the Svea field-campaign. Internal diameter: 1.6 m, length: 3 m (source CEDRE).....	17
Figure 3	Assembly of the 8 mesocosms in Svea (source CEDRE).....	17
Figures 4 (left) and 5 (right)	Mesocosms deployed in the Svea field-campaign (source: IRIS).....	18
Figure 6	Location of the mesocosms at the experimental site (source IRIS).....	18
Figure 7	Tiles during the oiling phase and their positioning in the icepack.....	19
Figure 8	Chart pie representing the chemical composition of the KOBBE crude oil by mass, analyzed by GC-FID.....	20
Figure 9	Comparison of the burned residue chromatogram (in grey) with the fresh oil one (in black).....	20
Figure 10	Schematic drawing of the field experimental setup at Svea.....	21
Figure 11	Pictures of the different treatments applied: a) Mesocosm with oil alone, b) Mesocosm with oil mixed with dispersant, c) Mesocosm with in situ burning residue (source: IRIS).....	22
Figure 12	Ice core melting at 2-4 °C. Sterile bags containing melted ice cores from oil contaminated mesocosm (right bag), and from oil+dispersant mesocosm (left bag). Source: IRIS.....	23
Figure 13	Left Panel: Hand pump used for the collection of seawater samples. Right Panel: Filtering set up for Seawater and melted sea-ice.....	24
Figure 14	Tiles collected from below the sea ice.....	25
Figure 15	Example of cores collected at T3: a) Cude oil treatment, b) Oil+dispersant treatment, c) Burnt oil treatment and d) Control treatment.....	31
Figure 16	Evolution of dissolved PAHs concentrations in the water column (in $\mu\text{g.L}^{-1}$) over the winter and spring seasons for the different treatments considered and the different	

	depths. Legend: Blue bars = naphthalene and its alkylated congeners; Red bars = three-four ring PAHs; Green bar = PAHs containing five or more rings).....	34
Figure 17	Evolution of dissolved PAHs concentrations (in $\mu\text{g.L}^{-1}$) and pure oil (Aromatics + Alkanes; in $\mu\text{g.g}^{-1}$) over the winter and spring seasons for the different treatments considered (crude oil, oil+dispersant, burnt oil, control and clean site). Legend: Blue bars = dissolved PAHs; Red bars = Aromatics in pure oil; Green bar = Alkanes in pure oil. The top scale is for Alkanes (from 0 to 160 000 $\mu\text{g.g}^{-1}$). The bottom scale is for Dissolved PAHs (from 0 to 20 000 $\mu\text{g.L}^{-1}$) and Aromatics compounds (from 0 to 20 000 $\mu\text{g.g}^{-1}$).	37
Figure 18	Evolution of the chemical composition of the oil trapped in ice (MCL) for each treatment with time	39
Figure 19	Overview of bacterial community structure in two pristine arctic sea ice locations (site 1 and 2) by Denaturing Gradient Gel Electrophoresis (DGGE). Analysis from total DNA samples extracted from the top layer of 3 different ice cores from each location are shown. Values on the left show the % similarity between bacterial communities	40
Figure 20	Overview of bacterial community structure in two pristine arctic sea ice locations (site 1 and 2) by Denaturing Gradient Gel Electrophoresis (DGGE). This analysis was based on total cDNA, derived from RNA samples extracted from the top layer of 3 different ice cores from each location. Values on the left show the % similarity between bacterial communities	40
Figure 21	Overview of bacterial community structure in two pristine arctic sea ice locations in February and March by DGGE. Analysis performed on total DNA extracted from samples collected from the top sea ice layer (in black) and from the bottom sea-ice layer (in blue). Values on the left show the % similarity between bacterial communities	41
Figure 22	Overview of bacterial community structure in the top layer sea ice from ice cores collected in the control and the oil contaminated mesocosms. DGGE analysis from total DNA extracted samples from different ice cores at each location, collected one month after exposure to oil. Values on the left show the % similarity between bacterial communities	42
Figure 23	Overview of bacterial community structure in the top layer sea ice from ice cores collected in May (after 3 months' exposure) in the control, Crude oil, Burnt oil and oil+dispersant mesocosms. DGGE analysis performed on total DNA. Values on the left show the % similarity between bacterial communities.....	43
Figure 24	Overview of the active bacterial community structure in the top layer sea ice from ice cores collected in May (after 3 months' exposure) in the control, Crude oil, Burnt oil and Oil+dispersant mesocosms. DGGE analysis performed on total RNA extracted from the samples. Values on the left show the % similarity between bacterial communities.	43
Figure 25	Quantification of the total number of bacteria (TNB), Oleispira and Colwellia genera and small Eukarya. Total number of 16 S rRNA gene copies per 1 ml melted sea-ice cores from the ice top, middle and bottom layers and in 1 ml of seawater from just below the ice surface (-1m because of the ice thickness). Results are shown here for the February samples taken before the start of the experiment. 3 distinct ice cores or water samples are used for each measurement. The results are shown here for 1 of the sites (see appendix for the results from the other site). The error is the standard error for the measurement. NB: The TNB value is shown on a different axis due to higher numbers.	44
Figure 26	Quantification of the total number of bacteria (TNB), Oleispira and Colwellia genera and small Eukarya. Total number of 16 S rRNA gene copies of per 1 ml melted sea-ice cores from the ice top and bottom layers and in 1 ml of seawater from just below the ice surface. Results are shown here after 1 month exposure (March samples) in the crude oil, oil+dispersants, burnt oil and control no treatment mesocosms. 3 distinct ice cores or water samples are used for each measurement. The error is the standard error for the measurement. NB: The TNB value is shown on a different axis due to higher numbers.....	46
Figure 27	Quantification of the total number of bacteria (TNB), Oleispira and Colwellia genera and small Eukarya. Total number of 16 S rRNA gene copies of per 1 ml melted sea-ice cores from the ice top and bottom layers and in 1 ml of seawater from just below the ice surface. Results are shown here after 2 months exposure (April samples) in the crude oil, oil+ dispersants, burnt oil residue and control no treatment mesocosms. 3	

	distinct ice cores or water samples are used for each measurement. The error is the standard error for the measurement. NB: The TNB value is shown on a different axis due to higher numbers.....	47
Figure 28	Quantification of the total number of bacteria (TNB), <i>Oleispira</i> and <i>Colwellia</i> genera and small Eukarya. Total number of 16 S rRNA gene copies of per 1 ml melted sea-ice cores from the ice top, mid section and bottom layers and in 1 ml of seawater from just below and 1m below ice surface. Results are shown here after 3 months exposure (May samples) in the crude oil, oil+dispersants, burnt oil and control no treatment mesocosms. 3 distinct ice cores or water samples are used for each measurement. The error is the standard error for the measurement. NB: The TNB value is shown on a different axis due to higher numbers.	48
Figure 29	Quantification of <i>Oleispira</i> (total number of bacterial 16S rRNA gene copies per 1ml seawater) under the sea-ice layer, Samples from May, 3 months after exposure in the control, crude oil, oil+dispersant and burnt oil mesocosms.	49
Figure 30	Normalized number of metabolically active <i>Oleispira</i> in the top 20cm ice layer from different treatments (Crude oil, oil+dispersant, burnt oil) and control mesocosms. Quantification of <i>Oleispira</i> 16S rRNA on total RNA extracted from 3 different ice-cores for each mesocosm 1, 2 and 3 months after start of exposure (March, April and May). Error bar is the standard error.....	50
Figure 31	Normalized number of metabolically active <i>Oleispira</i> in the bottom 20cm of ice from different treatments (crude oil, oil+dispersant, burnt oil) and control mesocosms. Quantification of <i>Oleispira</i> 16S rRNA on total RNA extracted from 3 different ice-cores for each mesocosm 1, 2 and 3 months after start of exposure (March, April and May). Error bar is the standard error.....	50
Figure 32	Contribution of metabolically active <i>Oleispira</i> in total active microorganisms. Quantification of <i>Oleispira</i> 16S rRNA on total RNA extracted from ice-cores from the top layer sea-ice in the control and different treatment mesocosms, 1,2 and 3 months after exposure (March, April and May).	51
Figure 33	Microbial community analysis (based on 16S rRNA gene sequencing by 454 pyrosequencing) from total DNA and RNA (metabolically active population). Sea-ice samples (from the top, middle and bottom 20cm sections of ice cores) collected from the pristine environment before the start of the mesocosm exposure experiment. Each analysis originates from the pooling of 3 distinct cores.	52
Figure 34	Microbial community analysis (based on 16S rRNA gene sequencing by 454 pyrosequencing) from total DNA and RNA (metabolically active population). Seawater samples (from 5, 10 and 25m depths) collected from the pristine environment before the start of the mesocosm exposure experiment. Each analysis originates from the pooling of 3 distinct samples.	53
Figure 35	Microbial community analysis (based on 16S rRNA gene sequencing by 454 pyrosequencing) from total RNA (metabolically active population). Sea-ice samples (top and bottom of ice layer) collected from the oil, oil+dispersant, burned oil residue and control, collected 1, 2 and 3 months after the start of the exposure (March, April and May). Each analysis originates from the pooling of 3 distinct samples.	54
Figure 36	Microbial community analysis (based on 16S rRNA gene sequencing by 454 pyrosequencing) from total DNA. Sea-ice samples (top and bottom of ice layer) collected from the crude oil, oil+dispersant, burnt oil and control, collected 1, 2 and 3 months after the start of the exposure (March, April and May). Each analysis originates from the pooling of 3 distinct samples.	55
Figure 37	Microbial community analysis (based on 16S rRNA gene sequencing by 454 pyrosequencing) from total DNA and total RNA (metabolically active population). Seawater samples collected from just below the sea-ice layer in the control and oil+dispersant mesocosms. Each analysis originates from the pooling of 3 distinct samples. Bacterial genera representing more than 2% of the total population are detailed in the caption. 'Other bacteria' comprise of genera present at less than 1% of the population.....	56
Figure 38	Air temperature during the two incubation period at Svea airport. Incubation at T2 started on 4/16/15. The incubation at T3 started on 5/8/15.....	57
Figure 39	Bacterial abundance in sea ice and water samples as measured by flow cytometry.	58

Figure 40	Bacterial growth rates (in day ⁻¹) fitted for exponential growth determined in incubation experiments with melted ice and water below the ice. The blue and green bars represent incubations performed over two incubation periods with added oil, whereas the red bars represent incubations without added oil. The bottom ice section was only investigated in May and only in the oiled treatment.	59
Figure 41	Oxygen consumption rates (in pmol O ₂ day ⁻¹ cell ⁻¹) determined in incubation experiments with melted ice and water below the ice.	60
Figure 42	First order naphthalene degradation rate constants (day ⁻¹) determined in incubation experiments. An asterisk (*) denotes negative degradation rates caused by analytical difficulties.	61
Figure 43	Concentrations of the 3 groups of alkanes during time on tiles.	62
Figure 44	Variation of nC17/pristane and nC18/phytane ratios during time for oil at the tiles surface.	63
Figure 45	Evolution of C1-fluo-pyrene/C4-phen and Phen/C4-Phen ratios during time in oil at the tiles surface.	63
Figure 46	Evolution of the aromatic fractions of oil extracted from tiles with time.	63
Figure 47	Quantification of total bacteria (TNB), Colwellia and Oleispira genera and small eukaryotes (expressed as total number of 16S rRNA gene copies) in biofilms extracted from 3 control non-oiled tiles (C1 to C3) and 3 oil-coated tiles (Oil1 to Oil3) 1, 2 and 3 months after exposure (respectively March, April and May). Error bars are the standard error between measurements. Analysis done by qPCR quantifications on total DNA.	65
Figure 48	Contribution of metabolically active Oleispira in the total active bacterial populations in biofilms extracted from 3 contaminated tiles and 3 non contaminated tiles. Analysis done by qPCR quantification on total RNA.	66
Figure 49	Bacterial community analysis (based on 16S rRNA gene sequencing by 454 pyrosequencing) from total DNA and RNA (metabolically active organisms) in biofilms extracted from 2 control non-oiled tiles (Control1 and 2) and 2 oil-coated tiles (Oiled1 and 2). This analysis was done 3 months after exposure (May). Each analysis originates from the pooling of 3 distinct samples.	67
Figure 1	a) Map of Svalbard archipelago. The red line illustrates the distance between Longyearbyen (airport location) and Svea, b) Svea mining town with the location of the living and working barracks marked with a blue point, and the field and sampling location marked with a red point. The red cross represents the location of the mesocosm set-ups (located 800 m from shore).	75
Figure 2	Industrial drawing of the mesocosms applied in the Svea field-campaign. Internal diameter: 1.6 m, length: 3 m (source CEDRE).	76
Figure 3	Assembly of the 8 mesocosms in Svea (source CEDRE).	76
Figure 4	Mesocosms deployed in the Svea field-campaign (source: IRIS).	77
Figure 5	Location of the mesocosms at the experimental site (source IRIS). Red crosses indicate the mesocosm area, whereas green crosses indicate clean sampling area.	77
Figure 6	Chart pie representing the chemical composition of the KOBBE crude oil by mass, analyzed by GC-FID.	78
Figure 7	Comparison of the burned residue chromatogram (in grey) with the fresh oil one (in black).	79
Figure 8	Schematic drawing of the field experimental setup at Svea.	80
Figure 9	Pictures of the different treatments applied: a) Mesocosm with oil alone, b) Mesocosm with oil plus dispersant, c) Mesocosm with in situ burning residue (source: IRIS).	81
Figure 10	Outer tubing inserted in drill hole of mesocosm.	82
Figure 11	(a) Experimental setup (left) showing an enclosure cut into the ice and bounded by a clear plastic box with a cover (further details in text). (b) Experimental design (right) shows the physical layout in duplicate of the control and the five treatments applied; the green ovals show the three overlapping holes drilled at the bottom of each enclosure (see details in text) that allow subsurface water to naturally fill each enclosure. Treatments are: oil slick (A, B), oil and dispersant (C, D), burned oil residue	

	(E, F), oil sheen (G, H), control (I, J), dispersant-only (I, J). (c) Picture of the setup in the field.	94
Figure 12	Sampling scheme.	95
Figure 13	The mean biomass ($\mu\text{g C L}^{-1}$) of (A-B) bacteria, (C-D) HNF, (E-F) dinoflagellates, and (G-H) ciliates in the control, burnt oil, oil+dispersant, and crude oil treatments in winter (left) and spring (right). Error bars represent ± 1 SD.	103
Figure 14	The mean biomass ($\mu\text{g C L}^{-1}$) of (A-B) picophytoplankton, (C-D) nanophytoplankton, and (E-F) diatoms in the control, burnt oil, oil+dispersant, and crude oil treatments in winter (left) and spring (right). Error bars represent ± 1 SD.	104
Figure 15	Average cumulated specific faecal pellet production (SPP) for <i>C. glacialis</i> females exposed to four treatments. Error bars show standard error (n=15).	107
Figure 16	Average cumulated specific egg production (SEP) for <i>C. glacialis</i> females exposed to four treatments. Error bars show standard error (n=15).	108
Figure 17	Cumulated mean specific faecal pellet production (SPP) for <i>C. glacialis</i> females exposed to four dilution series concentrations of mesocosm water from control, burnt oil, oil+dispersant and crude oil treatments. Initial exposure concentration in the 100% mesocosm water.	109
Figure 18	Cumulated mean specific egg production (SEP) for <i>C. glacialis</i> females exposed to four dilution series concentrations of mesocosm water from control, burnt oil, oil+dispersant and crude oil treatments. Initial exposure concentration in the 100% mesocosm water.	110
Figure 19	Average hatching success (7 days of incubation) of eggs from <i>C. glacialis</i> females exposed to four treatments (100% mesocosm water) over 13 days and initial unexposed. Error bars show standard error.	111
Figure 20	Proportion of deformed nauplii from eggs hatched by <i>C. glacialis</i> female copepods exposed to four treatments of mesocosm water (100%) in spring.	111
Figure 21	Nauplii of <i>Calanus glacialis</i> . Left single photo show a normal <i>C. glacialis</i> nauplii and the four images on the right illustrates different forms of deformations encountered.	112
Figure 22	Proportion of hatched nauplii of <i>C. glacialis</i> reaching second development level.	112
Figure 23	Total PAH concentration (sum of 21 PAHs) in water from mesocosms at Day 1 of the exposure experiments in both winter and spring campaign. Note the logarithmic scale on the Y-axis.	113
Figure 24	Ice thickness in the experimental mesocosms. Vertical dispersion bars give the range for duplicate mesocosms.	114
Figure 25	PAR at the ice-water interface in the experimental mesocosms (measured with a Seabird ECO-PAR cosine sensor mounted on an articulated pole). Snow was cleared before taking the measurement. No light was detected at T2 due to late sampling in the day (not shown). Vertical dispersion bars give the range for duplicate mesocosms.	115
Figure 26.	Concentration of nitrate in melted bottom-ice cores (+filtered seawater) in the different treatments for each sampling time. The horizontal dashed line provides the nitrate concentration in the surface water used for dilution. Vertical dispersion bars give the range for duplicate mesocosms.	116
Figure 27	Concentration of Chl a (bars) and contribution of phaeopigments* (green circles) in bottom-ice cores for the different treatments at each sampling time. Vertical dispersion bars give the range for duplicate mesocosms. *Calculated as $100 \times \text{phaeo} / (\text{chl a} + \text{phaeo})$	117
Figure 28	Number of pennate diatom species (richness) by genus within the bottom-ice of different mesocosms at (A) T1 on 27 March and (B) T3 on 6 May. The smallest and largest bubbles correspond to 1 and 14 species per genus, respectively. On the x-axis, mesocosm B = crude oil, C&D= oil+dispersant, E&F = burnt oil and I&J = contr.	118
Figure 29	Presence and abundance of different species belonging to the pennate diatom genus <i>Navicula</i> within the bottom-ice of different mesocosms on 6 May. The smallest and largest bubbles correspond to 40 and 560 individual cells per liter, respectively. On the x-axis, mesocosm B = crude oil, C&D= oil+dispersant, E&F = burnt oil and I&J = control.	119

Figure 30	Protist groups for which cellular abundance was positively (green circles) or not (red circles) related to the concentration of chl a in bottom ice, using pooled data from all mesocosms at T1 and T3. Note the change of vertical scale for the Primmiosphytes.....	121
Figure 31	Combined abundance of pennate diatoms, naked dinoflagellates, flagellates and cryptophytes in bottom-ice cores for the different treatments at T3 on 6 May. The horizontal and vertical lines are provided as visual references to help distinguish between treatments.	121
Figure 32	Relative contribution of pennate diatoms, naked dinoflagellates, flagellates and cryptophytes to their combined abundance in bottom-ice cores for the different treatments at T3 on 6 May. The horizontal and vertical lines are provided as visual help to distinguish between treatments. Letters indicate mesocosm treatments: B = crude oil, C&D= oil+dispersant, E&F = burnt oil and I&J = control.....	122
Figure 33	Cell densities of pico- and nanophytoplankton (left panels) and heterotrophic bacteria (right panels) determined using flow cytometry for replicate enclosures (blue [a] and red [b] lines) exposed to different oil treatments (Oil slick, oil sheen, burned residue, oil and dispersant, dispersant-only, and a control). Abundances are shown for surface layer (SL) and subsurface (SW) waters.	123
Figure 34	Daily net rate of change in bacterial (top) and pico/nanoplankton (bottom) abundance in surface layer (SL) and subsurface (SW) seawater after 72h of incubation in the control and experimental treatments. Mean value and standard deviation is shown for each treatment.	124
Figure 35	Microbial community analysis (based on 16s rRNA sequencing) for samples from the surface layer (left five bars) and 50cm below the water table (right bars). Several treatments (Oil slick, oil sheen, burned residue, oil and dispersant, and dispersant-only) were followed over five days. Groups shown account for 90% of the total abundance.	125
Figure 36	Bacterial community diversity (H) in the control (days 0, 1 and/or 5) and among treatments (day 5) in surface layer and subsurface waters.	126
Figure 37	(A) Cluster analysis of microbial community composition. Three main groups can be observed: (i) Surface layer ("SL") samples on day 5 (d5) plus the dispersant-only treatment samples from 50 cm depth (SW samples K and L), (ii) SL and SW samples of the control treatment at day 0 (d0), and (iii) samples from SW samples at day 5. Expect the dispersant-only samples. (B) Principle Component analysis of microbial community composition, showing the same tentative clustering. Control treatment is in red, dispersant-only in green, SL samples in yellow, and SW samples in black.....	126
Figure 38	PAH concentration in the subsurface seawater (50 cm depth) treated with oil (treatment A) and a combination of oil+dispersant (C), and control treatment (I) measured on days 1, 3 and 5.	127
Figure 39	PAH concentrations for surface layer treated with burned oil (treatment E), oil sheen (G) and the control treatment (I), measured on days 1, 3 and 5.....	128
Figure 40	Changes in the hydrocarbon composition in the oil phase during the incubation, as seen by GCxGC-FID chromatograms. Only the oil sheen treatment shows a slight change in composition, with volatile compounds being evaporated during the five days of incubation.	129
Figure 41	(A) THC and (B) Σ26 PAH concentrations at t24 (circles) and t48 (triangles) for all treatment groups in boxplots. Treatment mean concentrations that do not share a letter are significantly different (p<0.01).	130
Figure 42	Cumulative mortality (% of overall mortality) of polar cod during the course of the exposure and post exposure period (June 2015 – January 2016) for each treatment group. No significant difference in % mortality was found between treatment groups, control or unexposed groups.	131
Figure 43	Specific growth rate (SGR; % change in body weight per day) mean ± SE of fish during after exposure to different OSR measures or unexposed (n=40-49 per treatment [Unexp. n is 23-30 fish]). Different letters indicate significant differences between treatment groups.	132
Figure 44	(A) Histological representation of an early maturing female with cortical alveoli vesicles and early signs of vitellogenesis with yolk globules present in oocyte periphery; (B) Histological representation of an advanced maturing female with vitellogenic oocytes. Scale bare is 200 µm in both pictures.....	133

Figure 45	(A) Maturity stage frequency distribution of females from all treatments; (B) boxplots of GSI of female fish in different treatment groups, maturing females are plotted in the boxplots and immature and resting females are indicated at triangles. Different letters indicate significant differences between treatment groups where those groups with no letters in common are significantly different from one another and those sharing a letter are not. The number above each treatment refers to N.....	134
Figure 46	(A) Maturity stage frequency distribution of males from all treatments; (B) boxplot of GSI of male fish in different treatment groups, maturing males are plotted in the boxplots and immature and resting males are indicated at triangles	135
Appendix Figure 1	Active bacterial community composition (based on total RNA). Bottom layer of sea ice in Control no oil mesocosm in March (1 month after start of exposure). Silva NGS analysis. In blue are non classified organisms.	173
Appendix Figure 2	Active bacterial community composition (based on total RNA). Bottom layer of sea ice in Oil+dispersant mesocosm in March (1 month after start of exposure). Silva NGS analysis. In blue are non classified organisms.	174
Appendix Figure 3	Active bacterial community composition (based on total RNA). Bottom layer of sea ice in Control no oil mesocosm in May (3 months after start of exposure). Silva NGS analysis. In green are non-classified organisms.	175
Appendix Figure 4	Active bacterial community composition (based on total RNA). Bottom layer of sea ice in Oil+dispersant mesocosm in May (3 months after start of exposure). Silva NGS analysis. In blue are non classified organisms.	176
Appendix Figure 5	Active bacterial community composition (based on total RNA). Seawater collected from just under the ice layer in the Control no oil mesocosm in May (3 months after start of exposure). Silva NGS analysis. In green are non classified organisms.....	177
Appendix Figure 6	Active bacterial community composition (based on total RNA). Seawater collected from just under the ice layer in the oil+dispersant mesocosm in May (3 months after start of exposure). Silva NGS analysis. In green are non classified organisms.....	178
Appendix Figure 7	Active bacterial community composition (based on total RNA). Biofilm collected from control non-contaminated tiles in May (3 months after start of exposure). Silva NGS analysis. In green are non classified organisms.....	179
Appendix Figure 8	Active bacterial community composition (based on total RNA). Biofilm collected from oiled tiles in May (3 months after start of exposure). Silva NGS analysis. In green are non classified organisms.	180
Appendix Figure 9	Quantification of Oleispira (total number of bacterial 16S rRNA gene copies per 1ml seawater) under the sea-ice layer, Samples from May, 3 months after exposure in the control, oil, oil+dispersant and burned oil mesocosms.....	181

LIST OF TABLES

Table 1	Sampling schedule	22
Table 1	Sampling schedule.	81
Table 2	Sampling program for micro plankton exposure study.....	85
Table 3	Specific carbon conversion factors derived from the experiment in March 2015.	86
Continuation Table 3	Specific carbon conversion factors derived from the experiment in March 2015. 87	87
Table 4	Specific carbon conversion factors derived from the experiment in April 2015.....	88
Table 5	Carbon content of mature <i>C. glacialis</i> females and of egg and pellets (Swaethorp et al., 2011). Data are mean \pm SD.	89
Table 6	The average concentrations \pm SD of pH, nutrients (nitrate, phosphate, silicate; $\mu\text{M L}^{-1}$), and sum of 21 PAHs (ng L^{-1}) on Day 0 and Day 14 in post exposure laboratory experiments with water from control, burnt oil, oil+dispersant, and crude oil mesocosm water sampled in March 2015.	100
Table 7	The average concentrations \pm SD of pH, nutrients (nitrate, phosphate, silicate; $\mu\text{M L}^{-1}$), and PAH (ng L^{-1}) on Day 0 and Day 14 in post exposure laboratory experiments	


	with water from control, burnt oil, oil+dispersant, and crude oil mesocosm water sampled in April 2015.....	101
Table 8	The effect of burnt oil, dispersed oil, and crude oil treatments on the biomass of various organism groups in winter. Negative effect – the biomass of a specific organism group was lower in a particular oil treatment than in the control. Positive effect – the biomass of a specific organism group was higher in a particular oil treatment than in the control. No effect – the biomass of a specific organism group in a particular oil treatment did not differ from the biomass in the control.	105
Table 9	The effect of burnt oil, oil+dispersant, and crude oil treatments on the biomass of various organism groups in spring. Negative effect – the biomass of a specific organism group was lower in a particular oil treatment than in the control. Positive effect – the biomass of a specific organism group was higher in a particular oil treatment than in the control. No effect – the biomass of a specific organism group in a particular oil treatment did not differ from the biomass in the control.	106
Table 10	Bioaccumulation of PAHs in copepod females (ng/individual) and eggs (ng/egg) in copepod exposure experiments including dilution experiments. Second column is background concentrations and eggs are taken from females exposed to undiluted mesocosm water.....	114
Table 11	Summary of polar cod sampled in January after a 7-month monitoring period following 48 h exposure to in situ burned oil residues [BO], mechanically dispersed oil [MDO], and chemically dispersed oil [CDO] treatment, and a control group. Unexposed fish have size distributions which fall outside the intermediate range included in the exposure experiment. Age, as determined by otoliths, somatic weight, total length, hepatosomatic index (HSI), and condition factor were calculated for all fish. All values are mean ± SE.....	130
	Relative abundance (%) of bacteria/taxonomic group (> 1%) in pristine ice core samples from February, DNA and RNA approach.....	168
	Relative abundance (%) of bacteria/taxonomic group (> 1%) in pristine seawater at 5, 10 and 25 m depth, DNA and RNA approach.....	169
	Relative abundance (%) of bacteria/taxonomic group (> 1%) in seawater from mesocosm treatments, DNA and RNA approach.....	170
	Relative abundance (%) of bacteria/taxonomic group (> 1%) in ice core samples, different treatments in March, analysis on RNA level.....	170
	Relative abundance (%) of bacteria/taxonomic group (> 1%) in ice core samples, different treatments in April, analysis on RNA level.....	170
	Relative abundance (%) of bacteria/taxonomic group (> 1%) in ice core samples, different treatments in May, analysis on RNA level.....	171
	Relative abundance (%) of bacteria/taxonomic group (> 1%) in ice core samples, different treatments in March, analysis on DNA level.....	171
	Relative abundance (%) of bacteria/taxonomic group (> 1%) in ice core samples, different treatments in April, analysis on DNA level.....	171
	Relative abundance (%) of bacteria/taxonomic group (> 1%) in ice core samples, different treatments in May, analysis on DNA level.....	172
	Relative abundance (%) of bacteria/taxonomic group (> 1%) in the biofilm samples from May, analysis on DNA and RNA level.....	172

SECTION 1 UNIQUE ARCTIC COMMUNITIES AND OIL SPILL RESPONSE CONSEQUENCES- OIL BIODEGRADATION & PERSISTENCE.

Environmental Effects of Arctic Oil Spills and Arctic Spill Response Technologies
2014-2016

Final Report Project 2B

July 2017



Project Manager,
Lionel Camus, Akvaplan-niva

Quality Control: Lionel Camus & Hector Andrade
Akvaplan-niva, Tromsø, July 2017

Authors which contributed to this project:

Cedre

- Stéphane Le Floch
- Fanny Chever
- Justine Receveur

International Research Institute of Stavanger

- Catherine Boccadoro
- Elin Austerheim
- Mari Mæland
- Adriana Krolicka

Bigelow Laboratory for Ocean Sciences

- Christopher Aepli

1 INTRODUCTION

The biodegradation of oil spills and their hydrodynamic spreading and dispersion have been extensively studied and oil degrading microorganisms have been shown to bloom following exposures to hydrocarbons [Hazen et al., 2015]. In Arctic regions, weathering effects are likely to be slower and spill may stay frozen into the ice for long periods of time. Extensive studies have been performed in the Arctic to understand the biodegradation potential and the fate of the oil, and have suggested that the oil composition of oil trapped in ice may remain largely intact during the winter months [Brakstad et al., 2008].

In this work, Arctic petroleum exposures were conducted using purpose built mesocosms, which were designed to monitor the long-term fate, behavior, persistence and biodegradation of the oil and impact on the microbial communities, following different response scenarios. Oil exposures were conducted in large semi-contained mesocosm set-ups placed *in situ* in Van Mijenfjord (Svalbard, Norway) over a single winter and spring season encompassing the peak biological activity period (including the melting period). Natural environmental conditions prevailed, including, exchange with the atmosphere, exchange with the water column and weathering processes during the winter and spring seasons. Hence the biodegradation process and persistence of the oil was followed from the oil introduced in February to the melting in July. In addition, separate oil exposures were set-up to investigate the natural attenuation of the oil on immersed rock surfaces over the same time period.

For the purpose of this project, the following parameters were studied through the ice layer, within the water under the ice and on the rock surfaces, over the five-month period:

- Chemical composition of the oil,
- Bacterial populations and oil degrading microorganisms,
- Microbial activity and hydrocarbon biodegradation.

These experiments investigated the fate of the oil and the role of microorganisms in the natural oil biodegradation process in the Arctic by focusing on crucial questions concerning the oil weathering processes, biodegradation rate, oil behavior and migration through the ice, biodegradation potential of the *in-situ* microbial communities and their response to the oil.

2 MATERIAL AND METHODS

2.1 Location of field site

An extensive field campaign was conducted in Van Mijenfjord at Svea (Svalbard, Norway) from January to July 2015 (Figure 1). Svea is a coal-mining town located approximately 60 km south-east of Longyearbyen. A barrack at Polartun near Svea served as working/living quarters and laboratory facility. The sampling and field work took place a few hundred metres offshore Crednermorenen right across the fjord from the barracks (travelling distance of approximately 4 km). Sampling and handling of the samples, as well as a number of *in situ* measurements/analyses were performed on site.

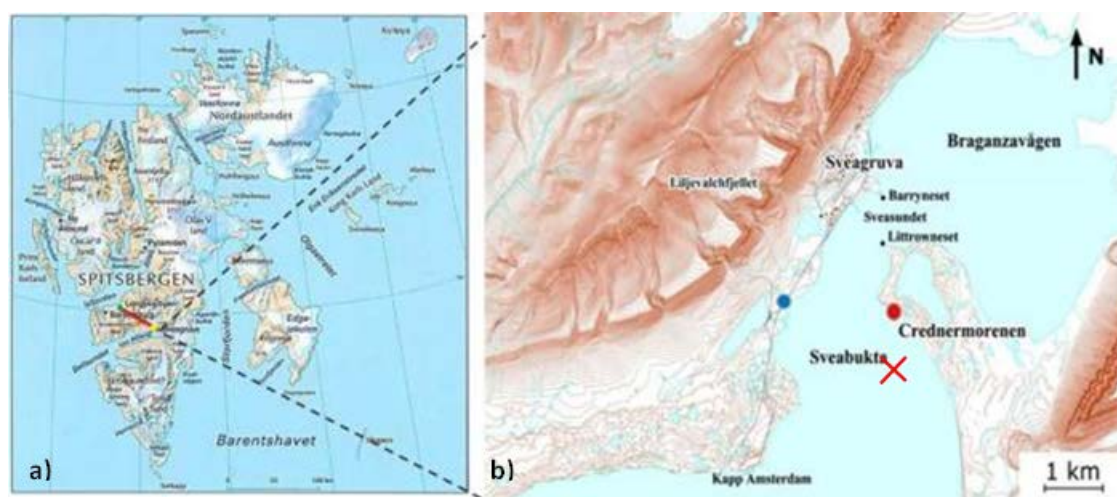


Figure 1 a) Map of Svalbard archipelago. The red line illustrates the distance between Longyearbyen (airport location) and Svea, b) Svea mining town with the location of the living and working barracks marked with a blue point, and the field and sampling location marked with a red point. The red cross represents the location of the mesocosm set-ups (located 800 m from shore).

2.2 Deployed experimental equipment

2.2.1 Mesocosms construction

Cedre designed 8 mesocosms that were used in this study (Figure 2). The French engineering company G2B manufactured them, in close cooperation with Cedre. The structure was checked by SOFRESID engineering and Eni Saipem SA. The mesocosms were designed to float in open water and be resistant to icing in order to stay on location from the fall freeze to the spring melt (the diameter of the mesocosms, 1.6 m, has been chosen in order to minimize stresses applied on the structure over the icing period). They consist of a floating opaque vertical cylinder (about 1 square meter section) open at the top and the bottom to allow natural exchanges with the atmosphere and the water column (dilution, evaporation, etc), but long enough (3 meters) to keep the oil contained. Once surrounded by floating ice, the mesocosms move with the ice according to the tidal movements; this prevents movement of water through the pipe, which could lead to

oil leakage out of the inner part of the mesocosm. Opaque vertical cylinders have been chosen (black plastic curtain).

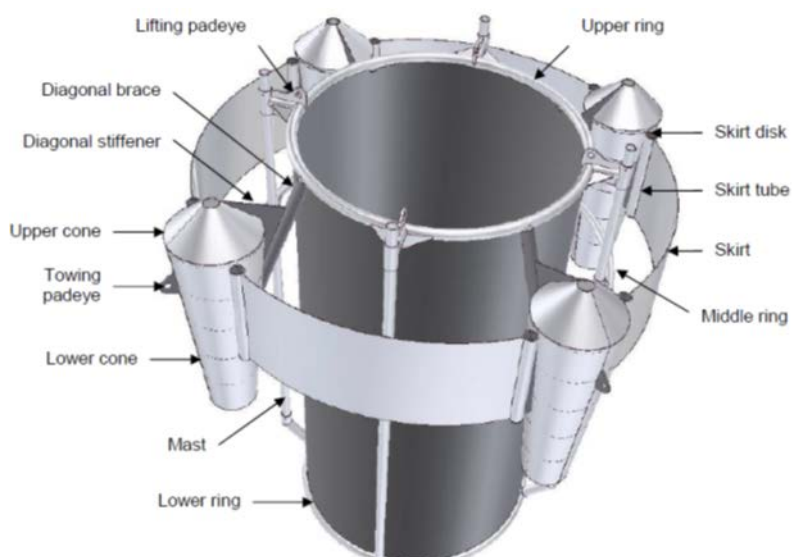


Figure 2 Industrial drawing of the mesocosms applied in the Svea field-campaign. Internal diameter: 1.6 m, length: 3 m (source CEDRE)

The 8 mesocosms were transported from Brest (October 2014) to Svea (November 2014) with Blue water Shipping company (by road transport from Brest to Tromsø, by boat from Tromsø to Svea). Once arrived in Svalbard, in January 2015, the structure of the mesocosms was assembled at Svea (Figure 3)



Figure 3 Assembly of the 8 mesocosms in Svea (source CEDRE)

The initial schedule (deployment in the water before icing) was not followed due to weather conditions (unstable and drifting sea ice that could create a lot of stress on the mesocosms structure and anchoring system) and administrative reasons. Consequently, the mesocosms were deployed once the fjord was covered with ice of sufficient thickness and stability (resistance to

storm and safe for people to work on). During weeks 7 and 8, large holes (3m x 3m) were cut in the 80cm thick ice with a chainsaw, and the ice blocks pulled out by means of man power and transported away from the site by snowmobile. The mesocosms were transported to the experimental site individually on a modified sledge pulled by a snowmobile. Once on site the mesocosms were lowered into the water (Figures 4, 5 and 6).



Figures 4 (left) and 5 (right) Mesocosms deployed in the Svea field-campaign (source: IRIS)



Figure 6 Location of the mesocosms at the experimental site (source IRIS)

2.2.2 Tiles

In addition to the mesocosms experiment that focus on the water and ice compartments, experiments with rock tiles were set up in the same location (~40 m away from the mesocosms). Tiles are cut in a granite block and they have the following size: 20 x 20 cm with a thickness of 3-4 cm (Figure 7).

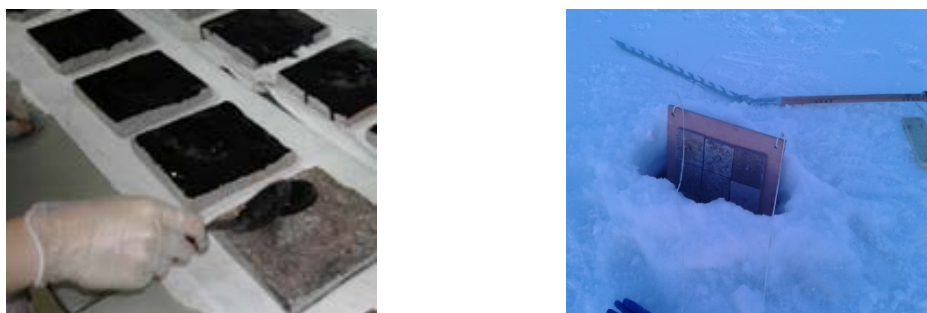


Figure 7 Tiles during the oiling phase and their positioning in the icepack

The tiles were treated with the same oil and deployed during the same period of time to study the fate of the oil, natural attenuation and biodegradation, on solid substrate. Measurements were taken to investigate the role of rock surface biofilms in the oil biodegradation process. The oil was applied to the surface of the tiles using a paintbrush. Three layers of oil were added with a 5 min drying period between each layer resulting in an oil film of ca. 1mm. Tiles were left to dry overnight before being deployed below the ice (suspended in the water column). They were left immersed during the whole experiment. Clean tiles (without oil addition) were also deployed to serve as a control.

2.3 Oil and dispersant used for treatments

2.3.1 Crude oil

The KOBBE crude oil (produced by the GOLIAT oil field in the Barents Sea) was chosen in agreement with IOGP and was supplied by Eni to Akaplan Niva in Tromsø. The total volume was divided into several batches before distributing it over the different experiments (see section 2.2). The total volume was calculated in order to lead to an oil thickness of ~0.25 cm once divided between the different experiments (thickness that is representative of a real oil spill, leading to a volume of 20 L per mesocosm).

Physical and chemical analyses of the fresh oil were performed at Cedre. The KOBBE oil is a relatively light crude oil centered on $n\text{-C}_{14}$, with a density of 0.816 g/mL (at 2 °C) and a viscosity of 6 mPa.s (at 2 °C and a shear rate of 10 s⁻¹). The distillation curve obtained during the sample preparation of the 250 °C residue is representative of the maximum evolution at sea, and results of this distillation provides a reliable prediction of the maximum evaporation rate expected when spilled at sea. The evaporation rate which was measured in the laboratory is 50 %. The content of asphaltenes is low (0.3 % w/w, i.e. by mass) and the content of wax is moderate (11 %). The crude oil pour point is -39 °C. The fresh oil is thus not in the solid form at the temperatures encountered during the field work. The pour point is related to the wax content, and it increases over time due to the evaporation process. The surface and interfacial tensions (measured between the oil and the air and the oil and the water) are of 24.73 and 13.44 mN/m, respectively. The maximum water content is of 77.9 %. The chemical composition of the crude oil is presented below (Figure 8).

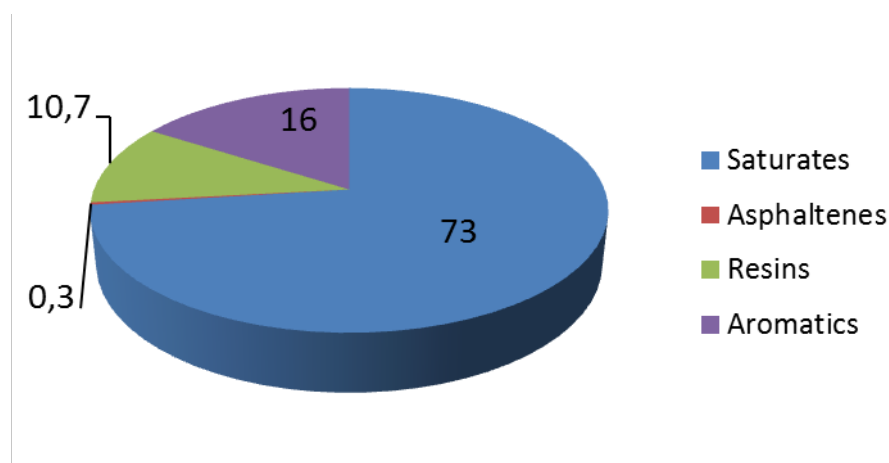


Figure 8 Chart pie representing the chemical composition of the KOBBE crude oil by mass, analyzed by GC-FID

The sum of 21 parent PAHs and their alkylated congeners analyzed in this study leads to a concentration of $9,300 \mu\text{g.g}^{-1}$ for this crude oil. The sum of the *n*-alkanes is of $82,000 \mu\text{g.g}^{-1}$.

2.3.2 Burnt oil residue

The production of burned residue was done in collaboration with the French institute INERIS (Verneuil-en-Halatte, France): 20 L of the KOBBE oil was burned in 3 min. This was the time needed for the fire to go out, leading to approx. 2 L burned residue (i.e., ~ 85 – 90 % of the fresh oil volume was burned).

Chromatogram of the burned residue compared to the fresh oil, analyzed by HT-GC/FID, is presented in Figure 9. This method provides a general view of the oil, from the light compounds (around 10 carbons) to the heaviest fractions corresponding to a vacuum residue (around 90 carbons). It can be observed that the light fraction of the burnt oil disappeared compared to the fresh oil.

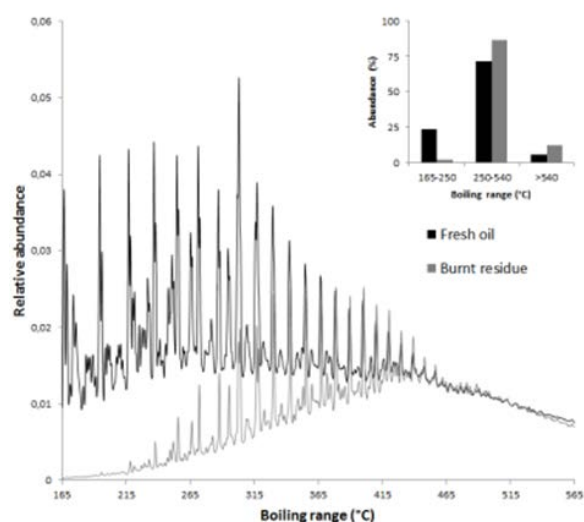


Figure 9 Comparison of the burned residue chromatogram (in grey) with the fresh oil one (in black)

2.3.3 Dispersant

The dispersant chosen is approved for use in many countries and produced by one of the industrial partners of the study, TOTAL: FINASOL OSR52 (TOTAL fluids)¹. This dispersant presents an efficiency of $79 \pm 3 \%$, measured using the IFP test (NF T 90-345) on viscosity oil of 1,300 cSt. In response of an acute toxicity test, the dispersant toxicity of brown shrimps (*Crangon crangon*) exposed during 6 hours to 960 mg.L^{-1} causes a mortality of 3.3 % (NF T90-349 method). Finally, the biodegradability of the dispersant is at least 50 % according to a test performed by INERIS (NF T 90-346).

2.4 Treatments applied and sampling schedule

The mesocosms were placed as 2 rows of 4 mesocosms, each row being separated by 20 - 25 m, and each mesocosm in a row being separated by approx. 13 m.

Four different treatments (2 replicates each) were applied to the mesocosms (Figure 10 and 11) and left to freeze in:

- **Natural attenuation (mesocosms A and B):** 20 L of crude oil was added to each of 2 mesocosms. This quantity poured on a surface of 8 m^2 leads to an oil thickness of 0.25 mm, which is representative of a real fresh oil slick.
- **Oil mixed with dispersant (oil+dispersant)(mesocosms C and D):** 20 L of crude oil was mixed with 1 L of dispersant and this mixture was added to each of 2 mesocosms, without additional mechanical mixing to mimic an ineffective dispersant application.
- **Residues of burnt oil (mesocosms E and F):** 2 L of residuals of burned crude oil was added to each of 2 mesocosms (2 L correspond to the volume of residues that remains after burning 20 L of this specific crude oil – KOBBE oil).
- **Control (mesocosms I and J):** 2 mesocosms were let free from oil and served as control. In addition, 2 additional controls were sampled ~120 m away from the mesocosms area (out of any mesocosms) and served as Clean Sites control (to check the effect of mesocosm location).

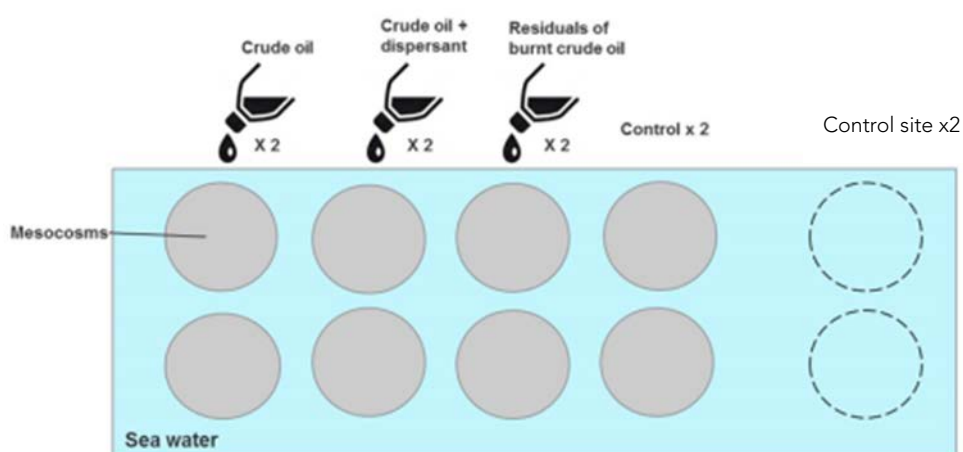


Figure 10 Schematic drawing of the field experimental setup at Svea

¹ FINASOL OSR 52 Material Safety Data Sheet (MSDS): <http://www.quickfds.com/out/17439-36840-24544-010574.pdf>.



Figure 11: Pictures of the different treatments applied: a) Mesocosm with oil alone, b) Mesocosm with oil mixed with dispersant, c) Mesocosm with in situ burning residue (source: IRIS)

Figure 11 Pictures of the different treatments applied: a) Mesocosm with oil alone, b) Mesocosm with oil mixed with dispersant, c) Mesocosm with in situ burning residue (source: IRIS)

Table 1 describes the sampling schedule. In addition to the three sampling points in the icing period, an additional sampling point after the melting period was included. This sampling took place in July before cleaning and decommissioning of the mesocosms. Fieldwork started end of January (mesocosms arrival at Svea) and lasted until the ice melting period in order to cover different winter temperatures and environmental conditions, as well as the spring peak of biological activity.

Table 1 *Sampling schedule*

Time Point	Month	Action
T0	17th-20th of February	Sampling point for microbial community. Mesocosms set up on the ice and oil spillage.
T1	March	Sampling point
T2	April	Sampling point
T3	May	Sampling point
Ice break up		
T4	July	Sampling point and mesocosms cleaning/dismounting

2.5 Sample collection and handling

2.5.1 General considerations

All sample collection, sampling handling and experimental work related to microbiology was performed in sterile conditions as far as possible. All equipment used was autoclaved at 121°C for 30 min when possible, or rinsed with ethanol prior to use. All sampling and handling equipment was rinsed with clean sterile seawater between samples. Dedicated equipment was used for the clean mesocosms and oil-exposure mesocosms and samples in order to avoid oil or dispersant contamination.

2.5.2 Sea ice sampling

At each time point during the ice period (T1, T2 and T3), three cores were collected from each mesocosm (random distribution of sampling points in each mesocosm) using a 9 cm diameter corer which was cleaned after drilling in each mesocosm. For the sampling of the Control mesocosm (x 2) and the sampling of the Clean site (x 2), a dedicated corer was used to avoid any transfer of petroleum residues or microorganisms. Once a core was obtained, length measurements and photographs were taken. The outside of the core was shaved with a clean sterile sharp blade in order to remove any contamination (oil or microorganisms) resulting from the coring. Each core was then cut at regular intervals with clean and sterile equipment into the following 3 or 4 sections, depending upon length: (i) a top section of packed snow of variable length (when present), (ii) a top of ice section (the first 20cm below the oil layer or T0 level), (iii) a 20 cm "middle ice section", and (iv) a 20 cm "bottom ice section", which was the interface ice-water. The location of the oil layer—i.e. the "most concentrated layer" (MCL) was reported for each core. Each section was transferred into a sterile airtight bag and rapidly transported to the on-site laboratory in insulated coolers.

2.5.3 Sea ice sample preparation

To avoid osmotic shock of microorganisms and to speed up the melting process, 500 mL of 3 °C filter-sterilized (0,2 µm filter) seawater from the clean environment sites (outside the mesocosm area) were added to each bag containing an ice core before being put into a refrigerator at 2-3 °C to melt, which took less than two days (Figure 12). After melting, a sample of seawater was kept for chemical analysis (for all sampling campaigns) and bacterial activity measurement (for the T2 and T3 sampling campaigns, details below), and the rest was filtered through a 0.2 µm filter using sterile equipment, for biological analysis. The volume of seawater filtered was recorded and the filter was flash frozen and stored at -80 °C then further transported and stored in the laboratories at -80 °C.



Figure 12 Ice core melting at 2-4 °C. Sterile bags containing melted ice cores from oil contaminated mesocosm (right bag), and from oil+dispersant mesocosm (left bag). Source: IRIS

2.5.4 Seawater sample collection

At each of the four sampling times (T1, T2, T3 and T4), water was collected at three different depths in mesocosms, using a manual pump for the shallow samples (Figure 13): for T1, T2 and T3, just below the ice, at 1 m below ice, and at 2 m below the ice. For the T4, at 0.7 m, 1 m and 2 m below the sea surface. The tubes used for water sampling (one dedicated to each treatment) were rinsed with ethanol before use, and nitrile gloves were used during handling of the equipment and when retrieving the water from the sampler. Deeper seawater samples were collected at the appropriate depths using Niskin bottles. Clean sites, located in the same fjord but approx. 120 m away from the mesocosms were also sampled. A total of 105 samples were collected and immediately transported to the on-site laboratory.

2.5.5 Seawater sample preparation

The seawater samples were immediately transferred into insulated coolers and transported to the laboratory at Svea. A 1,00 ml subsample of each water sample was collected for chemical analysis and the rest was filtered through a 42 mm diameter 0.22 μm pore size GSWP filter (Millipore, Billerica, MA, USA) in a sterile environment (1.5 L per filter) (Figure 13). The total volume filtered was recorded and the filters were placed in 2 ml Eppendorf tubes and stored at -80°C until used.



Source: IRIS



Source: IRIS

Figure 13 Left Panel: Hand pump used for the collection of seawater samples. Right Panel: Filtering set up for Seawater and melted sea-ice

2.6 Oil on tiles

At each sampling time (T0, T1, T2 and T3), three oiled tiles and two non-oiled tiles were collected for analysis.

2.6.1 Chemical analyses of oil on tiles

Concerning chemical analysis, tiles were stored at -20°C . The oil remaining on the rock surfaces was desorbed using ultrasonic bath after addition of internal standards and dichloromethane. The oil was then analyzed by High Temperature GC-FID and GC-MS in Scan and SIM modes. GC-

MS allowed the PAHs (21 PAHs and their ramified components) and alkanes ($nC_{10} - nC_{36}$) quantifications. A total of 29 tiles were collected.

2.6.2 Microbiological biofilm sample collection from tiles

Tiles were collected and 50 cm² surfaces for the oil contaminated tiles and 100 cm² for the non-oil-coated tiles were scraped under sterile conditions, using a sterile swab. This was done on the field site immediately upon retrieving the tiles (Figure 14). The biofilm collected was placed in Eppendorf tubes and immediately transported to the site laboratory and stored at -80°C until transport to IRIS laboratories.

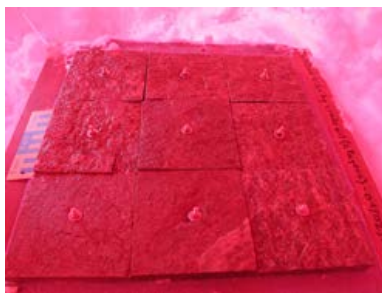


Figure 14 Tiles collected from below the sea ice

2.7 Analytical methods

2.7.1 Chemical analyses

For ice cores, melted ice cores were transferred into 100 mL bottles (see sea ice sample preparation). Dissolved PAHs were extracted using the Stir Bar Sorptive Extraction (SBSE) protocol (Roy et al., 2005). Stir Bars with the PAHs adsorbed on were stored at -20 °C. The water phase samples were analyzed in GC-MS in order to quantify water-soluble oil compounds (aromatics, determination of 21 parent and alkylated daughter PAHs). This information informs on the level of exposure to oil of living organisms of the top water column. A total of 339 samples were collected.

The pure oil layers (Most Concentrated Layer, MCL) were directly taken from the cores and stored at -20 °C in the freezer until analysis. The oil degradation was analyzed by High Temperature GC-FID and GC-MS in Scan and Single Ion Monitoring (SIM) modes. GC-MS allowed the PAHs (21 parent PAHs and their alkylated congeners) and alkanes ($n-C_{10} - n-C_{38}$) quantifications. A total of 78 samples were collected.

Seawater samples were extracted directly on site, and only, the stir bars were transported to the laboratory for PAH quantification.

2.7.2 Microbial community analyses

For microbial community analysis, the total DNA and RNA were extracted from each sample to determine the microbial community structure (DNA level) and structure of active counterparts of microbial assemblages (RNA level). Bacterial community composition was investigated, as well as microbial numbers and presence of oil degrading microorganisms. The DNA or the RNA

extracted from the triplicate samples from each mesocosm were pooled to consider oil and microbial community patchiness without losing ecological relevance and predictive power.

For microbial community analysis, total DNA and RNA were extracted from the same samples directly from the frozen filters. The samples from the three cores from the same mesocosm were pooled for most of the analyses planned (with the exception of samples which are analysed to investigate the variability between sampling points). This was done to consider oil and microbial community patchiness without losing ecological relevance and predictive power.

The extracted DNA was purified and either immediately used or stored at -80 °C. The RNA was immediately purified and traces of DNA were removed from the samples before reverse transcriptase reaction. To avoid any degradation, RNA samples were never stored. The resulting cDNA was either immediately used or stored at -80 °C for later analysis.

2.7.2.1 Total DNA and RNA extractions and DNA purification

For microbial community analysis, total DNA and RNA were extracted from the same samples directly from the frozen filters. The samples were kept on ice and the filters were crushed immediately upon collection from -80 °C in the 2-ml Eppendorf tube using a clean pipette tip. Total genomic DNA and RNA was extracted simultaneously using the Allprep DNA/RNA kit (Qiagen, Valencia, CA) according to the manufacturer's protocols with some modifications. DNA extractions were eluted in 50µl buffer for DNA and 20µl buffer for RNA.

Oligonucleotides used in this study

Analysis	Intended target	Gene	Individual primer or probe **	Sequences (5' - 3')	References
DGGE fingerprint	<i>Bacteria</i>	SSU rRNA	(GC-clamp)341 F 907R	CCTACGGGAGGCAGCA CCCCGTC AATTCCTTTGAGTT	Muyzer et al., 1993
454 sequencing	<i>Bacteria</i>	SSU rRNA	Bakt_341F Bakt_805R	CCTACGGGNGGCWGCAG GACTACHVGGGTATCTAATCC	Herlemann et al., 2011
qPCR	<i>Bacteria</i>	SSU rRNA	Uni331F Uni797R UniP514	TCCTACGGGAGGCAGCAGT GGACTACCAGGTATCTAATCCTG TT CGTATTACCGCGGCTGCTGGCAC	Nadkarni et al., 2002
qPCR	<i>Eukaryota</i>	SSU rRNA	EUK345f EUK499r	CACCAGACTTGCCCTCYAAT CCGCGGTAATCCAGCTC	Zhu et al., 2005
qPCR	<i>Archaea</i>	SSU rRNA	Arch349F Arch806R	GYGCASCAGKCGMGA AW GGACTACVSGGTATCTAAT	Takai and Horikoshi, 2000
qPCR	<i>Colwellia</i> sp.	SSU rRNA	COL134F COL209R	CCTTATGGTGGGGGACAACA AATCAAATGGCGAGAGGTCCG	Krolicka et al., 2014
qPCR	<i>Oleispira antarctica</i>	SSU rRNA	OLEA339F OLEA520R	TGGACGAAAGTCTGATGCAGCCAT G TCCGATTAACGCTTGACACCTTAGT	Krolicka et al., 2014

Analysis	Intended target	Gene	Individual primer or probe **	Sequences (5' - 3')	References
qPCR	<i>Cycloclasticus</i> sp.	GyrB	GyrbCycF GyrbCycR GyrbP (probe)	CGTAGATAAGAATGATGTGAATGT GG CCGTCTCTCTGAGGAATGTTATT AGGTGGCTTTGCAATGGAATGATT CT	Krolicka et al., 2014
qPCR	<i>Alcanivorax</i> sp.	SSU rRNA	Alcvx-464F Alcvx-675R 515RAlc (probe)	GAGTACTTGACGTTACCTACAG ACCGGAAATTCCACCTC CGTATTACCGCGGCTGCTGGCAC	Kostka et al., 2011 Krolicka et al., 2014
qPCR	<i>Alteromonas</i> sp., <i>Pseudoalteromonas</i> sp., <i>Neptunomonas naphthovorans</i>	<i>naphthalene</i> 1,2-dioxygenase large subunit	naphF naphR probe	ATTGGACCTCCTGCTCGTTG GGTAGCCCACTGCATCATGT	This study
qPCR	* <i>Alteromonas</i> , <i>Marinobacter</i> , <i>Alcanivorax</i>	SSU rRNA	UM1326F UW1445R	CCRTGAAGTCGGAATCGCTA TAATCGTCCTCCCGARGGTT	This study

*Hits many *Alteromonas*, *Marinobacter*, *Alcanivorax*, some uncultured *Oceanspirillales*, *Glaciecola* and *Oleiphilus* (Suppl. Table)

** Numbers in names of primers specific to SSU rRNA respond to *E. coli* position of 16S rRNA gene

2.7.2.2 16S rDNA PCR and Denaturing Gradient Gel Electrophoresis

Bacterial V3-V4 hypervariable region of the 16S rRNA gene was amplified using the following primers; (GC clamp) 341F and SD907r (Table above). A 900 µl PCR reaction was prepared in a 0.5 ml Eppendorf tube on ice by mixing 450 µl AccuPrime SuperMix I (Life Technologies), 4.5 µl of each primer (total concentration of 500nM of each), 369 µl of DNase free water and 4 µl of DNA. PCR amplifications were carried out with a DNA thermal cycler using one cycle at 94 °C 3 min, followed by 30 cycles of 30 s at 94°C, 30 s at 53°C, 70 s at 68°C, and a final extension at 68°C for 7min. Agarose gel electrophoresis (2% agarose) was performed to visualize the PCR products before the amplicons were stored at -20°C for DGGE analysis. Fifty microliters of PCR products generated by the (GC clamp) 341F and SD907r primer pair was subsequently analysed by DGGE on a DCode cooled gel electrophoresis unit (BioRad, Hercules, CA, USA). Denaturing gels were generated using a gradient mixer and a peristaltic pump by standard procedures. A linear gradient from 25% to 60% denaturant (urea/formamid) was used for all analysis. A 5 ml stacking polyacrylamide gel containing no denaturant was added after the denaturing gel polymerized for 30 min. The electrophoresis tank was placed on a stirrer for uniform distribution of heat during electrophoresis. All DGGE analysis was performed in 0.5X TAE buffer at a constant temperature of 60°C at 80V for 16 hours (960 mins). Gels were stained for 15 min in 200 ml 0.5XTAE buffer + 20 µl of SybrGreen. Pictures were captured with a Gel Doc 2000 Gel documentation system (BioRad, Hercules, CA, USA). Fingerprinting analysis of DGGE patterns was performed using the Pearson correlation coefficient implemented in Gel Compare II software (Applied Maths, Kortrijk, Belgium).

2.7.2.3 cDNA preparation

- **DNA digestion in RNA samples;** DNA free turbo kit (Ambion) was used according to the manufacture protocol
- **Reverse transcription** was performed using TaqMan® reverse transcription kit and random hexamers. The volume equivalent to 1 µl of RNA was used per 20 µl master mix.
- **Control of RNA samples in terms of DNA contamination**

The control of DNA contamination consisted of QPCR analysis of RNA samples and responding cDNA samples using universal primers (Nadkarni et al., 2002). Lack of amplification or very late amplification is allowed on further analysis using these cDNA samples.

2.7.2.4 Real Time PCR (RT-PCR) reactions

Quantitative PCR (qPCR) was performed on a StepOnePlus instrument using SYBR® Green Master Mixes (Life Technology) or TaqMan® Universal PCR Master Mix (Life Technology). The oligonucleotide sequences for these genes are presented in the appendix. Primers were added to SYBR Green master mixes or IQ TM SYBR® Green Supermix (BioRad) at 150nM concentrations or 500nM concentrations for TaqMan mixes. The probes were labelled with a 6-FAM fluorophore (6-carboxyfluorescein) and contained an Iowa Black quencher and internal ZEN quencher (Integrated DNA Technologies; Coralville, IA) except for the probe used for quantification of Bacteria, which possessed a TAMARA quencher (Life Technology). The final concentration of the probe in TaqMan reactions was 250 nM with the exception of the Bacteria assay where the mix contained 100 nM of each of the universal forward and reverse primers and the probe (Nadkarni et al., 2002). Annealing temperature was either 61 °C or 60 °C (only in the case of the Bacteria assay) and amplification was performed in 40 cycles. PCR mastermix (20 µl) contained 2 microliters of 10 times diluted DNA or cDNA mixture. Conditions of PCR reactions and concentration of oligonucleotides in the case of *Eukaryota* and *Archaea* assays were according to information in the relevant literature. For the construction of respective standard curves for quantitative PCR, we used synthetic gene fragments (gBlocks®, IDT, <https://www.idtdna.com/pages/products/genes/gblocks-gene-fragments>). Synthetic DNA sequences were longer (750 bp) and overlapped the target sequences. PCR efficiency was calculated automatically using the slope of the regression line in the standard curve (StepOnePlus Real-Time PCR system, Applied Biosystems). The number of gene copies will correspond to 1 ml of seawater. Analysis with a single assay was performed for samples derived from selected time points simultaneously on a single plate to avoid plate to plate variation.

2.7.2.5 454 Amplicon sequencing and analysis

The 16S rRNA gene was amplified using fusion primers designed according to Roche recommendations and containing specific sequences targeted on V3-V4 region 5' - CCTACGGGNGGCWGCAG - 3' (Bakt_340F) and 5' -GACTACHVGGGTATCTAATCC - 3' (Bakt_784R) (Herlemann et al., 2011). The PCR mastermix contained: 2,5 units of High Fidelity Polymerase (Roche) provided 1X buffer without MgCl₂, 250 µg BSA, 2 µl of DNA template, 200 µM of each dNTPs, 2.5 mM MgCl₂, 0.25 µM of each primer and H₂O to a final volume of 50 µl. PCR was performed under the following conditions: 3 min at 95°C followed by 32 cycles of 30 sec at 95°C, 40 sec at 55°C and 60 sec at 72°C followed by a final extension for 10 min at 72°C. Agarose electrophoresis was performed to visualize the PCR products. All samples were pooled in equal molar amounts, purified and sequenced at the Department of Biochemistry, University of Cambridge, UK. The pyrosequencing reaction was performed on a FLX sequencer using Titanium chemistry. The initial processes (removing low quality and short sequences (<150 bp), splitting

according to the barcodes, trimming barcoding sequences) was performed using the pipeline available on the Ribosomal Data Project II webpage <http://rdp.cme.msu.edu/> (Cole and Wang, 2014). Sequences were screened against chimera structures using USEARCH 6.0. Then, all non-chimeric sequence reads were processed by the NGS analysis pipeline of the SILVA rRNA gene database project (<https://www.arb-silva.de/ngs/>) (Quast et al., 2013). Each sequence was aligned using the SILVA Incremental Aligner tool (SINA v1.2.10 for ARB SVN (revision 21008)) (Pruesse et al., 2012). Then the initial steps of quality control were performed and identical reads were identified. The unique reads were clustered (OTUs) per sample and the reference read of each OTU was classified. The process of dereplication and cluster analysis was performed using cd-hit-est (version 3.1.2; <http://www.bioinformatics.org/cd-hit>) (Li and Godzik, 2006). The classification was performed by a local nucleotide BLAST search against the non-redundant version of the SILVA SSU Ref dataset using blastn (version 2.2.30+) (Camacho et al., 2009) with custom settings. Reads without any BLAST hits or reads with weak BLAST hits, remain unclassified (where the suitability function used in pipeline of the SILVA the did not exceed the value of 93).

2.7.2.6 Sample preparation and incubation for bacterial activity measurements

Short-term incubation experiments were conducted to determine bacterial activity and hydrocarbon degradation potential under in-situ conditions. From each mesocosm, melted ice from the top ice section of the core (i.e., the 20 cm below the "most concentrated layer") and water samples (collected just below the ice) were investigated during T2 and T3. To this end, 20-day (at sampling point T2) and 10-day incubation experiments (at sampling point T3) were conducted.

Subsamples (10 mL) of the ice cores (after melting) and seawater were filtrated with a 0.8 µm surfactant-free cellulose acetate filter (Corning SFCA filters; in order to remove particles and larger phytoplankton) and transferred in individual 10-mL serum vials (nominal volume 12 mL). The vials were equipped with oxygen sensor spots (oxygen microsensor spots type PSt7; PreSens, Germany). For each sample, four replicate serum vials were prepared. Three of the replicate vials were amended with 20 µL of crude oil that was pre-weathered in the laboratory (evaporated all volatile compounds up to n-C₁₀ in a rotary evaporator). To prevent the oil from sticking to the glass surface or stopper, the oil was added on a small piece of pre-combusted glass fiber filter (GF/F, approx. 5 mm diameter). The vials were crimp-sealed with rubber butyl stoppers and placed in acrylic vial rack boxes that were lined with non-transparent tape to protect the vials from light. Holes in the boxes allowed the vials to be immersed in seawater. These acrylic vial racks boxes were placed in a mesh bag and lowered in seawater (at approx. 1 m depth below the ice) though a hole in the ice approx. 100 m away from the mesocosms. Temperature data loggers (Titbit HOBO loggers; Onset Computer Corporation, Bourne, MA) were placed in two vial racks to monitor the seawater temperature.

2.7.3 Bacterial activity measurements: Analytical methods

Sampling procedure: To monitor microbial activity, the oxygen saturation in the vials was measured using optical methods (Microx4 optode; PreSens, Germany). To this end, the vials were briefly removed from the seawater and put in an ice water bath during oxygen measurement. At defined times, select vials were removed from the incubation and sacrificed for flow cytometry and hydrocarbon analysis.

Flow cytometry: For enumeration of bacteria, vials were opened, and 1 mL water samples were transferred in a 2 mL cryogenic vial preloaded with 50 μ L aqueous paraformaldehyde (10 %). The cryogenic vials were kept at 4 °C for 1 hour to stop microbial activity, and then transferred to -80°C. The samples were transported from the field site to Bigelow Laboratory on dry ice and stored at -80°C until analysis. Immediately before analysis, samples were thawed, stained and bacteria were enumerated at the Center for Aquatic Cytometry at Bigelow Laboratory (East Boothbay, ME, USA) using flow cytometry.

Hydrocarbon analysis: After sampling for flow cytometry, hydrocarbons in the remaining 9 mL of solution and on the glass fiber filter were extracted by adding 3 mL of hexane (GC Resolv grade, Fisher Scientific), and vortexing the vials for 30 sec. The hexane layer was then carefully transferred into pre-combusted 4 mL glass vials using Pasteur pipettes, and the vials were closed with PTFE-lined screw caps, and the caps were sealed with PTFE tape. To remove any remaining water phase, each vial contained approx. 2 g anhydrous Na_2SO_4 . The samples were shipped to Bigelow Laboratory at ambient temperature, and were stored at 4 °C until analysis. Volumes of 1 μ L were injected into a gas chromatograph (GC) coupled to a mass spectrometer (MS) through a split/splitless (at 320 °C) using an autoinjector (Agilent 789B GC, Agilent 5977 MSD, Agilent 7693A autoinjector; Agilent Technologies, Wilmington DE, USA). The GC oven was held at 40 °C for 10 min and ramped to 320 °C at 5 °C/min (held 15 min). He (ultrahigh purity 99.999%) was used as carrier gas at a flow rate of 1 mL/min. The following mass traces were monitored in Single Ion Monitoring (SIM) mode: m/z 57 (alkanes); 128, 142, 156, 170 (naphthalenes); 178, 192, 206, 220 (phenanthrene); 166, 180, 194, 208 (fluorenes); 228, 242, 256 (chrysens); 191 (hopanes). In order to calculate degradation of petroleum hydrocarbons, compounds were normalized to the recalcitrant compound 17 α (H),21 β (H)-hopane present in crude oil, and these ratios were compared to ratios of samples at time 0 (immediately before the incubation).

3 RESULTS AND DISCUSSION - MESOCOSM EXPERIMENT

3.1 Visual observations

Figure 15 presents the picture of a core collected at T3 for each treatment applied. The cores were very different depending on the treatment applied. A brown centered layer can be observed for the crude oil treatment (below the ice/slush layer) (Figure 15a), an oil dispersion through the most concentrated layer to the bottom can be observed for the oil+dispersant treatment (Figure 15b) whereas traces of burnt oil (in a thin layer) is observed for the burnt treatment (Figure 15c). The last core (control treatment) shows the quality of the sampling (no oil visible) (Figure 15d). These observations were similar across all the cores collected.



Figure 15 Example of cores collected at T3: a) Cude oil treatment, b) Oil+dispersant treatment, c) Burnt oil treatment and d) Control treatment

Additionally, at the end of the experiment (T4, after the ice broke up), no visual differences were observed between the mesocosms (the oil color and viscosity looked similar). In the mesocosm containing the residue of burning, the quantity was less important (because 2 L was added instead of 20 L for the other treatments), but the remaining oil looked the same as in the other mesocosms. It is to be mentioned that, at the end of the experiments, three of the eight mesocosms were detached from their anchors and were washed ashore. Those three mesocosms corresponded to the following treatments: two "control" and one "burnt oil". This explains the reduced amount of data at T4.

3.2 Chemical analysis in the mesocosm experiment

3.2.1 Sea water compartment

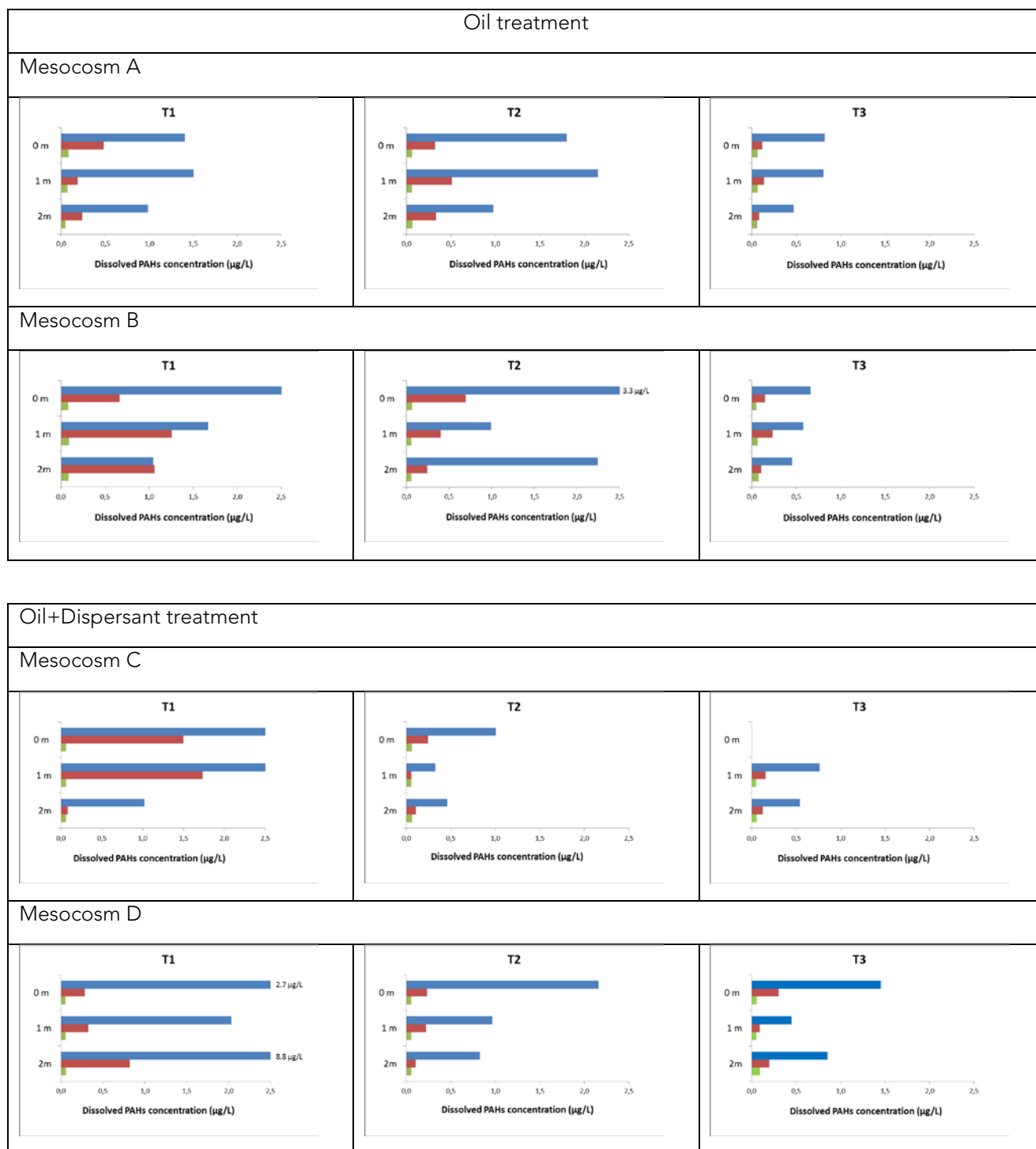
In order to determine the different processes potentially affecting the PAHs behaviour during this study (i.e., evaporation, dissolution, biodegradation...), the 21 PAHs (and their ramified compounds) were divided in three groups, from the lightest to the heaviest compounds. The first group gathers the naphthalene compounds (naphthalene and ramified C₁, C₂ and C₃-naphthalene, compounds referred as N to N3 hereafter), the second group, from benzothiophene to C₃-chrysene (referred to BT to C3), represents medium compounds (with 3 – 4 aromatic rings), and the third group gathers the heaviest compounds (5 rings and more) from benzo(b,k)fluoranthene to benzo(g,h,i)perylene (BBF to BPE).

Figure 16 presents the evolution with time of the dissolved PAHs in the three groups (N-N3, BT-C3 and BBF-BPE), for all mesocosms (mesocosms A and B, C and D, E and F and I and J). No oil droplets were detected. This figure shows that the majority of the dissolved PAHs in the water column are composed of the lightest compounds, i.e. naphthalene and its ramified compounds. They represent about 90 % for the oil+dispersant treatment and about 75 % for the crude oil and the burnt oil mesocosms. The medium compounds (BT - C3) represent less than 20 % of the total PAHs and the heaviest compounds less than 5 % of the total PAHs. These results suggest that dissolution in the water column concerns the lightest compounds.

The oil+Dispersant treatment exhibits the most dynamic behaviour with values reaching 8.8 µg.L⁻¹ at 2 m depth for the naphthalene group at T1. At this sampling time, the highest dissolved PAHs concentrations are observed for the oil+dispersant treatment but, at T2, the highest values are observed for the crude oil treatment. This result underlines the fact that dispersant increases the dissolution kinetics of light PAHs and this result is in accordance with the scientific literature (Guyomarch et al., 2002). These compounds are released from the ice into the water column over time.

The burnt oil treatment depicts low concentrations during the season studied, the maximum reached being observed at T3 (1 m) with 1.5 µg.L⁻¹ (first group of PAHs). Considering the total sum of the PAHs and the 3 depths combined, concentrations ranged from 0.5 ± 0.4 µg.L⁻¹ to 1.8 ± 1.8 µg.L⁻¹. These values are close to those observed in the control treatment leading to the hypothesis that very little dissolution of compounds occurred when using the residue of burnt oil. During the burning step, the fresh oil loses its lightest compounds partially responsible for the dispersion efficiency. Additionally, no clear increase is observed in the water column after the ice break up (T4) as seen in the crude oil and oil+dispersant treatments.

Concerning the control, tap water, sterile seawater used for microbial experiments, water collected at the clean sites (CS) and at control oil sites (CO, i.e. between mesocosms) was sampled and compared to the mesocosms I and J (CTL treatment). The concentrations obtained for the different controls for the total sum of the PAHs and the three depths are in the same range (below ~1.0 µg.L⁻¹) and in agreement with the values measured in the control treatment (mesocosms I and J), ranging from 0.7 ± 0.3 µg.L⁻¹ to 1 ± 0.2 µg.L⁻¹. These results show that no contamination is observed in the control treatment and, that no cross contamination occurred between the mesocosms. Nevertheless, these results also show a background contamination level by dissolved PAHs in the Svea fjord.



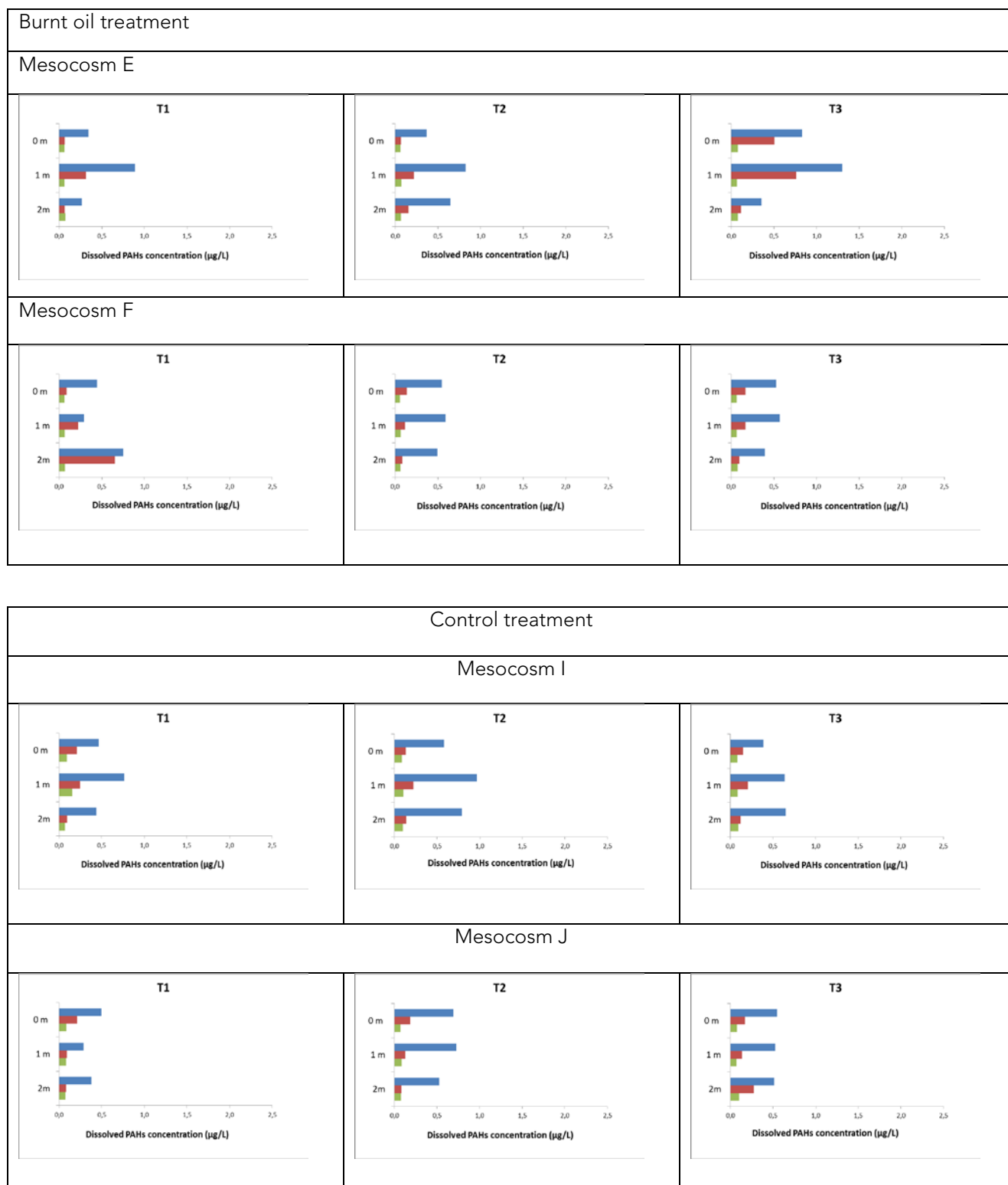


Figure 16 Evolution of dissolved PAHs concentrations in the water column (in $\mu\text{g}\cdot\text{L}^{-1}$) over the winter and spring seasons for the different treatments considered and the different depths. Legend: Blue bars = naphthalene and its alkylated congeners; Red bars = three-four ring PAHs; Green bar = PAHs containing five or more rings)

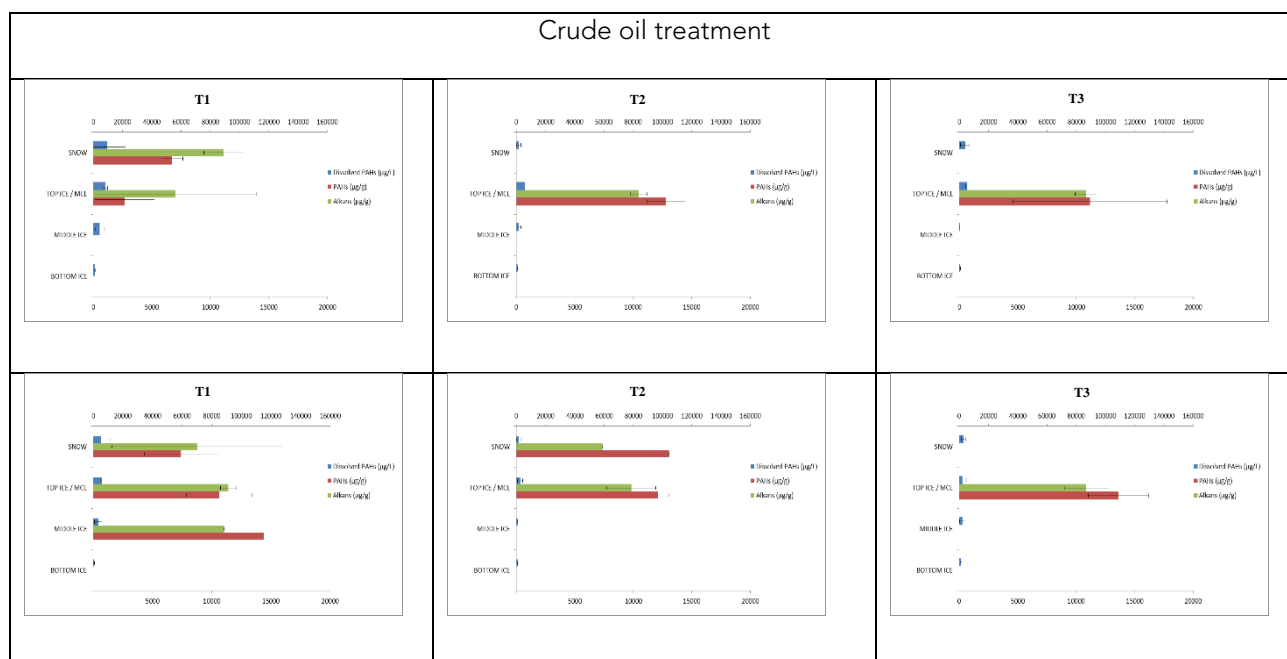
The dissolution kinetics of PAHs were very slow during the winter period and only light compounds were significantly detected for oil+dispersant and crude oil treatments. For both treatments, these compounds were detected at the 3 monitored depths suggesting a diffuse flow out of the mesocosm. Dissolution processes took place even if the oil was trapped in the icepack, if the temperature was below 0 °C.

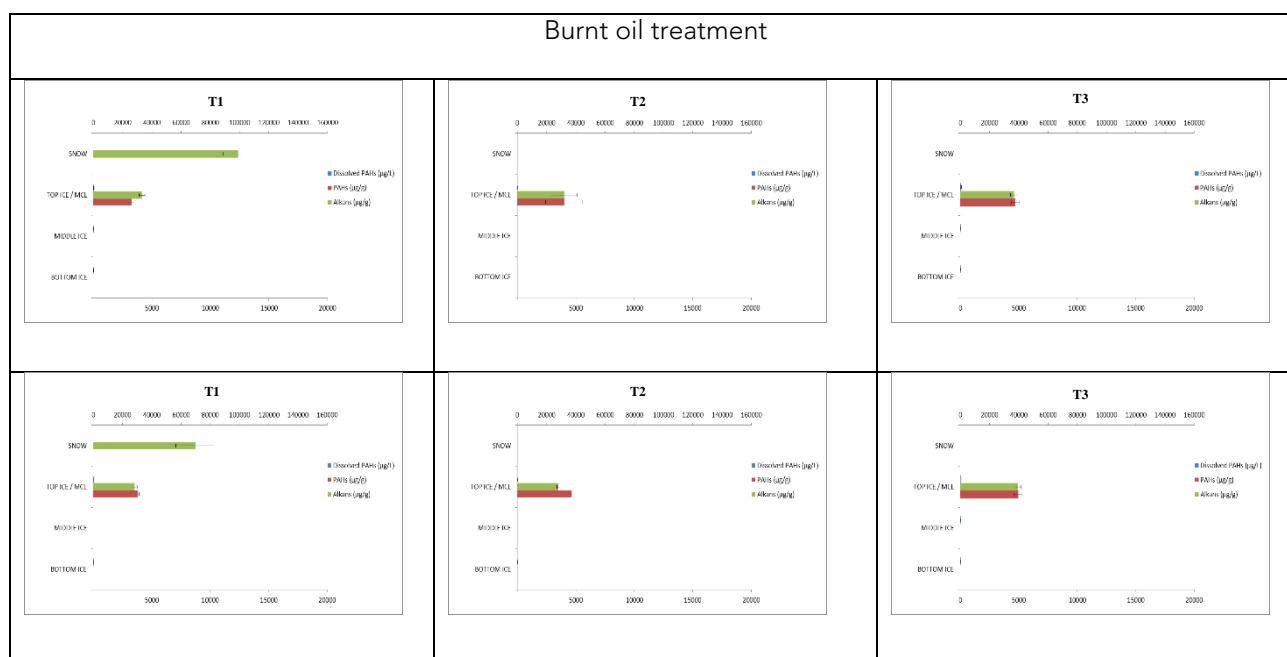
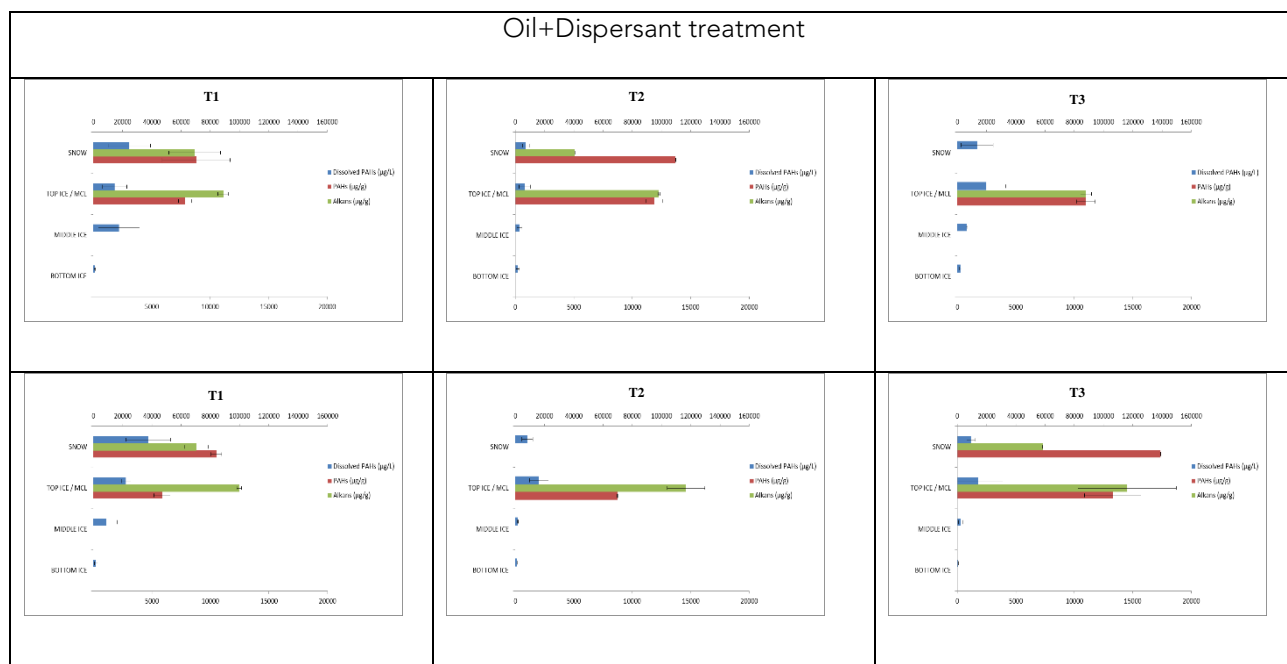
3.2.2 Ice compartment

Chemical analysis. All the core sections were analyzed (packed **Snow** of variable thickness –when present; **Top** ice section which contained the Most Concentrated Layer -MCL; **Middle** ice section; and **Bottom** ice section which was the ice - water interface). The bottom section is a key section in ensuring a better understanding of the migration of dissolved compounds from the ice to the water column.

Figure 17 presents the distribution of the oil in the different sections of cores: the results are expressed in $\mu\text{g.g}^{-1}$ when pure oil was detected in the ice (green bars = alkanes, and red bars = aromatics) and the results are expressed in $\mu\text{g.L}^{-1}$ when dissolved PAHs were detected in melted ice (blue bars).

First of all, the results show that the oil slick was frozen in the Top section of the ice core. Nevertheless and in some cases, pure oil was also detected in the snow layer.





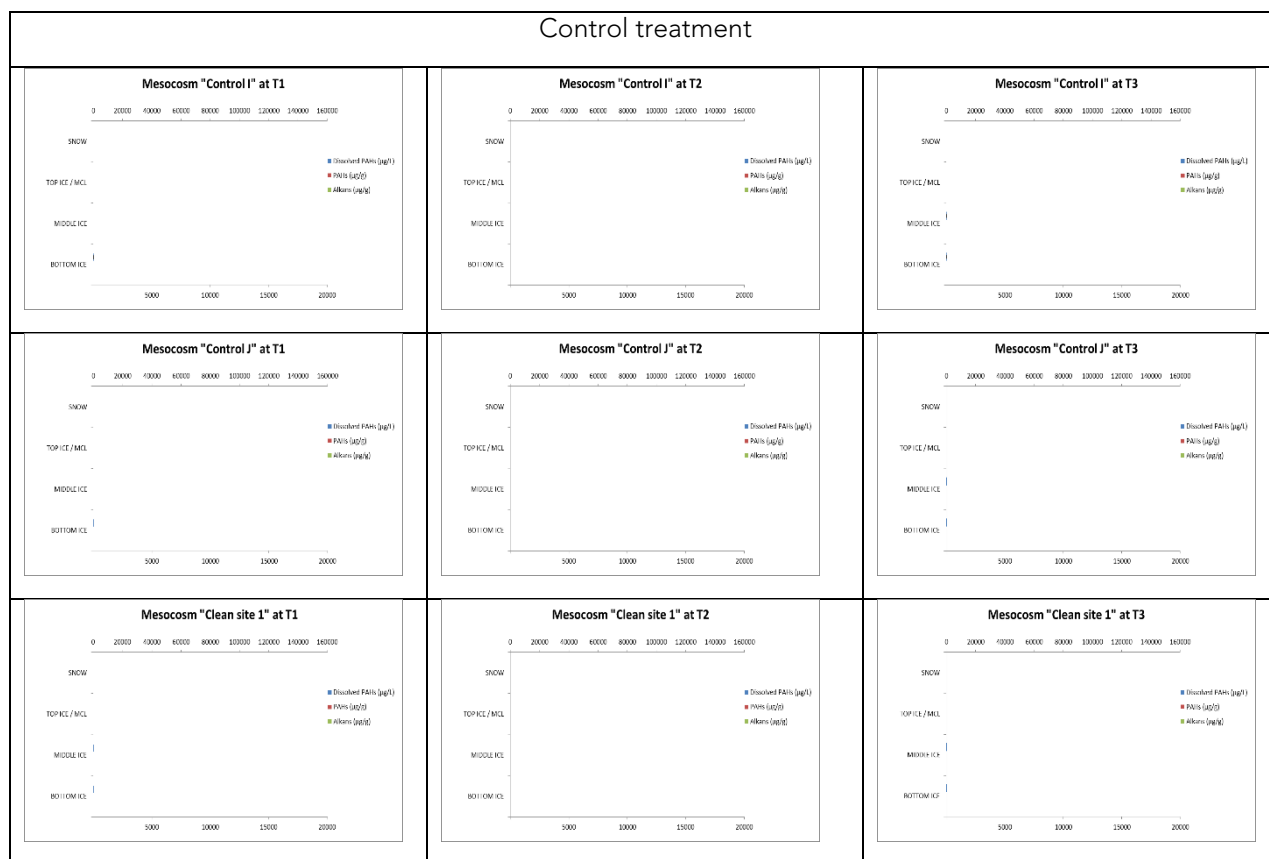


Figure 17 Evolution of dissolved PAHs concentrations (in $\mu\text{g.L}^{-1}$) and pure oil (Aromatics + Alkanes; in $\mu\text{g.g}^{-1}$) over the winter and spring seasons for the different treatments considered (crude oil, oil+dispersant, burnt oil, control and clean site). Legend: Blue bars = dissolved PAHs; Red bars = Aromatics in pure oil; Green bar = Alkanes in pure oil. The top scale is for Alkanes (from 0 to 160 000 $\mu\text{g.g}^{-1}$). The bottom scale is for Dissolved PAHs (from 0 to 20 000 $\mu\text{g.L}^{-1}$) and Aromatics compounds (from 0 to 20 000 $\mu\text{g.g}^{-1}$).

3.2.3 Dissolved Polycyclic Aromatic Hydrocarbons (PAHs) in ice cores

Dissolved PAHs were detected in all core sections and for all oil treatments. The same pattern is observed in the ice and in the water column: the oil+dispersant treatment exhibits the highest value (maximum value $\sim 5,000 \mu\text{g.L}^{-1}$), the crude oil treatment exhibits mean values (maximum value $\sim 1,500 \mu\text{g.L}^{-1}$), the burnt oil treatment exhibits the lowest value (maximum value $\sim 50 \mu\text{g.L}^{-1}$). Clearly, a diffusion of dissolved PAHs from the Top section of the ice core to the Bottom section is observed. Nevertheless, the concentrations encountered in the bottom parts of the ice are approximately ten times higher than those measured in the water column (around $200 \mu\text{g.L}^{-1}$ in the ice compared to $\sim 20 \mu\text{g.L}^{-1}$ in the water column). The transfer from the ice to the water column seems to be slower than the vertical diffusion of PAHs in the ice core. Concerning the chemical nature of the dissolved PAHs detected, the same result as in the water column is also observed: more than 90 % of the PAHs are composed of Naphthalene and its ramified compounds.

No dissolved PAHs were detected in the control treatment and for the clean site. This result confirms that dissolved PAHs detected in the water column for the control treatment are due to a background contamination of the fjord.

From these results, a clear migration of dissolved PAHs compounds (especially light compounds) can be observed from the oil layer to the bottom part of the ice. This confirms the dissolution of the light compounds encountered in the water column for the crude oil and oil + dispersant treatments.

It is important to underline that dissolved compounds are considered readily available for microbial uptake by passive diffusion or active transport through cell membranes, while hydrocarbons trapped in oil droplets are less available (Parales and Ditty, 2010).

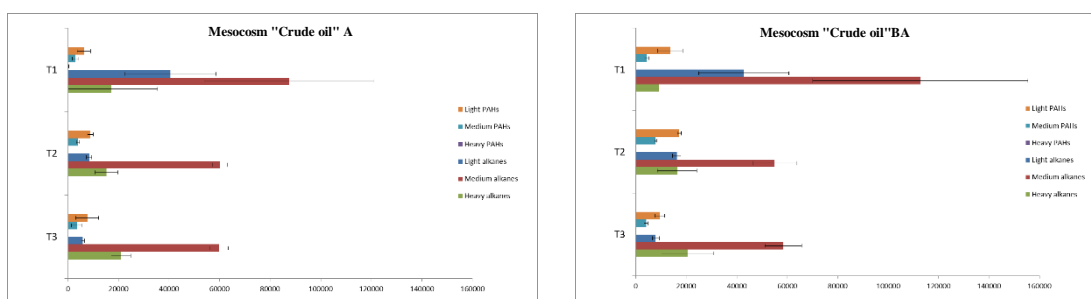
3.2.4 Oil concentration in ice cores

For the Top section of the ice cores, the Most Concentrated Layer (MCL), chemical analyses were performed on the alkane and aromatic fractions. Free oil was observed in each MCL section of the cores which explains why the results are expressed in $\mu\text{g.g}^{-1}$.

The behaviour of the oil was monitored through the concentration of 3 groups of alkanes (nC10-nC14, nC15 – nC25 and nC26 – nC36) and 3 groups of aromatics (naphthalene and ramified C1, C2 and C3-naphthalene or Light PAHs; from benzothiophene to C3-chrysene or medium PAHs, i.e. with 3 – 4 aromatic rings; and from benzo(b,k)fluoranthene to benzo(g,h,i)perylene or Heavy PAHs, i.e. 5 rings and more).

Concerning the groups of alkanes, the highest concentrations were obtained for the Medium fraction, followed by the heavy fraction, and finally the lightest one. These distributions are observed in all mesocosm independently of the treatment applied and at each sampling time (Figure 18). The highest variation is observed for the lightest alkanes (nC₁₀-nC₁₄): their relative abundance decrease with time can be explained by dissolution or biodegradation processes. As their dissolution rate is very low, notably due to their solubility limit, we can suspect that biodegradation processes occurred. This explanation is confirmed by the fact that the heaviest fraction (nC₂₆ – nC₃₆), reluctant to any biodegradation processes, increased in term of relative abundance. In addition, light alkanes are well known to be readily biodegradable (Le Floch et al., 1999).

Concerning the groups of aromatics, no significant trend is observed. Indeed, the concentration of these compounds is very variable over time and from one mesocosm to the other. No difference between treatments can be observed.



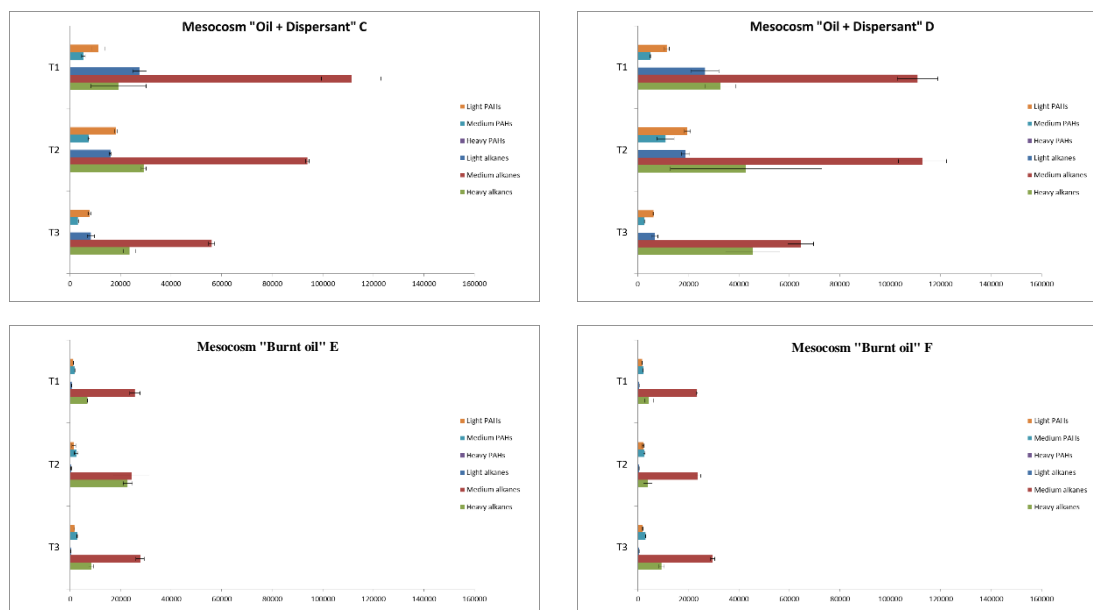


Figure 18 Evolution of the chemical composition of the oil trapped in ice (MCL) for each treatment with time

3.3 Screening of general shifts in microbial populations in the mesocosm experiment

Pre-screening of the microbial populations was performed by Denaturing Gradient Gel Electrophoresis (DGGE) (Muyzer, 1993) (see material and methods section...). This method allows the visualization of the most prominent organisms within the microbial community of a given sample.

3.3.1 Microbial communities – variability between samples and locations

Denaturing Gradient Gel Electrophoresis (DGGE) was used to evaluate the overall natural variability of the bacterial community structure in the sea-ice, both at the DNA level (organisms present) and the RNA level (active organisms). DNA and RNA was extracted from the top section of the sea-ice from 3 samples in 2 pristine locations and then amplified using 16S rDNA specific set of primers. Results of the cluster analysis of bacterial community are shown in Figure 19 and Figure 20.

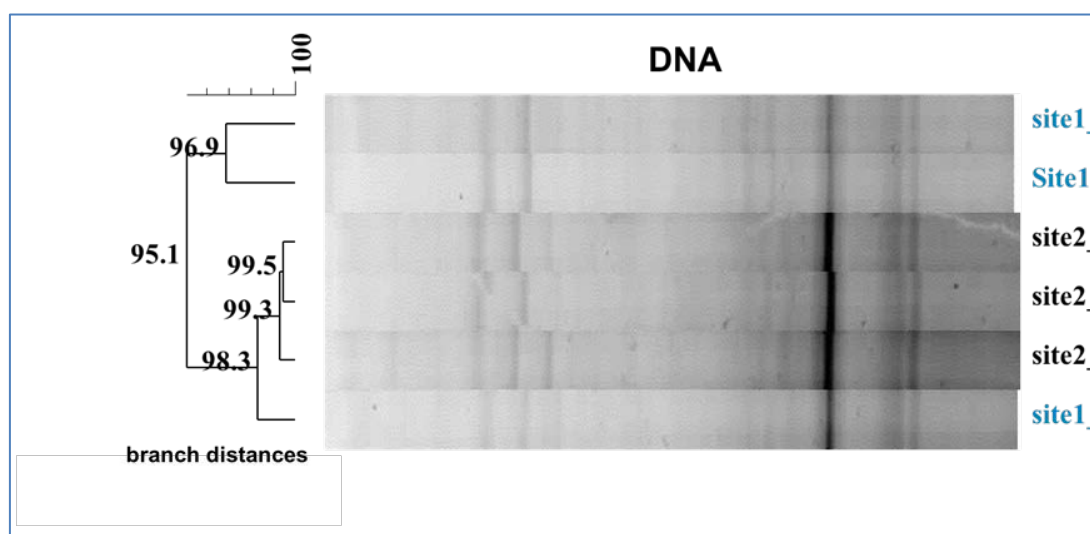


Figure 19 Overview of bacterial community structure in two pristine arctic sea ice locations (site 1 and 2) by Denaturing Gradient Gel Electrophoresis (DGGE). Analysis from total DNA samples extracted from the top layer of 3 different ice cores from each location are shown. Values on the left show the % similarity between bacterial communities

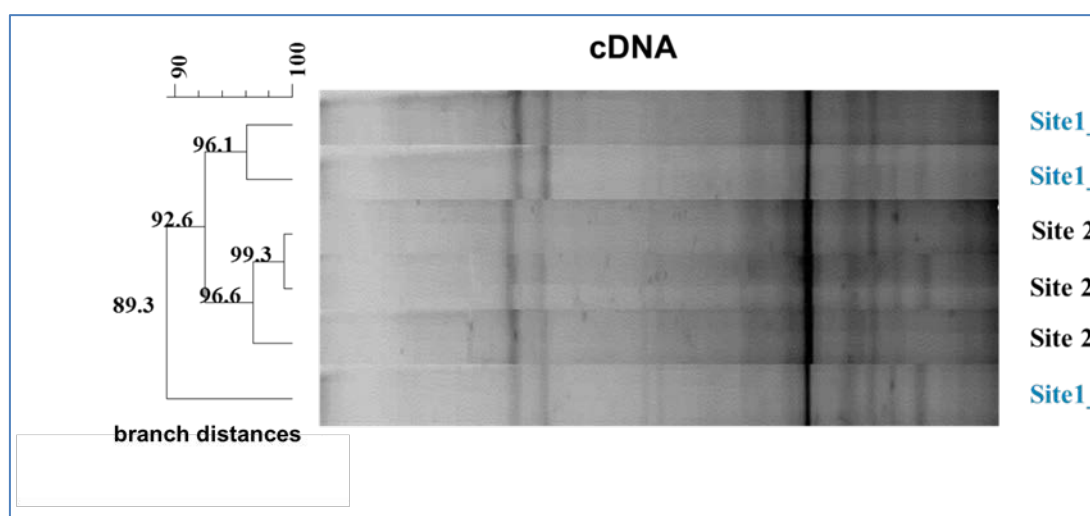


Figure 20 Overview of bacterial community structure in two pristine arctic sea ice locations (site 1 and 2) by Denaturing Gradient Gel Electrophoresis (DGGE). This analysis was based on total cDNA, derived from RNA samples extracted from the top layer of 3 different ice cores from each location. Values on the left show the % similarity between bacterial communities

Results show similar microbial community structures between the samples from the ice cores from the same site or the different sites. This low variability is particularly noticeable on the DNA level (more than 95% similarity between samples). At the RNA level (active microbial community), there is still very little variability in the community structure (more than 89% similarity). Such an observation is important for the analysis and interpretation of results obtained after exposure to oil or treatment methods to some mesocosms.

3.3.2 Microbial communities – seasonal variability and variability through the ice layer

The results show more than 80% similarity in the microbial community structure between locations, even within a month interval. More variability in microbial communities can be seen within the ice layers depending on depth (Figure 21). The community structure in the top layer of the ice was only 50% similar to that of the bottom layer of the ice (1m depth). This demonstrates the need to consider separate layers of the ice separately.

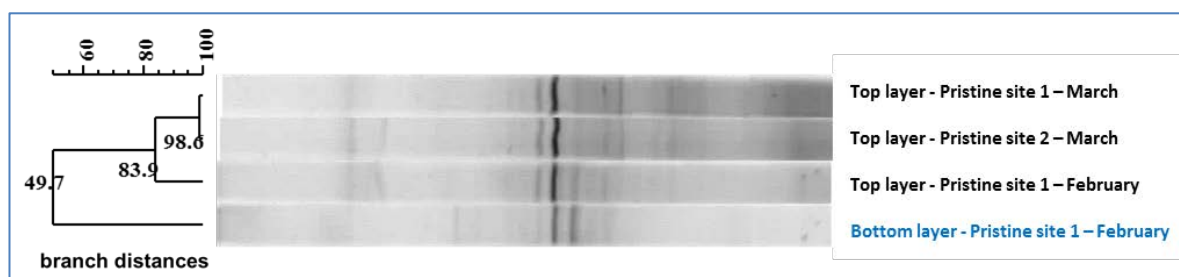


Figure 21 Overview of bacterial community structure in two pristine arctic sea ice locations in February and March by DGGE. Analysis performed on total DNA extracted from samples collected from the top sea ice layer (in black) and from the bottom sea-ice layer (in blue). Values on the left show the % similarity between bacterial communities

3.3.3 Screening of bacterial community structure shifts in response to oil exposure

Effect of oil on microbial communities

The results from the overview of the microbial community structure at the DNA level from 10 samples from the top sea-ice layer from oil (10 samples) and control (12 samples) mesocosms are shown in Figure 22. The results show a low variability in the microbial structure between the different samples and mesocosms subjected to the same treatment (no oil or oil contamination). All samples from the control mesocosms clustered together, with the exception of two oil contaminated samples which contained only low levels of DNA. However, the community structure in the oil exposed mesocosms after one month exposure show clear shifts in community structure, with some organisms becoming more dominant and some organisms growth being inhibited by oil.

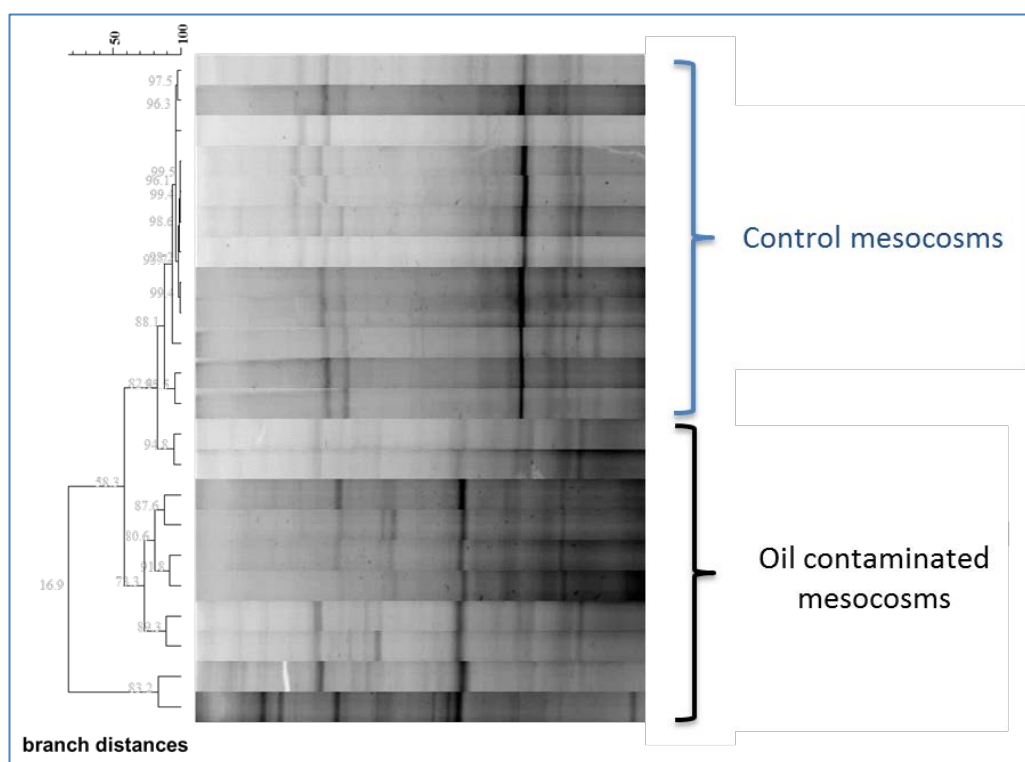


Figure 22 Overview of bacterial community structure in the top layer sea ice from ice cores collected in the control and the oil contaminated mesocosms. DGGE analysis from total DNA extracted samples from different ice cores at each location, collected one month after exposure to oil. Values on the left show the % similarity between bacterial communities

Effect of oil and different spill remediation treatments on microbial communities

The total bacterial community structure overview (from total DNA extraction from samples), following oil exposure and different treatment scenarios, is shown in Figure 23. The same analysis done for the metabolically active portion of the community (total RNA extractions from samples) is shown in Figure 24.

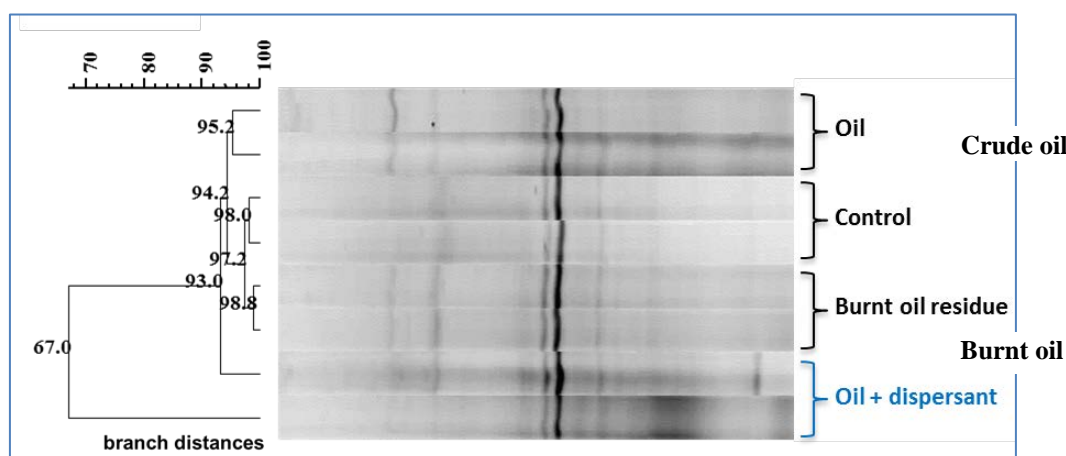


Figure 23 Overview of bacterial community structure in the top layer sea ice from ice cores collected in May (after 3 months' exposure) in the control, Crude oil, Burnt oil and oil+dispersant mesocosms. DGGE analysis performed on total DNA. Values on the left show the % similarity between bacterial communities.

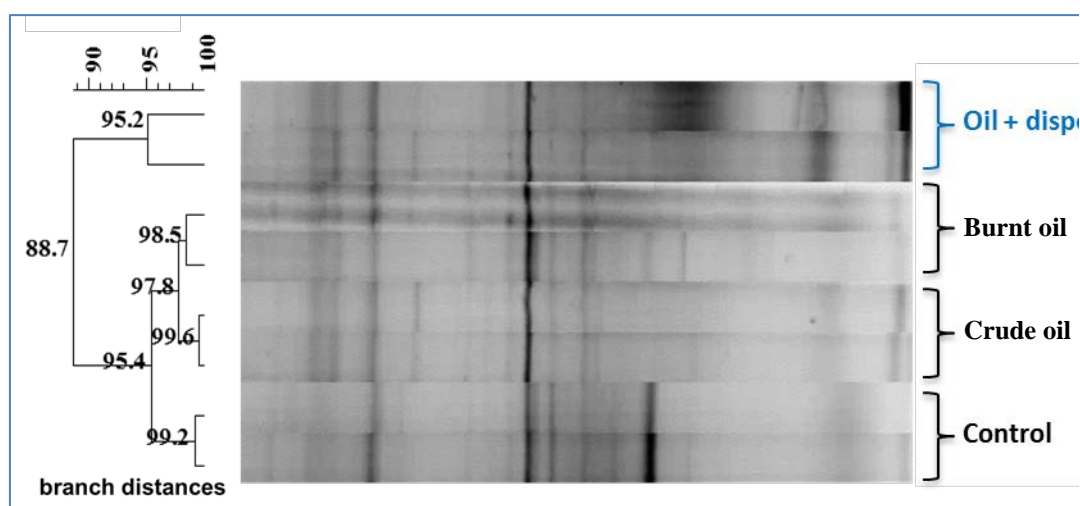


Figure 24 Overview of the active bacterial community structure in the top layer sea ice from ice cores collected in May (after 3 months' exposure) in the control, Crude oil, Burnt oil and Oil+dispersant mesocosms. DGGE analysis performed on total RNA extracted from the samples. Values on the left show the % similarity between bacterial communities.

The results on the relative similarities between the bacterial communities show a clear clustering of samples from the mesocosms that have been exposed to the same treatment. Control mesocosms I and J differ clearly from samples in the exposed mesocosms, particularly when considering the active portions of the microbial communities (Figure 24). Samples exposed to oil and dispersant exhibit a lower similarity to the other samples.

3.4 Microbial biomass in the mesocosm experiment - Quantification of bacteria, archaea and small eukaryotes

The impact of oil on microbial numbers was investigated by a quantification method based on quantitative polymerase chain reaction (qPCR) on total DNA and RNA extracted from ice core

and seawater samples collected from the experimental mesocosms as well as the surrounding environment (see method of sampling collection and analysis in section...). Three samples from three different cores and water samples were analysed for each mesocosm or location.

Sea-ice and seawater samples were collected from two sites in February just before the installation of the mesocosms, to get information on the environments and microbial communities before the start of the different exposures. Samples were then collected from all mesocosms (2 control non contaminated, 2 crude oil contaminated, 2 oil+dispersant and 2 burnt oil in March, April and May, respectively 1,2 and 3 months after the start of the exposure.

The results of all the quantitative PCR results are expressed in number gene copy numbers per ml of melted sea ice or seawater so the numbers differ from direct number of cell counts (there are approximatively 8 copy numbers of the 16S r RNA gene par cell for bacteria, but sometimes many times higher for small Eukaria).

3.4.1 Microbial communities in the pristine arctic environment

The results for the total number of bacteria, *Colwellia* and *Oleispira* genera and number of Eukarya in the different ice layers (top 20cm, middle 20cm section, and bottom 20cm of the sea ice) and depths of seawater (-1m or right below the sea ice, 5m, 10m and 25m depths) for control samples collected before the start of the experiment in February (before installing the mesocosms or performing the exposures) are shown in Figure 25.

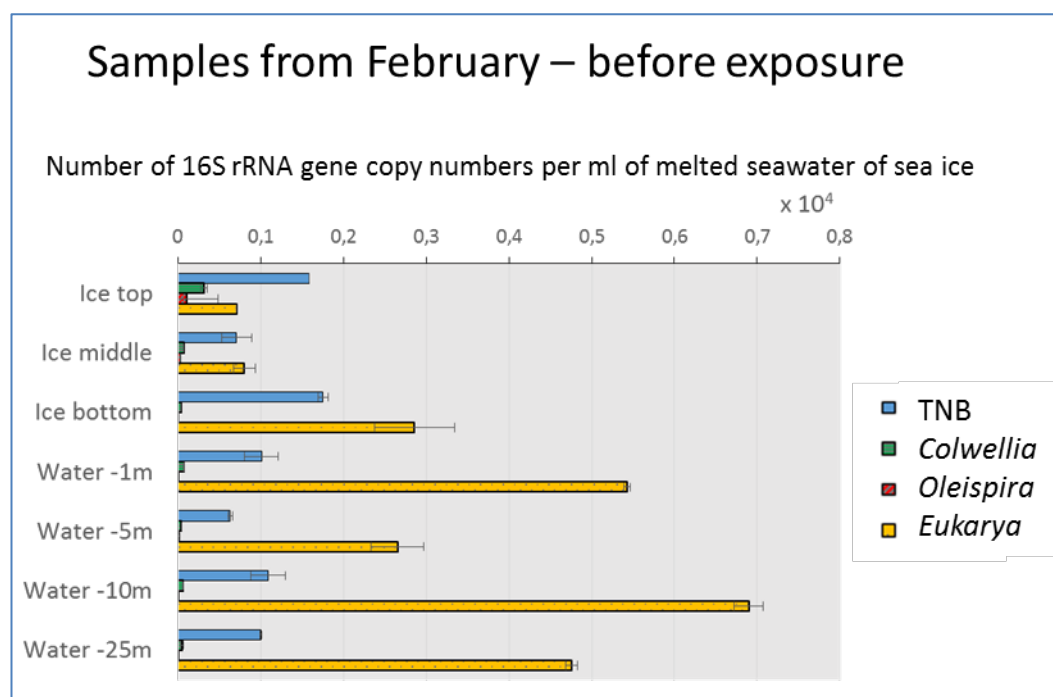


Figure 25 Quantification of the total number of bacteria (TNB), *Oleispira* and *Colwellia* genera and small Eukarya. Total number of 16 S rRNA gene copies per 1 ml melted sea-ice cores from the ice top, middle and bottom layers and in 1 ml of seawater from just below the ice surface (-1m because of the ice thickness). Results are shown here for the February samples taken before the start of the experiment. 3 distinct ice cores or water samples are used for each measurement. The results are shown here for 1 of the sites (see appendix for the results from the other site). The error is the standard error for the measurement. NB: The TNB value is shown on a different axis due to higher numbers.

The results show a relatively constant number of organisms and very similar results between the two sites. *Oleispira* organisms are found at levels higher than expected from Arctic environmental samples (Krolicka *et al.*, article in preparation), which could be indicative of these locations having been previously exposed to very low concentrations of hydrocarbons (this would be consistent with the location of the experimental site, in proximity to Svea mining, as well as the chemical analysis of samples). Eukarya are found in lower abundance in the top and middle sections of the sea ice layers than in the bottom of the ice layer of water column.

3.4.2 Microbial communities during exposure to crude oil, oil+dispersant or burnt oil

The results for the total number of bacteria, number of *Colwellia* and *Oleispira* genera and *Eukarya* in the different ice layers and depths of seawater in all mesocosms (two oil contaminated, two oil + dispersant, two burned oil residue or in situ burning and two non-contaminated mesocosms) are shown in Figure 26 (March samples collected one month after exposure start), Figure 27 (April samples collected two months after exposure start) and Figure 28 (May samples collected three months after exposure start).

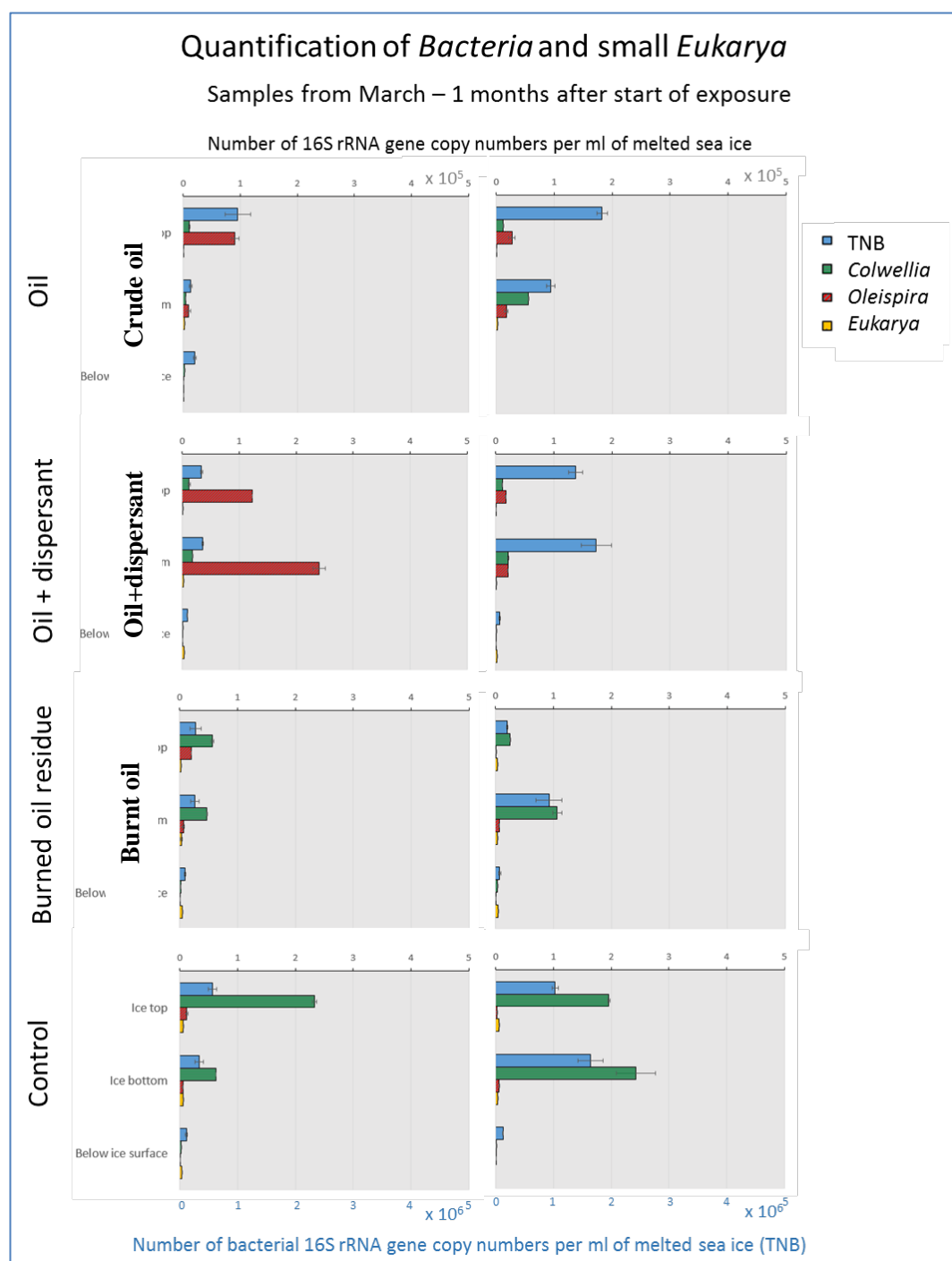


Figure 26 Quantification of the total number of bacteria (TNB), *Oleispira* and *Colwellia* genera and small *Eukarya*. Total number of 16 S rRNA gene copies of per 1 ml melted sea-ice cores from the ice top and bottom layers and in 1 ml of seawater from just below the ice surface. Results are shown here after 1 month exposure (March samples) in the crude oil, oil+dispersants, burnt oil and control no treatment mesocosms. 3 distinct ice cores or water samples are used for each measurement. The error is the standard error for the measurement. NB: The TNB value is shown on a different axis due to higher numbers.

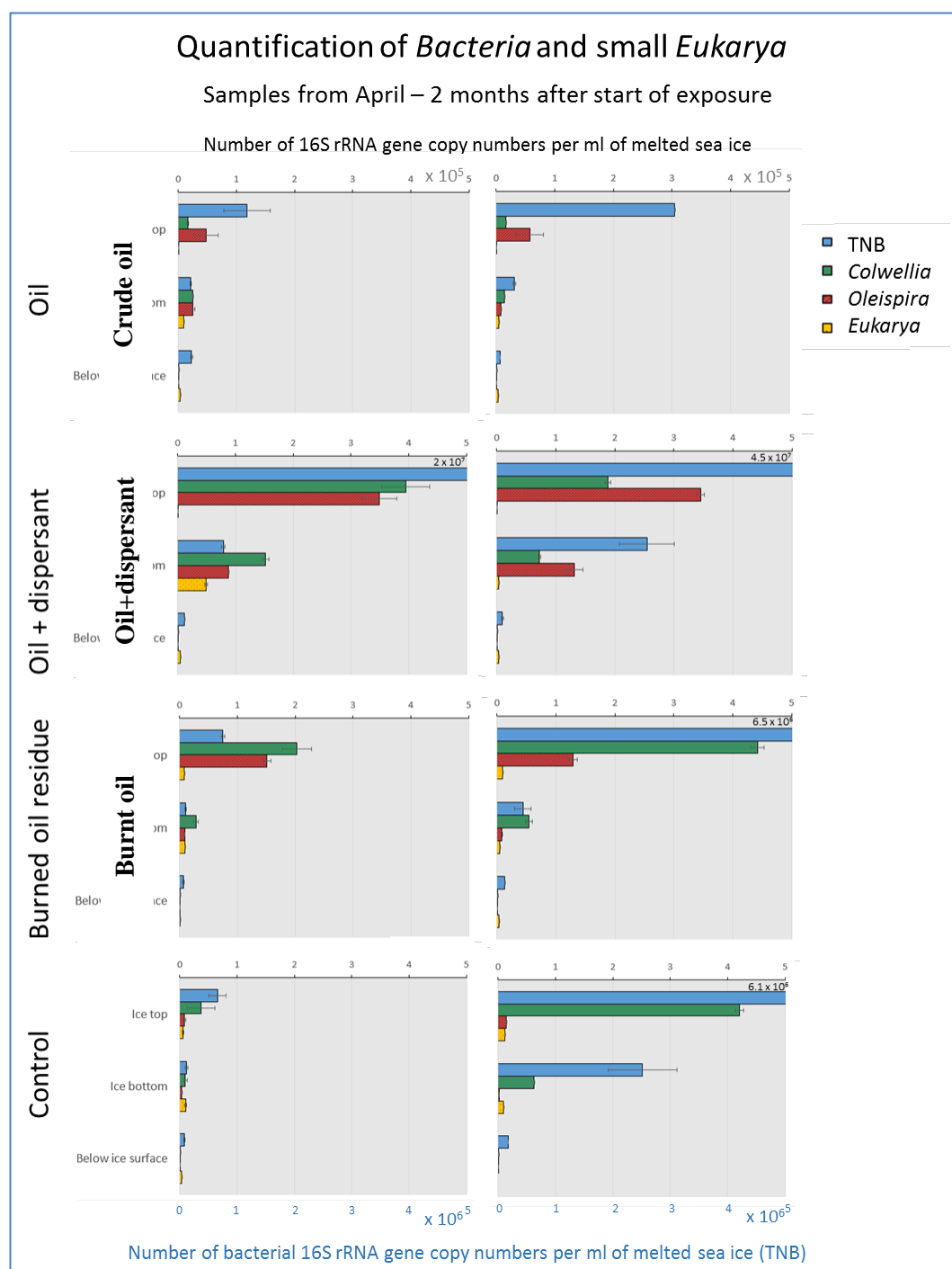


Figure 27 Quantification of the total number of bacteria (TNB), *Oleispira* and *Colwellia* genera and small *Eukarya*. Total number of 16 S rRNA gene copies of per 1 ml melted sea-ice cores from the ice top and bottom layers and in 1 ml of seawater from just below the ice surface. Results are shown here after 2 months exposure (April samples) in the crude oil, oil+ dispersants, burnt oil residue and control no treatment mesocosms. 3 distinct ice cores or water samples are used for each measurement. The error is the standard error for the measurement. NB: The TNB value is shown on a different axis due to higher numbers.

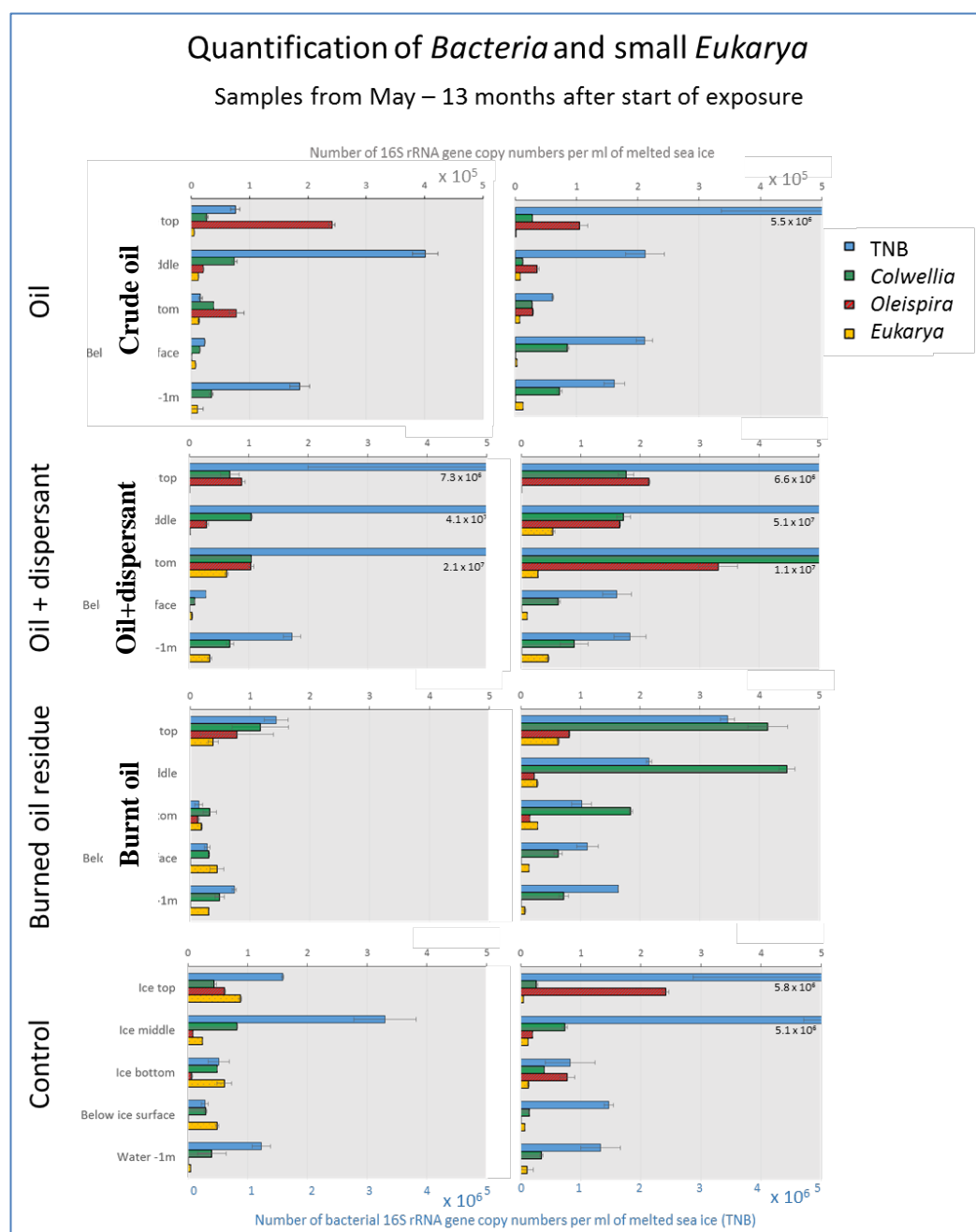


Figure 28 Quantification of the total number of bacteria (TNB), *Oleispira* and *Colwellia* genera and small *Eukarya*. Total number of 16 S rRNA gene copies of per 1 ml melted sea-ice cores from the ice top, mid section and bottom layers and in 1 ml of seawater from just below and 1m below ice surface. Results are shown here after 3 months exposure (May samples) in the crude oil, oil+dispersants, burnt oil and control no treatment mesocosms. 3 distinct ice cores or water samples are used for each measurement. The error is the standard error for the measurement. NB: The TNB value is shown on a different axis due to higher numbers.

The number of Archaea was extremely low throughout the experiment in all mesocosms and ice layers or water depths, and the results are therefore not shown here. Archaea were detected in sea-ice core samples only, with an abundance lower than 1×10^3 per mL of melted ice. In pristine samples in February (before contamination), low numbers of Archaea were found in the middle

and bottom sections of the ice cores, but never in the top layer. During March very low numbers were found in the bottom layer of the control, crude oil, and burnt oil mesocosm. During April and May, these low numbers were only detected in the bottom section of the control and burnt oil mesocosms, indicating a possible toxicity of oil on the Archaea population. Detailed analyses in this report were therefore focused on quantification and identification of bacterial populations and to a limited extend small eukaryotic organisms.

The results for the total number of bacteria, total number of *Oleispira* spp., *Colwellia* spp. and total number of small eucaryotes in February before the start of the experiment (T0) are shown in Figure 25. These analyses are the results of 3 cores and 3 water samples from each depths collected at 2 different sites within the mesocosm area. The results for the different mesocosms (2 crude oil mesocosms, 2 oil+dispersant, 2 burnt oil and 2 control mesocosms) are shown Figure 26 for March samples (1 month after exposure), Figure 27 for April samples (2 months after exposure) and Figure 28 for May samples (3 months after exposure).

Bacterial numbers in the respective ice layers and water depths are relatively stable (less than an order of magnitude variation) throughout the duration of the experiment in the crude oil, burnt oil and control mesocosms, implying that the oil and treatments do not greatly change overall number of bacteria present. Two months after oil exposure (April samples), however, bacterial numbers in the oil+dispersant mesocosms are considerably higher (10 fold) than other mesocosms. The dispersant allows both an enhanced bioavailability of the oil and may also reduce the toxicity to other microorganisms by reducing the concentration of oil in the upper layers of the ice.

In the oil+dispersant mesocosms, the bottom layers exhibit a growth in bacterial populations, suggesting a higher oil contamination and biodegradation through the ice layer in this treatment compared to crude oil or burnt oil (Figure 31).

The quantification of eukaryotes show an increase of these organisms in the control and burnt oil mesocosms in the top ice-layer, but not in the crude oil and oil+dispersant, suggesting a toxic effect of the oil. This effect is seen to a lesser extent in the top ice layer.

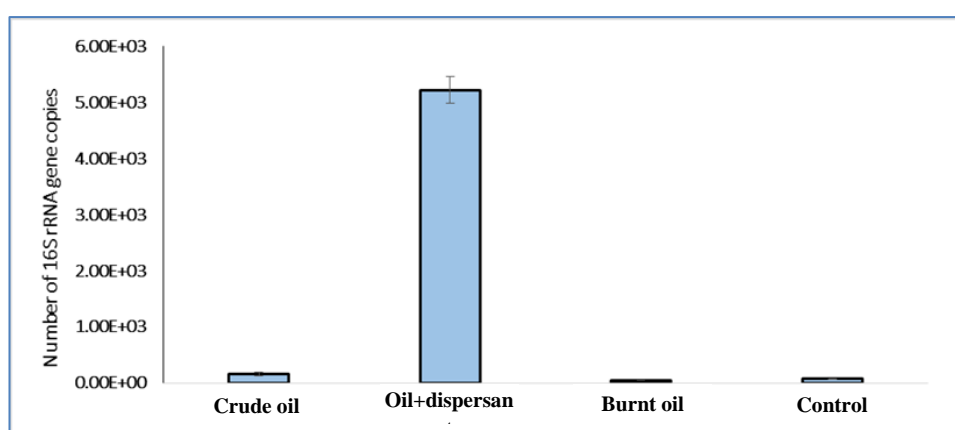


Figure 29 Quantification of *Oleispira* (total number of bacterial 16S rRNA gene copies per 1ml seawater) under the sea-ice layer, Samples from May, 3 months after exposure in the control, crude oil, oil+dispersant and burnt oil mesocosms.

3.4.3 Active microbial communities after exposure to crude oil, oil+dispersant or burnt oil

The activity of the different microorganisms was investigated by specific gene quantification on total RNA extracted from samples collected.

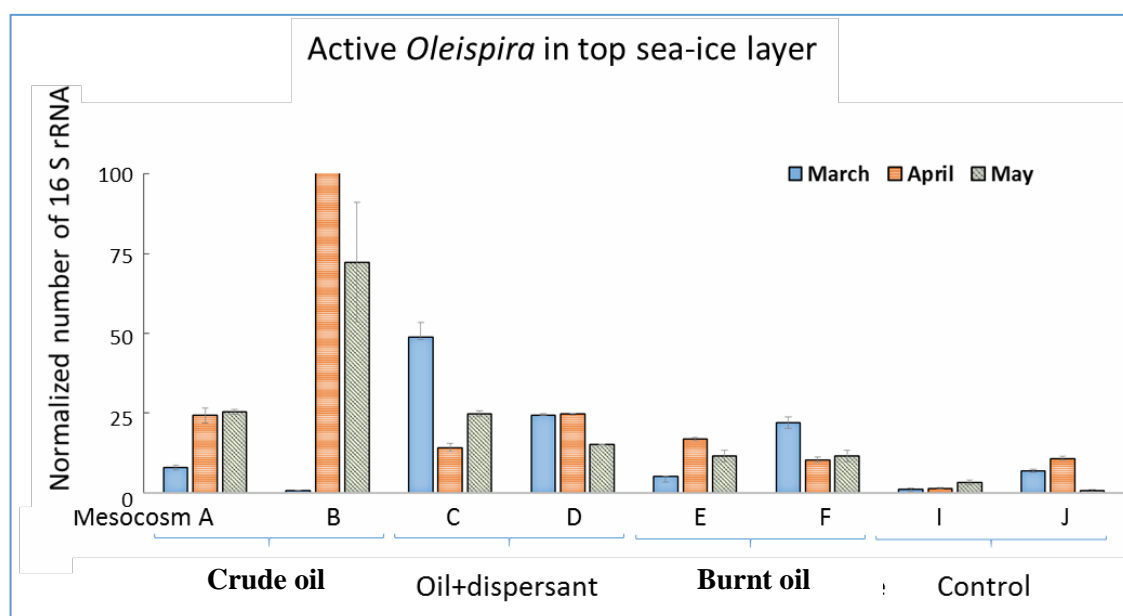


Figure 30 Normalized number of metabolically active *Oleispira* in the top 20cm ice layer from different treatments (Crude oil, oil+dispersant, burnt oil) and control mesocosms. Quantification of *Oleispira* 16S rRNA on total RNA extracted from 3 different ice-cores for each mesocosm 1, 2 and 3 months after start of exposure (March, April and May). Error bar is the standard error.

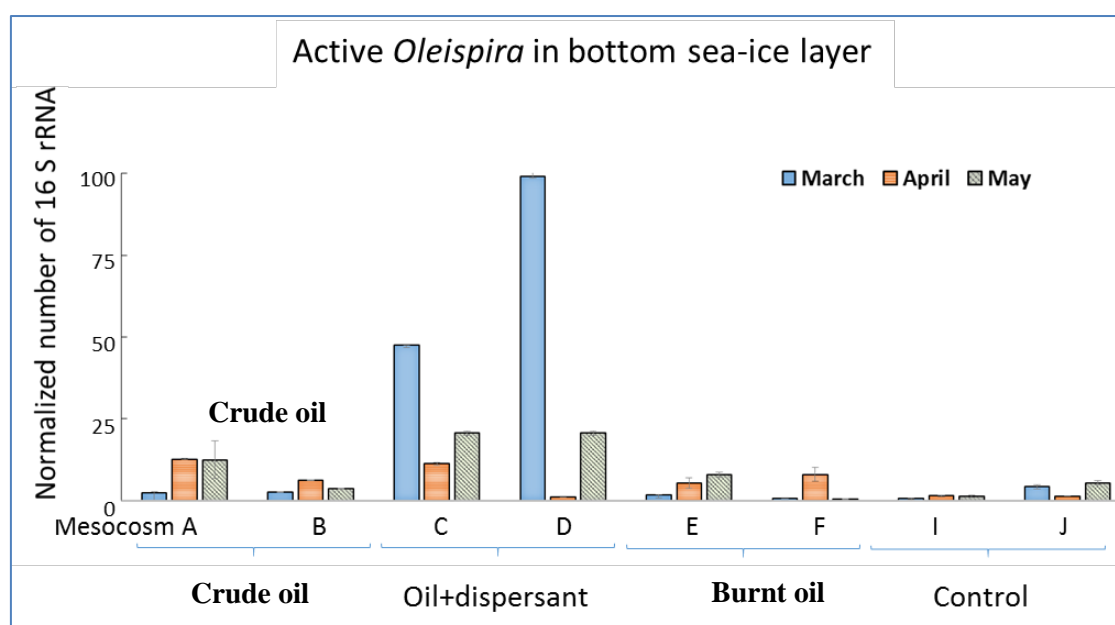


Figure 31 Normalized number of metabolically active *Oleispira* in the bottom 20cm of ice from different treatments (crude oil, oil+dispersant, burnt oil) and control mesocosms. Quantification of *Oleispira* 16S

rRNA on total RNA extracted from 3 different ice-cores for each mesocosm 1, 2 and 3 months after start of exposure (March, April and May). Error bar is the standard error.

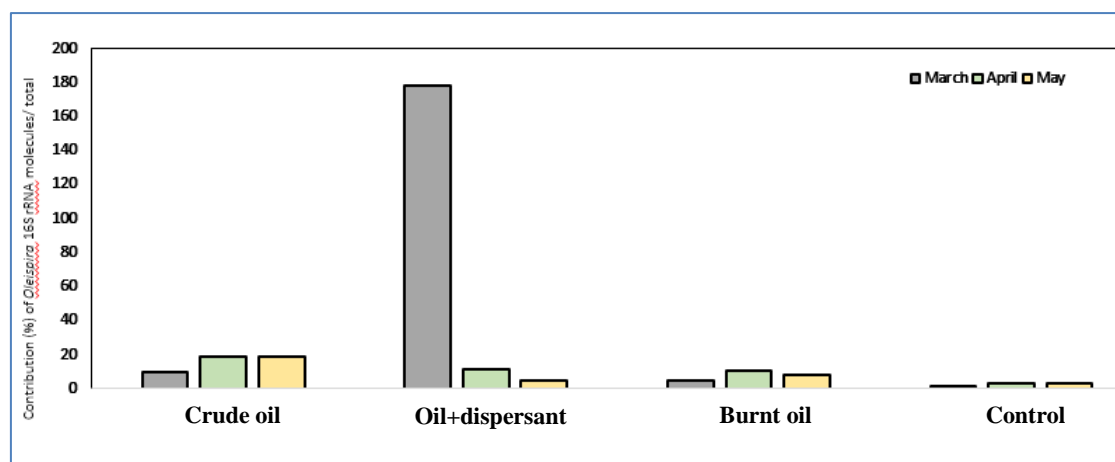


Figure 32 Contribution of metabolically active *Oleispira* in total active microorganisms. Quantification of *Oleispira* 16S rRNA on total RNA extracted from ice-cores from the top layer sea-ice in the control and different treatment mesocosms, 1,2 and 3 months after exposure (March, April and May).

Results show that *Oleispira* is present in the sea ice in Svea in very low numbers (of order 10^3 per mL of melted sea ice). Within the first month following the oil spill (March samples), these organisms become more dominant in both the crude oil and the oil+dispersant contaminated mesocosms (more than 10-fold increase), and to a lesser extent in the burnt oil treatment (2two-fold increase) (Figure 31). In the second month of exposure, *Oleispira* become much more abundant (100-fold) in the oil+dispersant mesocosms, suggesting the oil may be more bioavailable to these organisms, allowing the oil degrading community to be more active and grow faster.

The results from the bottom of the ice-core show an enhanced bioavailability and degradation of the oil in the oil+dispersant mesocosms compared to the other mesocosms (Figure 32).

3.5 Bacterial community analysis in the mesocosm experiment

The total environmental bacterial communities were investigated on the basis of 16S rDNA 454 pyrosequencing and identification of the organisms present, following the protocols detailed in section 2. The sequencing was performed on both PCR products from DNA (all organisms present) and cDNA made from total RNA (only active organisms) extractions. Samples from 3 different ice cores or seawater samples were pooled for each sequencing analysis, to get a more accurate representation of the environment.

As for the analysis of the quantification of different organisms described in the previous section, sea-ice and seawater samples for total bacterial community analysis were collected from two sites in February just before the installation of the mesocosms, to get information on the environments and bacteria present before the start of the different exposures. Samples were then collected from the control non contaminated, crude oil contaminated, oil+dispersant and burnt oil

mesocosms, in March, April and May, respectively 1,2 and 3 months after the start of the exposure.

The results are presented showing the contribution of different bacterial families, sometimes regrouping them into orders, or detailing into genera when they were particularly abundant. Results from the sea-ice layer and the seawater are shown on different figures to be able to highlight different organisms as the community structures in there compartments are very different. Clearly, Arctic petroleum-degrading microorganisms were detected and this result is in accordance with the scientific litterature (McFarlin et al., 2014).

3.5.1 Bacterial community structure in the pristine arctic environment before treatments

The results for the total bacterial community analysis for control samples collected before the start of the experiment in February (before installing the mesocosms or performing the exposures) are shown in Figure 33 for the different ice layers (top 20cm, middle 20cm section, and bottom 20cm of the sea ice) and Figure 34 for the different depths of seawater (-1m or right below the sea ice, 5m, 10m and 25m depths).

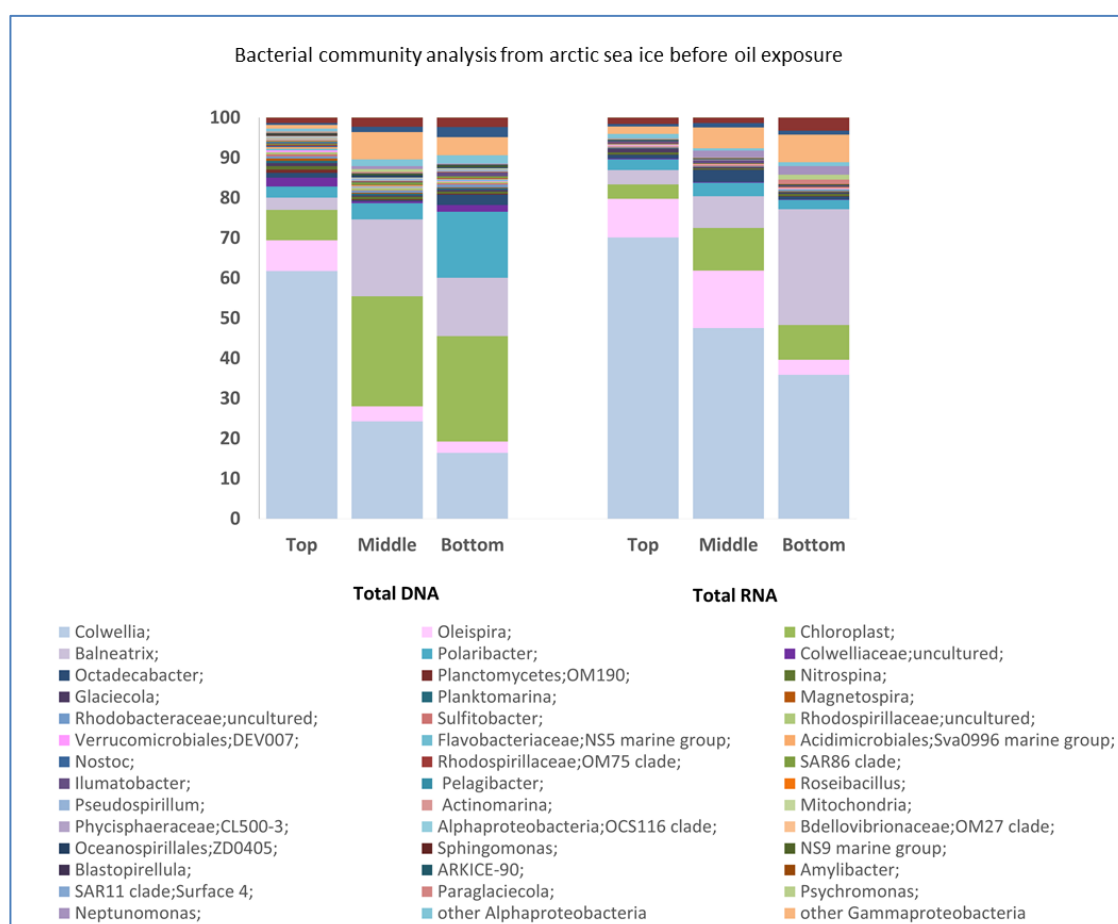


Figure 33 Microbial community analysis (based on 16S rRNA gene sequencing by 454 pyrosequencing) from total DNA and RNA (metabolically active population). Sea-ice samples (from the top, middle and bottom 20cm sections of ice cores) collected from the pristine environment before the start of the mesocosm exposure experiment. Each analysis originates from the pooling of 3 distinct cores.

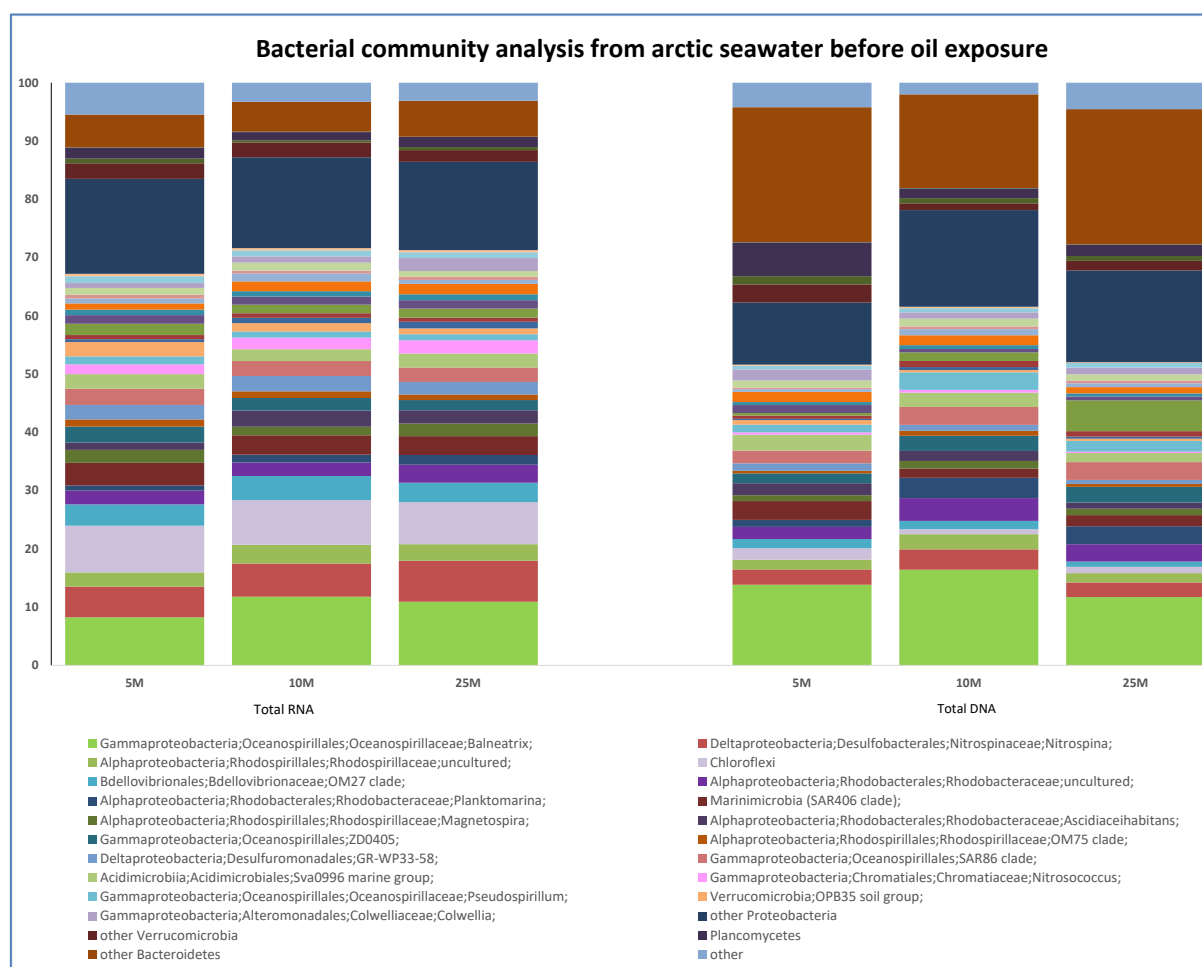


Figure 34 Microbial community analysis (based on 16S rRNA gene sequencing by 454 pyrosequencing) from total DNA and RNA (metabolically active population). Seawater samples (from 5, 10 and 25m depths) collected from the pristine environment before the start of the mesocosm exposure experiment. Each analysis originates from the pooling of 3 distinct samples.

In all samples, the Gammaproteobacteria (amongst which are found the genera *Colwellia*, *Oleispira*, *Balneatrix*), Alphaproteobacteria, and Flavobacteria (amongst which the genus *Polaribacter*) composed most of the bacterial communities in sea-ice and seawater. Among these, Gammaproteobacteria (dominated by bacteria from the genera *Colwellia*) were the most abundant in the sea-ice layer, particularly in the top section (with more than 60 of the total community from this genus). The activity of the organisms (community from RNA analysis) was found to be very dominated by *Colwellia* in the whole sea-ice layer.

The results show changes in the bacterial community structure through the ice layer depth, towards a more diverse community at lower depth. The seawater bacterial community was found to be much more diverse, with only few changes with water depth.

Oleispira organisms were found at levels higher than expected from Arctic environmental samples (Krolicka et al, article in prep), *Eukarya* were found in lower abundance in the top and middle sections of the sea-ice layers than in the bottom of the ice layer of water column.

3.5.2 Bacterial community structure during exposure to crude oil, oil+dispersant or burnt oil

The results for the total bacterial community analysis in the top and bottom of the ice layer in the control, oil, oil + dispersant and burned oil residue mesocosms in March, April and May are shown in Figure 35 (RNA) and Figure 36 (DNA).

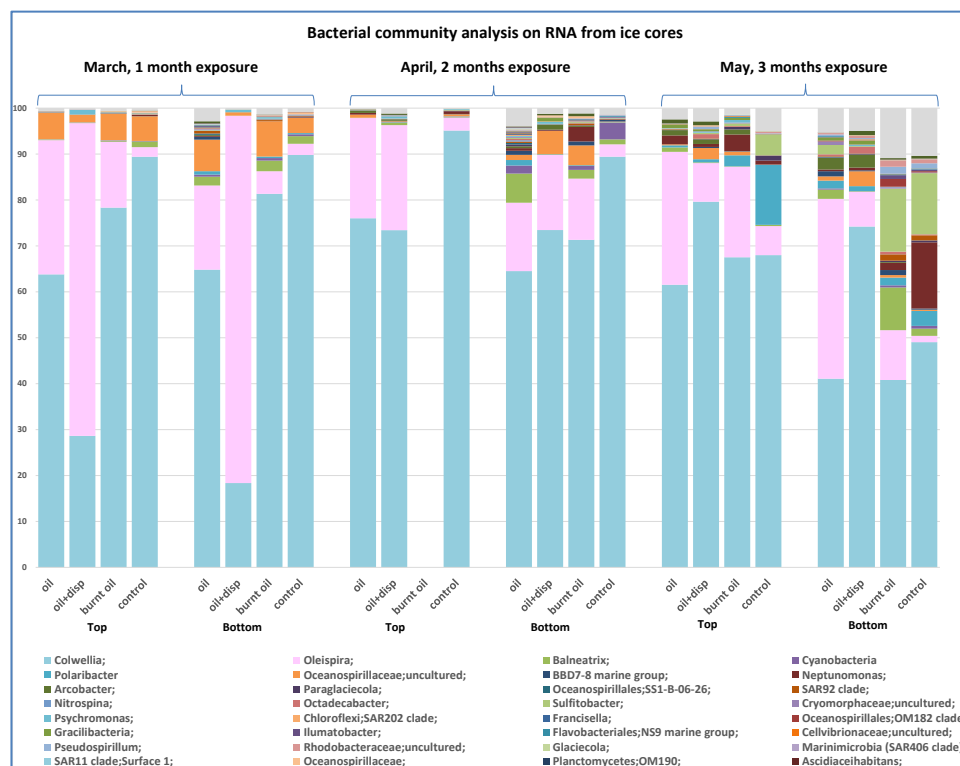


Figure 35 Microbial community analysis (based on 16S rRNA gene sequencing by 454 pyrosequencing) from total RNA (metabolically active population). Sea-ice samples (top and bottom of ice layer) collected from the oil, oil+dispersant, burned oil residue and control, collected 1, 2 and 3 months after the start of the exposure (March, April and May). Each analysis originates from the pooling of 3 distinct samples.

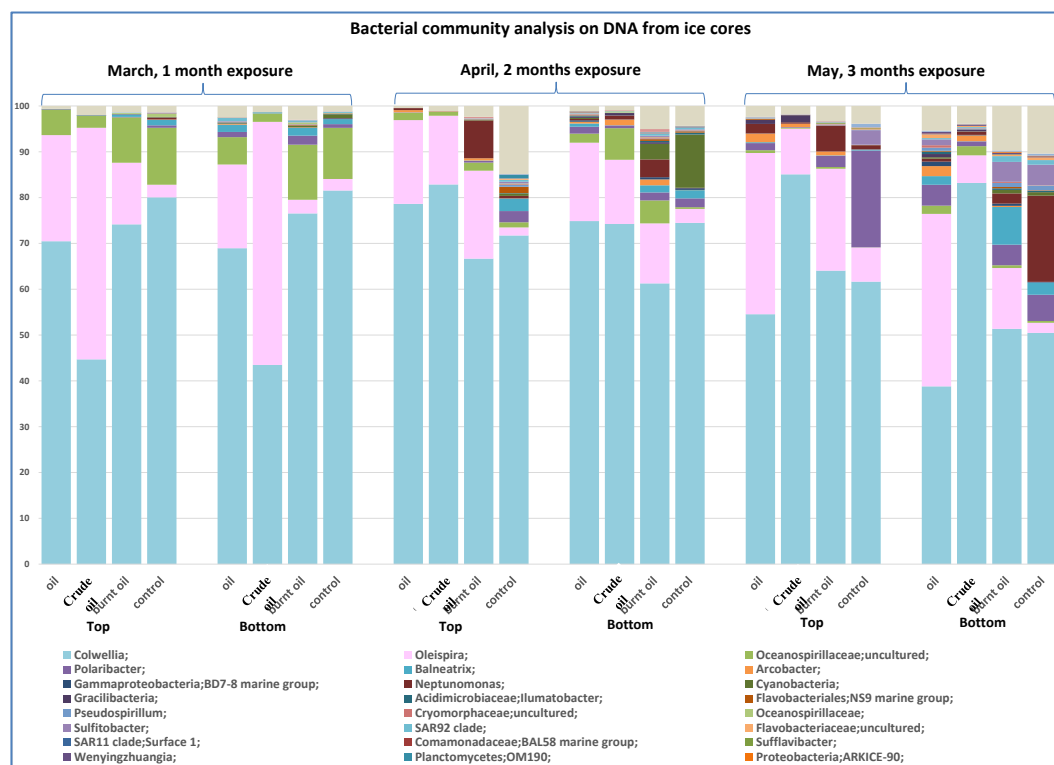


Figure 36 Microbial community analysis (based on 16S rRNA gene sequencing by 454 pyrosequencing) from total DNA. Sea-ice samples (top and bottom of ice layer) collected from the crude oil, oil+dispersant, burnt oil and control, collected 1, 2 and 3 months after the start of the exposure (March, April and May). Each analysis originates from the pooling of 3 distinct samples.

As for the samples from February, the Gammaproteobacteria (amongst which are found the genera *Colwellia*, *Oleispira*, *Balneatrix*), Alphaproteobacteria, and Flavobacteria (amongst which the genus *Polaribacter*) composed most of the bacterial communities in sea-ice and seawater. Among these, bacteria from the genera *Colwellia* were found to be the most abundant.

The bacterial community was found to be more diverse in the bottom section of the ice layer, and increased over time in all mesocosm. The community was found to be less diverse in the oil treatments than in the controls (particularly with the addition of dispersant, and to a lesser extent in the burnt oil mesocosm). *Oleispira* organisms, which have been found to be able to degrade oil are found in much higher abundance in all oil exposures and treatments. In the oil+dispersant treatments, *Oleispira* are found in high abundance (more than 50% of the total community) within the 1st month of exposure. In the crude oil mesocosm, the bacterial community changed more progressively, to reach more than 30% *Oleispira* in May (3 months after the start of the exposure).

In the bottom section of the ice cores only small differences are visible between the control and the burnt oil mesocosm.

The results for the total bacterial community analysis in the seawater collected just below the sea-ice layer in the control and oil+dispersant mesocosms in May (3 months after exposure) are shown in Figure 37.

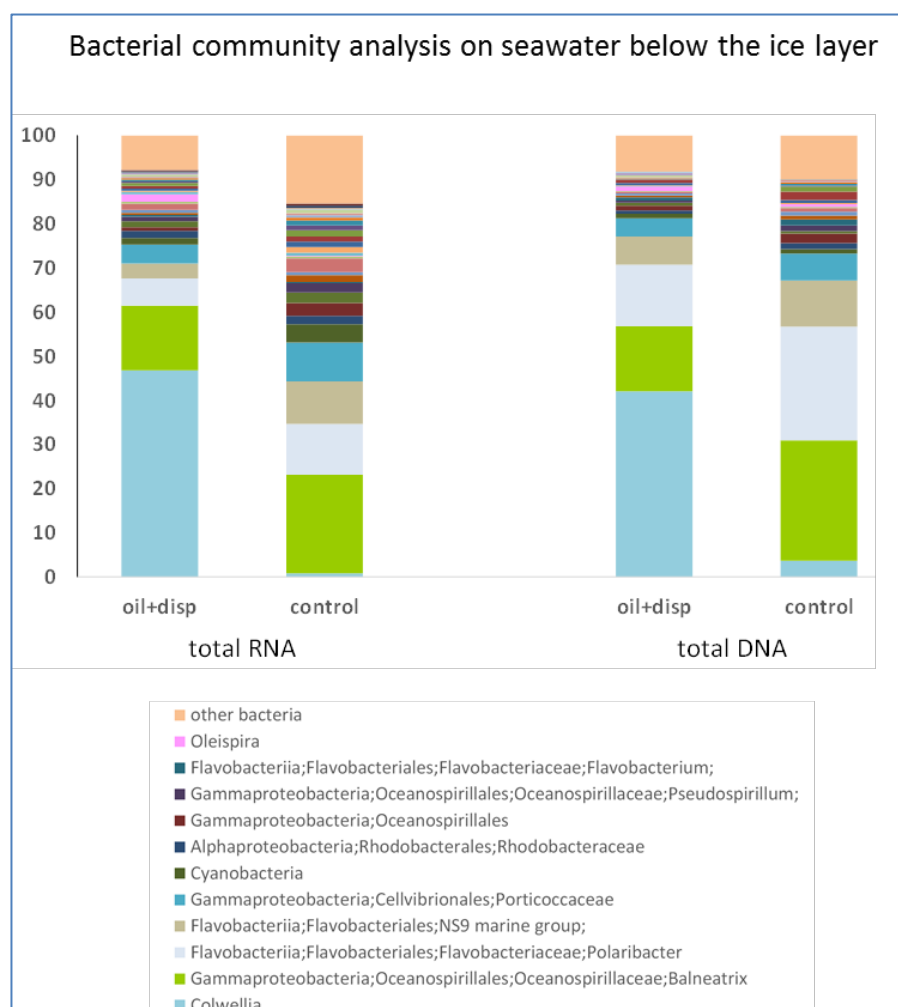


Figure 37 Microbial community analysis (based on 16S rRNA gene sequencing by 454 pyrosequencing) from total DNA and total RNA (metabolically active population). Seawater samples collected from just below the sea-ice layer in the control and oil+dispersant mesocosms. Each analysis originates from the pooling of 3 distinct samples. Bacterial genera representing more than 2% of the total population are detailed in the caption. 'Other bacteria' comprise of genera present at less than 1% of the population.

The samples collected bellow the ice layer from the oil + dispersant exhibited a lower bacterial community diversity than in the control mesocosms. Moreover, a much higher abundance of *Colwellia* organisms were found, as well as a higher *Oleispira* activity. Previous work by Liv Guri Faksness (Brakstad et al., 2008) investigating the presence of oil compounds beneath the ice and they showed very low concentrations of hydrocarbons below the ice.

4 RESULTS AND DISCUSSION ON SHORT-TERM INCUBATION EXPERIMENTS

During the April (T2) and May (T3) sampling campaigns, short-term incubation experiments with melted sea ice and with seawater were conducted to determine microbial activity and hydrocarbon degradation potential. During both incubation periods, the ice thickness at the incubation sites was 50 – 70 cm. The air temperature recorded at a nearby weather station is shown in Figure 38 (Svea airport weather station; data from www.yr.no/sted/Norge/Svalbard/Sveagruva_målestasjon/). During both periods the temperature was mostly below 0 °C, with short periods above freezing temperature. The seawater temperature as recorded by temperature loggers attached to the incubation boxes was rather constant around -1.8 °C.

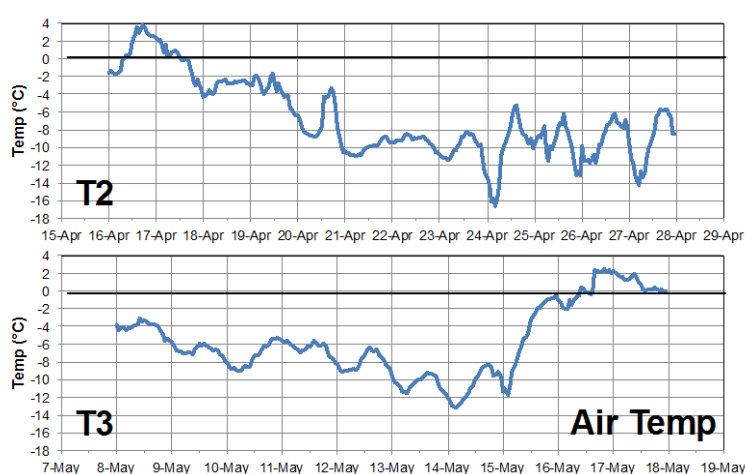


Figure 38 Air temperature during the two incubation period at Svea airport. Incubation at T2 started on 4/16/15. The incubation at T3 started on 5/8/15.

4.1 Microbial Abundance in ice and water samples

The abundance of bacteria in sea ice and seawater was determined before the start of the incubation (Figure 39). For the control mesocosm, the bacterial abundance was similar in the water and the ice, and the abundance slightly increased from April to May. For the oiled mesocosm and the burnt oil, the microbial abundances were generally slightly higher than in the control, but did not significantly increase from April to May. Again, the abundances in the water and ice were comparable. In contrast, the April oil+dispersant treatment showed a significantly higher bacterial abundance in the ice as compared to the underlying seawater. This abundance was also higher than in the ice layer of the other treatments.

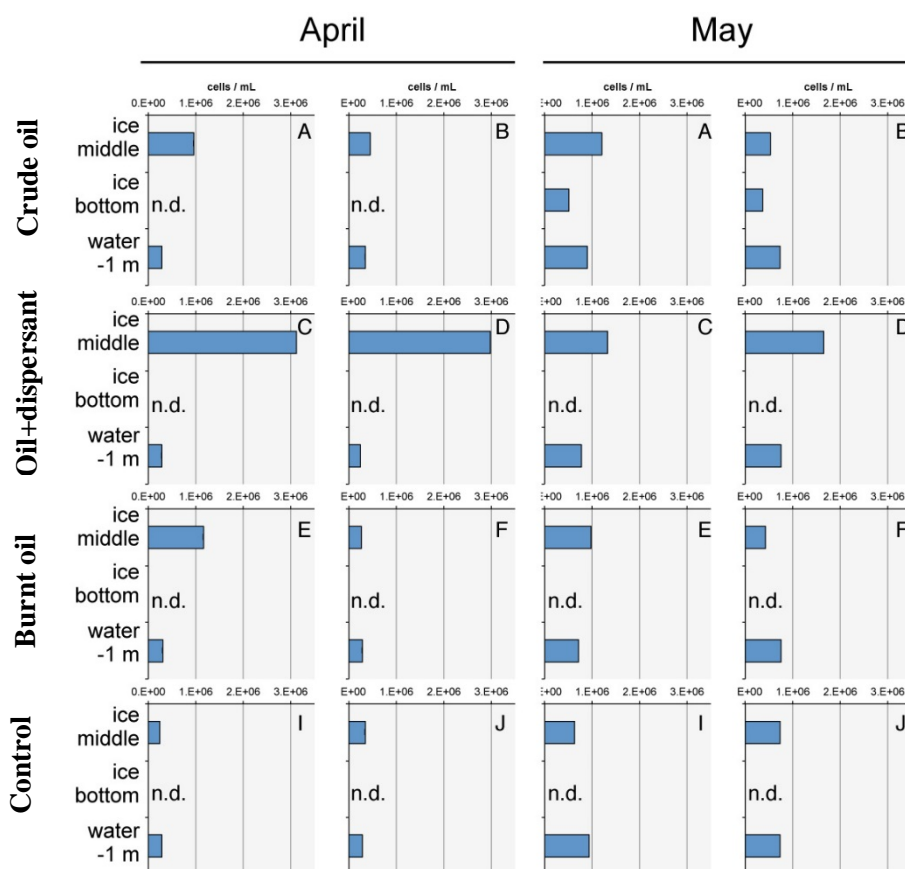


Figure 39 Bacterial abundance in sea ice and water samples as measured by flow cytometry.

4.2 Microbial growth and oxygen consumption

The bacterial abundance was measured during the 10- to 20-day incubation during both sampling campaigns. The following four observations were made. First, an increase of bacteria was observed in all treatments (Figure 40). Second, bacterial growth was observed both in incubation where oil was added (as additional carbon source) as well as in incubation where no additional oil was amended. This signifies that even without added hydrocarbons, dissolved organic matter or dissolved hydrocarbons present in the seawater or melted ice can serve as a carbon source to support bacterial growth. The growth of bacteria might also have been facilitated by the absence of a major phytoplankton fraction, which was removed through filtration before the incubation (using a 0.8 μ m filter). A third observation is that the growth rate for the ice samples increased from April to May, whereas it remained approximately constant in the seawater. Lastly, it was observed that the oil+ dispersant treatment experienced no significant growth during the incubation experiment in the ice layer in April, but similar growth during the incubation experiment as the other treatments in May.

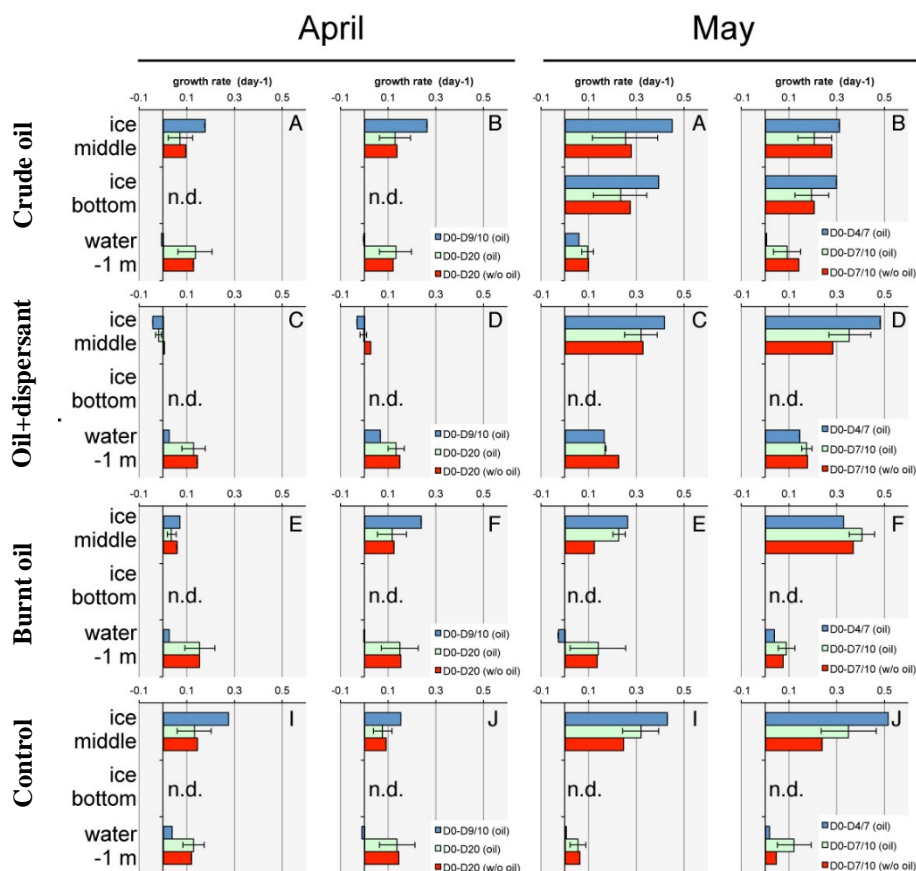


Figure 40 Bacterial growth rates (in day⁻¹) fitted for exponential growth determined in incubation experiments with melted ice and water below the ice. The blue and green bars represent incubations performed over two incubation periods with added oil, whereas the red bars represent incubations without added oil. The bottom ice section was only investigated in May and only in the oiled treatment.

The growth of bacteria was also accompanied by oxygen consumption (Figure 41). The following three observations can be made: First, more oxygen consumption occurred in April than in May. Second, oxygen consumption was higher for bacteria from seawater than for bacteria from ice. Third, no significant difference in oxygen consumption rate was observed between treatments that have been amended with oil as compared to treatment that were not amended. These observations suggest that bacteria from sea ice and seawater are very versatile and can use a multitude of substrates (such as dissolved organic carbon or petroleum) for growth.

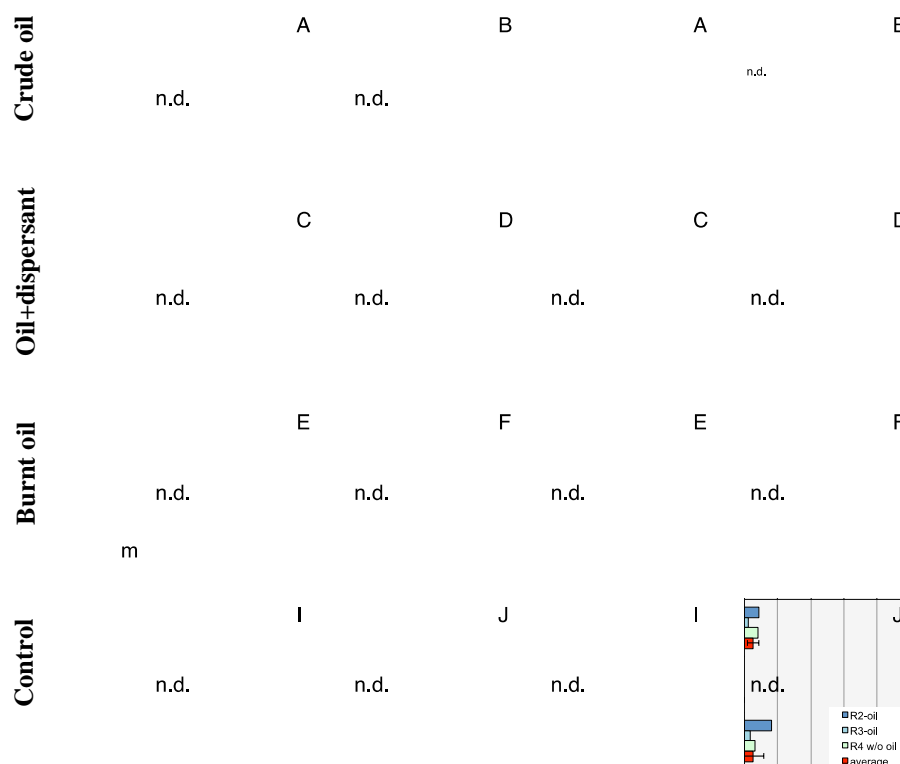


Figure 41 Oxygen consumption rates (in $\text{pmol O}_2 \text{ day}^{-1} \text{ cell}^{-1}$) determined in incubation experiments with melted ice and water below the ice.

4.3 Naphthalene degradation rates in short-term incubation experiments

The hydrocarbon depletion relative to a native, recalcitrant petroleum compound (hopane) was quantified during the incubation experiments. A degradation of various hydrocarbons was indeed observed during the experiments: a small (<10%) but significant degradation of naphthalene and its alkylated congeners, fluorene, phenanthrene and dibenzothiophene was observed after just 7 days of incubation at seawater temperature (-1.8°C). This preferential degradation of non-alkylated parent PAHs is clearly indicative of biodegradation and was not caused by evaporation or dissolution effects, as confirmed by analysis of sterile controls. Furthermore, cell growth (Figure 40) and oxygen consumption (Figure 41) was observed in all incubations. Together, these findings strongly support the hypothesis that bacteria present in sea-ice are able to degrade petroleum hydrocarbons at seawater temperatures during a relatively short incubation period.

To systematically investigate the effect of mesocosms treatment (crude oil, oil+dispersant, burnt oil), we calculated first-order degradation rates for naphthalene as a representative PAH (Figure 42). Interestingly, naphthalene degradation was observed in all treatments, even in samples from the control mesocosms. This signifies that bacteria present in sea-ice have the ability to quickly respond to the presence of hydrocarbons, and degrade them.

We also determined degradation rates for seawater collected from the mesocosms (Figure 42). For the April incubations, similar degradation rates were observed in incubations prepared from

sea-ice as compared to incubation prepared from seawater. Note that for the May incubation, analytical challenges prevented us from calculating meaningful degradation for all but one seawater incubation.

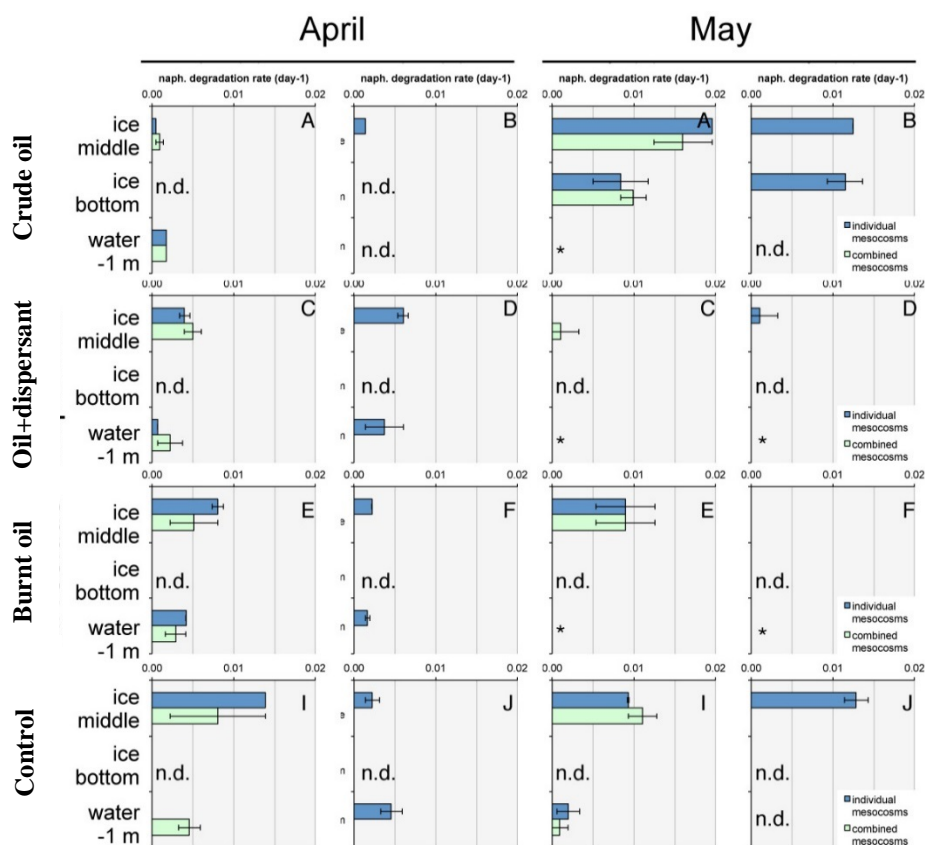


Figure 42 First order naphthalene degradation rate constants (day⁻¹) determined in incubation experiments. An asterisk (*) denotes negative degradation rates caused by analytical difficulties.

5 RESULTS AND DISCUSSION ON BIOFILM ON TILES EXPERIMENT

Tiles coated with oil and control tiles were incubated in Arctic seawater just below the sea-ice. Chemical analysis of the oil as well as characterisation of the microbial biofilm formations were performed at different time intervals (1, 2 and 3 months) on 9 tiles per time point.

5.1 Results and discussion from the chemical analysis from tiles

5.1.1 Chemical analyses

For the chemistry, the same approach as the one used for the MCL has been chosen to present data obtained for tiles experiment. First, results on alkanes are presented and, secondly, those obtained with the aromatic fraction.

Alkanes. Results show a significant decrease in nC10-nC14 group of alkanes during time but not for the heaviest groups (Figure 43). This decrease implies a lost of the lightest oil compounds due to weathering processes.

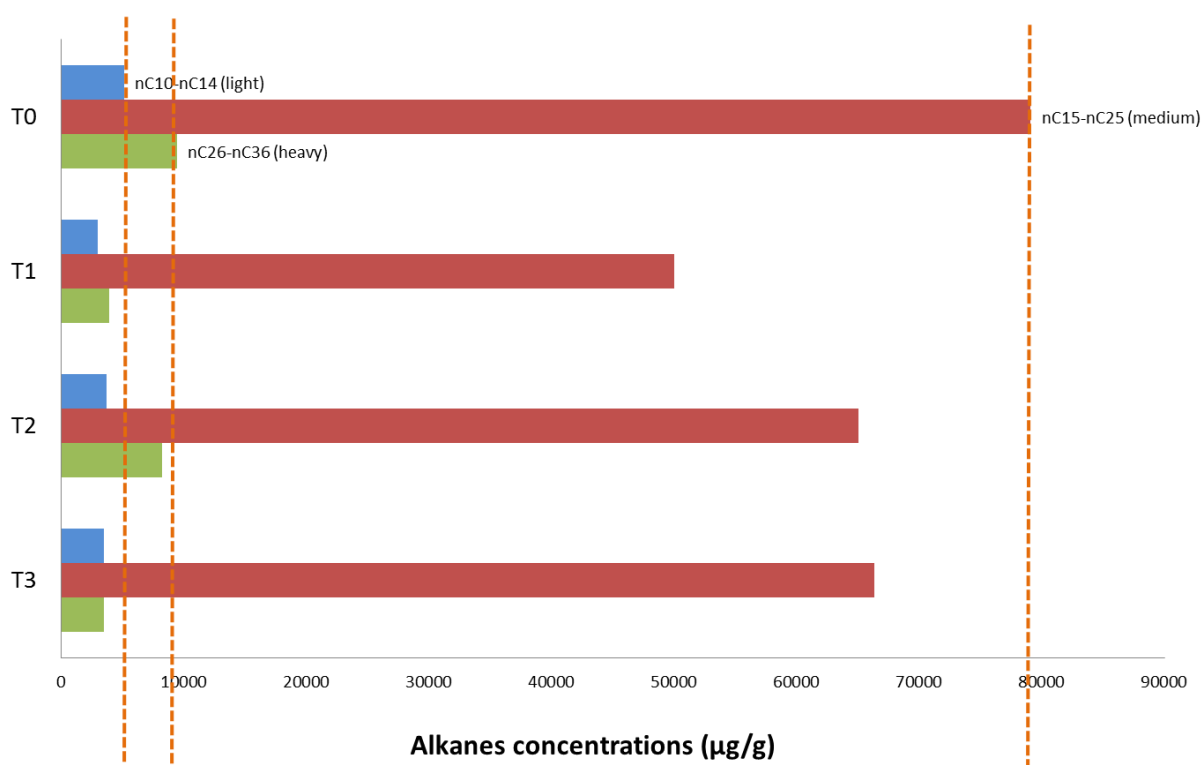


Figure 43 Concentrations of the 3 groups of alkanes during time on tiles.

The same trend, than for the nC10-nC14 group of alkanes, is observed with nC₁₇/pristane and nC₁₈/phytane ratios which demonstrate that biodegradation processes occurred at the tiles surface (Figure 44).

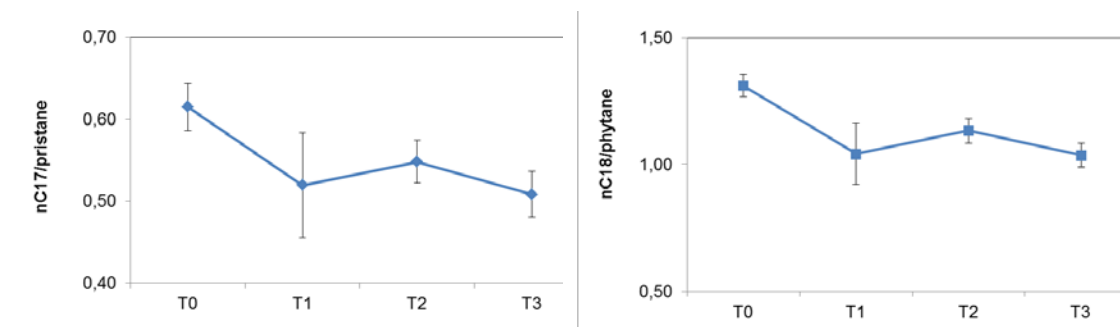


Figure 44 Variation of nC17/pristane and nC18/phytane ratios during time for oil at the tiles surface

Aromatics. The C1-fluo-pyrene/C4-phen and the Phen/C4-Phen ratios are used to follow, respectively, photooxydation and dissolution processes. These processes were not significant as no trend is clearly observable; both ratios are stable during time (Figure 45).

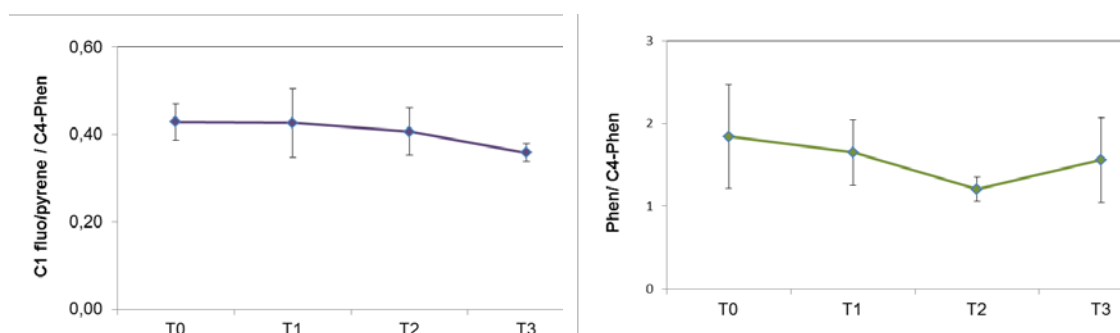


Figure 45 Evolution of C1-fluo-pyrene/C4-phen and Phen/C4-Phen ratios during time in oil at the tiles surface

Concerning the chemical nature of aromatics, no significant trend is observed: the Light, Medium and heavy fractions followed the same trend (Figure 46).

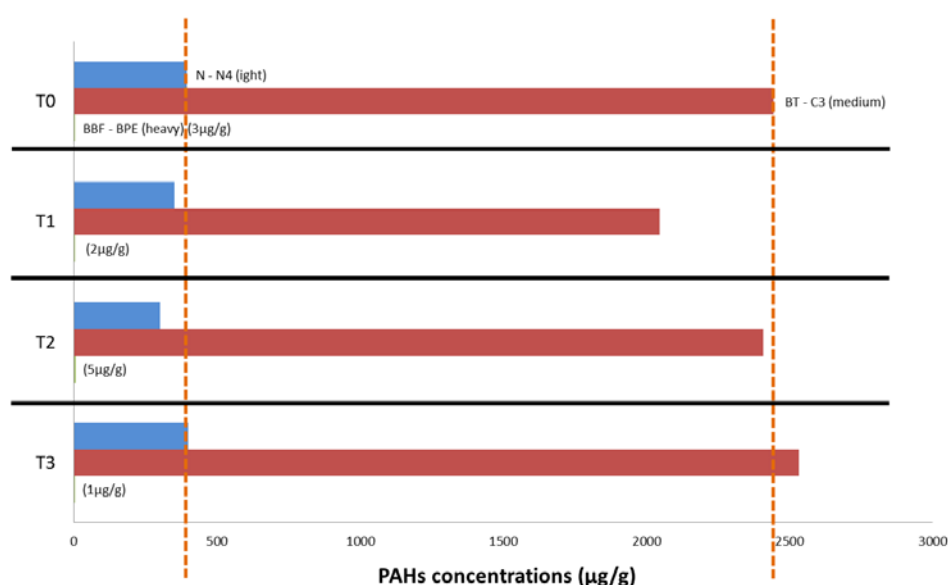


Figure 46 Evolution of the aromatic fractions of oil extracted from tiles with time

5.2 Results and discussion from the microbial analysis from tiles

Pristine and oil coated tiles were incubated in Arctic seawater just below the sea-ice to investigate the fate of the oil and biodegradation on rock surfaces. For the microbial analysis, 3 pristine non-contaminated tiles and 3 oil-coated tiles were collected after 1, 2 and 3 months incubation time. Biofilms were collected according to material and methods section 3.5. The microbial communities from the biofilm formations on tiles were investigated by extracting the total DNA (organisms present) and RNA (active portion of the community) from the biofilm samples collected.

5.2.1 Microbial biomass, microbial activity and oil degraders from biofilms on tiles

The total number of bacteria, *Colwellia* and *Oleispira* genera, as well as Eukaryotes were quantified by qPCR with appropriate assays and standards. The results are shown in Figure 47. The numbers are expressed as gene copy numbers per cm² of tile biofilm.

Less than 500 gene copy numbers of total bacteria were found in biofilms in non-contaminated tiles amongst which less than 0,01% were *Oleispira* organisms. These numbers went up to 1000 gene copies for the total bacteria, which was still less than 2 orders of magnitude that of oiled tiles. The number of *Eukarya* followed the same trend.

Tiles coated with oil before incubation were, after 1 month exposure, already heavily covered in a microbial biofilm, with $6-15 \times 10^4$ gene copy numbers per cm² of tile found in the 3 samples analysed. A high number of *Oleispira* organisms were also detected, making up to half the total microbial communities, and 7 order of magnitudes higher than in control tiles.

Over time, the number of bacterial and *Oleispira* detected diminished to less than a third of those detected in March, but were still more than 3 orders of magnitudes higher than for controls for total number of bacteria, *Oleispira* genera, as well as for number of small Eukaryotes.

The number of small eucaryotes detected increased over time during the experiment, with most of the increase taking place during the last month of incubation (3 months after the start of the exposure to oil) in contaminated and non contaminated surface biofilms, but with still 2 order of magnitude higher numbers in oil contaminated tiles (Figure 48).

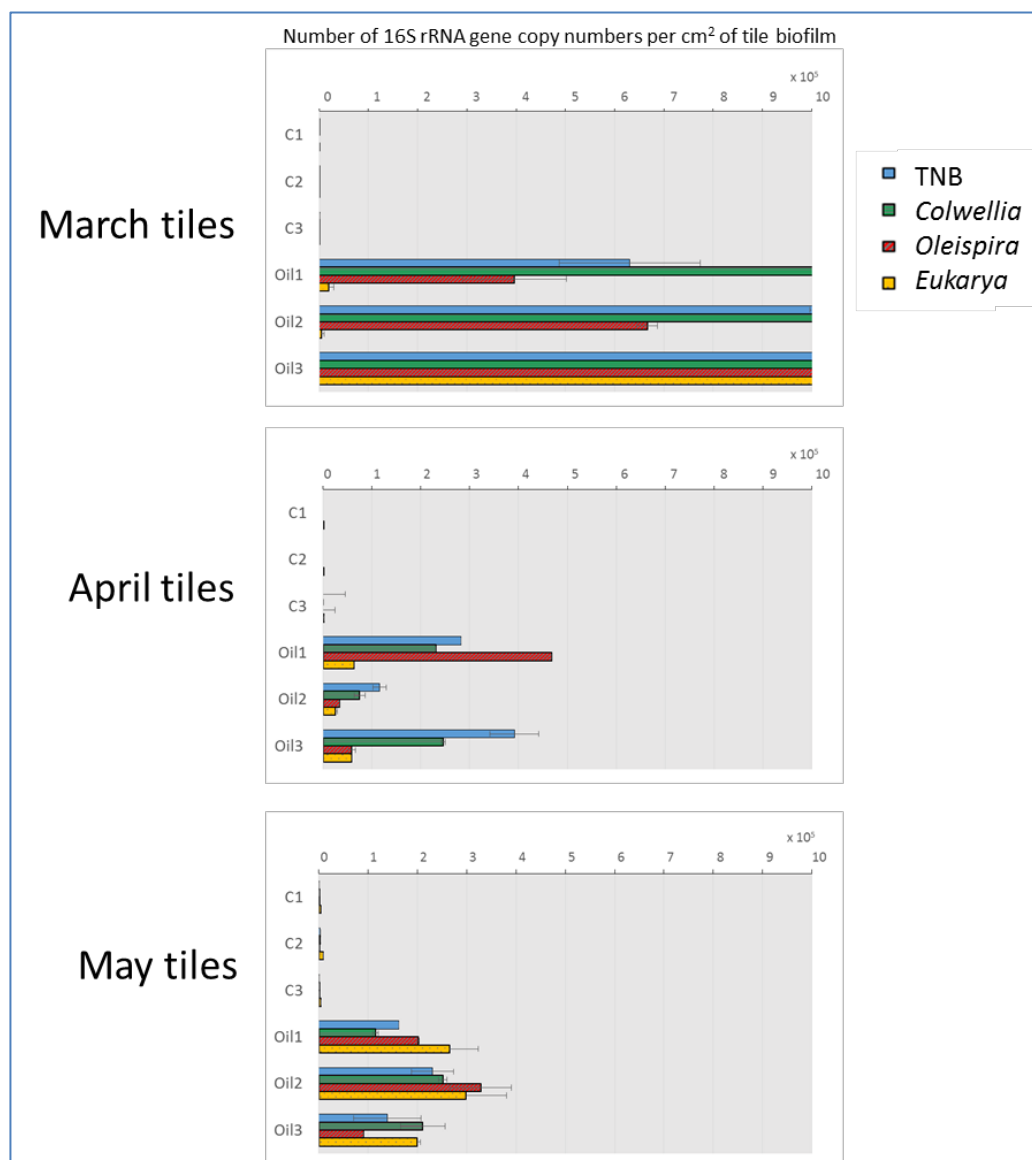


Figure 47 Quantification of total bacteria (TNB), *Colwellia* and *Oleispira* genera and small eukaryotes (expressed as total number of 16S rRNA gene copies) in biofilms extracted from 3 control non-oiled tiles (C1 to C3) and 3 oil-coated tiles (Oil1 to Oil3) 1, 2 and 3 months after exposure (respectively March, April and May). Error bars are the standard error between measurements. Analysis done by qPCR quantifications on total DNA.

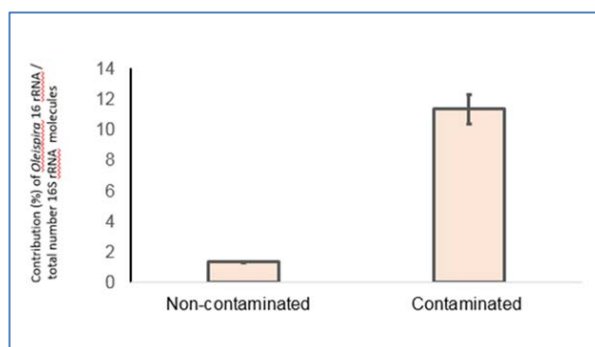


Figure 48 Contribution of metabolically active *Oleispira* in the total active bacterial populations in biofilms extracted from 3 contaminated tiles and 3 non contaminated tiles. Analysis done by qPCR quantification on total RNA.

The results clearly show that the biofilms collected from oil contaminated surface are highly enriched in oil degrading microorganisms and communities and that these are active.

5.2.2 Total Bacterial community analysis

The total bacterial community of biofilm formations on tiles were investigated by extracting the total DNA and RNA from biofilms formed on 2 oiled and 2 non-oiled (control) tiles. 16S rDNA 464 pyrosequencing was performed and the sequences obtained were identified (see material and methods Section). The results are shown in Figure 49.

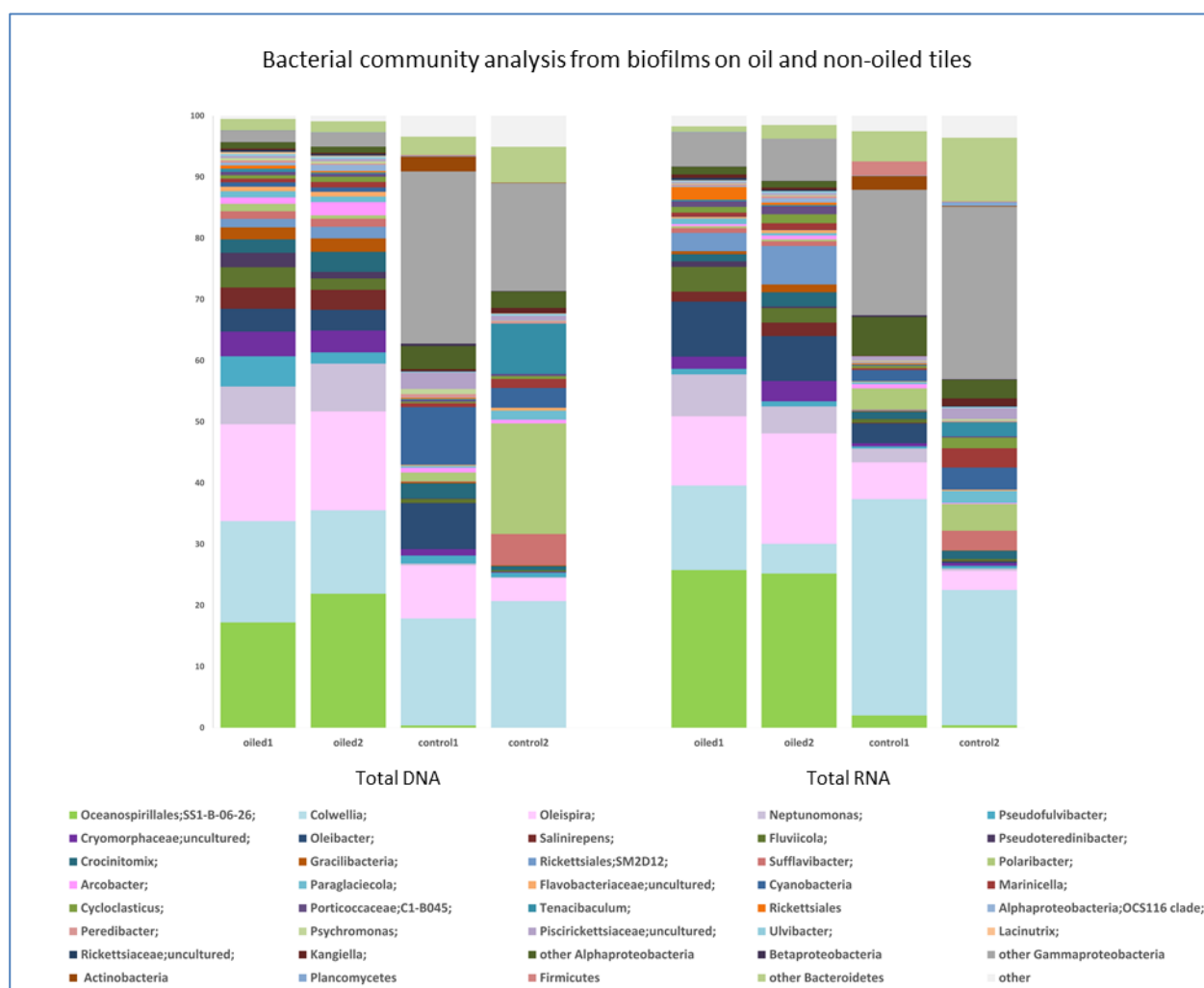


Figure 49 Bacterial community analysis (based on 16S rRNA gene sequencing by 454 pyrosequencing) from total DNA and RNA (metabolically active organisms) in biofilms extracted from 2 control non-oiled tiles (Control1 and 2) and 2 oil-coated tiles (Oiled1 and 2). This analysis was done 3 months after exposure (May). Each analysis originates from the pooling of 3 distinct samples.

The results show a high bacterial diversity in the biofilm samples from both the pristine and oil contaminated biofilms. A high proportion of the *Colwellia* genus is found in the non oil contaminated samples, with them representing approximately 20% of the total bacterial community and 30% of the active portion of the population (analysis performed on total RNA), more than twice the numbers observed in oil contaminated samples.

In oil contaminated samples, the order of the Oceanospirillales represent more than 45% of the total DNA and 55% of the total RNA of the samples (more than twice the portion of these organisms seen in pristine samples). Amongst these, the *Oleispira* genus represents more than 15% of the total or active population, which is approximately 3 fold that of non-contaminated biofilm samples.

6 CONCLUSIONS

6.1 Fate of oil and biodegradation through the sea-ice layer

In the mesocosms study, the majority of oil seems to be trapped in the ice during the ice season, and relatively undegraded oil was recovered in the mesocosms after the ice melted. The observation that the basic chemical composition of the oil layer frozen in the ice does not significantly change over the winter months is supported by previous studies. In addition, the mobility of the oil components was observed and this result is in accordance with the scientific literature (Fingas and Hollebone, 2003). A diffusion of dissolved petroleum compounds (PAHs) from the top sections of the ice cores to the bottom sections was observed. The applied oil in each of the mesocosms was encapsulated in the ice in the upper section of the ice core, and dilution processes occurred followed by a diffusion of dissolved compounds downwards in the core until the ice – seawater interface. This diffusion process explains the concentration of dissolved PAHs measured in the water column under the ice in all mesocosms. Nevertheless, the kinetic of these phenomenon was higher for the oil+dispersant treatment. In addition, and for the oil trapped in the top section of the ice pack, biodegradation of light alkanes was observed for oil+dispersant and crude oil.

The results from the microbial analysis in control sites (outside of the mesocosms) before the start of the exposures were found to be consistent with low background levels of hydrocarbon being present in the environment, which could be indicative of this locations having been previously exposed (this would be consistent to the location of the experimental site, in proximity to Svea where coal mining was ongoing). The microbial communities were found to be very similar between different locations and over time (during the experiment from February to May). Microbial communities were found to be different at different ice-layer depths and significant changes between communities from ice and seawater were found. However, Arctic microbial communities were found to shift in response to an oil spill within the first month of exposure. This study shows that Arctic microbial communities potentially able to biodegrade oil compounds are present and active in the sea-ice layers in the event of an oil spill even during the winter months. Investigating the active portions of the bacterial community has shown that some changes are more visible on the activity of organisms rather than on the total population. From the hydrocarbon degradation incubation experiments we conclude that bacteria present in sea ice are able to respond to and degrade petroleum hydrocarbons within weeks. This microbial activity showed a strong seasonable influence. During the April incubations, the observed microbial growth and degradation rates was less pronounced than in May.

This study confirms previous biodegradation studies (McFarlin et al. 2014) showing that Arctic microbial populations are able to degrade petroleum compounds in cold seawater.

6.2 Leakage of oil and biodegradation in the seawater below the ice layer.

Bacterial community structure analysis showed a significant difference in the oil+dispersant mesocosms compared to the control and other treatments. The bacterial community shifted towards very high numbers of *Colwellia* organisms as well as a higher activity of *Oleispira* genus. Members of these genera have been previously identified in crude oil contaminated seawater in Greenland and are known to include many oil degrading species. These results indicated that oil

components may have leaked through from the ice layer to the seawater, where it was actively being degraded by microorganisms. The biodegradation potential of bacteria present in seawater was confirmed by the short term incubation experiments performed herein. Our findings are supported by previous work by (Brakstad et al., 2008) investigating the presence of oil compounds beneath the ice as a result of a frozen in oil layer in Svalbard also showed very low concentrations of hydrocarbons below the ice. However, although it only represents a small fraction of the spill, the microbial response and activity seen in the present study demonstrates the *in situ* capability of the microorganisms to degrade the low concentrations of hydrocarbons. This observed microbial activity limits the concentration of hydrocarbon and minimizes the impact of the low level long term exposure these compounds would cause on marine organisms.

6.3 Fate of oil and biodegradation of oil on rock tiles

The analyses performed herein support that a strong biodegradation of oil components takes place on rock surface in the Arctic environment. The much higher number of bacterial observed on the oiled rock surface and the high portion of potentially oil degrading organisms observed within the first months of exposure of rock surface of the tiles to oil in the Arctic marine environment is indicative of a biofilm constituted for a large part of oil degrading organisms forming on the surfaces. Two and three months after exposure the concentration of oil compounds had diminished, and bacterial including oil degrading bacteria were less densely populating the rock surfaces.

Small Eukaryotes were found to increase on the rock surfaces over the duration of the experiment. These were found to increase during the last month of exposure when little oil was left and bacterial numbers were lower, indicating the Eukaryotes may be feeding on the bacterial biomass and taking advantage of the high nutrient content of the environment on the previously contaminated tiles.

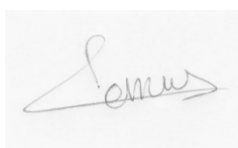
In summary, the tiles experiment show that biofilms are formed by microorganisms on rock surfaces submerged in arctic seawater. On oil contaminated surfaces, the microbial community established is dominant in metabolically active oil degrading microorganisms implying that these are likely able to biodegrade at least some of the oil components from the environment.

7 REFERENCES

- Brakstad O.G., Nonstad, I., Faksness, L.-G. and Brandvik, P.J., (2008) "Responses of Microbial Communities in Arctic Sea-ice After Contamination by Crude Petroleum Oil.", *Microb. Ecol.* 55:540–552.
- Camacho, C., G. Coulouris, et al. (2009). "BLAST+: architecture and applications.(Software)." *BMC Bioinformatics* 10: 421.
- Cole, J. R., Q. Wang, et al. (2014). "Ribosomal Database Project: data and tools for high throughput rRNA analysis." *Nucleic acids research* 42(Database issue): D633.
- Fingas, M.V., Hollebone B.P. 2003. Review of behavior of oil in freezing environments. *Marine Pollution Bulletin*, 47, 333-340
- Guyomarch J., Le Floch S., Merlin F. 2002. Effect of suspended mineral load, water salinity and oil type on the size of oil-mineral aggregates in the presence of chemical dispersant. *Spill Science & Technology Bulletin*, 8, 95-100
- Hazen, T.C., Prince, R.C., Mahmoudi, N. (2015) "Marine Oil Biodegradation.", *Env. Sci. Techn.* 50:2121–2129.
- Herlemann D. P., Labrenz M., et al. (2011). "Transitions in bacterial communities along the 2000 km salinity gradient of the Baltic Sea." *The ISME Journal* 5(10): 1571.
- Krolicka A., C. Boccadoro, et al. (2014). "Detection of oil leaks by quantifying hydrocarbonoclastic bacteria in cold marine environments using the Environmental Sample Processor". *Proceedings of the 37th AMOP Technical Seminar on Environmental Contamination and Response, Canada*, 791-807
- Le Floch S., Merlin F., Guillerme M., Dalmazzone C., Le Corre P. 1999. A Field Experimentation on Bioremediation: BIOREN. *Environmental Technology*, 20, 897-907
- Li, W. and A. Godzik (2006). "Cd-hit: a fast program for clustering and comparing large sets of protein or nucleotide sequences." *Bioinformatics* 22(13): 1658-1659.
- McFarlin, K. M. R.C. Prince, et al. (2014). "Biodegradation of Dispersed Oil in Arctic Seawater at -1°C." *PLoS ONE* 9(1): e84297. doi:10.1371/journal.pone.0084297
- Muyzer, G., E. C. Dewaal, et al. (1993). "Profiling of complex microbial-populations by denaturing gradient gel-electrophoresis analysis of polymerase chain reaction-amplified genes-coding for 16s ribosomal-rna." *Appl. Environ. Microbiol.* 59(3): 695-700.
- Nadkarni, M. A., F. E. Martin, et al. (2002). "Determination of bacterial load by real-time PCR using a broad-range (universal) probe and primers set." *Microbiology* 148(Pt 1): 257-266.
- Parales, R. E., Ditty, J. L. (2010) Substrate transport. In: Timmis, K. N. (ed) *Handbook of Hydrocarbon and Lipid Microbiology*, Springer-Verlag, Berlin, ISBN: 978-3-540-77584-3, pp. 1546-1553.
- Pruesse, E., J. Peplies, et al. (2012). "SINA: Accurate high-throughput multiple sequence alignment of ribosomal RNA genes." *Bioinformatics* 28(14): 1823-1829.
- Quast, C., E. Pruesse, et al. (2013). "The SILVA ribosomal RNA gene database project: improved data processing and web-based tools." *Nucleic acids research* 41(Database issue): D590.
- Roy G., Vuillemin R., Guyomarch J. 2005. "On-site determination of polynuclear aromatic hydrocarbons in seawater by stir bar sorptive extraction (SBSE) and thermal desorption GC–MS". *Talanta*, Vol 66, Issue 3, 540–546.
- Takai, K. and K. Horikoshi (2000). "Rapid Detection and Quantification of Members of the Archaeal Community by Quantitative PCR Using Fluorogenic Probes." *Applied and Environmental Microbiology* 66(11): 5066.
- Zhu, F., R. Massana, et al. (2005). "Mapping of picoeucaryotes in marine ecosystems with quantitative PCR of the 18S rRNA gene." *FEMS Microbiology Ecology* 52(1): 79-92.

SECTION 2 UNIQUE ARCTIC COMMUNITIES AND OIL SPILL RESPONSE CONSEQUENCES - RESILIENCE AND SENSITIVITY

*Environmental Effects of Arctic Oil Spills and
Arctic Spill Response Technologies
2014-2016
Final Report Project 2A*



Project Manager,
Lionel Camus, Akvaplan-niva

Quality Control: Magnus Aune & Hector Andrade,
Akvaplan-niva, Tromsø, July 2017



Authors which contributed to this report:

Bigelow Laboratory for Ocean Sciences

- Christopher Aeppli & Patricia Matray

COWI

- Morten Hjorth & Kirstine Toxværd

DTU

- Marina Pančić, Torkel Nielsen, Pil Hansen, & Kirstine Toxværd

Cedre

- Stephane L. Floch & Camille Lacroix

UNIS

- Janne Søreide & Helene Eide

Akvaplan-niva

- Marianne Frantzen, Jocelynn Palerud, Magnus Aune, Lionel Camus

UiT – the Arctic University of Norway

- Jasmine Nahrgang and Morgan L Bender

1 INTRODUCTION

1.1 Background and research objectives

The goal of the Arctic Oil Spill Response Technology Joint Industry Programme (JIP) was to advance arctic oil spill response strategies and equipment as well as to increase understanding of potential impacts of oil on the Arctic marine environment to enhance oil spill response decision making.

As part of the JIP, a unique long-term mesocosm experiment was executed to improve the scientific knowledge of the fate and biodegradation of oil and oil spill response residues in ice, as well as the environmental effects to ice associated ecology. Eight mesocosms were installed in the sea ice of the Van Mijenfjord in Svea, Svalbard in February 2015 and remained in place until July 2015. Oil was introduced into two mesocosms to follow natural attenuation. In two other mesocosms oil mixed with dispersant was introduced and another pair contained burned residues mimicking an in situ burn response. The oil mixed with dispersant treatment mimics an ineffective dispersant application where, instead of the oil getting dispersed in the water column, the oil mixed with dispersant freezes into the ice. The two remaining mesocosms served as controls (no oil). The study was designed to study the long term impact of these different scenarios on under-ice phyto & zooplankton communities. Similar treatments were applied in situ in microcosms to study the impact on the communities of the sea surface microlayer. Finally, polar cod were exposed in the laboratory to mechanically and chemically dispersed oil, along with burnt residue of oil to measure the effect on the resilience.

The primary and secondary objectives for each of the study were:

1.1.1 Zoo and micro plankton

The main objective was to investigate the effects from oil compounds migrating through the sea ice and potentially exposing key plankton species and groups and compare any effects between treatments. The main hypothesis was that the investigated oil spill response technologies would cause differences in the transport of crude oil components, through the sea ice to the water column below and therefore lead to different exposure regimes for the sea ice communities in the water column beneath the oil spill. A different development over time from winter period to spring and sea ice breakup was also hypothesised. The focus was set on the microbial web, which plays an important role in transfer energy and carbon in the sea as well as copepods as important secondary producers and key species in the arctic food web. In the study, microbial food web was divided into functional groups and copepods were represented by the arctic species *Calanus glacialis*.

The study endpoints of the microbial communities were production estimated as a change in biomass ($\mu\text{g C L}^{-1}$) over time of the main microbial groups observed in the area (viruses, bacteria, hetero-nanoflagellates (HNF), dinoflagellates, ciliates, picophytoplankton, nanophytoplankton, and diatoms). The sampled communities were followed for two weeks under controlled laboratory conditions (light intensity, temperature). The biomass of viruses, bacteria, HNF, picophytoplankton, and nanophytoplankton were measured, as well as the biomass of dinoflagellates, ciliates, and diatoms.

This study compares the impact of oil (natural attenuation), oil mixed with chemical dispersant (Finasol OSR52) and residues of burnt crude oil on grazing, egg production, egg hatching, nauplii malformation and development of the key pelagic sea ice associated copepod *Calanus glacialis*. Effects are evaluated on two occasions, during the fast ice period and just before the ice break-up. We also looked at the impact on the microplankton (bacteria, virus etc.) of the bacterial loop.

The nature of exposure of the communities was also investigated through chemical analyses of sampled water in both campaigns. Likewise, any potential bioaccumulation was investigated by analysing exposed copepod females and eggs for oil compounds.

1.1.2 Light penetration, nutrients and ice-algal growth

The production of microalgae in sea ice and surface waters is necessary to support the benthic and pelagic food webs. As example, a keystone copepod species of Arctic environments, *Calanus glacialis*, depends on the biomass of ice algae to feed and complete its reproductive cycle every spring.

The presence of oil immediately under or within the ice can affect organisms directly through toxicity or indirectly by modifying their growth environment. Direct responses of microalgae to chronic or acute exposure to oil and dispersants are very diverse and depend on the species considered, the nature of the contaminant, dose, etc. (Lewis and Pryor, 2013). These responses include, for example, changes in cellular composition (proteins, carbohydrates and/or nucleic acids), a reduction in chlorophyll *a*, photosynthesis or growth, with particularly strong adverse effect under nutrient-limited conditions for phytoplankton. Changes in community composition and succession have also been reported (Lewis and Pryor, 2013), which may impact the biogeochemical functions performed by the bottom-ice biota. Conversely, stimulation of growth as well as rapid recovery and acclimation of phytoplankton have also been reported under weak exposure in cold waters (Hsiao et al., 1978). The rare data available for ice algae suggests a lack of toxic effect at the species and community levels during short-term exposure (Cross, 1982; Cross, 1987). Indirect effects of oil and dispersants on algae may occur through alterations of light and nutrient availability, which regulate the timing, quantity and quality of primary production. Likewise, burnt oil and black carbon can contribute to attenuate light penetration (e.g. Doherty et al., 2013). The accumulation of biomass by ice algae and the consumers that rely on this biomass is contingent on the supply of essential nutrients at the ice-water interface and within brine channels (Vancoppenolle et al., 2010) and this supply can be affected by the presence of oil or dispersants. In the present project, these indirect effects were evaluated in the experimental study using the mesocosms containing naturally-forming sea ice.

The main goal was to examine the effect of different experimental treatments on the lowest portion of the sea ice where ice algae grow. The following measurements or sample collections were performed:

1. concentration of plant nutrients in bottom sea-ice and the water below the ice;
2. photosynthetically-available radiation (PAR) above and below sea-ice;
3. concentration of plant pigments (chlorophyll *a*, phaeopigments) and particulate organic matter in bottom sea-ice (including particulate organic carbon and total particulate nitrogen);
4. taxonomic composition of protist assemblages in bottom ice;
5. daily rates of primary production and nitrogen uptake in bottom sea ice

1.1.3 Sea Surface Layer Microbial Community

Little or no data are available on the chemical and biological properties of the surface microlayer in the Arctic Ocean. Investigations from lower latitudes reveal that surface microlayers are dynamic ecotones, enriched in particulate and dissolved organic matter, gases and neuston with respect to the underlying subsurface seawater (Liss and Duce 1997, Keith Bigg et al., 2004, Kuznetsova et al., 2004, Yang et al., 2005, Wurl et al., 2011). Within the Arctic pack ice, it is the presence of leads or the onset of sea ice melting in spring with resulting increases in biological activity that may allow for the formation of thin surface microlayers. Organic material in arctic surface microlayers around sea ice, whether alive, active or detrital, will most likely originate from sea ice flora exudates and brine early in the growth season and from planktonic organisms later on. Both can lead to accumulation of dissolved and particulate organic matter, the dynamics of which will depend somewhat on the onset and intensity of microbial growth and the resulting foodweb interactions.

The presence of oil and oil-derived or related products in permanently cold waters and in the presence of sea ice may affect the formation of sea surface microlayers and any associated neuston community differently than in lower latitudes. The existing gap in knowledge motivated the objective of Project 2A herein addressed which was to characterize biological exposure, sensitivity and resilience of Arctic species in sea surface micro layer communities that are exposed to oil, dispersant/oil mixtures, and burned oil residue.

1.1.4 Polar cod

Polar cod (*Boreogadus saida*) is a keystone species with a pan Arctic distribution (Bradstreet and Cross, 1982) that has been used as an indicator species in Arctic environments to understand the effects and mechanisms of oil pollution (Christiansen and George, 1995; Jonsson et al., 2010; Andersen et al., 2015; Nahrgang et al., 2010; 2016; Bender et al., 2016). Growth and reproductive investment are physiological end-point that can provide an integrative measure of the effects of pollutants on whole organisms, and give important insights into the potential risks to populations. Polar cod starts to build up their gonads in early autumn and final maturation and spawning takes place in late February/early March. Throughout the active spermatogenesis/vitellogenesis period, male fish display a more rapid developmental rate in terms of increased plasma sex steroid concentrations and increased gonadosomatic index (GSI) than female fish (Bender et al., 2016).

The main objective of this study was to investigate long-term resilience in polar cod exposed to environmentally realistic and dynamic exposure conditions likely to occur following an actual oil spill. Long-term effects on survival, growth and reproductive investment was monitored for seven months after acute (48 h) exposure to mechanically dispersed oil (MDO), chemically dispersed oil (CDO) or burned oil residue.

2 MATERIAL & METHODS

2.1 Location of field site

An extensive field campaign was conducted in Van Mijenfjord at Svea (Svalbard, Norway) from January to July 2015 (Figure 1). Svea is a coal-mining town located approximately 60 km south-east of Longyearbyen. A barrack at Polartun near Svea served as working/living quarters and laboratory facility. The sampling and field work took place a few hundred metres offshore Crednemoenen right across the fjord from the barracks (travelling distance of approximately 4 km). Sampling and handling of the samples, as well as a number of *in situ* measurements/analyses were performed on site.

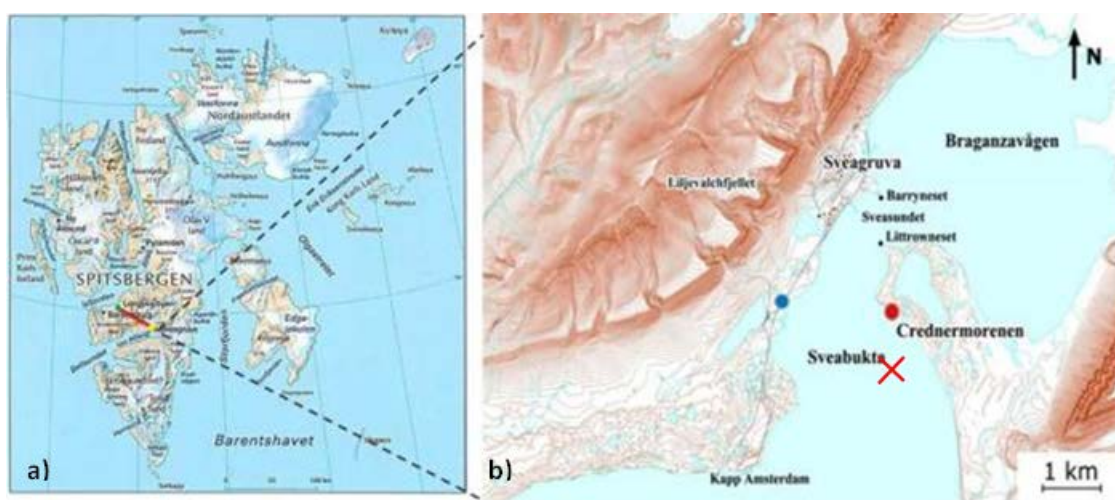


Figure 1 a) Map of Svalbard archipelago. The red line illustrates the distance between Longyearbyen (airport location) and Svea, b) Svea mining town with the location of the living and working barracks marked with a blue point, and the field and sampling location marked with a red point. The red cross represents the location of the mesocosm set-ups (located 800 m from shore).

2.2 Deployed experimental equipment

2.2.1 Mesocosms construction

Cedre designed the 8 mesocosms that were used in this study (Figure 2). The French engineering company G2B manufactured them, in close cooperation with Cedre. The structure was checked by SOFRESID engineering and Eni Saipem SA.

The mesocosms were designed to float in open water and be resistant to icing in order to stay on location from the fall freeze to the spring melt (the diameter of the mesocosms, 1.6 m, has been chosen in order to minimize stresses applied on the structure over the icing period). They consist of a floating opaque vertical cylinder (about 1 square meter section) open at the top and the bottom to allow natural exchanges with the atmosphere and the water column (dilution, evaporation, etc), but long enough (3 meters) to keep the oil contained. Once surrounded by floating ice, the mesocosms move with the ice according to the tidal movements; this prevents movement of water through the pipe, which could lead to oil leakage out of the inner part of the mesocosm. Opaque vertical cylinders have been chosen (black plastic curtain). In case of real oil

spills (oil slick of few hundred meters), the slick would induce a UV-light blockage at the surface of the ice (i.e. stop the penetration of light in the water column or through the ice pack). Considering this observation, the black color of the cylinders can be used in the frame of this project, without inducing any bias in the results.

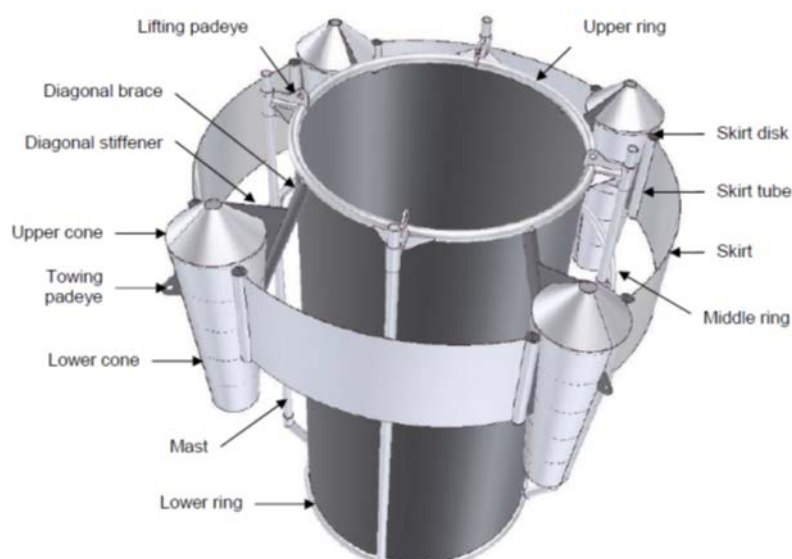


Figure 2 Industrial drawing of the mesocosms applied in the Svea field-campaign. Internal diameter: 1.6 m, length: 3 m (source CEDRE).

The 8 mesocosms were transported from Brest (October 2014) to Svea (November 2014) with Blue water Shipping company (by road transport from Brest to Tromsø, by boat from Tromsø to Svea). Once arrived in Svalbard, in January 2015, the structure of the mesocosms was assembled at Svea (Figure 3).



Figure 3 Assembly of the 8 mesocosms in Svea (source CEDRE).

The initial schedule (deployment in the water before icing) was not followed due to weather conditions (unstable and drifting sea ice that could create lot of stress on the mesocosms structure and anchoring system) and administrative reasons. Consequently the mesocosms were deployed once the fjord was covered with ice of sufficient thickness and stability (resistance to storm). During weeks 7 and 8, large holes (3m x 3m) were cut in the 80cm thick ice with a chainsaw,

and the ice blocks pulled out by means of man power and transported away from the site by snow scooter. The mesocosms were transported to the experimental site individually on a modified sledge pulled by a snow scooter. Once on site the mesocosms were lowered into the water (Figure 4 and Figure 5).



Figure 4 Mesocosms deployed in the Svea field-campaign (source: IRIS).



Figure 5 Location of the mesocosms at the experimental site (source IRIS). Red crosses indicate the mesocosm area, whereas green crosses indicate clean sampling area.

2.3 Oil and dispersant used for treatments

2.3.1 Crude oil

The KOBBE crude oil (produced by the GOLIAT oil field in the Barents Sea) was chosen in agreement with IOGP and was supplied by Eni to Akaplan Niva in Tromsø. The total volume was divided into several batches before distributing it over the different experiments. The total volume was calculated in order to lead to an oil thickness of ~0.25 cm once divided between the different experiments (thickness that is representative of a real oil spill, leading to a volume of 20 L per mesocosm).

Physical and chemical analyses of the fresh oil were performed at Cedre. The KOBBE oil is a relatively light crude oil centered on $n\text{-C}_{14}$, with a density of 0.816 g/mL (at 2 °C) and a viscosity of 6 mPa.s (at 2 °C and a shear rate of 10 s^{-1}). The distillation curve obtained during the sample preparation of the 250 °C residue is representative of the maximum evolution at sea, and results of this distillation provides a reliable prediction of the maximum evaporation rate expected when spilled at sea. The evaporation rate is 50 %. The content of asphaltenes is low (0.3 % w/w, i.e. by mass) and the content of wax is moderate (11 %). The crude oil pour point is -39 °C. The fresh oil is thus not in the solid form at the temperatures encountered during the field work. The pour point is related to the wax content, and it increases over time due to the evaporation process. The surface and interfacial tensions (measured between the oil and the air and the oil and the water) are of 24.73 and 13.44 mN/m, respectively. The maximum water content is of 77.9 %. The chemical composition of the crude oil is presented below (Figure 6).

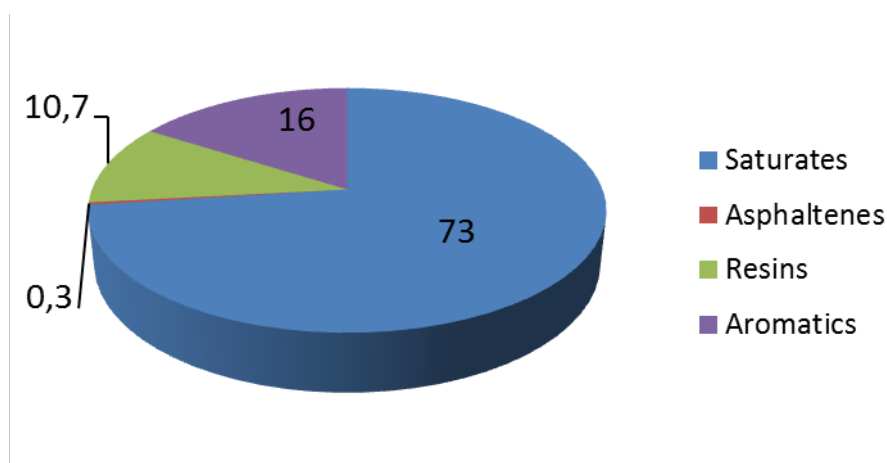


Figure 6 Chart pie representing the chemical composition of the KOBBE crude oil by mass, analyzed by GC-FID.

The sum of 21 parent PAHs and their alkylated congeners analyzed in this study leads to a concentration of $9,300\text{ }\mu\text{g.g}^{-1}$ for this crude oil. The sum of the n -alkanes is of $82,000\text{ }\mu\text{g.g}^{-1}$.

2.3.2 Burned oil residue

The production of burned residue was done in collaboration with the French institute INERIS (Verneuil-en-Halatte, France): 20 L of the KOBBE oil was burned in the course of 3 min. This was the time needed for the fire to go out, leading to approx. 2 L burned residue (i.e., ~ 85 – 90 % of the fresh oil volume was burned).

Chromatogram of the burned residue compared to the fresh oil, analyzed by HT-GC/FID, is presented in Figure 7. This method provides a general view of the oil, from the light compounds (around 10 carbons) to the heaviest fractions corresponding to a vacuum residue (around 90 carbons). It can be observed that the light fraction of the burned oil disappeared compared to the fresh oil.

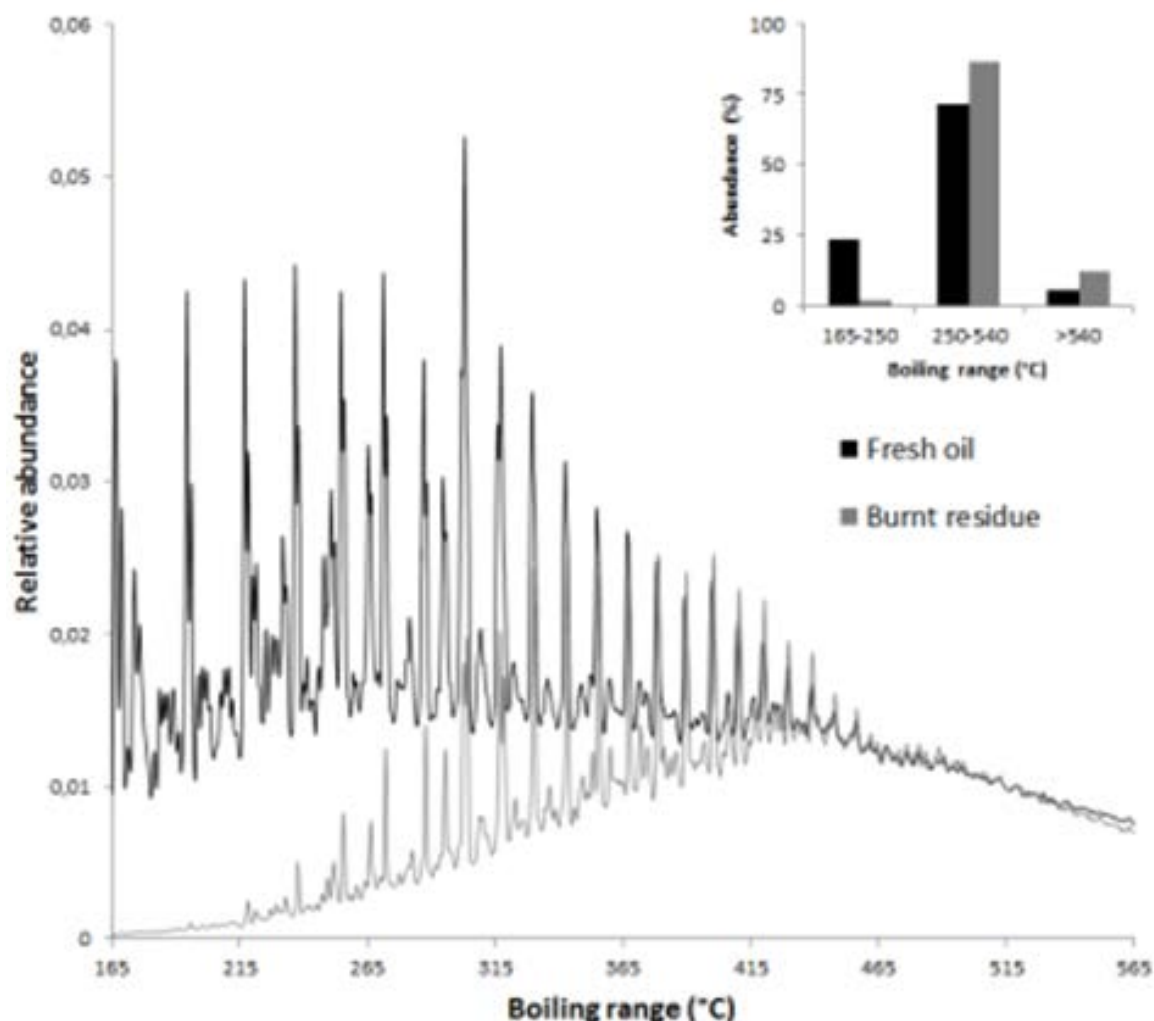


Figure 7 Comparison of the burned residue chromatogram (in grey) with the fresh oil one (in black).

2.3.3 Dispersant

The dispersant chosen is approved for use in many countries and produced by one of the industrial partners of the study, TOTAL: FINASOL OSR52 (TOTAL fluids)². This dispersant presents an efficiency of $79 \pm 3\%$, measured using the IFP test (NF T 90-345) on viscosity oil of 1,300 cSt. In response of an acute toxicity test, the dispersant toxicity of brown shrimps (*Crangon crangon*) exposed during 6 hours to 960 mg.L^{-1} causes a mortality of 3.3 % (NF T90-349 method). Finally, the biodegradability of the dispersant is at least 50 % according to a test performed by INERIS (NF T 90-346).

2.4 Treatments applied and sampling schedule

The mesocosms were deployed February 17th and 18th 2015 (T0, see below for sampling schedule), once the fjord was covered with ice of sufficient thickness and stability (resistance to storm). Large

² FINASOL OSR 52 Material Safety Data Sheet (MSDS): <http://www.quickfds.com/out/17439-36840-24544-010574.pdf>.

holes (3 m x 3 m) were cut in the 80 cm thick ice with a chainsaw, and the ice blocks pulled out by means of man power and transported away from the site by snowmobile. The mesocosms were transported to the experimental site individually on a modified sledge pulled by a snowmobile. Once on site the mesocosms were lowered into the water. The mesocosms were placed as 2 rows of 4 mesocosms, each row being separated by 20 - 25 m, and each mesocosm in a row being separated by approx. 13 m illustrated in Figure 8. In total, 4 different treatments (2 replicates each) were applied to the mesocosms and allowed to freeze in (Figures 8 and 9):

- **Natural attenuation (mesocosms A and B):** 20 L of crude oil was added to each of 2 mesocosms. This quantity poured on a surface of 8 m² leads to an oil thickness of 0.25 mm, which is representative of a real fresh oil slick.
- **Oil mixed with dispersant (oil+dispersant)(mesocosms C and D):** 20 L of crude oil was mixed with 1 L of dispersant and this mixture was added to each of 2 mesocosms, without additional mechanical mixing to mimic an ineffective dispersant application.
- **Residues of burnt oil (mesocosms E and F):** 2 L of residuals of burned crude oil was added to each of 2 mesocosms (2 L correspond to the volume of residues that remains after burning 20 L of this specific crude oil – KOBBE oil).
- **Control (mesocosms I and J):** 2 mesocosms were let free from oil and served as control. In addition, 2 additional controls were sampled ~120 m away from the mesocosms area (out of any mesocosms) and served as Clean Sites control (to check the effect of mesocosm location).

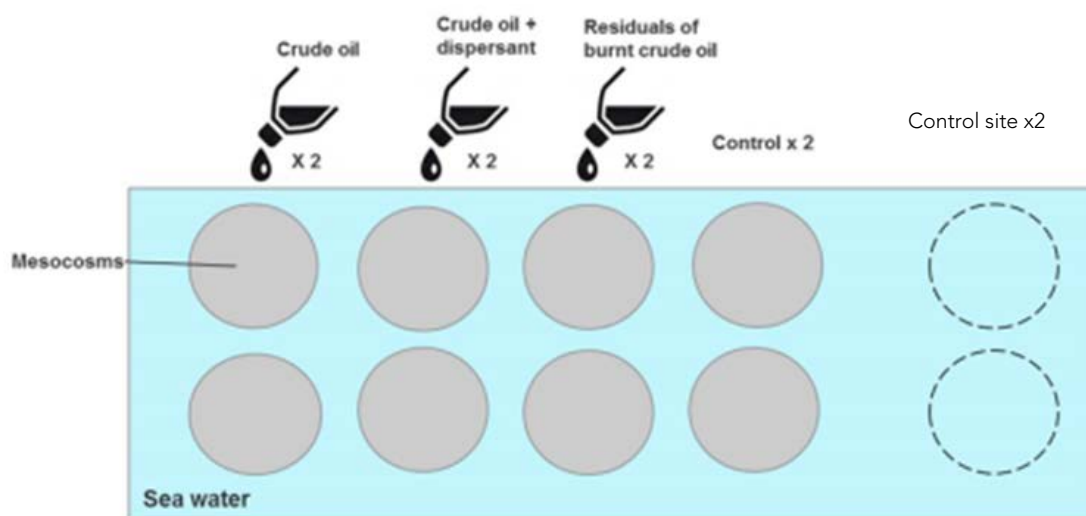


Figure 8 Schematic drawing of the field experimental setup at Svea.

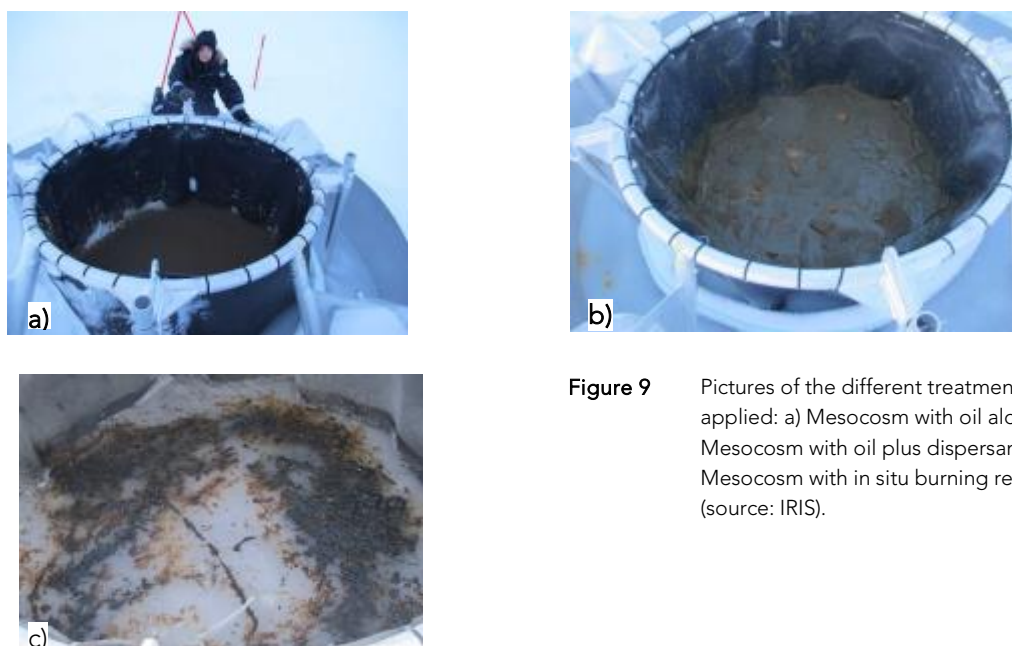


Figure 9 Pictures of the different treatments applied: a) Mesocosm with oil alone, b) Mesocosm with oil plus dispersant, c) Mesocosm with in situ burning residue (source: IRIS).

Table 1 describes the sampling schedule in the mesocosms. In addition to the 3 sampling points in the icing period, an additional sampling point after the melting period was included. This sampling took place in July before cleaning and decommissioning of the mesocosms. Field work started end of January (mesocosms arrival at Svea) and lasted until the ice melting period in order to cover different winter temperatures and environmental conditions, as well as the spring peak of biological activity.

Table 1 Sampling schedule.

Time Point	Month	Action
T0	17th-20th of February	Sampling point for microbial community. Mesocosms set up on the ice and oil spillage.
T1	March	Sampling point
T2	April	Sampling point
T3	May	Sampling point
Ice break up		
T4	July	Sampling point and mesocosms cleaning/dismounting

2.5 Plankton

The study of plankton responses to oil spill technologies was done through a field campaign with exposure experiments in mesocosms outside Svea in Van Mijenfjord in Svalbard, Norway. Post exposure response studies were performed simultaneously on two occasions on water and plankton community samples from the mesocosms taken to laboratory facilities in UNIS, Longyearbyen. Mesozooplankton (*Calanus glacialis* copepods) were not present at the mesocosm site and were sampled from Billefjorden and exposed to mesocosm water in the laboratory.

The study of sea ice communities took place over two campaigns; the first one on March 26-27 before the pelagic spring bloom, and the second on May 14 during the bloom a few days before

ice break up. The methodological approach was identical in both campaigns. Below follows the methodology of the sampling of water and plankton communities from the mesocosms, the laboratory exposure experiments and the chemical analyses of water and copepods.

2.5.1 Sampling of water and under sea ice communities

Water was sampled from each mesocosm by a plastic hand pump at the sea ice – water interface through drilled holes in the ice (Figure 10). The holes were pre drilled one day before to obtain sea ice cores for other studies. The boreholes were gently cleaned of slush ice, and water was pumped from 10 cm above the lower ice edge using a hand-operated vacuum pump with a 200 μm filter to remove larger zooplankton. To avoid contamination of the sampling tube, an outer tubing was inserted in the drill hole prior to pumping. On both sampling events, 40 L of water from each mesocosm ($-2.4\text{ }^{\circ}\text{C}$, 34 psu in March and 32 psu in May) was sampled, corresponding approximately to the top 2.2 cm of the water column. The water was pumped by hand (4.6 L min^{-1}) into 23 L insulated glass bottles to prevent freezing and stored dark at 1°C until returning to the laboratory (12-24 h). Each pump cycle lasted 8-10 minutes. In the laboratory, water from replicate mesocosms were mixed in glass beakers to ensure homogeneity between replicates. Part of the water was transferred to the micro plankton exposure study (see below) and the remaining water was used for the copepod exposure study.



Figure 10 Outer tubing inserted in drill hole of mesocosm.

2.5.2 Sampling of copepods

At the site of the mesocosm, the water depth was rather shallow so there is no available populations of *Calanus glacialis* for the copepod exposure study. Therefore, specimens of *C. glacialis* were collected elsewhere on Svalbard in Isfjorden (Karls Kronta Djupet, bottom depth $\sim 250\text{ m}$, position $78.1944^{\circ}\text{N } 14.55.046^{\circ}\text{E}$) on March 21 and May 14, 2015. Samples were collected from boat with 3 vertical plankton hauls from depth of 200 m to the surface using a plankton net (WP2 200 μm in March and WP3 1 mm in May) with a 1 L plastic container as non-filtering cod-

end to reduce stress and damage to the organisms. After collection, samples were diluted with surface seawater and kept in 3 L plastic containers at in situ temperature (0 °C) until returning to the laboratory.

In the laboratory, sampled copepods were stored in large 25 L buckets at 4 °C (6 days in March, 1 day in May) until they were sorted for the exposure experiment. Mature female *Calanus glacialis* were identified based on the criteria in Nielsen et al., 2014 and were gently selected with a plastic pipette on ice-chilled petri dishes under a stereomicroscope (Olympus SZ40, 20X magnification) and placed in 10 mL ice chilled glass containers with 0.2 µm filtered seawater until the initiation of the experiment (<1h).

2.5.3 Micro plankton post exposure study

Microplankton community responses were investigated by studying the development of communities for 2 x 14 days at two times during the mesocosm exposure. Water (4 x 20 L) from each treatment were pooled, and incubated in 5 L glass bottles in triplicates for 14 days. The cultures were stored at ≤1 °C at 40-50 µmol photons m⁻² s⁻¹ following a light:dark cycle of 16:8 h, and stirred manually at least twice a day (ten gentle vertical rotations). Salinity of the water samples was 33.8 and 31.9 in March and May, respectively (VWR SympHony SP90M5, VWR International, Inc.). The air and water temperature were measured continuously using HOBO Data Loggers, whereas the light intensity and pH were measured every second day at approximately the same time using LI-COR Biosciences, model LI-1400 Data Logger (Biosciences, Lincoln, NE, USA) and Thermo Electron Corporation, Orion Star Series with a ROSS Ultra combination pH electrode (Thermo Electron Corporation, Beverly, MA, USA), respectively. The pH electrode was calibrated weekly (2-point calibration) using Thermo Electron Corporation, Orion Application Solution buffers of pH 7.0 and 10.0 dilutions.

Samples (3 x 60 mL) for measurements of inorganic nutrients (nitrate NO³⁻, phosphate PO³⁻ and silicate Si(OH)₄) were withdrawn from the culturing bottles using 60 mL syringes, and filtered through 0.2 µm Q-Max syringe filters into acid-washed collection bottles on days 0, 4, 8, and 14 (Table 1). The samples were immediately stored at -80 °C, and later analysed at the National Institute of Aquatic Resources, Technical University of Denmark. To determine dissolved PAH concentrations, samples (3 x 100 mL) were collected from each culturing bottle on days 0, 8, and 14 (Table 2), and immediately stored at -20 °C. The samples were analysed at CEDRE, France, according to procedures described below.

2.5.3.1 Size-fractionated chlorophyll-a concentration

Samples (3 x 100 mL) for size-fractionated concentrations of Chl-a were withdrawn from each replica on days 0, 4, 8, 12, and 14 (Table 2), and filtered sequentially through 50, 10 and 0.7 µm pore size filters. The pigments were extracted in 5 mL methanol (99.5%) for 24 hours in darkness at room temperature. The fluorescence of the extracts was measured before and after addition of 100 µL HCl (37%) with a Turner Designs, model 10-AU Fluorometer (Turner Designs, Sunnyvale, CA, USA). The fluorometer was calibrated prior to use with pure Chl-a standard (Sigma).

2.5.3.2 Biomass measurements

Every second day, samples for determining the abundance and biomass of viruses and prokaryotes, small phytoplankton, and hetero nanoflagellates (HNF), and every fourth for protozoa were taken (Table 2).

Viral, bacterial, small phytoplankton, and HNF samples (3×2 mL) were enumerated using an Attune Acoustic Focusing Cytometer (Applied Biosystems by Life Technologies, CA, USA). The data were analysed using Attune® Cytometric Software (version 2.1; Life Technologies Corporation, CA, USA). The enumeration was performed on 2 mL samples fixed with glutaraldehyde (1% final concentration) for 3 hours in the dark at 4 °C, and stored at -80 °C until the analysis after 5 months at University of Bergen, Norway. The samples were thawed immediately before analysis.

The thawed viral and bacterial subsamples of 100 µL were diluted 10-fold in 0.2 µm filtered TE buffer (Tris 10 mM, EDTA 1 mM, pH 8), and stained with SYBR Green I (Molecular Probes Inc., Eugene, OR, USA) for 10 min at 80 °C in a water bath to provide optimal staining of viruses (Marie et al., 1999).

The samples of 200 µL were analysed at a 100 µL min⁻¹ flow rate, and the discriminator was set on the basis of their side scatter (proportional to cell size) and pigment (green and red fluorescence). Fluorescent yellow-green microspheres of the 2 µm diameter (FluoSpheres® Carboxylate-Modified Microspheres, UK) were added to the samples as an internal standard. The small phytoplankton subsamples of 400 µL were analysed directly after thawing at a flow rate of 200 µL min⁻¹, and the discriminator was set on the basis of their side scatter (proportional to cell size) and pigment (red and orange fluorescence) (Larsen et al., 2004).

The thawed HNF subsamples of 1.4 mL were stained with SYBR Green I (Molecular Probes Inc., Eugene, OR, USA) for 4-6 hours at 4 °C in the dark. The subsamples were enumerated at a flow rate of 500 µL min⁻¹, and the discriminator was set on the basis of their pigment (green and red fluorescence). Fluorescent yellow-green microspheres of the 0.5 µm diameter (FluoSpheres® Carboxylate-Modified Microspheres, UK) were added to the samples as an internal standard (Zubkov et al., 2007).

The samples for biomass of small phytoplankton and HNF (3×15 mL) were fixed with glutaraldehyde (1% final concentration) for 3 hours at 4 °C in the dark, and stored at -80 °C. For each treatment, the thawed triplicates from Day 0, and Day 14 were pooled ($V_{\text{Day 0}} = 45$ mL; $V_{\text{Day 14}} = 45$ mL), and sequentially filtered through 8, 5, 3, 2 and 1 µm pore size filters. The size fractionation was implemented to estimate the percentage of various phytoplankton and HNF groups within the given size intervals. For the winter season, the phytoplankton and HNF filtrates of 0.9 mL and 1.8 mL were enumerated at flow rates of 200 µL min⁻¹ and 500 µL min⁻¹, and the spring phytoplankton and HNF filtrates of 0.5 mL and 0.9 mL were enumerated applying the same flow rates as before. The discriminators for phytoplankton and HNF were set as described above. The abundance of small phytoplankton and HNF within different size intervals was converted to the weighted arithmetic mean size, and used for biomass estimates based on the carbon conversion factors (Table 3 and Table 4).

Protozoan (ciliates and dinoflagellates) and diatoms samples (3×110 mL) were fixed with acidic Lugol (3% final concentration), and stored in darkness and cooled until analysis at the National Institute of Aquatic Resources, Denmark. The samples were allowed to settle, and the upper volume of 10 mL was gently removed. Afterwards, the remaining volume was settled in a 100 ml Utermöhl sedimentation chamber for 24 hours. The samples were examined in an inverted microscope (Leica DM IL LED, Leica Microsystems GmbH, Wetzlar, Germany) at a magnification of $\times 200$. Ciliates and dinoflagellates were identified morphologically, enumerated and divided into size classes covering 10 µm ranges of equivalent spherical diameter (ESD). The ESD of every

specimen was measured, and the cellular volume determined using the appropriate geometric shape. The cellular volume was converted to biomass using specific carbon conversion factors given in Table 3 and Table 4. Loricata and aloricate forms were discriminated for ciliates, and thecate and athecate forms were discriminated for dinoflagellates.

Table 2 Sampling program for micro plankton exposure study.

Sampling	DAY 0	DAY 2	DAY 4	DAY 6	DAY 8	DAY 10	DAY 12	DAY 14
pH	•	•	•	•	•	•	•	•
Salinity	•							
Temperature	•	•	•	•	•	•	•	•
Light	•	•	•	•	•	•	•	•
Chl-a	•		•		•		•	•
Nutrients	•		•		•			•
PAH	•				•			•
Plankton	•	•	•	•	•	•	•	•
Protozoa	•		•		•		•	•

Table 3 Specific carbon conversion factors derived from the experiment in March 2015.

Functional group	ESD (µm)	Biomass (pg C cell ⁻¹)	Winter biomass (µg C L ⁻¹)															
			Control				Burnt oil				Oil + dispersant				Crude oil			
			Day 0		Day 14		Day 0		Day 14		Day 0		Day 14		Day 0		Day 14	
			Mean	SD	Mean	SD	Mean	SD	Mean	SD	Mean	SD	Mean	SD	Mean	SD	Mean	SD
Thecate dinoflagellates	<10	128	-	-	-	-	-	-	-	-	-	-	-	-	-	-	-	-
	16.5	439	-	-	0.01	0.00	-	-	-	-	0.01	0.00	-	-	0.01	0.00	0.01	0.00
	25.9	1336	-	-	0.01	0.00	0.00	0.01	0.00	0.01	0.01	0.01	0.00	0.01	0.01	0.01	0.01	0.02
	35.7	2921	0.01	0.02	0.04	0.06	-	-	-	-	-	-	-	-	0.00	0.02	0.01	0.02
	45.6	5316	-	-	-	-	-	-	-	-	0.00	0.04	0.02	0.03	-	-	-	-
	>50	6684	-	-	-	-	-	-	-	-	-	-	-	-	-	-	-	-
Athebate dinoflagellates	<10	128	0.42	0.22	6.72	6.37	0.33	0.20	3.58	1.99	0.30	0.21	4.68	2.79	0.29	0.30	4.99	2.10
	16.5	439	0.63	0.38	1.16	0.21	0.47	0.29	1.28	0.79	0.35	0.26	0.98	0.46	0.40	0.35	0.81	0.34
	25.9	1336	0.50	0.40	1.19	0.64	0.31	0.19	0.95	0.35	0.30	0.07	1.05	0.30	0.31	0.06	0.82	0.13
	35.7	2921	0.52	0.61	1.30	0.52	0.26	0.33	0.94	0.61	0.18	0.25	1.12	0.83	0.10	0.74	1.09	0.70
	45.6	5316	0.11	0.09	0.32	0.30	0.11	0.09	0.19	0.03	0.05	0.04	0.43	0.14	0.08	0.15	0.41	0.25
	>50	6684	0.16	0.17	0.30	0.14	0.11	0.10	0.22	0.15	0.00	0.19	0.18	0.14	0.20	0.14	0.22	0.15
Loricata ciliates	<10	28	-	-	-	-	-	-	-	-	-	-	-	-	-	-	-	-
	16.5	125	-	-	-	-	-	-	-	-	-	-	-	-	-	-	-	-
	25.9	486	-	-	-	-	-	-	-	-	-	-	-	-	-	-	-	-
	35.7	1263	-	-	0.01	0.01	-	-	-	-	-	-	-	-	0.01	0.00	-	-
	45.6	2622	0.01	0.02	-	-	-	-	-	-	0.00	0.02	0.01	0.02	0.01	0.00	0.03	0.03
	>50	3469	0.01	0.02	-	-	0.01	0.02	-	-	-	-	0.03	0.03	0.02	0.02	-	-
Aloricate ciliates	<10	99	-	-	-	-	-	-	-	-	-	-	-	-	-	-	-	-
	16.5	448	0.01	0.01	0.01	0.00	0.01	0.01	0.01	0.01	0.01	0.00	-	-	0.01	0.01	0.01	0.01
	25.9	1741	0.01	0.01	-	-	0.01	0.01	0.01	0.02	0.19	0.26	0.01	0.01	0.02	0.01	0.02	0.01
	35.7	4527	0.02	0.03	-	-	0.02	0.03	-	-	0.02	0.00	0.02	0.03	0.00	0.06	0.00	0.06
	45.6	9401	-	-	0.05	0.07	-	-	-	-	0.00	0.02	-	-	-	-	-	-
	>50	12435	-	-	-	-	0.04	0.07	-	-	-	-	-	-	-	-	-	-
HNF	3.4	4.6	0.18	0.03	2.33	0.60	0.22	0.02	0.81	0.13	0.19	0.03	0.89	0.27	0.20	0.04	0.52	0.14
	5.8	22.7	0.18	0.05	0.45	0.18	0.38	0.13	0.25	0.10	0.31	0.03	0.34	0.11	0.20	0.03	0.22	0.04
Bacteria	-	0.02	3.18	0.21	9.51	2.21	3.18	0.18	7.32	0.41	3.49	0.17	9.38	1.05	3.82	0.14	7.33	0.20
Viruses	-	0.0002	0.22	0.10	0.13	0.01	0.38	0.01	0.40	0.13	0.41	0.07	0.40	0.09	0.47	0.04	0.56	0.00
Diatoms	39.8	1330	0.08	0.03	111.60	45.27	0.06	0.02	99.81	76.58	0.08	0.07	134.25	17.09	0.11	0.06	103.48	13.05

Continuation Table 3 Specific carbon conversion factors derived from the experiment in March 2015.

Functional group	ESD (µm)	Biomass (pg C cell ⁻¹)	Winter biomass (µg C L ⁻¹)															
			Control				Burnt oil				Oil + dispersant				Crude oil			
			Day 0		Day 14		Day 0		Day 14		Day 0		Day 14		Day 0		Day 14	
Nanoplankton	4.0	7.5	0.07	0.02	1.11	0.36	0.08	0.06	0.70	0.38	0.06	0.02	0.90	0.25	0.10	0.01	0.79	0.02
	9.3	91.2	-	-	19.28	9.65	0.15	0.13	17.22	12.84	0.15	0.13	24.77	3.44	0.15	0.26	18.98	1.58
Picoplankton	1.6	0.4	0.01	0.00	0.18	0.10	0.02	0.01	0.13	0.08	0.01	0.00	0.08	0.04	0.02	0.01	0.05	0.01

Table 4 Specific carbon conversion factors derived from the experiment in April 2015

Functional group	ESD (µm)	Biomass (pg C cell ⁻¹)	Spring biomass (µg C L ⁻¹)															
			Control				Burnt oil				Oil + dispersant				Crude oil			
			Day 0		Day 14		Day 0		Day 14		Day 0		Day 14		Day 0		Day 14	
			Mean	SD	Mean	SD	Mean	SD	Mean	SD	Mean	SD	Mean	SD	Mean	SD	Mean	SD
Thecate dinoflagellates	<10	128	0.01	0.00	-	-	0.01	0.00	0.01	0.01	-	-	3.68	0.70	-	-	-	-
	16.5	439	0.15	0.16	0.10	0.01	0.10	0.06	0.09	0.04	0.00	0.02	0.45	0.01	0.04	0.04	0.07	0.01
	25.9	1336	0.01	0.01	0.01	0.01	0.01	0.02	0.01	0.01	0.00	0.01	0.04	0.02	0.01	0.01	0.01	0.01
	35.7	2921	-	-	-	-	-	-	-	-	-	-	0.03	0.03	-	-	-	-
	45.6	5316	-	-	-	-	-	-	-	-	-	-	-	-	-	-	-	-
	>50	6684	-	-	-	-	-	-	-	-	-	-	-	-	-	-	-	-
Athebate dinoflagellates	<10	128	0.39	0.14	8.87	1.96	0.56	0.39	7.60	1.46	0.20	0.23	-	-	0.55	0.34	2.00	0.42
	16.5	439	0.97	0.38	1.41	0.12	0.71	0.27	1.30	0.26	0.17	0.34	0.01	0.01	0.27	0.16	0.88	0.17
	25.9	1336	0.19	0.09	0.14	0.01	0.14	0.08	0.15	0.10	0.01	0.08	-	-	0.05	0.04	0.16	0.05
	35.7	2921	0.01	0.02	0.10	0.06	0.06	0.03	0.04	0.07	0.00	0.02	-	-	0.03	0.04	0.05	0.06
	45.6	5316	0.03	0.04	0.03	0.04	0.05	0.05	0.04	0.06	-	-	-	-	-	-	-	-
	>50	6684	-	-	-	-	-	-	-	-	-	-	-	-	-	-	0.02	0.04
Loricata ciliates	<10	28	-	-	-	-	-	-	-	-	-	-	-	-	-	-	-	-
	16.5	125	-	-	-	-	-	-	-	-	-	-	-	-	-	-	-	-
	25.9	486	-	-	0.01	0.01	-	-	-	-	-	-	-	-	-	-	-	-
	35.7	1263	0.02	0.01	0.02	0.01	-	-	0.02	0.01	0.00	0.01	-	-	0.01	0.02	-	-
	45.6	2622	-	-	-	-	-	-	-	-	0.00	0.02	-	-	-	-	-	-
	>50	3469	-	-	-	-	-	-	-	-	-	-	-	-	-	-	-	-
Aloricate ciliates	<10	99	0.04	0.03	-	-	0.03	0.02	0.01	0.01	0.03	0.04	-	-	0.05	0.05	-	-
	16.5	448	0.25	0.14	0.07	0.02	0.23	0.10	0.12	0.03	0.05	0.02	0.01	0.01	0.04	0.01	0.03	0.00
	25.9	1741	0.07	0.02	0.03	0.02	0.09	0.11	0.07	0.02	0.02	0.01	0.02	0.02	0.02	0.06	0.01	0.01
	35.7	4527	0.09	0.00	0.05	0.00	0.05	0.05	-	-	-	-	-	-	0.00	0.03	-	-
	45.6	9401	-	-	-	-	-	-	-	-	-	-	-	-	-	-	-	-
	>50	12435	0.06	0.09	-	-	-	-	-	-	-	-	-	-	-	-	-	-
HNF	3.5	5.0	0.43	0.06	4.17	0.46	0.52	0.11	3.50	0.14	9.10	1.09	4.66	1.18	1.05	0.07	2.18	0.09
	8.4	67.8	1.22	0.35	16.76	2.31	1.24	0.38	15.02	0.86	4.61	1.33	9.15	3.21	1.50	0.37	4.87	0.30
Bacteria	-	0.02	11.91	0.43	3.24	0.38	12.61	0.41	8.77	1.15	14.65	0.31	4.36	0.21	11.90	0.18	9.67	0.41
Viruses	-	0.0002	0.66	0.07	0.82	0.02	0.62	0.03	0.69	0.13	1.14	0.07	1.44	0.11	0.68	0.05	0.68	0.06
Diatoms	39.8	1330	0.01	0.02	7.46	9.55	0.17	0.07	24.90	7.44	0.01	0.02	1.16	0.54	0.19	0.21	5.49	3.55
Nanoplankton	3.9	7.1	3.35	0.87	16.76	1.43	3.57	0.25	11.81	2.00	6.81	0.47	1.90	0.08	5.38	0.71	3.50	0.35
	9.8	107.4	1.00	0.33	5.25	1.70	0.90	0.16	3.50	1.50	0.99	0.56	5.03	0.68	1.88	0.97	1.44	0.87
Picoplankton	1.7	0.6	4.15	1.15	0.62	0.16	4.56	0.43	3.59	0.56	3.29	0.17	1.51	0.14	5.32	0.16	4.23	0.40

2.5.4 Copepod exposure study

The exposure experiment was conducted to investigate effects of the exposure of oil spill treatments on grazing and egg production of exposed females. The experiment consisted of bottle incubations of *Calanus glacialis* in mesocosm water and daily quantification of faecal pellet and egg production.

The 200 µm filtered mesocosm water from the three oil spill treatments and the control was transferred to 1 L red cap glass bottles (N=15 per treatments), and three *C. glacialis* were transferred to each bottle. Bottles were incubated for 14 days in a climate-regulated room at 0 °C and kept dark to prevent phototoxicity. Every second day, *T. weissflogii* culture was added at increasing concentrations from 30-110 µg C L⁻¹ to prevent food limitation.

Every 24 h, each bottle content was gently filtered through a submerged 50 µm filter. Filtrate was returned to the bottle, while females, pellets and eggs were rinsed onto a glass petri dish with chilled 0.2 µm filtered seawater. Copepod survival was determined under a stereo microscope (Olympus SZ40, 20Xmagnification), and live females were immediately returned to the bottle using a plastic pipette.

Faecal pellets and eggs were counted under a stereo microscope (Leica S4E, 20Xmagnification) on ice-chilled petri dishes to determine daily production. Every second day, the length and width of 100 pellets and all eggs from random samples of each treatment were measured using an inverted microscope (Leica DMIL LED, 40x magnification) and used to calculate carbon content. Pellet width was measured to the nearest 8 µm and pellet length to the nearest 25 µm, and pellets were only considered for the study if the length was minimum 3 x width (Swalethorp et al., 2011).

Pellet volume was calculated assuming cylinder shape and egg volume as the shape of a sphere. Specific faecal pellet production (SPP) was calculated using number of pellets, the mean pellet volume for pellets produced the entire period, and a pellet volume to carbon conversion factor of 4.30×10^{-6} µg C pellet⁻¹ (Swalethorp et al., 2011). Specific egg production (SEP) was calculated using number of eggs, a mean egg volume for the entire period, and an egg volume to carbon conversion factor of 1.10×10^{-7} µg C egg⁻¹ (Swalethorp et al., 2011) (Table 5).

Table 5 Carbon content of mature *C. glacialis* females and of egg and pellets (Swalethorp et al., 2011). Data are mean ±SD.

	Pre-bloom	Bloom
Carbon content (µg C female ⁻¹)	213 ± 132	406 ± 177
Egg carbon (µg C egg ⁻¹)	1.10×10^{-7}	1.10×10^{-7}
Faecal pellet carbon (µg C pellet ⁻¹)	4.30×10^{-6}	4.30×10^{-6}

To avoid effects from starvation during the exposure experiment, copepods were fed a culture of the diatom *Thalassiosira weissflogii* for feeding was grown in 1 L plastic containers and kept at 12 °C and constant aeration at 50-60 µmol photons m⁻² s⁻¹ with a 16:8h light:dark cycle. The medium used for *T. weissflogii* cultures was B1 (Hansen 1989) with silicate based on autoclaved 0.2 µm filtered seawater with a salinity of 33 ppm.

An exposure study on mesozooplankton was performed simultaneously in both campaigns, to investigate potential threshold effect concentrations. The experiment consisted of bottle

incubations of *C. glacialis* in dilutions of mesocosm water and quantification of daily faecal pellet and egg production. A dilution series of four concentrations (100%, 10%, 1% and 0.1% of mesocosm water) was prepared for each of the three oil spill treatments and the control. For the 100%, 1000 mL of the 200 μm filtered mesocosm water was transferred to 1 L red cap glass bottles (fifteen replicates \times four treatments (three oil treatments and a control)). For the 10%, 100 mL mesocosm water was added to 900 mL 0.2 μm filtrated seawater (FSW) (five replicates \times four treatments). For the 1%, 10 mL mesocosm water was added to 990 mL FSW (five replicates \times four treatments) and for the 0.1%, 1 mL mesocosm water was added to 999 mL FSW (five replicates \times four treatments). Three females of *C. glacialis* were transferred to each bottle. Bottles were incubated for 14 days in a climate-regulated room at 0 °C. Because toxicity of oil compounds can increase if exposed to light (Pelletier et al., 1997) the bottles were kept in darkness to prevent phototoxicity. Every second day, *T. weissflogii* culture was added at increasing concentrations from 30-110 $\mu\text{g C L}^{-1}$ as the culture grew denser. The investigated endpoints and the remaining methodology were identical to the above.

2.5.5 Egg hatching experiment

Hatching experiments were conducted to investigate effects of the oil spill treatments on hatching success of eggs from exposed females.

In March, eggs produced within a 24 h period from females in the control treatment and from all treatments after 13 days of incubation were transferred to Nunclon Multidishes (6-well trays) with 10 mL 0.2 μm filtered seawater and stored in darkness at 0 °C for 7 days. 1-46 eggs were incubated in each well. Samples were then fixed with a drop of acidic lugol (3 % final concentration) before nauplii and unhatched eggs were counted under a stereo microscope (Leica S4E, 20X magnification).

In May, eggs produced within a 24 h period from females in the control treatment and eggs from all treatments after 3, 4, 5, 11, 12 and 13 days of incubation were stored in petri dishes with 40 mL 0.2 μm filtered seawater and stored in darkness at 0 °C. 1-46 eggs were incubated in each petri dish. The number of nauplii was counted after 7 days, and hatching success was calculated as the proportion of the initial number of eggs that hatched into nauplii. The development of hatched nauplii was monitored to investigate potential post exposure effects. Samples with less than three eggs were removed from the dataset prior to analysis.

2.5.6 Chemical analysis of oil compounds

To investigate the chemical composition of oil compounds in the mesocosm water during the exposure experiment, 100 mL (twelve replicates) was subsampled into acid washed glass bottles after 0, 7 and 14 days of incubation and frozen (-20 °C) for later analysis. The analyses included 21 PAHs, among which the 16 compounds listed as priority pollutants by US EPA, and was performed by stir bar sorptive extraction-thermal desorption-gas chromatography-tandem mass spectrometry (SBSE-TD-GC-MS/MS). Briefly, 10 mL of an ethanolic solution containing 10 ng of 7 deuterated PAH (internal standards) were added to 90 mL of seawater sample. Then, analytes were extracted for 2 hours at 700 rpm using polydimethylsiloxane stir-bars (Twister 20 mm \times 0.5 mm, Gerstel). Bars were subsequently analyzed using a gas chromatography system Agilent 7890A coupled to an Agilent 7000 triple quadrupole mass spectrometer (Agilent Technologies) and equipped with a Thermal Desorption Unit (TDU) combined with a Cooled Injection System

(Gerstel). Thermodesorption and GC-MS/MS conditions were as previously described (Lacroix et al., 2014). Analytes were quantified relatively to deuterated compounds using a calibration curve ranging from 0.01 ng to 30 ng per bar. Two compounds, benzo(b)fluoranthene and benzo(k)fluoranthene, were quantified as a sum, named benzo(b+k)fluoranthene, due to a poor resolution. Results are expressed as ng/L of seawater. Limits of quantification (LOQ) were calculated by the calibration curve method (Shrivastava et al., 2011) and limit of detection (LOD) were estimated by dividing LOQ by 3.

To investigate bioaccumulation in *C. glacialis*, 15 females from an initial sample and 15 females from the four treatments after 14 days of post exposure were rinsed in 0.2 µm filtered seawater, transferred individually to 8 mL glass vials and frozen (-20 °C) for later analysis. The content of PAHs was quantified in pools containing between 5 and 10 adult copepods. 21 PAHs were analysed, among which the 16 compounds listed as priority pollutants by US EPA. Analyses were performed by stir bar sorptive extraction-thermal desorption-gas chromatography-tandem mass spectrometry (SBSE-TD- GC-MS/MS) using a procedure adapted from Lacroix et al., (2014). Copepods pools were resuspended in 2 ml of an ethanolic solution containing 0.05 g.ml⁻¹ of hydroxide potassium and were digested for 3h at 80°C by alkaline digestion. Visual observations indicated this procedure allowed a disruption of copepod exoskeleton and a release of the body content. After addition of 20 ml of reverse osmosis water, analytes were extracted from digested samples for 2 hours at 700 rpm using polydimethylsiloxane stir-bars (Twister 20 mm x 0.5 mm, Gerstel). Bars were subsequently analysed using a gas chromatography system Agilent 7890A coupled to an Agilent 7000 triple quadrupole mass spectrometer (Agilent Technologies) and equipped with a Thermal Desorption Unit (TDU) combined with a Cooled Injection System (Gerstel). Thermodesorption and GC-MS/MS conditions were as previously described (Lacroix et al., 2014). Analytes were quantified relatively to deuterated compounds using a calibration curve ranging from 0.01 ng to 10 ng per bar. Two compounds, benzo(b)fluoranthene and benzo(k)fluoranthene, were quantified as a sum, named benzo(b+k)fluoranthene, due to a poor resolution. Results are expressed as ng analytes/copepod.

Limits of quantification (LOQ) were calculated by the calibration curve method (Shrivastava et al., 2011) and limit of detection (LOD) were estimated by dividing LOQ by 3.

To investigate transfer of oil compounds from exposed females to eggs, eggs were subsampled for chemical analysis in May. Subsampling was not done in March due to low egg production. 20-60 eggs produced within a 48 h period from females in the control treatment and from all treatments after 7 and 14 days of incubation were rinsed in 0.2 µm filtered seawater, transferred to 8 mL glass vials (three replicates) and frozen (-20 °C) for later analysis. The content of PAHs was quantified identically to waster and copepod PAH quantification (see description above) in copepod eggs. Copepod eggs were resuspended in 6 ml of an ethanolic solution containing 0.05 g.ml⁻¹ of hydroxide potassium. Samples were digested for 1.5h at 80°C by alkaline digestion and were submitted to 10 min of ultrasounds before another 1.5h of alkaline digestion at 80°C. Due to the low amount of eggs in each sample, visual observation fail to confirm if this procedure allowed a complete disruption of eggs shell. Results are expressed as ng analytes/copepod egg.

Limits of quantification (LOQ) were calculated by the calibration curve method (Shrivastava et al., 2011) and limit of detection (LOD) were estimated by dividing LOQ by 3.

All chemical analyses were performed at CEDRE.

2.5.7 Statistical analysis

2.5.7.1 Micro plankton

Analysis of variance (ANOVA) was used for comparison of computed mean values of each replica on measurements of pH, nutrients, PAH, and biomass of organisms among the treatments. If ANOVAs were significant, pairwise comparisons of pooled standard deviations using Benjamini and Hochberg's test of variability were performed. All data were normally distributed (Shapiro-Wilk test), and did not require transformations. The homogeneity of variances was tested using Levene's test. These analyses were performed in RStudio, and the level of significance used was 0.05.

2.5.7.2 Copepods

Data was tested for normal distribution using the Shapiro-Wilks test and, transformed by square root or power two if they were not normally distributed. Data was tested for equal variance using Bartlett's test, or Levene's test in case of non-normal distribution. Analyses of Variance (one-way ANOVA) with Dunnett's post hoc test were used for the average specific faecal pellet and egg production rates (SPP and SEP) of control and exposed organisms, as well as for hatching success. Where there was no homogeneity of variance, one-way ANOVA with Welch's correction was performed. When data was not normal distributed Kruskal-Wallis test was performed. Calculations were performed using the R 3.2.1 software and a significance level of $\alpha = 0.05$ was used in all statistical tests.

2.6 Light penetration, nutrients and ice-algal growth

2.6.1 Experimental design and sampling

The mesocosms consisted of an open-ended circular aluminum frame with semi-rigid, opaque side walls designed to prevent lateral exchange with the surrounding water (Figure 11). The mesocosms were deployed in late February 2015 through holes made in young ice. The four experimental conditions included an unaltered control (mesocosms i and j), 20 liters of crude Kobe oil (mesocosms a and b), a mixture of 20 liters of Kobe Oil and Finasol dispersant (mesocosms c and d), and the residue obtained after burning of 20 liters of crude Kobe oil (mesocosms e and f), all in duplicates. The treatments were applied to surface water inside the ice-free mesocosms in February, after which the ice was allowed to grow for ca. 1 month before the first sampling. In each of the eight mesocosms we collected ice cores from the top with a Kovacs mark II ice corer (diameter of 9 cm). The bottom 5 cm of each core was sectioned and retained for the determination of nutrients, chlorophyll a, the elemental composition of organic matter, the taxonomic composition of microalgae as well as the estimation of primary production rates on 26 March (T1), 14 April (T2) and 6 May (T3). Before processing, the cores were slowly melted in the dark with filtered seawater to minimize osmotic stress (1 part ice for 3 parts of water). Nutrients were also measured in the surface water used to dilute the melting ice cores.

2.6.2 Light measurements

Photosynthetically available irradiance (PAR) at the ice-water interface in the experimental mesocosms was measured with a Seabird ECO-PAR cosine sensor mounted on an articulated pole. To avoid the confounding effect of variable snow covers and incident solar radiation, the

snow was cleared before taking the measurement and all mesocosms were measured within minutes of each other. The pole was lowered through the hole left by the ice corer, the articulated section was bent to place the probe away from the hole and measurements were taken during a 360° rotation of the sensor. The data presented below represent the average of all data for a full rotation.

2.6.3 Nutrient measurements

Samples were filtered through GF/F filters, collected in acid-cleaned 15 ml polyethylene tubes and stored frozen until analysis at the home laboratory (Laval University). The concentration and composition of major inorganic nutrients (nitrate, phosphate, silicate) were measured on the preserved samples using routine colorimetric techniques according to Martin et al., (2010). Ammonium was measured in the field using the sensitive fluorometric method of Holmes et al., (1999).

2.6.4 Pigments and particulate organic matter

Samples for the determination of pigments (chl a), particulate organic carbon (POC), and total particulate nitrogen (TPN) were collected on GF/F filters. All filters except those for pigments were dried in a field oven for 24 hours at 60°C. Pigment concentrations were determined at UNIS with the fluorometric method (Parsons et al., 1984a). At the home laboratory, POC and TPN filters were combusted in a CHN elemental analyzer (Costech ECS-4010) and the total amounts of C and N as well as their stable isotopic compositions were determined by mass spectrometry (Thermo Finnigan Delta Plus Advantage) using the methods described in Pineault et al., (2013).

2.6.5 Algal taxonomy

Melted ice samples for cell enumeration and identification were preserved with acidic Lugol's solution (Parsons et al., 1984a) and stored in the dark at 4°C until analysis. Cells $\geq 2 \mu\text{m}$ were identified to the lowest possible taxonomic rank using inverted microscopy (Zeiss Axiovert 10) according to Lund et al., (1958). At least 400 cells were enumerated at a magnification of 400X (Lund et al., 1958) in each 50 mL settling chamber. The abundance of each taxon was computed according to the equation of Horner (2002). The limit of detection was 40 cells mL^{-1} . The main references used for cell identification were Poulin and Cardinal (1982), Medlin and Hasle (1990), Poulin (1991), Tomas (1997), Bérard- Therriault et al., (1999), von Quillfeldt (2001), and Throndsen et al., (2007). The sample from mesocosm A at T3 was anomalous (unusual aggregation which rendered homogenization difficult) and excluded from analyses.

2.7 Sea Surface Layer Microbial Community

2.7.1 Experimental Setup

The experiments were conducted in six pairs of rectangular holes referred to as "enclosures" for the rest of this report), which were cut in the sea ice on 5/12/15. Each enclosure was 40 cm x 55 cm, and fitted with plastic (polypropylene) boxes that had bottoms cut-out in order to confine the area of the experiment. The boxes were dug down into the snow and a few cm into the ice, in order to freeze into the ice (Figure 11). Within the area covered by each box, a bottom layer of sea ice was left that was then drilled through with several 20 cm-diameter holes, allowing seawater

to fill the box. At the time of construction of these enclosures, the air temperature was above freezing, preventing re-freezing of seawater that entered the enclosures.

Lids made of UV-transparent foils (ACLAR® embedding film, 7.9 mil thick, Ted Pella inc, Redding, CA) were placed on top of the plastic boxes to prevent slush build up from blown snow while allowing oil photochemistry. A polycarbonate tube (2.22 cm ID, 61 cm length) fastened to the inside of each box allowed for sampling of bulk seawater underneath the surface layer at a depth of 50 cm.

The experimental design avoided the accumulation of snow from extensive drift (i.e., depending on the wind, enclosure holes could be filled with snow within hours). In addition, snow on top of the ice is very heavy such that seawater can come up through the hole and flood the surface of the ice with approx. 5 – 10 cm water layer; this results on a snow-water-air, rather than the desired ice-water-air, boundary, with subsequent slush formation that were not part of our experimental design.

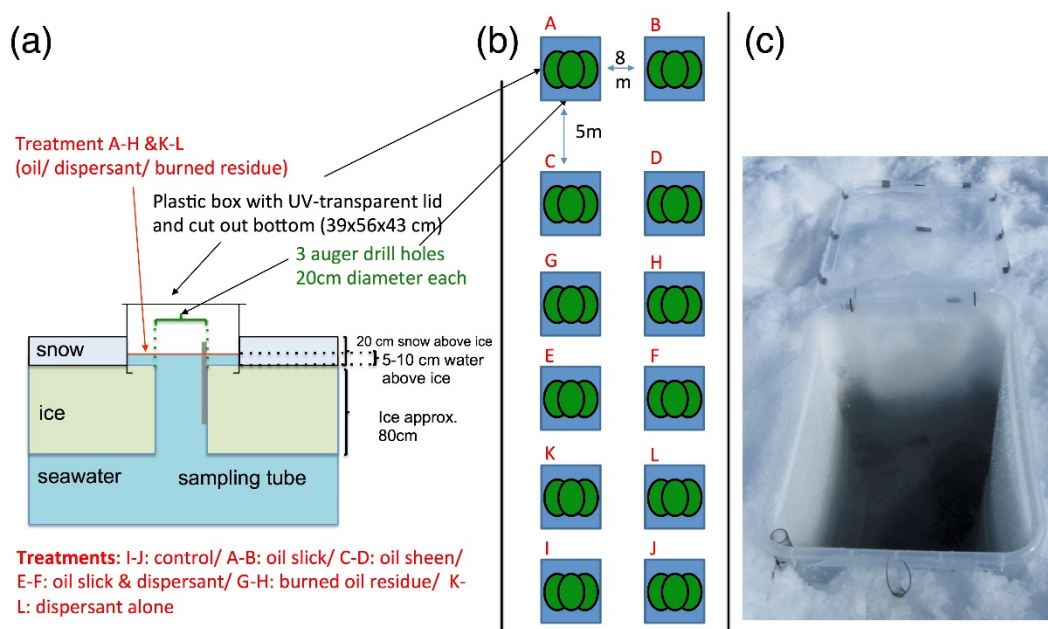


Figure 11 (a) Experimental setup (left) showing an enclosure cut into the ice and bounded by a clear plastic box with a cover (further details in text). (b) Experimental design (right) shows the physical layout in duplicate of the control and the five treatments applied; the green ovals show the three overlapping holes drilled at the bottom of each enclosure (see details in text) that allow subsurface water to naturally fill each enclosure. Treatments are: oil slick (A, B), oil and dispersant (C, D), burned oil residue (E, F), oil sheen (G, H), control (I, J), dispersant-only (K, L). (c) Picture of the setup in the field.

This box-bound sea ice enclosure design prevented (i) the various treatments (oil, oil with dispersants, burned oil, dispersant-only) from leaching into the surrounding snow/slush layer, (ii) slush formation, and –importantly – (iii) seals from disturbing the experiments, while, simultaneously, it maximized the probability of sampling the water-ice-air interface. These adaptations were done in discussion with Akvaplan-niva and approved by the IOGP before field deployment.

2.7.2 Sampling

Sampling occurred at Day 0 (D0; immediately before application of the treatments), Day 1 (D1; 12h after application of the treatment), Day 3 and Day 5 (Figure 12). Samples were stored cold and dark until subsampling, extraction or filtration in the laboratory.

(i) Surface Layer. Surface layer water was collected using glass plates (30 x 46 cm, with chemically-resistant plastic handles) and transferred to glass jars using silicon blades. Each enclosure was sampled with an individual, clean glass plate; prior to each sampling time, glass plates were cleaned with detergent, rinsed with water, soaked in alcohol, rinsed with Milli-Q® water, air dried and stored in individual plastic bags. If oil was part of the surface layer sample, a sample of the oil phase was also taken.

(ii) Subsurface Water. Subsurface water (50 cm below sea surface) was collected with a hand vacuum pump connected to polytetrafluoroethylene (PTFE) hoses into 250-mL glass bottles (for hydrocarbon extraction) and 500-mL plastic bottles (for DNA extraction and flow cytometry). The PTFE hoses were guided through sampling tubes installed in the plastic boxes (Fig. 11) prior to application of the treatments to prevent contact of the surface treatment (oil, dispersant) with the PTFE hoses.

		D0 (5/12)	D1 (5/13)	D3 (5/15)	D5 (5/17)
oil (1cm)	A		x	x	x
	B				
			x	x	x
oil (1mm)	G		x	x	x
	H			x	x
			x	x	x
oil & dispersant	C		x	x	x
	D				
			x	x	x
burnt residue	E		x	x	x
	F		x	x	x
			x	x	x
dispersant only	K		x	x	x
	L		x	x	x
			x	x	x
control	I	x	x	x	x
	J				
		x	x	x	x

Figure 12 Sampling scheme.

2.7.3 Experimental Treatments

Five treatments were applied into pairs of replicate enclosures. These included:

1. addition of Kobbe light crude oil as an oil slick (1.7L of crude oil to a final thickness of ~1 cm; enclosures A, B);
2. an oil sheen (100mL of crude oil to a final thickness of ~10 mm; enclosures G, H);
3. oil pre-mixed with dispersant before the mixture was applied to the water surface (1.7L crude and 850 mL Finasol OSR52, from Total Special Fluids in a 20:1 ratio; enclosures C, D);
4. burned oil residue (100mL; enclosures E, F);
5. In addition, two sets of paired control enclosures were prepared by addition of dispersant-only (850 mL dispersant per 1 m²; enclosures K, L) and without any additions (enclosures I, J). The burned oil was prepared by Cedre (Brest, France) off-site in a special facility. This burning process removed approx. 85% mass of the Kobbe crude oil (personal communication, S. Le Floche, Cedre, Brest/France).

2.7.4 Sample Preparation and Analytical Methods

(i) Phytoplankton and Bacterial Abundance: 1 mL of sample was transferred into 2-mL cryo vials pre-loaded with 50 μ L paraformaldehyde (10%) (Vaulot et al., 1989). The samples were incubated at 4°C for 1 hour, and then transferred into a -80°C freezer. The samples were transported to Bigelow Laboratory for Ocean Sciences on dry ice and stored at -80°C until analysis. Samples were analyzed for the cell density of heterotrophic bacteria and pico/nanophytoplankton using flow cytometry (Sieracki et al., 2005).

(ii) Bacterial Community Analysis: 50 mL to 1,000 mL of samples were filtered through 0.20 μ m cellulose nitrate filters. The filters were placed in cryovials and immediately transferred into a -80°C freezer. The samples were shipped to Bigelow Laboratory for Ocean Sciences on dry ice and stored frozen (-80°C). DNA was extracted using PowerSoil® DNA isolation kits (MO BIO Laboratories, Carlsbad, CA) sent to Research and Testing Laboratories (Lubbock, TX) for 16S rRNA genes amplification, Illumina® sequencing, and bacterial community composition assignment (Degnan and Ochman 2012).

(iii) Hydrocarbon Analysis: Samples were liquid/liquid extracted with dichloromethane and shipped to Bigelow Laboratory for Ocean Sciences. A recovery standard was added (o-terphenyl) and the volume of the solvent was reduced to approx. 1 mL. Sub-samples were transferred into gas chromatography (GC) vials equipped with 200 μ L inserts. An internal standard mixture was added (containing deuterated PAHs and alkanes), and select PAHs (naphthalene and phenanthrene and their alkylated congeners) were quantified using GC/MS (Aeppli et al., 2012). In addition, select samples were analyzed on comprehensive two-dimensional gas chromatography coupled to a flame ionization detector (GC \times GC-FID) according to previously published methods (Aeppli et al., 2014).

2.8 Polar cod

2.8.1 Fish collection and husbandry

Wild polar cod were collected in Svalbard fjords in September 2014 by bottom trawl during a cruise aboard the RV Helmer Hanssen and thereafter transported to the Akvaplan-niva marine laboratory in Tromsø, Norway. The fish were reared in a single common 5000 L tank for an eight-month acclimation and maintain period and hand fed twice a week on a commercial marine fish feed (ration equal to 4% body weight per feeding; Skretting, 3-4 mm dry pellets). The light regime was maintained on a simulated Svalbard light throughout acclimation, exposure and post-exposure periods. The seawater temperature in the tank followed the annual variation of Grøtsundet, the fjord outside the marine laboratory where seawater was collected from 50 m depth, with a high of $8.6 \pm 0.1^\circ\text{C}$ in September and low of $3.74 \pm 0.02^\circ\text{C}$ in February and yearly average of $6.2 \pm 0.1^\circ\text{C}$. Oxygen saturation was kept above 90% for acclimation and post-exposure period. On the 19th of May 2015, all fish (n=310) were anesthetized (Metacaine at 0.08 g/L seawater) and received a passive integrated transponder tag (Trovan®) inserted intraperitoneally with no mortality or negative effects observed in the first weeks post tagging.

2.8.2 Exposure design

The exposure commenced in late June 2015 and growth was followed over a seven-month period (i.e. until January 2016) coincident with the active vitellogenesis/ spermatogenesis period of polar cod (Bender et al., 2016). The dispersant mixtures were generated according to Frantzen et al., (2015, 2016) following the protocol developed by Cedre, France for the DISCOBIOL project (e.g. Milinkovitch et al., 2011). The set-up consisted of four treatments and three replicates per treatment; control (no oil, Ctrl), mechanically dispersed oil (MDO) or chemically dispersed oil (CDO; premixed with dispersant FINASOL®; 5% w/w) and burned oil residues (BO). The BO was prepared using the whole oil residue from an artificially burned crude oil (Cedre) and its concentration equaled 10% of the nominal oil concentration used in the mechanically and chemically dispersed oil treatments. The initial concentration of the BO treatment is reduced compared to the MDO and CDO treatment as it is assumed that 90% of the oil would be burned off with only 10% remaining in the water (Buist et al., 2013). For directly comparison between dispersed oil toxicity (MDO, CDO) and BO toxicity, the same exposure protocol was used for all treatments. The oil used in these experiments was Goliat (Kobbe) crude oil which is a sweet light crude oil with a density of 0.83 kg /L, an °API gravity of 40.3 and a sulphur content of 0.14% wet weight (Eni Norge, 2015).

Briefly, the oil treatments (MDO and CDO; nominal concentration of 67 mg/L) or BO (nominal concentration of 6.7 mg/L) were introduced to individual 120 L exposure tanks through a funnel fixed at the surface. A pump in the bottom of each tank provided fixed and continuous mixing energy in all tanks. In order to ensure a homogeneous exposure mixture in the tanks and to allow some weathering of the oil to take place prior to exposure start, water and oil/ oil premixed with dispersant/ BO were mixed for 24 hours before the introduction of fish to the system. The water system was static and oil exposures were conducted for 48 hours after the introduction of the animals (water temperature 6.4 ± 0.3 °C and O₂ saturation was held >80% with aide of aerators). In total, 236 specimens were transferred to the exposure tanks (n=18-20 fish per replicates) and exposure occurred from the 26th to the 28th of June 2015. After 48 hours, all fish from each treatment were transferred to individual 500 L flow-through tanks supplied with clean seawater for two days before being growth registered (T1 on June 30th; see section 2.3). The fish were fasted two days prior to exposure start, during the 48h exposure period, and two days prior to every growth measurement.

2.8.3 THC and PAHs in seawater

Water samples (approximately 1L) were taken from all exposure tanks (n=3 per treatment) at the beginning of the experiment (t 0h), after 24 hours (t 24h), and at the end of the 48h exposure (t 48h). Analysis of total hydrocarbon content (THC) and 26 PAHs (16 Environmental Protection Agency [EPA] priority parent PAHs and C1–C3-alkylated naphthalenes, phenanthrenes and dibenzothiophenes) concentrations followed the protocol by Frantzen et al., (2016) using Gas Chromatography-Flame Ionization Detector and Gas Chromatography–Mass Spectrometry for THC and PAH quantification, respectively. The measured THC and PAH concentrations represent dissolved components as well as oil droplets. In the determination of $\Sigma 26$ PAH concentrations, single components with values below the limit of detection (LOD) were assigned a value of zero. Due to a technical instrument failure, water samples from t0h at the start of the exposure gave unreliable results and were excluded from further analysis.

2.8.4 Post-exposure monitoring and final sampling

The 48h exposure period was followed by a 48h recovery period in 500 L flow-through tanks and subsequent growth registration (T1; see paragraph below) before the fish were transferred back to the common 5000 L rearing flow-through tank. The common tank ensured identical post-exposure rearing conditions for all treatment and replicate groups (including unexposed fish remaining in the tank).

Mortality was recorded daily over the entire experiment. Growth was recorded at monthly intervals by first anesthetizing, then measuring the total weight (± 0.01 g) and total length (± 0.1 cm) at the following time points: T0 (May 19th, pit tagging), T1 (June 30th, 2 days post-exposure), T2 (July 30th), T3 (Sept. 3rd), T4 (Oct. 5th), T5 (Nov. 3rd), T6 (Dec. 9th), T7 (Jan. 5th). An additional group of "unexposed" polar cod was included in the common rearing tank which consisted of the remaining acclimation fish that fell below (Unexp. 1) and above (Unexp. 2) the desired intermediate size range and were therefore not included in the exposure experiment ($n=74$). These additional unexposed fish provided a control for experimental handling stress related to the exposure with growth measurements undertaken at T0, T2-T7 (excluded from T1 due to logistical limitations).

On the 5th of January, all remaining experimental fish and the unexposed fish, were sacrificed by a sharp blow to the head and the following measurements were collected: total length (± 0.1 cm), total weight (± 0.01 g wet weight [wwt]), sex, gonad weight (± 0.01 g wwt), liver weight (± 0.01 g wwt) and somatic weight (empty carcass weight, ± 0.01 g wwt). The middle section of the testis and ovaries were fixed in a buffered formaldehyde solution (4%) for later histological analysis. Otoliths were collected for age determination and read under a dissection microscope (Leica M205C).

Specific growth rate (SGR) for individual fish for the entire experimental period was determined according to the equation:

$$SGR = [(\ln tW2 - \ln tW1) / t - 1] 100$$

where SGR is % increase in body weight per day. $tW1$ and $tW2$ are the total weights of the fish recorded at times 1 and 2 respectively, and t is the number of days between weighting events.

Gonadosomatic index (GSI) and hepatosomatic index (HSI) were calculated according to the following equations:

$$GSI = (\text{gonad weight} / \text{somatic weight}) * 100$$

$$HSI = (\text{liver weight} / \text{somatic weight}) * 100$$

Condition factor for the different time points (T0-T7) was calculated:

$$CF = (W / L^3) * 100$$

where W is total weight in g and L is the total length in cm.

2.8.5 Histological analysis

Briefly, gonad tissues were rinsed of buffered formalin, dehydrated in a series of 70% ethanol baths and embedded in paraffin wax (Aldrich, USA) overnight using Histo-clear® as a clearing agent in a Shandon Citadel 1000 (Micron AS, Moss, Norway). Tissues were then embedded into paraffin and sliced at 5 μm (females) and 3 μm (males) thickness, using a Leica RM 2255 microtome

before being stained with haematoxylin and eosin. Two slides were prepared for each fish. Gonad maturity stages in females were classified using the development stage of oocytes within the respective categories of immature, resting, and early and advanced stages of maturation. Immature and resting females had only primary growth (PG) oocytes while maturing females had vitellogenic oocytes present. Resting females were identified by the presence of residual oocytes from previous spawning events with otherwise only PG oocytes. Maturing females exhibited different phases of oocyte development with varying extents of vitellogenin derived oil droplets in the oocyte cytoplasm (Figure 4ab). Oil droplets were present but filling less than $\frac{1}{2}$ of the cytoplasm in early maturing females while advanced females had oocytes completely filled or nearly filled with oil droplets. Abnormal oocyte development was noted with regard to the location of cortical alveolar vesicles and oil droplet within the oocyte. Oocyte diameter ($n \geq 3$ oocytes per slide) was counted for oocytes in the most advanced cohort on both slides then averaged for each female using the image processing software (Leica DFC 295 camera attached to a Leica DM 2000 LED microscope and Leica analysis software). Oocyte stage frequency disruption was determined by classifying all oocytes with a nucleus in area of 20 mm² placed randomly on the tissue slice. Frequency counts were averaged over both replicate slides. Presence of residue oocytes was noted and relative frequencies atretic oocytes were semi-quantified using a 0-3 scale ranging from absent (0% of oocytes were atretic) to obvious (20-30% of oocytes were atretic) for each female. Male testes were classified into the four different maturity stages of immature, resting, and maturing with late spermatocytes stage I or with late spermatocytes stage II.

2.8.6 Statistical Analysis

All statistical analyses were performed with R 3.1.1 (R Core Team, 2014). A Levene's test was used to test for normality and homogeneity of variance. When homogeneity criteria were met, a one-way analysis of variance (ANOVA) was used, and when a significant treatment effect was found, the Tukey's HSD post hoc for unequal sample sizes was used to distinguish differences between treatment groups. In cases where homogeneity criteria were not met, a nonparametric Kruskal Wallis ANOVA was used, followed by a multiple comparison of mean rank of all group tests. Difference in variance was tested using an F-test. Maturity stage frequency distributions were tested using a Fishers exact test with the null hypothesis that all treatments have similar maturity stage distributions. With a significant Fishers exact test result, a chi squared test was run comparing all treatment groups and control against one another. A probability level of $p \leq 0.05$ was considered significant for all tests. All values are presented as mean \pm standard error of the mean (SE).

3 RESULTS

3.1 Plankton

3.1.1 Exposure and effects of oil spill treatments on micro plankton

3.1.1.1 The effect on biotic factors in winter

In winter, temperature, salinity, light intensity, and pH concentration in the post exposure studies in the laboratory varied little among the treatments, although the pH levels increased on an overall level in all treatments during the experiments (Table 6). However, no significant differences in pH were found among the treatments (ANOVA, $p > 0.05$). The air and water temperatures remained stable over time, with the average temperatures of 1.05 ± 0.26 °C and 1.00 ± 0.00 °C, respectively. The salinity measured 33.8, and the light intensity at the water surface in the experimental bottles was 55 ± 12 $\mu\text{mol photons m}^{-2} \text{s}^{-1}$. Concentration of inorganic nutrients (nitrate NO_3^- , phosphate PO_4^{3-} and silicate Si(OH)_4) decreased in all treatments during the experiments (Table 6), yet, no significant differences were found among the treatments for any nutrient specimen (ANOVA, $p > 0.05$). Concentration of sum of 21 polycyclic aromatic hydrocarbon (PAH) also decreased over time in all treatments (Table 6), however, the sum PAH concentrations in the water samples significantly differed among the treatments (ANOVA, $p < 0.05$). The concentrations of sum PAH were significantly higher in dispersed oil and crude oil treatments than in control or burnt oil treatments (t-test, $p < 0.05$), but were not significantly different between the former two groups (t-test, $p > 0.05$). Similarly, no significant differences in the sum PAH concentrations were found between control and burnt oil (t-test, $p > 0.05$).

Table 6 The average concentrations \pm SD of pH, nutrients (nitrate, phosphate, silicate; $\mu\text{M L}^{-1}$), and sum of 21 PAHs (ng L^{-1}) on Day 0 and Day 14 in post exposure laboratory experiments with water from control, burnt oil, oil+dispersant, and crude oil mesocosm water sampled in March 2015.

Treatment	Time	Winter concentration ($\mu\text{M L}^{-1}$ for nutrients; ng L^{-1} for PAH)				
		pH	Nitrate	Phosphate	Silicate	PAH
Control	Day 0	7.56 ± 0.00	7.59 ± 0.69	0.55 ± 0.07	4.74 ± 0.24	100 ± 123
	Day 14	7.68 ± 0.03	6.21 ± 0.37	0.32 ± 0.07	4.24 ± 0.59	55 ± 62
Burnt oil	Day 0	7.56 ± 0.00	7.34 ± 0.58	0.40 ± 0.08	3.87 ± 0.19	65 ± 19
	Day 14	7.65 ± 0.02	6.36 ± 0.54	0.36 ± 0.06	4.83 ± 0.67	35 ± 18
Oil + dispersant	Day 0	7.61 ± 0.00	7.00 ± 0.39	0.45 ± 0.21	4.36 ± 0.56	624 ± 39
	Day 14	7.63 ± 0.02	5.45 ± 0.21	0.29 ± 0.15	4.68 ± 0.98	311 ± 85
Crude oil	Day 0	7.61 ± 0.00	6.70 ± 0.96	0.48 ± 0.04	4.08 ± 0.22	615 ± 275
	Day 14	7.65 ± 0.01	5.68 ± 0.80	0.35 ± 0.17	4.42 ± 0.31	249 ± 33

3.1.1.2 The effect on abiotic factors in spring

In spring, temperature, salinity, and light intensity also varied little among the treatments. The average air and water temperatures were 1.04 ± 0.26 °C and 1.00 ± 0.00 °C, respectively. The salinity of 31.9 ‰ or PSU was measured, and the light intensity at the water surface in the experimental bottles was 57 ± 8 $\mu\text{mol photons m}^{-2} \text{s}^{-1}$. The pH concentrations decreased in all treatments over time (Table 7); however, significant differences in pH among the treatments were found (ANOVA, $p < 0.05$). The levels of pH were significantly lower in all treatments compared to

the control group. Significant differences were also found among the other treatments, except for the pair burnt oil – crude oil (t-test, $p < 0.05$).

Overall, the concentration of nutrients and sum PAH decreased in all treatments during the experiments (Table 7). Significant differences were found in nutrient concentrations among the treatments (ANOVA, $p < 0.05$). The nitrate concentration was significantly lower in the control group compared to dispersed oil and crude oil treatments (t-test, $p < 0.05$). Significant differences were also found between all the other treatment pairs (t-test, $p < 0.05$), with the highest concentration of nitrate measured in crude oil treatment, followed by dispersed oil, and finally by burnt oil and control.

Similarly, the phosphate concentration was significantly lower in the control group compared to the other groups (t-test, $p < 0.05$). Significant differences were found among all the other treatments (t-test, $p < 0.05$), except between burnt oil and dispersed oil treatments. The highest concentration of phosphate was measured in crude oil, followed by dispersed oil and burnt oil treatments, and lastly by the control group. Finally, the concentration of silica was again significantly higher in the crude oil compared to the other three groups (t-test, $p < 0.05$). No significant differences were found between any other treatment combinations. Moreover, significant differences were found in the sum PAH concentration among the treatments (ANOVA, $p < 0.05$). The lowest concentrations of sum PAH were measured in control and burnt oil treatments, which were not significantly different (t-test, $p > 0.05$), but were significantly lower than the concentrations found in dispersed oil and crude oil groups (t-test, $p < 0.05$). Additionally, in terms of sum PAH concentration, dispersed oil and crude oil treatments were also significantly different (t-test, $p < 0.05$).

Table 7 The average concentrations \pm SD of pH, nutrients (nitrate, phosphate, silicate; $\mu\text{M L}^{-1}$), and PAH (ng L^{-1}) on Day 0 and Day 14 in post exposure laboratory experiments with water from control, burnt oil, oil+dispersant, and crude oil mesocosm water sampled in April 2015.

Treatment	Time	Spring concentration ($\mu\text{M L}^{-1}$ for nutrients; ng L^{-1} for sum of 21 PAHs)				
		pH	Nitrate	Phosphate	Silicate	PAH
Control	Day 0	7.65 \pm 0.00	5.32 \pm 0.96	0.24 \pm 0.04	3.40 \pm 0.67	90 \pm 70
	Day 14	7.58 \pm 0.03	4.33 \pm 0.36	0.26 \pm 0.03	3.18 \pm 0.15	27 \pm 15
Burnt oil	Day 0	7.63 \pm 0.00	5.94 \pm 0.66	0.45 \pm 0.07	3.88 \pm 0.54	261 \pm 62
	Day 14	7.49 \pm 0.03	4.51 \pm 0.11	0.31 \pm 0.08	2.88 \pm 0.17	59 \pm 51
Oil+dispersant	Day 0	7.60 \pm 0.00	6.47 \pm 0.13	0.45 \pm 0.03	3.76 \pm 0.17	20,269 \pm 4,219
	Day 14	7.47 \pm 0.02	5.19 \pm 0.07	0.34 \pm 0.01	2.86 \pm 0.00	9,519 \pm 3,620
Crude oil	Day 0	7.62 \pm 0.00	8.05 \pm 0.13	0.66 \pm 0.11	5.15 \pm 1.08	2,190 \pm 1,152
	Day 14	7.50 \pm 0.02	7.79 \pm 0.28	0.61 \pm 0.05	4.02 \pm 0.04	1,421 \pm 651

3.1.1.3 The effect on community succession in winter

In all four treatments, bacteria and heterotrophic-nanoflagellates grew exponentially as a function of time, with an acclimation period of 4 days observed in the bacterial growth (Figure 13A and 13C). However, significant differences in bacterial and HNF biomass were observed among the treatments (ANOVA, $p < 0.05$; Table 8). The biomass of bacteria in control and oil+dispersant treatments were significantly higher compared to the biomass in burnt oil and crude oil groups (t-test, $p < 0.05$). The differences in bacterial biomass between control and oil+dispersant groups were insignificant (t-test, $p > 0.05$), and the differences in biomass between burnt oil and crude oil treatments were insignificant as well (t-test, $p > 0.05$). The highest biomass of HNF was found

in the control group, which was significantly different from the HNF biomass in the other three treatments (t-test, $p < 0.05$). The biomass of HNF in burnt oil, oil+dispersant, and crude oil were not significantly different among each other (t-test, $p > 0.05$). As opposed to the exponential growth of bacteria and HNF, dinoflagellates grew linearly as a function of time (Figure 13E). There were no significant differences in biomass of dinoflagellates among the treatments (ANOVA, $p > 0.05$; Table 8). Ciliates overall ceased to establish a growing population in the treatments, with more or less comparable biomass among the groups (Figure 13G; ANOVA, $p > 0.05$; Table 8). Photosynthetic picoplankton grew exponentially as a function of time, with a long acclimation period (6 – 8 days; Fig. 14A). However, no significant differences were found in the picophytoplankton biomass among the treatments (ANOVA, $p > 0.05$; Table 8). The growth of nanophytoplankton and diatoms followed a linear function (Fig. 14C and E), with no significant differences in the biomass among the treatments of either of the two groups (ANOVA, $p > 0.05$; Table 8).

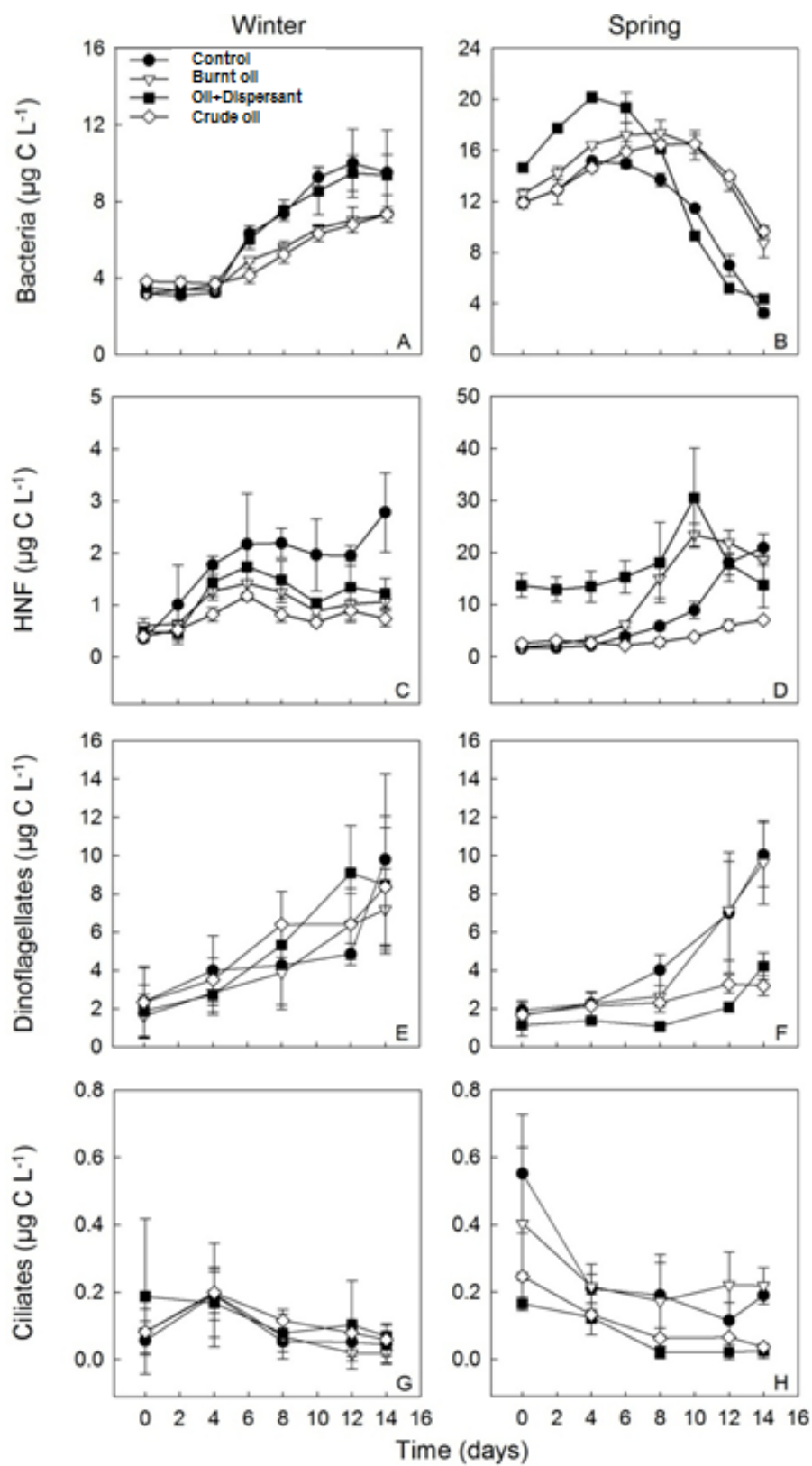


Figure 13 The mean biomass ($\mu\text{g C L}^{-1}$) of (A-B) bacteria, (C-D) HNF, (E-F) dinoflagellates, and (G-H) ciliates in the control, burnt oil, oil+dispersant, and crude oil treatments in winter (left) and spring (right). Error bars represent ± 1 SD.

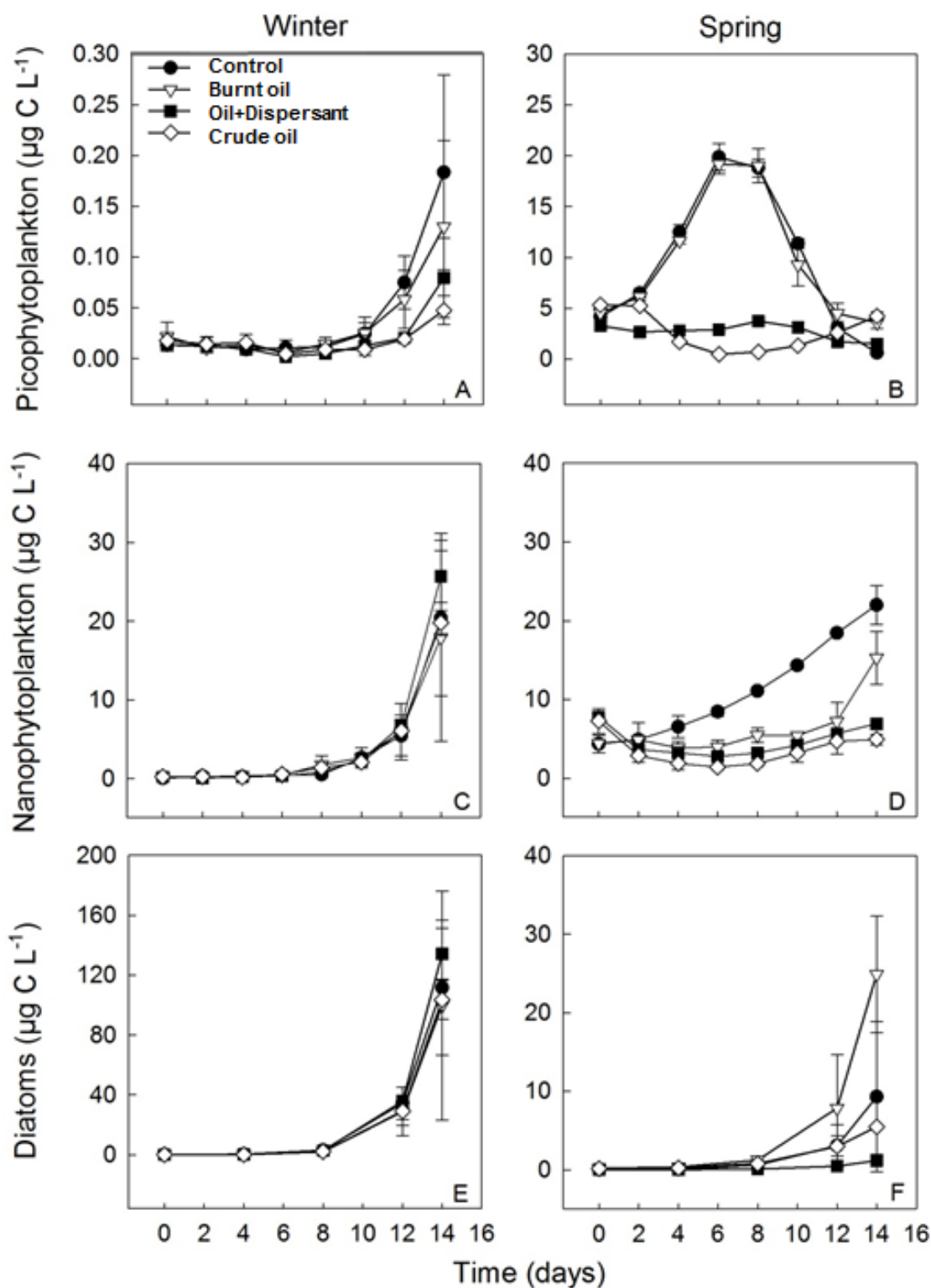


Figure 14 The mean biomass ($\mu\text{g C L}^{-1}$) of (A-B) picophytoplankton, (C-D) nanophytoplankton, and (E-F) diatoms in the control, burnt oil, oil+dispersant, and crude oil treatments in winter (left) and spring (right). Error bars represent ± 1 SD.

Table 8 The effect of burnt oil, dispersed oil, and crude oil treatments on the biomass of various organism groups in winter. Negative effect – the biomass of a specific organism group was lower in a particular oil treatment than in the control. Positive effect – the biomass of a specific organism group was higher in a particular oil treatment than in the control. No effect – the biomass of a specific organism group in a particular oil treatment did not differ from the biomass in the control.

Winter			
Organism group	Control vs Burnt oil	Control vs oil+dispersant	Control vs Crude oil
Bacteria	Negative effect	No effect	Negative effect
HNF	Negative effect	Negative effect	Negative effect
Dinoflagellates	No effect	No effect	No effect
Ciliates	No effect	No effect	No effect
Picophytoplankton	No effect	No effect	No effect
Nanophytoplankton	No effect	No effect	No effect
Diatoms	No effect	No effect	No effect

3.1.1.4 The effect on community succession in spring

In all treatments, bacteria grew linearly at first, and after 6 – 10 days the biomass started decreasing until the end of the experimental period (Figure 13B). Significant differences in the bacterial biomass were found among the treatments (ANOVA, $p < 0.05$; Table 8). The biomass of bacteria in the control group was significantly lower compared to the oil treatments (t-test, $p < 0.05$). Significant differences in the bacterial biomass were also observed among all the other treatment combinations (t-test, $p < 0.05$), with the highest biomass found in burnt oil, followed by crude oil and oil+dispersant treatments, and finally by control. In all four treatments, the growth of heterotrophic- nanoflagellates followed linear function (Figure 13D). Significant differences in the HNF biomass were observed among the groups (ANOVA, $p < 0.05$; Table 8). The biomass of HNF in control and burnt oil treatments was significantly lower than the biomass in oil+dispersant (t-test, $p < 0.05$), but significantly higher compared to the biomass in crude oil (t-test, $p < 0.05$). The biomass in control and burnt oil groups was not significantly different (t-test, $p > 0.05$). The highest biomass was observed in oil+dispersant treatment, followed by control and burnt oil, and finally by crude oil treatment. The growth of dinoflagellates followed a linear function in all the treatments (Figure 13F), yet, the biomass differed significantly among the groups (ANOVA, $p < 0.05$; Table 8). The biomass of dinoflagellates in control and burnt oil groups was significantly higher than the biomass in oil+dispersant and crude oil treatments (t-test, $p < 0.05$). However, the difference in the dinoflagellates biomass between the former two groups was insignificant (t-test, $p > 0.05$), and similarly, the difference in the biomass between oil+dispersant and crude oil treatments was insignificant as well (t-test, $p > 0.05$). The biomass of ciliates was decreasing during the first four days in all four treatments, which later stabilized in control and burnt oil groups, but kept decreasing in oil+dispersant and crude oil treatments (Figure 13H). The ciliates biomass in control and burnt oil treatments was significantly higher compared to the biomass in oil+dispersant and crude oil groups (t-test, $p < 0.05$). No significant differences were found between the biomass in control and burnt oil treatments, and between oil+dispersant and crude oil treatments (t-test, $p > 0.05$).

The biomass of picophytoplankton in control and burnt oil treatments was increasing linearly during the first week, and then started decreasing until the end of the experimental period (Figure 14B), however, the biomass between the two treatments did not differ significantly (t-test, $p > 0.05$; Table 9). On the other hand, the picophytoplankton communities in oil+dispersant and crude oil treatments ceased to establish growing populations altogether, with no significant

difference between the biomass in the two groups (t-test, $p > 0.05$; Table 9). The picophytoplankton biomass in control and burnt oil groups was significantly higher than the biomass in oil+dispersant and crude oil treatments (t-test, $p < 0.05$). The nanophytoplankton biomass was increasing linearly in all four treatments, however, an acclimation period of approximately 6 days was observed in the oil treatments (Figure 14D). Significant differences in the biomass of nanophytoplankton were observed among the groups (ANOVA, $p < 0.05$; Table 9). The biomass of nanophytoplankton in the control group was significantly higher compared to the oil treatments (t-test, $p < 0.05$). Significant differences in the nanophytoplankton biomass were also observed among all the other treatment combinations (t-test, $p < 0.05$), except for the combination oil+dispersant – crude oil (t-test, $p > 0.05$). The highest biomass was found in control, followed by burnt oil, and finally oil+dispersant and crude oil treatments. The growth of diatoms followed a linear function in all the treatments (Figure 14F), however, significant differences in the biomass were found (ANOVA, $p < 0.05$; Table 9). The highest biomass was observed in burnt oil treatment, and was significantly higher than the biomass in the other three treatments (t-test, $p < 0.05$). No significant differences were observed among any other treatment combination (t-test, $p > 0.05$).

Table 9 The effect of burnt oil, oil+dispersant, and crude oil treatments on the biomass of various organism groups in spring. Negative effect – the biomass of a specific organism group was lower in a particular oil treatment than in the control. Positive effect – the biomass of a specific organism group was higher in a particular oil treatment than in the control. No effect – the biomass of a specific organism group in a particular oil treatment did not differ from the biomass in the control.

SPRING			
Organism group	Control vs Burnt oil	Control vs oil+dispersant	Control vs Crude oil
Bacteria	Positive effect	Positive effect	Positive effect
HNF	No effect	Positive effect	Negative effect
Dinoflagellates	No effect	Negative effect	Negative effect
Ciliates	No effect	Negative effect	Negative effect
Picophytoplankton	No effect	Negative effect	Negative effect
Nanophytoplankton	Negative effect	Negative effect	Negative effect
Diatoms	Positive effect	No effect	No effect

3.1.2 Exposure and effects of oil spill treatments on copepods

3.1.2.1 The effect on grazing activity

The average faecal pellet production rate for *C. glacialis* for all treatments was 25.4 faecal pellets female⁻¹ day⁻¹ during in March and 23.7 in May respectively. The increase in average cumulated specific faecal pellet production rate (SPP) for all treatments was 0.24 µg C female⁻¹ day⁻¹ in March and 0.15 in May. There was no significant effect of any of the oil spill treatments on average cumulated SPP during the experimental period in March or May (ANOVA, $\alpha = 0.05$, $p > 0.12$) (Figure 15).

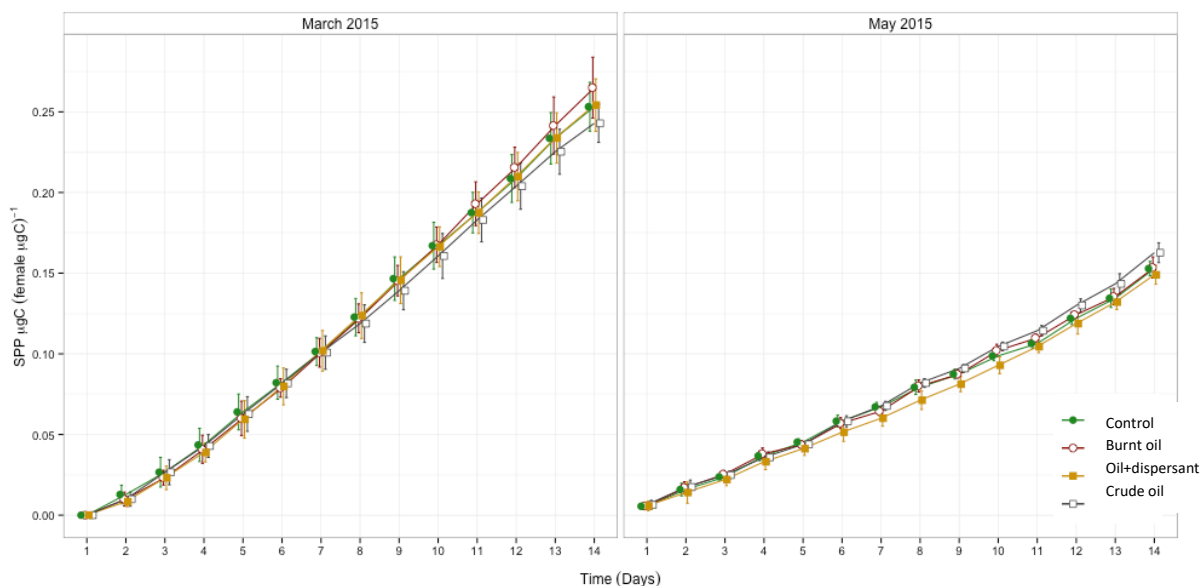


Figure 15 Average cumulated specific faecal pellet production (SPP) for *C. glacialis* females exposed to four treatments. Error bars show standard error (n=15).

3.1.2.2 The effect on egg production

The average egg production rate for *C. glacialis* for all treatments was 2.26 eggs female⁻¹ day⁻¹ during March and 4.44 in May respectively. The increase in average cumulated specific egg production rate (SEP) for all treatments was 0.057 µg C female⁻¹ day⁻¹ in March and 0.050 in May.

There was no significant effect of any of the oil spill treatments on average cumulated SEP during the experimental period in March. In May, the average cumulated SEP was significantly higher in the oil+dispersant treatment compared to the control from day 2 (+ 169 %) until the end of the experiment (+ 41 %) (Dunnett's test, $p < 0.0332$) (Figure 16).

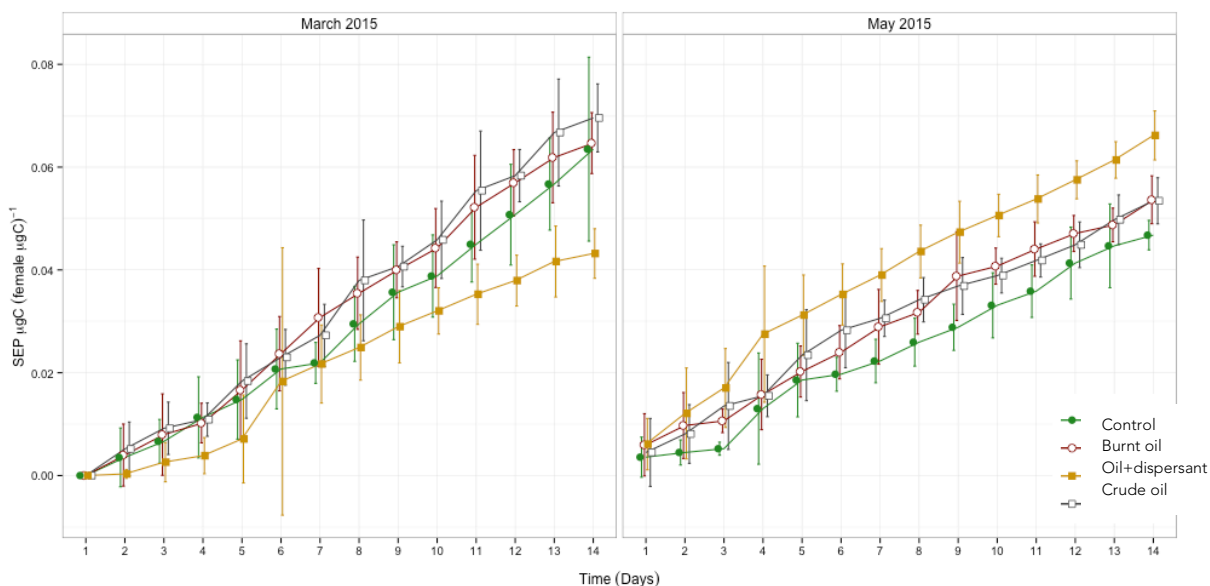


Figure 16 Average cumulated specific egg production (SEP) for *C. glacialis* females exposed to four treatments. Error bars show standard error (n=15).

3.1.3 Dilution exposure study

A series of dilutions of mesocosm water were prepared to perform identical exposure studies on to observe potential threshold effect concentrations on mature female copepods and eggs using the identical endpoints as described in the above experiment. Mesocosm water was diluted with filtered sea water where a dilution series of four concentrations (100%, 10%, 1% and 0.1% of mesocosm water) was prepared for each of the three oil spill treatments and the control. For the 100%, 1000 mL of the 200 µm filtered mesocosm water was transferred to 1 L red cap glass bottles (fifteen replicates × four treatments (three oil treatments and a control)). For the 10%, 100 mL mesocosm water was added to 900 mL 0.2 µm filtrated seawater (FSW) (five replicates × four treatments). For the 1%, 10 mL mesocosm water was added to 990 mL FSW (five replicates × four treatments) and for the 0.1%, 1 mL mesocosm water was added to 999 mL FSW (five replicates × four treatments). Three females of *C. glacialis* were transferred to each bottle. Bottles were incubated for 14 days in a climate-regulated room at 0 °C. The results are given in this paragraph and the results from undiluted mesocosm water as described above are presented in figures for reference (100 %).

3.1.3.1 The effect on specific faecal pellet production exposed to diluted mesocosm water

There was no significant effect of the oil spill treatments and concentrations on average cumulated SPP after the 14 day experimental period (ANOVA, $\alpha = 0.05$, $p > 0.110$) (Figure 17). The average daily specific fecal pellet production (SPP) for *Calanus glacialis* for all treatments and concentrations was $0.012 \pm 0.006 \mu\text{g C } \mu\text{g C female}^{-1} \text{ day}^{-1}$ (mean \pm SD) during the 14 day exposure period. The average cumulated specific fecal pellet production (cumulated SPP) after 14 days for all treatments and dilution series concentrations was $0.162 \pm 0.037 \mu\text{g C } \mu\text{g C female}^{-1}$ (mean ± 2 SD).

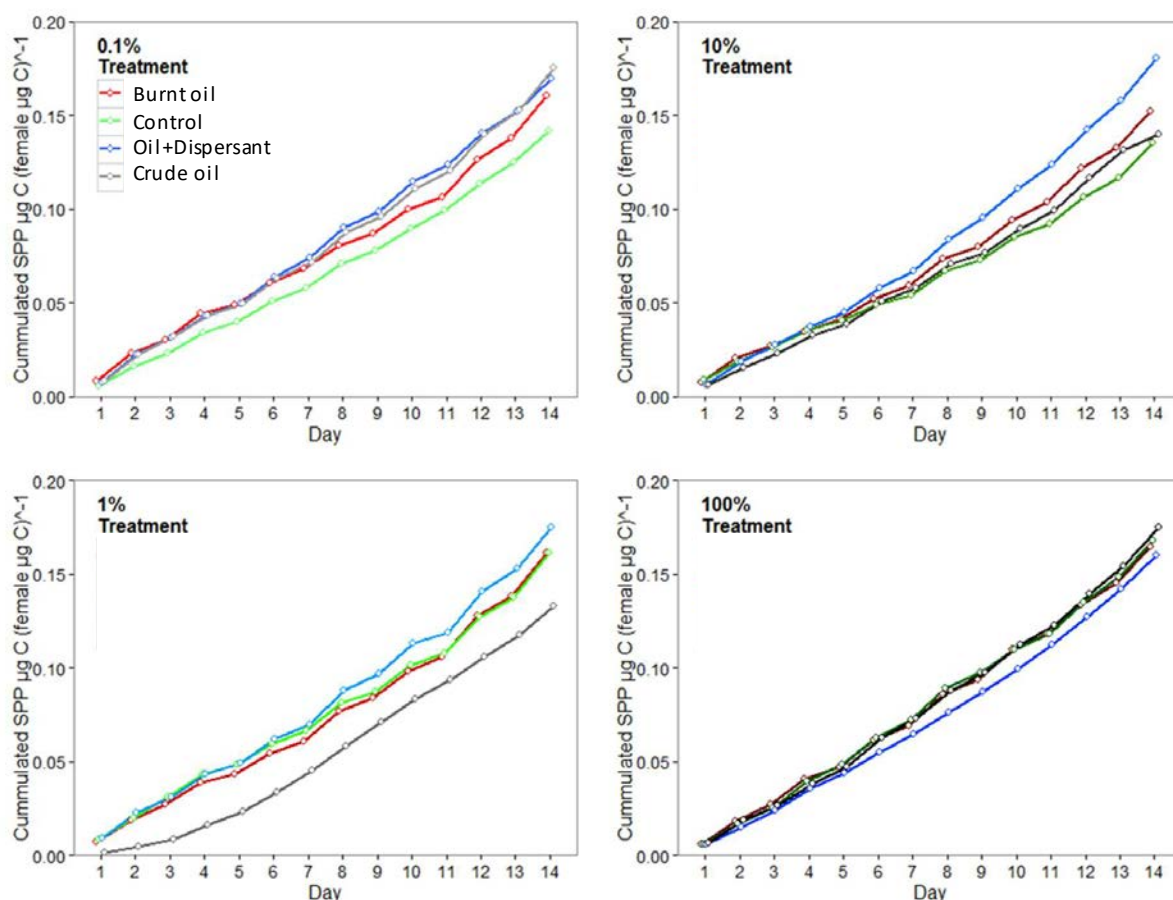


Figure 17 Cumulated mean specific faecal pellet production (SPP) for *C. glacialis* females exposed to four dilution series concentrations of mesocosm water from control, burnt oil, oil+dispesant and crude oil treatments. Initial exposure concentration in the 100% mesocosm water.

3.1.3.2 The effect on specific egg production exposed to diluted mesocosm water

The mean daily specific egg production (SEP) for *Calanus glacialis* for all treatments and concentrations was $0.004 \pm 0.006 \mu\text{g C } \mu\text{g C female}^{-1} \text{ day}^{-1}$ (mean \pm SD) during the 14 days exposure period (Figure 18). The mean cumulated specific egg production (cumulated SEP) for all treatments and concentrations was $0.051 \pm 0.023 \mu\text{g C female}^{-1}$ (mean \pm SD). Egg production tended to be higher in crude oil than the other treatments at 1% and 10% concentration and egg production in the burn oil treatments seemed to be highest in the 100% concentration (Figure 18). There was however no statistical significant effect of the oil spill treatments ((ANOVA), $\alpha = 0.05$, $p > 0.077$) and concentrations ((ANOVA, Post hoc DUNNETT), adjusted p - value, $p > 0.054$) on average cumulated SEP after the 14 days experimental period (Figure 18).

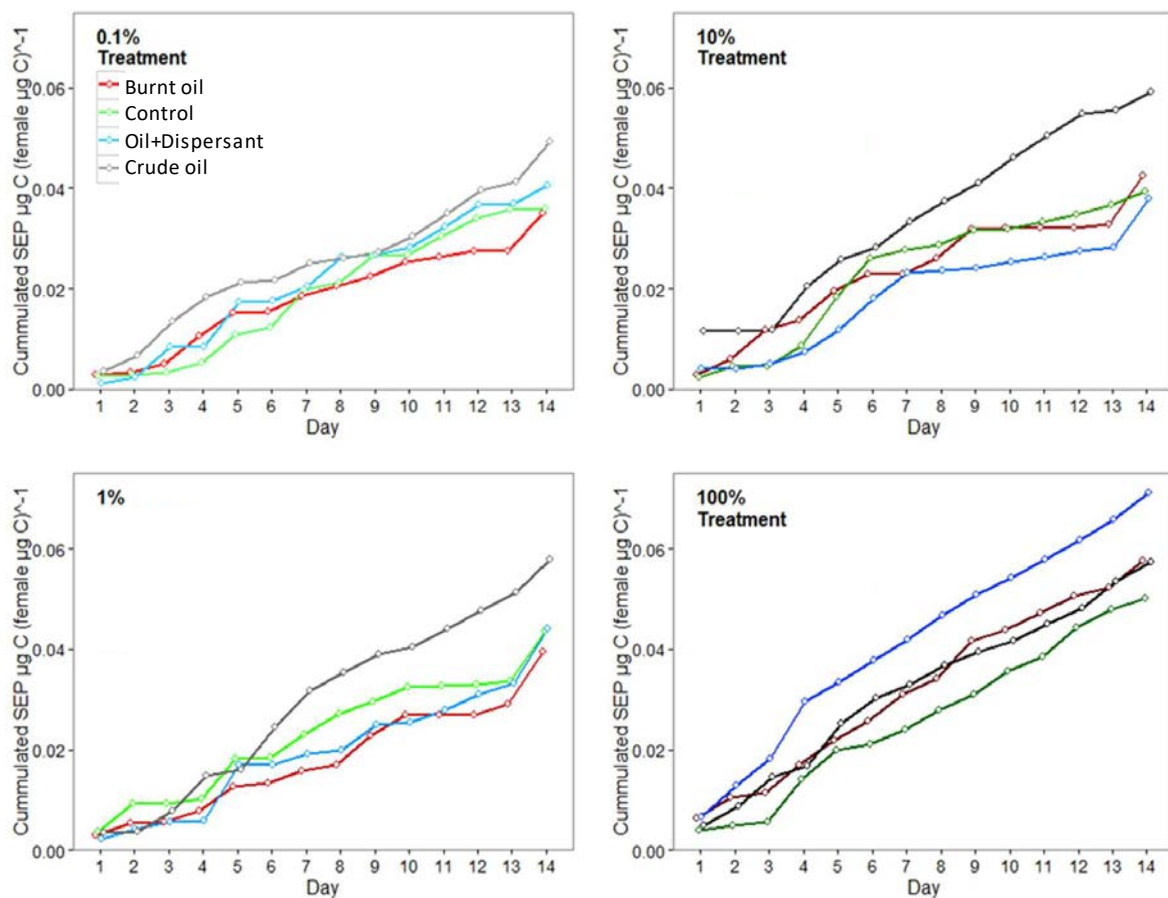


Figure 18 Cumulated mean specific egg production (SEP) for *C. glacialis* females exposed to four dilution series concentrations of mesocosm water from control, burnt oil, oil+dispersant and crude oil treatments. Initial exposure concentration in the 100% mesocosm water.

3.1.3.3 The effect on hatching success of eggs from females exposed to undiluted mesocosm water

Average hatching success was moderate in both March and May, and showed a tendency for reduced hatching success in the crude oil treatment (37 %) compared to the control (83 %). However, there was no significant effect of any of the oil spill treatments on hatching success after 13 days of exposure in either March or May (Figure 19).

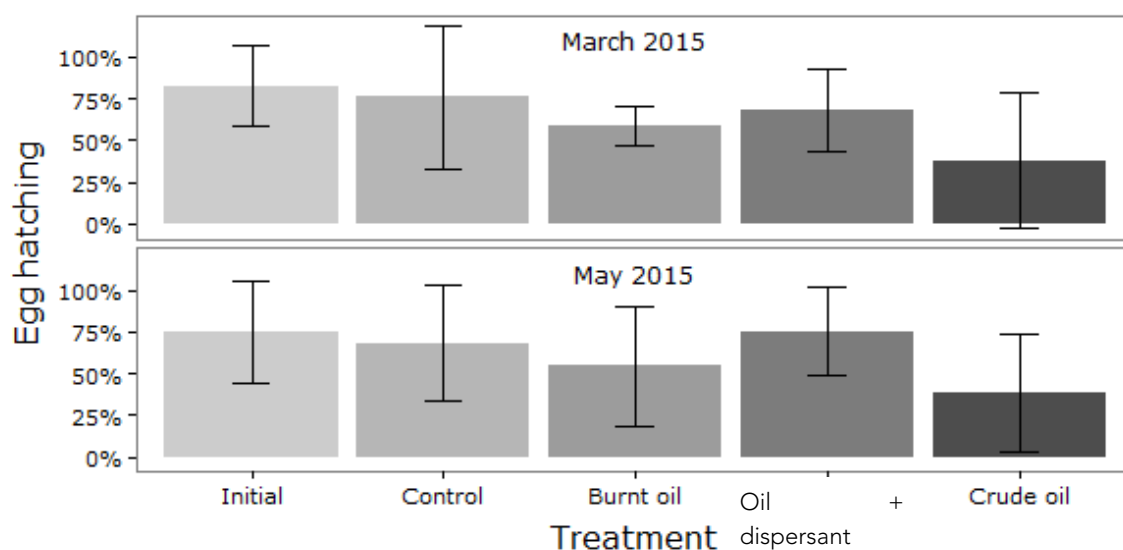


Figure 19 Average hatching success (7 days of incubation) of eggs from for *C. glacialis* females exposed to four treatments (100% mesocosm water) over 13 days and initial unexposed. Error bars show standard error.

3.1.3.4 Post exposure effects on Nauplii development exposed to undiluted mesocosm water

During the spring campaign, hatched nauplii were screened during their initial development to observe for potential post exposure effects. The investigated hatched nauplii from females exposed to water from the oil+dispersant mesocosm, showed a tendency of a higher proportion of deformations (Figure 20).

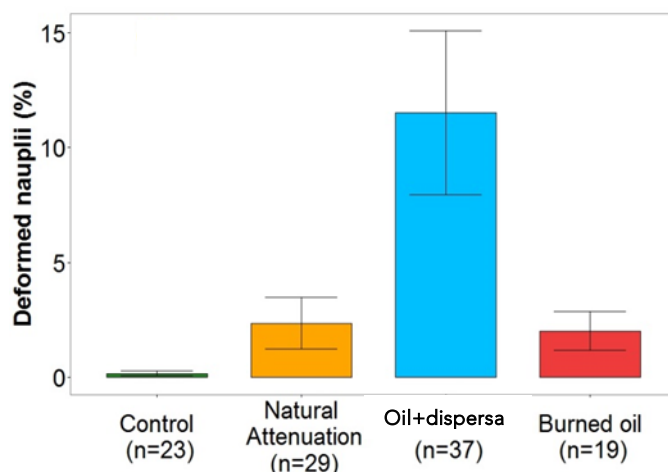


Figure 20 Proportion of deformed nauplii from eggs hatched by *C. glacialis* female copepods exposed to four treatments of mesocosm water (100%) in spring.

Only nauplii with severe deformation were counted as deformed (Figure 21), and subsequently the proportion of hatched nauplii which reached the second naupliar stage was determined (Figure 22).

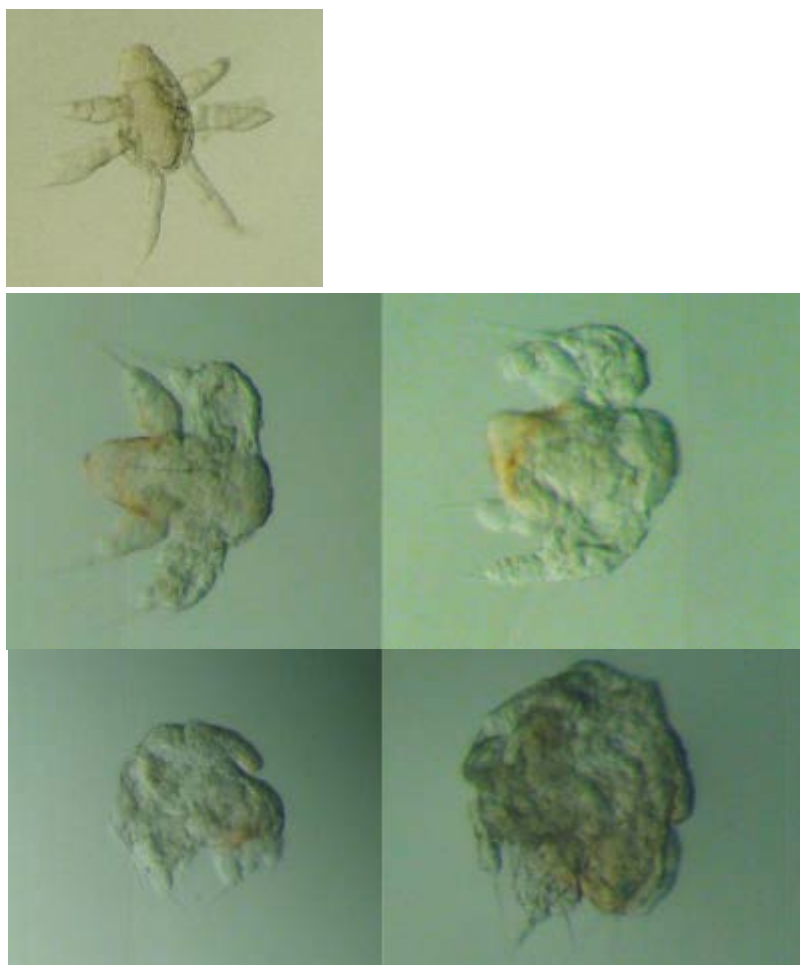


Figure 21 Nauplii of *Calanus glacialis*. Left single photo show a normal *C. glacialis* nauplii and the four images on the right illustrates different forms of deformations encountered.

There was a tendency of fewer nauplii reaching the next naupliar stage in the oil+dispersant treatment. However, the tendency was not significant due to a large variation in the data.

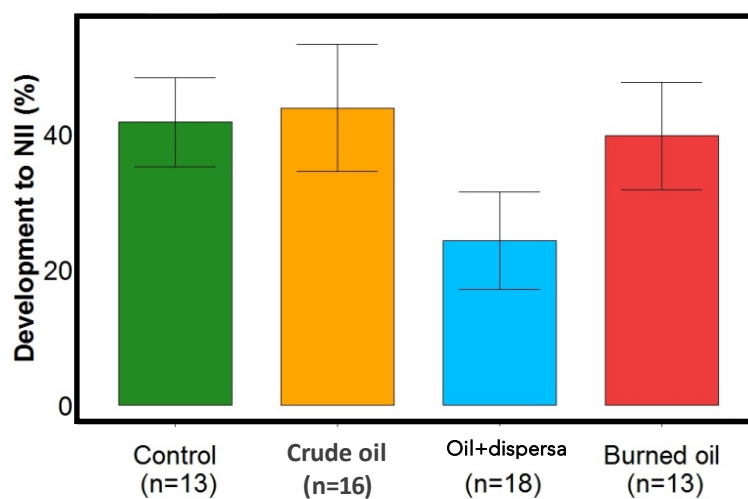


Figure 22 Proportion of hatched nauplii of *C. glacialis* reaching second development level.

3.1.4 Chemical analyses

In the presentation of results from the micro plankton exposure study, data on PAHs in the water was included. Below follows the chemical analyses, which describes the exposure regime that resulted from the mesocosms. Data are herein presented as total PAH concentrations in ng L^{-1} , determined as sum of up to 21 different PAHs.

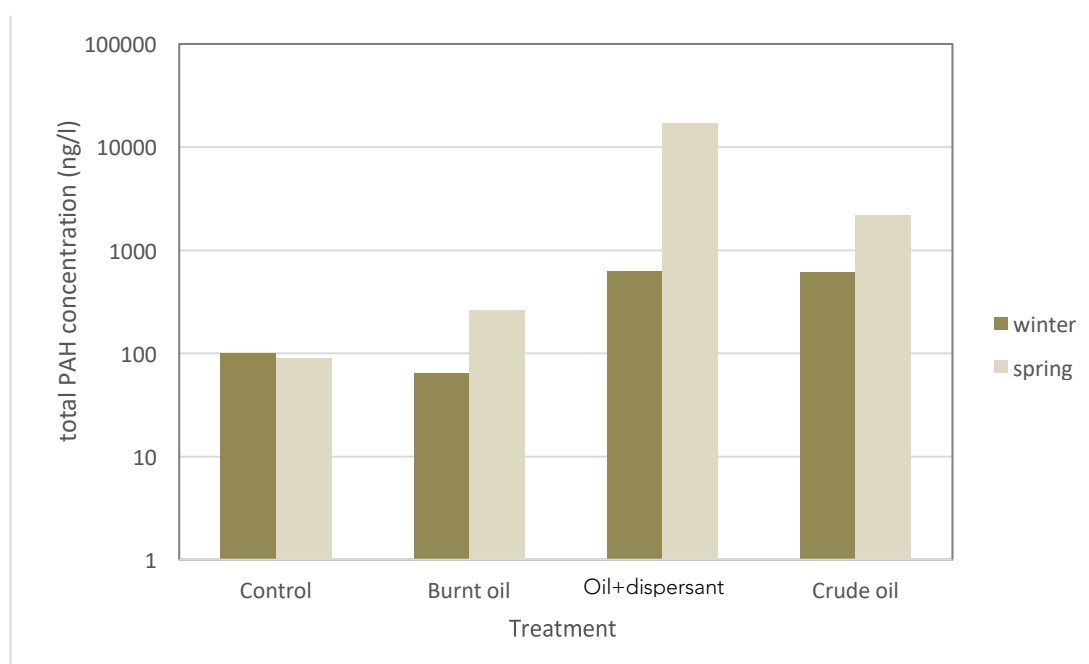


Figure 23 Total PAH concentration (sum of 21 PAHs) in water from mesocosms at Day 1 of the exposure experiments in both winter and spring campaign. Note the logarithmic scale on the Y-axis.

Figure 23 shows the initial PAH concentration in mesocosm waters used for the exposure studies in both the winter and spring campaigns. It can be seen, there is a background level in controls in both campaigns. In winter, the exposure level is as anticipated with the lowest concentrations in the burnt oil mesocosm and similar highest concentrations in oil+dispersant and crude oil mesocosms. In spring, the exposure pattern is similar, except for dispersants, where highest concentrations of PAHs were measured.

To investigate if copepods accumulated PAHs internally, measurements of total PAHs in whole body copepod and their egg were done. Data are presented in Table 10. Concentrations of PAHs in copepods at day 0 are normal background levels, which vary considerably in winter and spring. The general pattern shows some accumulation after 14 days of exposure. It should be noted, that values are extremely low and close to detection limits. There is also considerable variation among treatments with no consistent pattern.

Table 10 Bioaccumulation of PAHs in copepod females (ng/individual) and eggs (ng/egg) in copepod exposure experiments including dilution experiments. Second column is background concentrations and eggs are taken from females exposed to undiluted mesocosm water.

Winter	Background	100%	10%	1%	0.1%	Eggs
Day	0	14	14	14	14	14
Control	0,10	0,25	0,31	0,21	0,05	
Burnt oil	0,10	0,29	0,24	-	0,11	
Oil+Dispersant	0,10	0,75	0,12	0,21	0,03	
Crude oil	0,10	0,56	0,15	0,10	0,12	
Spring	0,41	0,14	0,32	0,05	0,27	
Control	0,41	0,31	0,13	0,03	0,39	0,32
Burnt oil	0,41	2,14	0,85	0,46	0,21	0,00
Oil+Dispersant	0,41	0,90	0,26	0,35	-	0,01
Crude oil	0,41	0,14	0,32	0,05	0,27	0,05

3.2 Light penetration, nutrients and ice-algal growth

3.2.1 Ice thickness

Ice thickness generally increased during the experiment and there was no consistent difference between duplicates for a given treatment. The different treatments had no discernible effect on ice thickness (Figure 24).

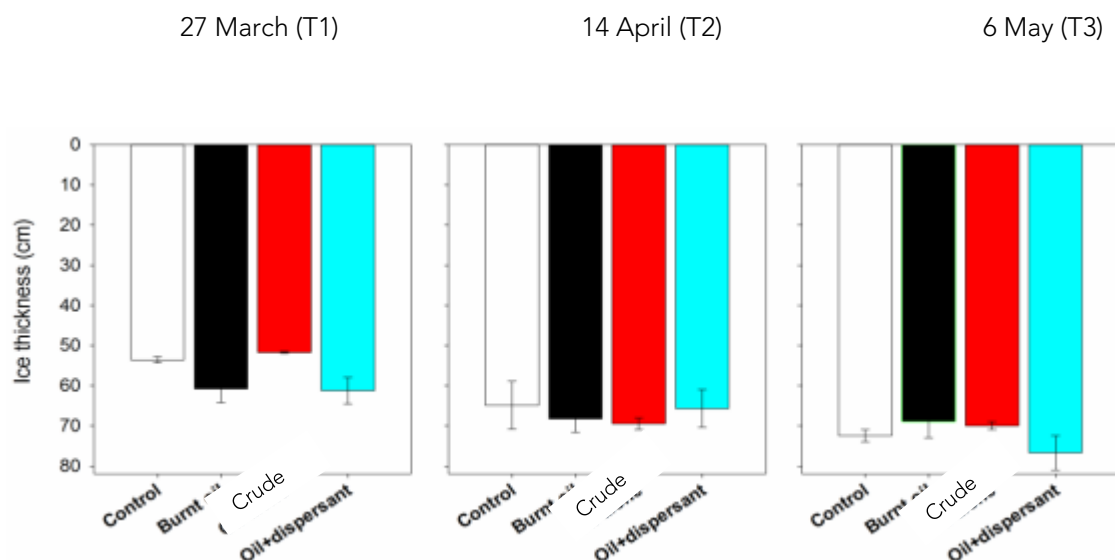


Figure 24 Ice thickness in the experimental mesocosms. Vertical dispersion bars give the range for duplicate mesocosms.

3.2.2 Light

Irradiance at the ice-water interface was systematically highest in the control treatment, sometimes barely detectable in the "burnt oil" treatment and never detected in other treatments (Figure 25). Given the near evenness of ice thickness for a given sampling date (Figure 24), the relatively low irradiance prevailing in the contaminated treatments can be ascribed to the

presence of oil, oil mixed with dispersants and burnt oil residues captured in the ice. Even the controls exhibited a very low penetration of light (i.e. % of above-ice PAR remaining below the ice), which we ascribe to lateral absorption of light by the opaque walls of the mesocosms (see Discussion). Due to logistic constraints, the measurement of light during T2 occurred too late in the day to get a signal below the ice.

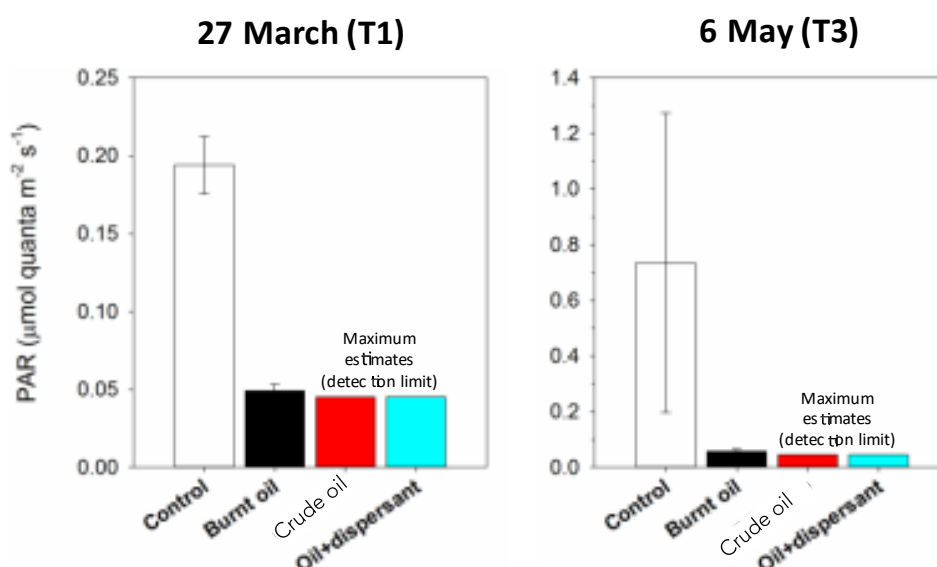


Figure 25 PAR at the ice-water interface in the experimental mesocosms (measured with a Seabird ECO-PAR cosine sensor mounted on an articulated pole). Snow was cleared before taking the measurement. No light was detected at T2 due to late sampling in the day (not shown). Vertical dispersion bars give the range for duplicate mesocosms.

3.2.3 Nutrients

With the exception of T1 for the "control" and "burnt oil" treatments, there were no clear differences in the concentrations of nitrate, phosphate and silicate between treatments (Figure 26, in order to simplify the visual presentation, only the nitrate data are shown, but phosphate and silicate qualitatively followed the same patterns). We find no evidence that the presence of contaminants in sea ice had an adverse impact on nutrient availability in bottom ice, possibly because those contaminants were mostly located above the bottom few centimeters, which would not impede upward supply of nutrients from the water to the algal layer. Concentrations of ammonium at T2 and T3 (Table 2; data from T1 are considered uncertain and excluded from analyses as the samples had to be frozen due to a chemical that was not delivered to Svalbard in time) were generally highest in the "control" and "burnt oil" treatments, suggesting enhanced biological activity and microbial recycling relative to the other treatments (ammonium is produced by algal exudations, bacterial decomposition and excretion by the grazers of ice algae).

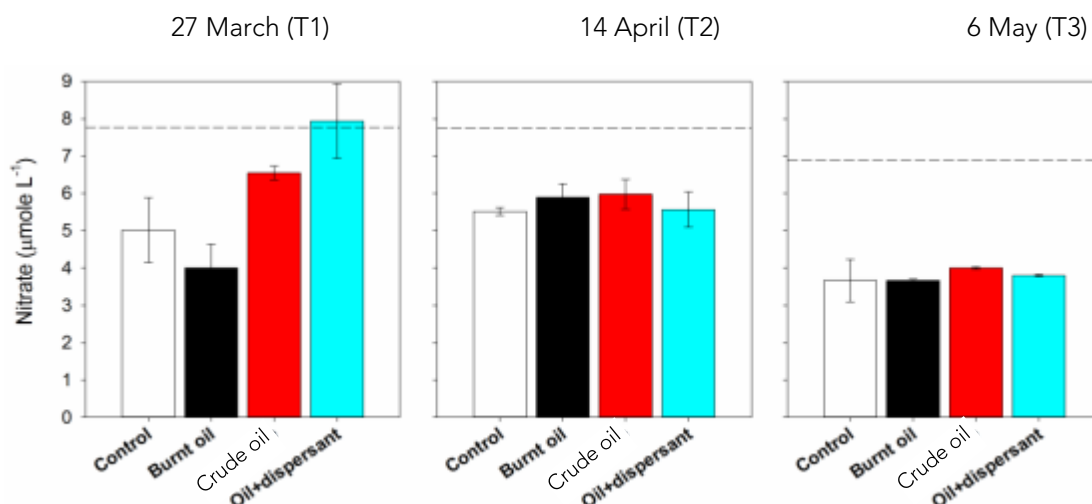


Figure 26. concentration of nitrate in melted bottom-ice cores (+filtered seawater) in the different treatments for each sampling time. The horizontal dashed line provides the nitrate concentration in the surface water used for dilution. Vertical dispersion bars give the range for duplicate mesocosms.

3.2.4 Pigments and particulate matter

Overall, chl *a* stocks were extremely low (Figure 27) for the region and the Arctic in general (see Discussion). Values were lowest at T2, possibly reflecting a net loss of algal material by physical ablation, sloughing or grazing (Fig. 4). The lowest chl *a* stocks were associated with a high degradation state (dominance of phaeopigments), possibly linked to the presence of unhealthy algae and/or detrital material. The highest values were observed in the "controls" (especially at T1), followed by the "burnt oil" treatment. The "oil + dispersant" treatment had no detectable chl *a* at T1 and T2. The mesocosms were more similar at T3 than at the other sampling dates, which suggests that mesocosms for which ice-algal growth is slower (oil alone, oil + dispersant) eventually catch up partly with the other ones during spring. Ratios of particulate organic carbon to chl *a* (POC:Chl) and ratios of particulate organic carbon to total particulate nitrogen (C:N) calculated from the data in Table 3 were generally high, especially in the "oil" and "oil+dispersant" treatments, suggesting a strong dominance of detrital material in bottom ice. Data from T1 and T3 for the "control" and "burnt oil" were consistent with a somewhat higher contribution of healthy ice algae to the organic matter contained in the brine channels of bottom sea-ice. Despite the sizable inventories of POC in bottom-ice, the mass spectrometer did not detect any labeling of the incubated samples with the ¹³C added as a tracer, even in the controls. We worked with the maximal sample size possible given the number of cores that could be extracted from any given mesocosms. This unfortunate result can be explained by the adverse effects of very low chl *a* concentrations and near- darkness on photosynthesis, which are attributable to the design of the mesocosms and not the experimental treatments *per se*.

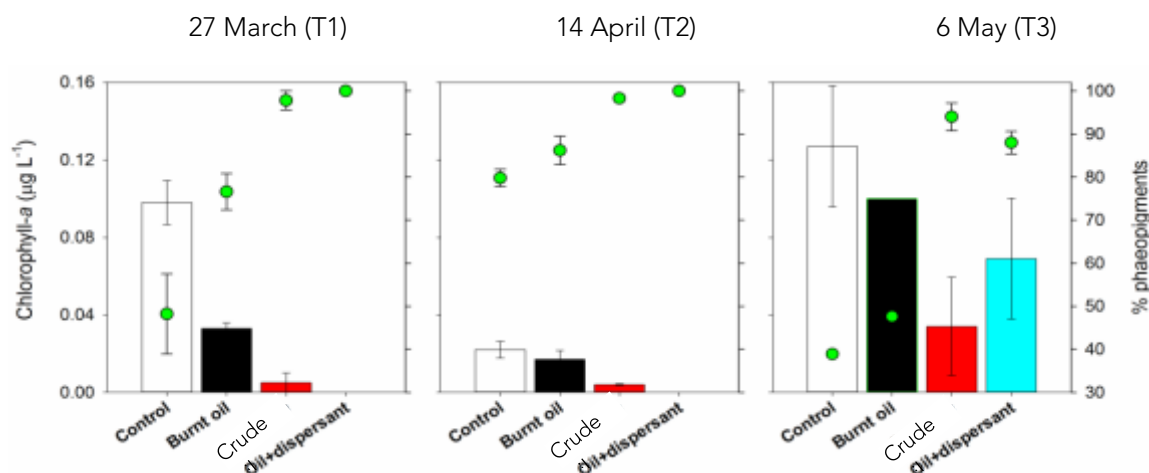


Figure 27 Concentration of Chl a (bars) and contribution of phaeopigments* (green circles) in bottom-ice cores for the different treatments at each sampling time. Vertical dispersion bars give the range for duplicate mesocosms. *Calculated as $100 \times \text{phaeo} / (\text{chl } a + \text{phaeo})$.

3.2.5 Taxonomic composition of ice protists: richness and diversity

Although the visual enumeration and identification of protists is highly labor-intensive and time consuming, this approach was preferred over molecular techniques given the need to quantitatively assess the abundance, size and aspect of the material present in the samples (i.e. intact vs. empty diatoms). Given the financial constraints of the project, available funds were used to provide a detailed taxonomic analysis of duplicate mesocosms at T3 (end point) and of one mesocosm for each treatment at T1 (baseline for comparison). These samples were prioritized because of the evident loss of ice material at T2 (Figure 26) and the need to compare the cumulated impacts of each treatment at T3.

Several metrics can be used to assess the effect of the experimental treatments on community composition. Here we considered the abundance of cells and species richness (number of different species present in a sample) either for the overall community or particular taxonomic groups. The analysis included strictly autotrophic taxa (diatoms, naked dinoflagellates, cryptophyceae, chrysophyceae, prymnesiophyceae) as well as mixotrophic (flagellates) and heterotrophic (thecate dinoflagellates, choanoflagellates) organisms to provide a complete overview of the community. A total of 195 distinct protist species were identified across the 11 samples analyzed. Note that the total of species provided in the bottom row does not necessarily correspond to the sum of the rows above it since some species occurred in more than one mesocosm but were counted only once in the total. Most taxonomic groups exhibited low species richness with the exception of pennate diatoms, which had the highest number of species by far, followed by dinoflagellates and choanoflagellates. Experimental treatments had no effect on species richness for most groups, except for pennate diatoms, whose maximum richness occurred in the controls at T1 and in the controls and "burnt oil" treatments at T3. Pennate richness remained low throughout the entire experiment in the "oil" and "oil+dispersant" treatment. It was initially low in the burnt treatment (T1) but reached high values similar to those of the controls at T3. A closer look at pennates shows that the number of genera represented remained low in the "oil" and "oil+dispersant" treatments at both T1 and T3 (Figure 28). For the "burnt oil" treatment this number increased dramatically between March and May, mostly through the diversification of the *Navicula* genus and the inclusion of species from the *Nitzschia*, *Navicula* and

Entomoneis genres. In the controls, the representation of different pennate genres and species richness within those genres remained high and similar throughout the experiment.

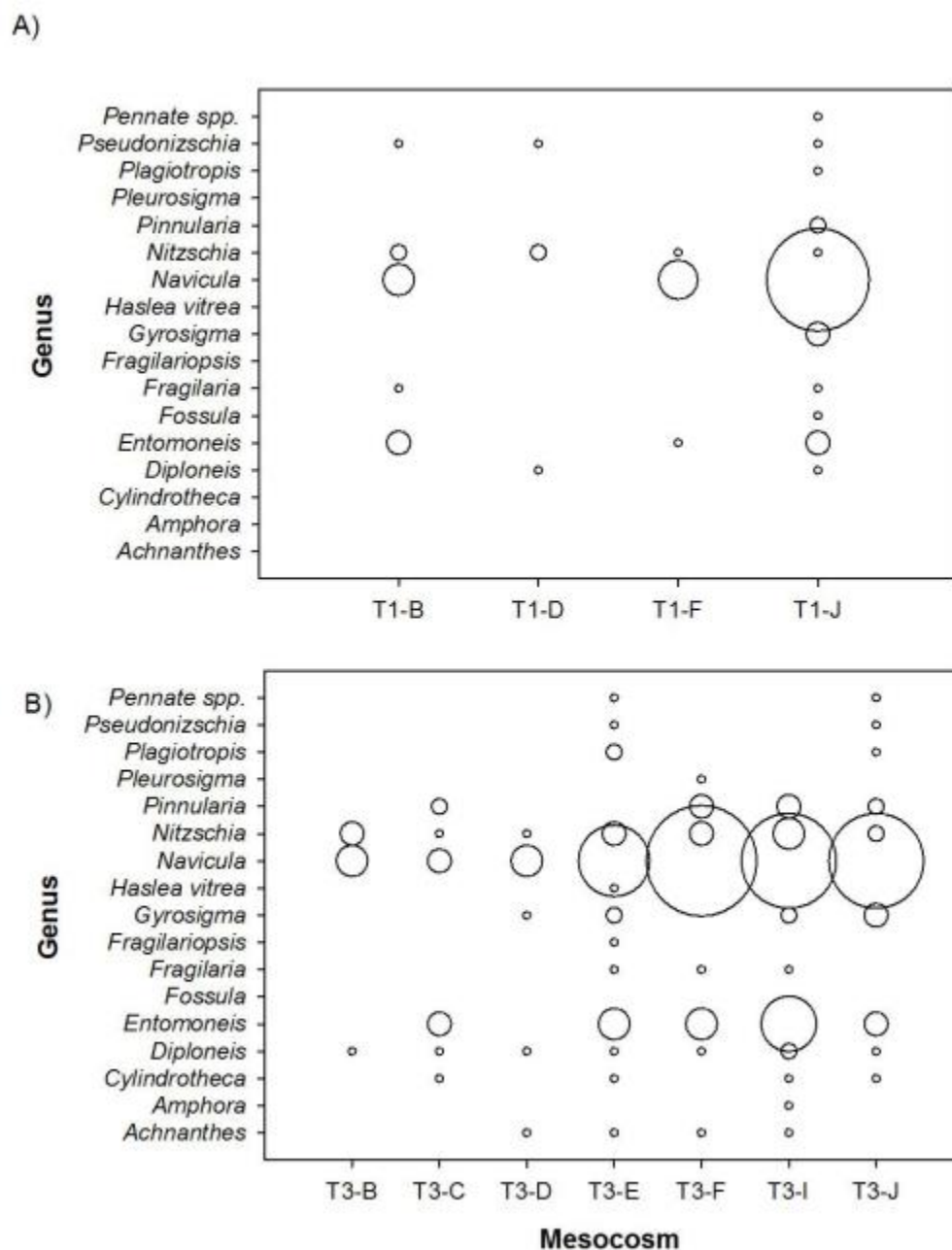


Figure 28 Number of pennate diatom species (richness) by genus within the bottom-ice of different mesocosms at (A) T1 on 27 March and (B) T3 on 6 May. The smallest and largest bubbles correspond to 1 and 14 species per genus, respectively. On the x-axis, mesocosm B = crude oil, C&D= oil+dispersant, E&F = burnt oil and I&J = contr

The *Navicula* genus was the most diverse overall and a detailed look at its species composition on 6 May shows that 11 of the species (most notably *N. arctica* and *N. septentrionalis*) present in the controls and/or the "burnt oil" treatment were not observed in the "oil" and "oil+dispersant" treatments (Figure 29). The dominant pennate species in controls and the "burnt oil" mesocosms,

Navicula directa, was either absent or in negligible abundance in the other treatments. Despite some variability between replicate mesocosms, the results clearly imply that the "oil" and "oil+dispersant" treatments had an adverse effect on the establishment of several species of pennate diatoms (the *Navicula* genus in particular) in bottom sea-ice, but the ultimate cause(s) of this effect cannot be ascertained. It could result from one or a combination of the following: extremely low light, which may have favored strongly shade-adapted species, or toxicity, which may have favored species with a relatively high resistance to crude Kobe oil. A previous toxicity study of *Navicula directa* reported a decrease in abundance upon exposure to sediments contaminated with hydrocarbons (Cunningham et al., 2003).

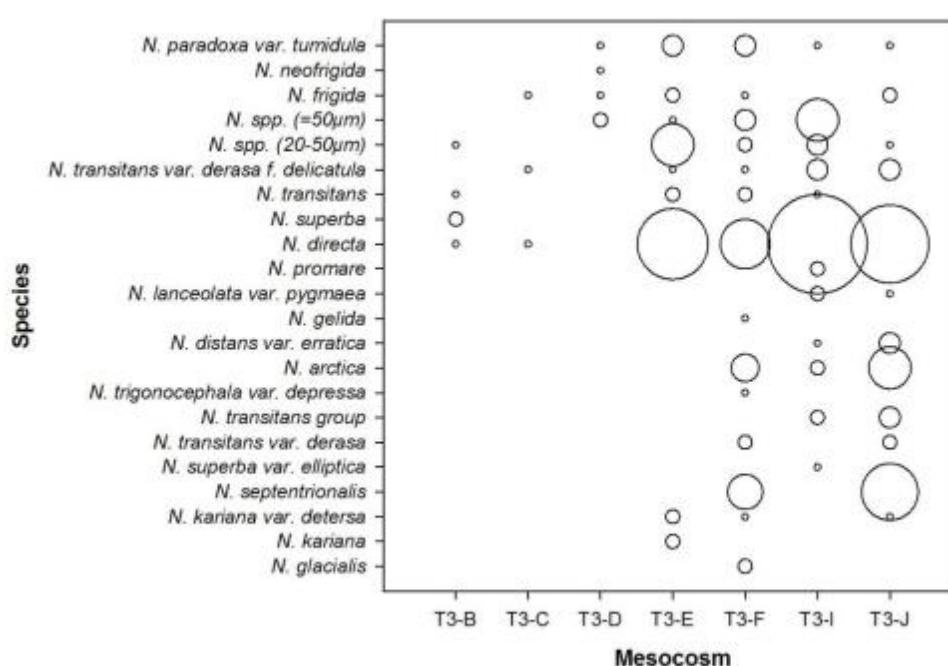


Figure 29 Presence and abundance of different species belonging to the pennate diatom genus *Navicula* within the bottom-ice of different mesocosms on 6 May. The smallest and largest bubbles correspond to 40 and 560 individual cells per liter, respectively. On the x-axis, mesocosm B = crude oil, C&D= oil+dispersant, E&F = burnt oil and I&J = control.

3.2.6 Abundance of selected groups of ice protists

In order to provide a workable arrangement of all abundance data for presentation purposes, the different species were pooled within broad taxonomic groupings, but only those groups that individually accounted for at least 5% of total cell counts were conserved for further analysis (i.e. pennate diatoms, centric diatoms, empty diatom frustules, naked dinoflagellates, thecate dinoflagellates, cryptophytes, primnesiophytes and flagellates). Collectively, these groups amounted to > 95% of all cells identified in any given mesocosm. Figure 30 shows the relationship between total chlorophyll a and algal abundance in each of the groups. There was a robust positive relationship for most groups, except the centric diatoms and primnesiophytes. For centric diatoms this is explained by the fact that this group grows exclusively in the water column. Their presence in the samples reflects passive trapping of presumably inactive pelagic cells when

the ice forms. This explanation also applies to prymnesiophytes, at least partially, since the planktonic species *Phaeocystis pouchetii* made up a large fraction of total cell counts in this class. Empty diatom frustules (mostly pennates) are dead cells, which have been subjected to lysis or grazing by consumers. The positive correlation between the number of empty frustules and chl *a* suggests that mortality was proportional to diatom growth and may have removed a significant portion of their biomass. As example, empty frustules amounted to 53% of the total number of intact diatoms in the control treatment at T3 (mesocosm I). This proportion varied across mesocosms but did not consistently differ between treatments. The presence of several groups of heterotrophic organisms in the samples (not detailed here, but including thecate dinoflagellates, ciliates, choanoflagellates etc.) supports this interpretation. The relatively high abundance of dead diatoms in the controls and "burnt oil" treatments is consistent with the accumulation of ammonium that reflects enhanced grazing and microbial activity.

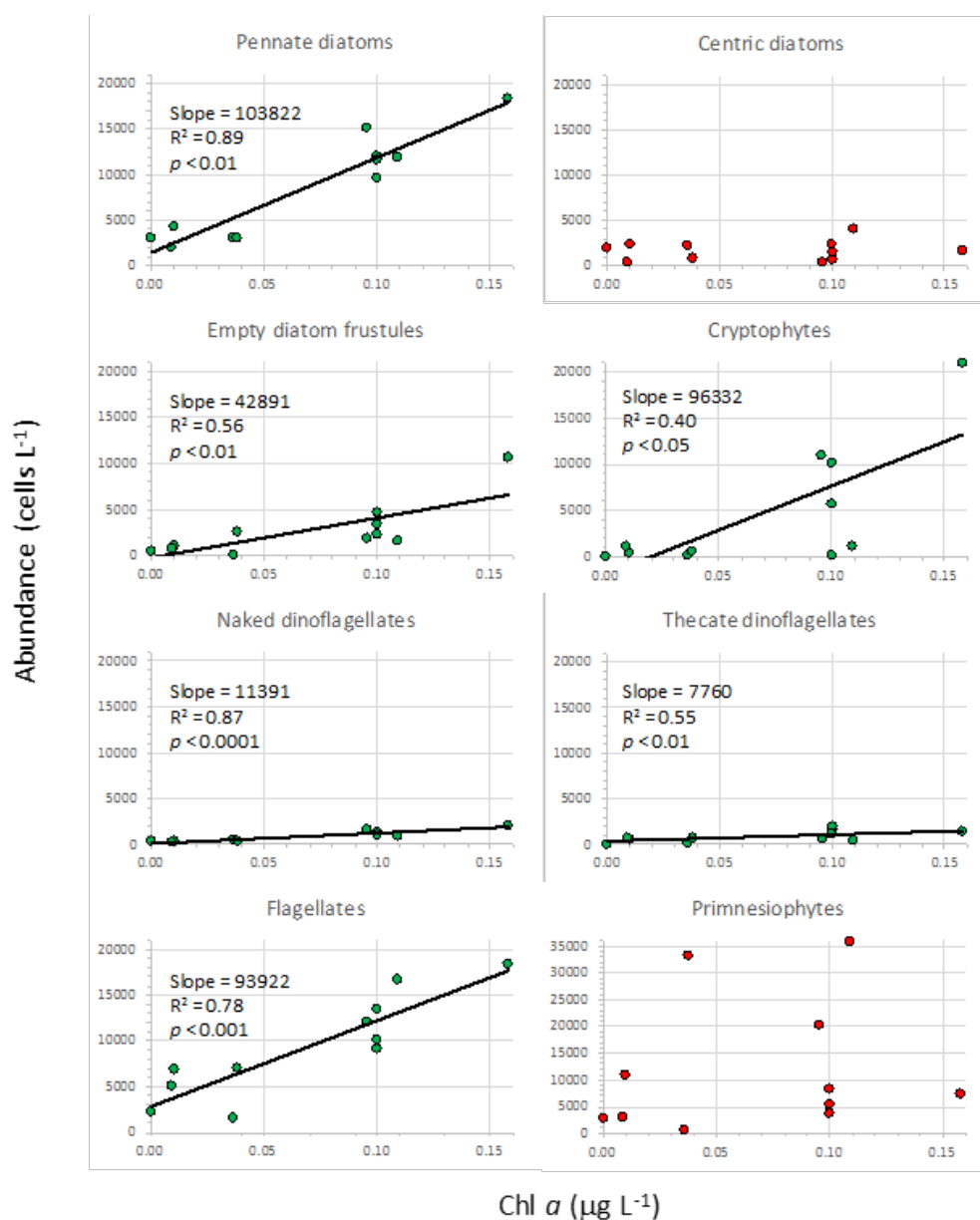


Figure 30 Protist groups for which cellular abundance was positively (green circles) or not (red circles) related to the concentration of chl a in bottom ice, using pooled data from all mesocosms at T1 and T3. Note the change of vertical scale for the Primnesiophytes.

A weighted analysis of the regression slopes given in Figure 30, excluding empty frustules and thecate dinoflagellates (heterotrophs), indicates that pennate diatoms drove, on average, 34% of the biomass difference between mesocosms, followed by cryptophytes (32%) and flagellates (31%), and a much lesser extent naked dinoflagellates (4%). Consistent with the analysis presented in Figure 27, the cumulated abundance of these four groups (i.e. those that comprise organisms known for their capacity to grow in sea ice) at T3 was relatively high in the controls and to a lesser extent the "burnt oil" treatment but conspicuously low in the other two treatments.

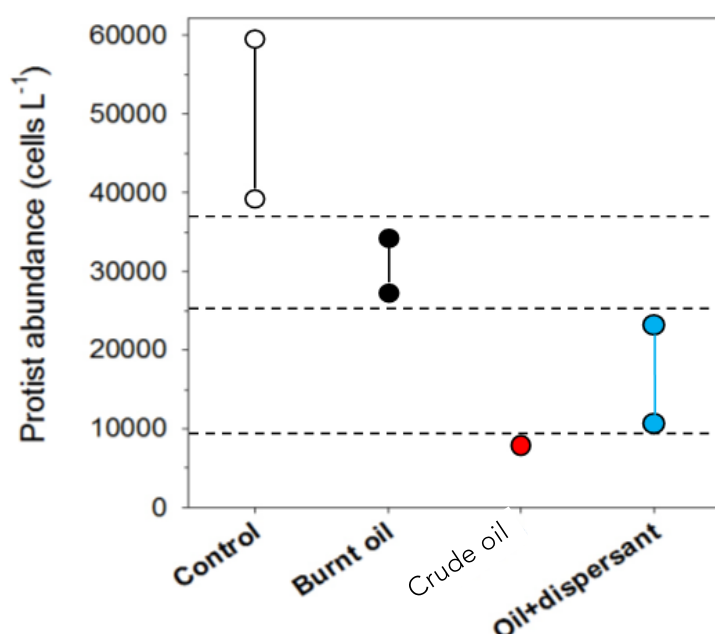


Figure 31 Combined abundance of pennate diatoms, naked dinoflagellates, flagellates and cryptophytes in bottom-ice cores for the different treatments at T3 on 6 May. The horizontal and vertical lines are provided as visual references to help distinguish between treatments.

A detailed analysis of the relative contribution of the same protist groups used in Figure 31 to their combined abundance is shown in Figure 32 for T1 and T3. This figure allows to assess the changes in community composition over time in mesocosms J, F, B and D, and to compare the different treatments at each sampling time. What emanates from this figure overall is the numerical importance of pennate diatoms and flagellates in all mesocosms. Together these two groups generally account for 62 to 95% of the total cell numbers. For the "oil" and "oil+dispersant" mesocosms that were sampled both at T1 and T3, the relative importance of flagellates tended to increase over time to the detriment of pennate diatoms. This shift was not apparent in the control and the "burnt oil" mesocosms (J and F), where flagellates and pennate diatoms maintained similar shares. In these mesocosms, however, cryptophytes greatly gained in importance between T1 to T3. This community shift was not apparent in the other treatments. Collectively these observations suggest that growth conditions for cryptophytes and pennate diatoms were more suitable in the controls and the "burnt oil" treatments than in the other ones.

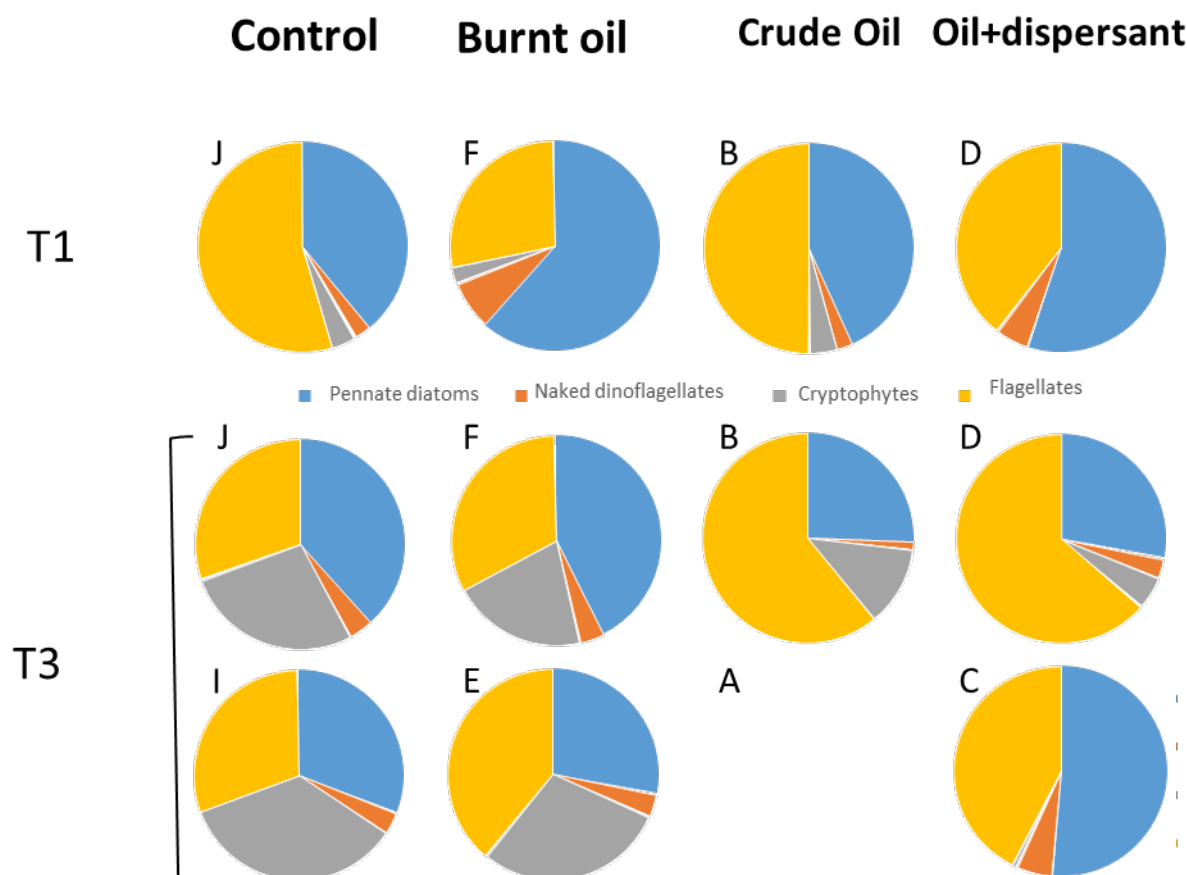


Figure 32 Relative contribution of pennate diatoms, naked dinoflagellates, flagellates and cryptophytes to their combined abundance in bottom-ice cores for the different treatments at T3 on 6 May. The horizontal and vertical lines are provided as visual help to distinguish between treatments. Letters indicate mesocosm treatments: B = crude oil, C&D= oil+dispersant, E&F = burnt oil and I&J = control

3.3 Sea Surface Layer Microbial Community

3.3.1 Physical Appearance of the Surface Layer.

The enclosures' surface layer responded differently to the air temperatures that were experienced; although air temperatures were gently rising prior to the experiment, a brief cold event lowered air temperatures from -5°C to -13°C on day 4 and then increased again to +2°C on day 5. Thus, the surface layer was liquid in all enclosures on day 0 after the removal of ice. On day 1, all treatments retained a liquid surface layer, except for the control and the dispersal-only enclosures that were freezing or frozen. On day 3, the control, dispersal-only, oil sheen and burned oil enclosures were freezing or frozen. This freezing resulted in the absence of a surface microlayer; although we sampled with glass plates, we define these samples as surface layer, with a thickness of 6-8 mm for the burned oil, oil and dispersant, and dispersant-only treatments. As a reference, a surface layer in the control enclosures increased in thickness from 6 to 9 mm over the course of the 5-day experiment, often sampled under sea ice. It was impossible to determine a surface layer thickness for the oil slick and oil sheen treatments as the oil coated the plates instantly, as expected. On the last day of the experiment, all enclosures had either about ¼ of the

surface area frozen (control, sheen, and burned oil treatments), were covered by ice slurry (dispersant only treatments) or were not frozen at all (oil and oil/dispersant treatments).

3.3.2 Microbial Abundance

Abundance of bacteria and nano/picoplankton in the surface layer was measurable only during the latter part of the experiment (Day 3 and 5) due to the various oil-related treatments and/or the presence of sea ice (Figure 33); only the control enclosures show a 5-day trend with almost no change during the first three days and a decrease in cell number on day 5. When available, bacterial and nano/picoplankton cell abundance in surface layer water was lower than in subsurface water (i.e., 50cm below the air-ice-water interface). Over 72h, bacterial cell abundance clearly decreased in the dispersant-only treatment in surface layer water (-5.2×10^4 cells mL^{-1} d^{-1} ; Figure 34 top) while no significant changes were observed in the subsurface water. Nano and picoplankton, though less abundant than bacteria by an order of magnitude to begin with, also showed a slight decrease in surface layer water in the control, dispersant-only, oil sheen and burned residue over 72h (Figure 34 bottom), with a 75-100% loss in cell number after 5days (Figure 33 left panels). No significant change in nano/picoplankton abundance was observed in subsurface water in any of the treatments or the control (Figure 34 bottom).

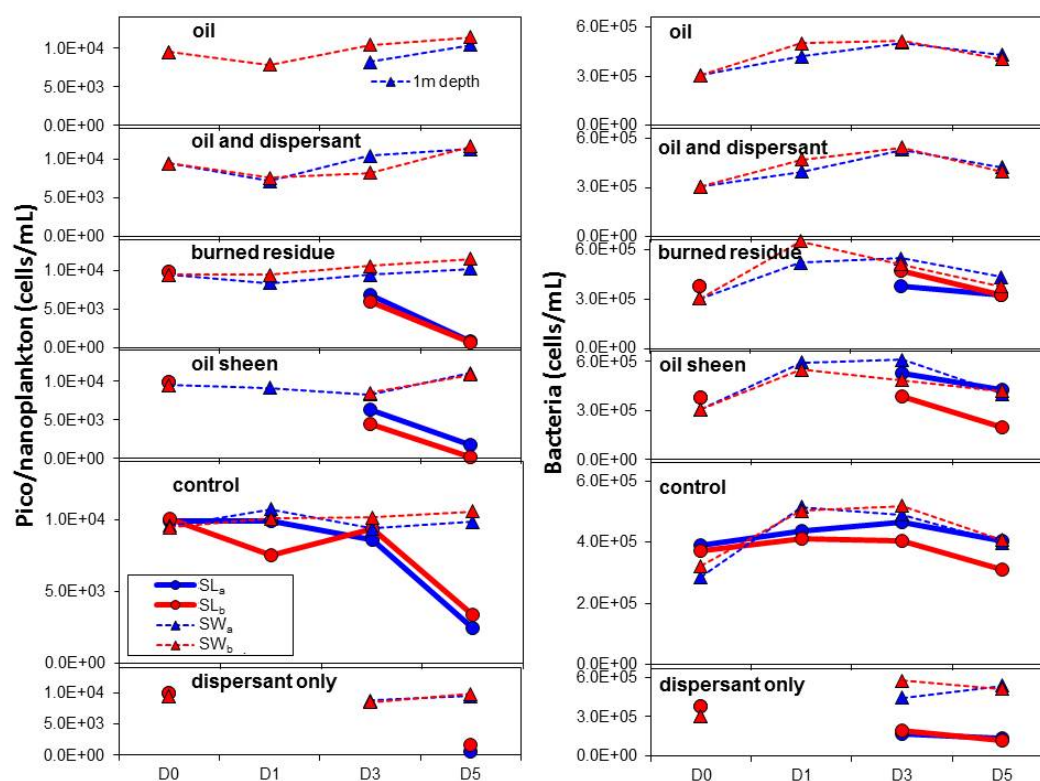


Figure 33 Cell densities of pico- and nanophytoplankton (left panels) and heterotrophic bacteria (right panels) determined using flow cytometry for replicate enclosures (blue [a] and red [b] lines) exposed to different oil treatments (Oil slick, oil sheen, burned residue, oil and dispersant, dispersant-only, and a control). Abundances are shown for surface layer (SL) and subsurface (SW) waters.

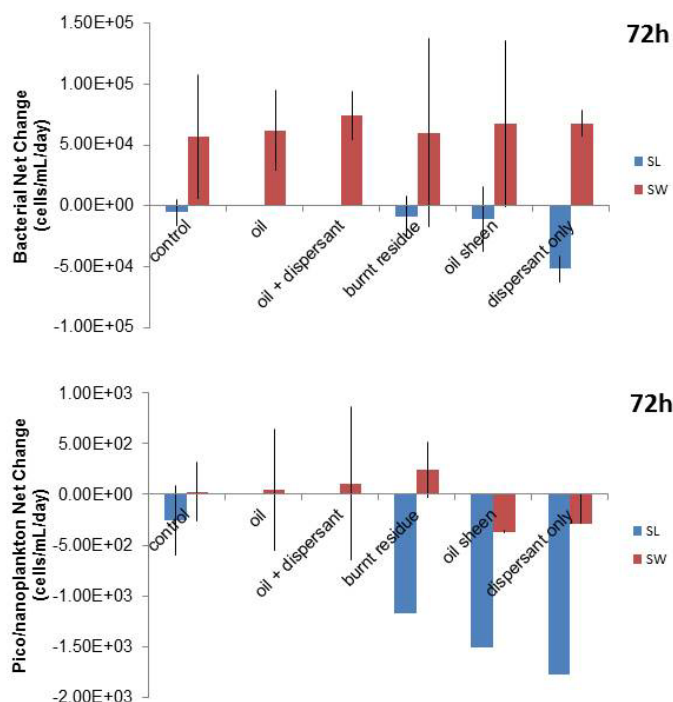


Figure 34 Daily net rate of change in bacterial (top) and pico/nanoplankton (bottom) abundance in surface layer (SL) and subsurface (SW) seawater after 72h of incubation in the control and experimental treatments. Mean value and standard deviation is shown for each treatment.

3.3.3 Bacterial Community Composition

Bacterial community composition was dominated by *Polaribacter*, *Colwellia*, *Balneatrix*, *Bacteroidetes*, and unidentified Proteobacteria that together accounted for over 80% of the relative bacterial abundance (Figure 35), with another 10 groups accounting for most of the remaining 20%. *Bacteroidetes* and *Colwellia* increased in relative importance over the 5-day experiment in surface layer waters only in the oil sheen and burned oil enclosures, respectively. In subsurface water, only *Colwellia* showed any change, increasing in the dispersant-only treatment. *Oleispira*, a bacterial species usually observed in oiled systems, was conspicuously absent (abundance <0.2%) in all enclosures.

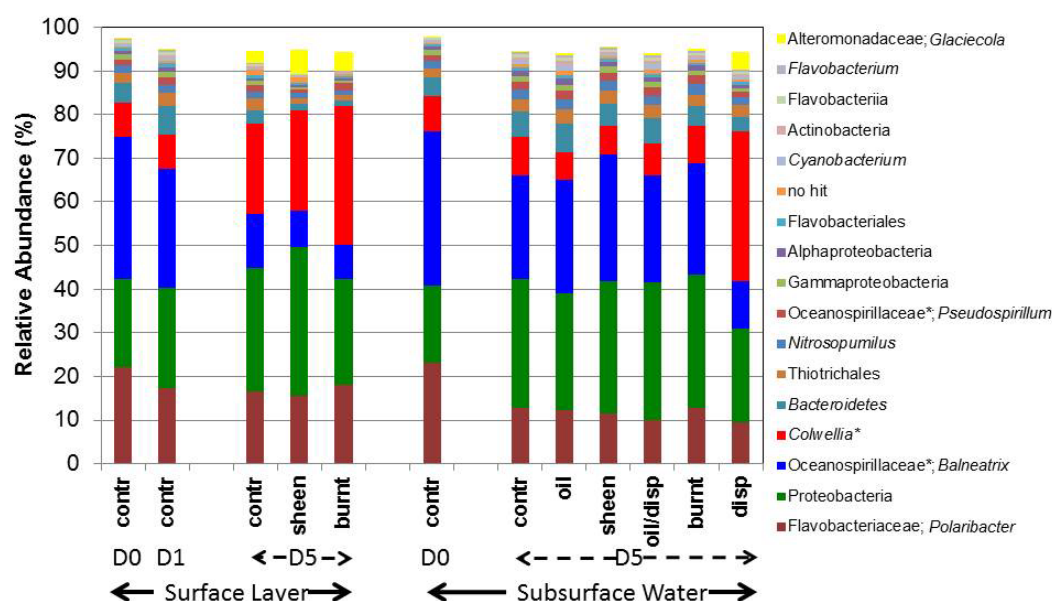


Figure 35 Microbial community analysis (based on 16s rRNA sequencing) for samples from the surface layer (left five bars) and 50cm below the water table (right bars). Several treatments (Oil slick, oil sheen, burned residue, oil and dispersant, and dispersant-only) were followed over five days. Groups shown account for 90% of the total abundance.

The diversity of the entire bacterial community in surface layer water, as measured by the Shannon index H (Shannon and Weaver 1949), decreased more in the control than in the oil sheen and burned oil enclosures over 5 days (Figure 36 top); due to presence of an oil slick throughout the incubation, no water samples could be collected for the other oil treatments. A similar pattern was observed in subsurface water, with bacterial diversity decreasing in the control enclosure, with no observable difference in the oil slick, oil and dispersant, and dispersant-only treatments; again, a slight—but not statistically significant— increase was observed in the oil sheen and burned oil enclosures (Figure 36 bottom).

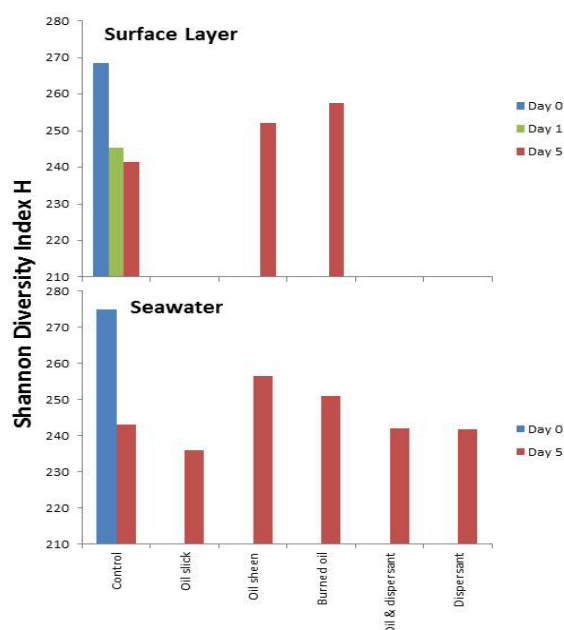


Figure 36 Bacterial community diversity (H) in the control (days 0, 1 and/or 5) and among treatments (day 5) in surface layer and subsurface waters.

To gain more details into shifts in the bacterial community, we performed a cluster analysis and principle component analysis using the 100 most abundant detected species detected (Figure 37). Both analyses show the same trend. First, the initial microbial community at the beginning of the experiment (i.e., at day 0, 6h after creating the ice holes) is distinct from all other microbial communities. The bacterial communities at the surface and at 50 cm depth are very similar. Second, at day 5 all samples with oil or oil/dispersant treatments (including burned oil residue) as well as the control treatment are similar for the 50 cm depth samples. Interestingly, the non-oiled control treatment does not appear to be significantly different from the oiled treatment. However, the dispersant-only treatment behaves differently. Third, the bacterial communities in the surface layer samples cluster together, and are different from the communities at 50 cm depth.

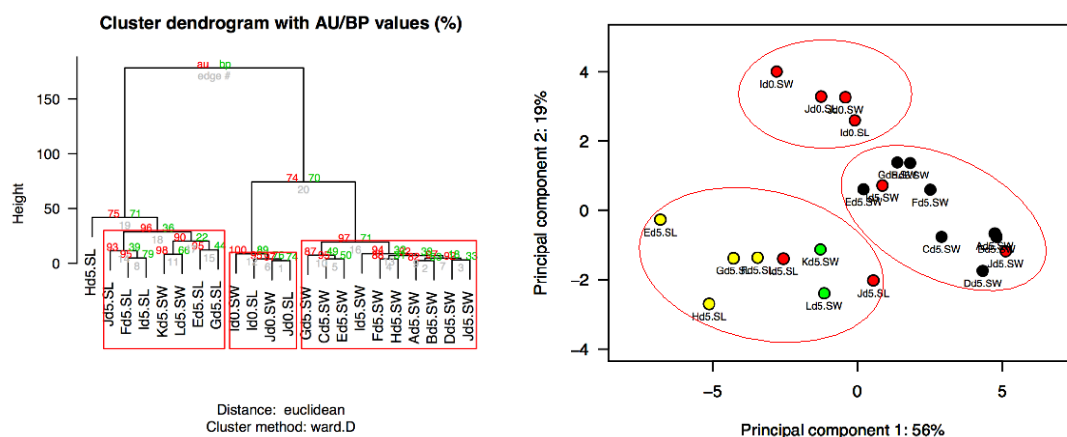


Figure 37 (A) Cluster analysis of microbial community composition. Three main groups can be observed: (i) Surface layer ("SL") samples on day 5 (d5) plus the dispersant-only treatment samples from 50 cm depth (SW samples K and L), (ii) SL and SW samples of the control treatment at day 0 (d0), and (iii) samples from SW samples at day 5. Expect the dispersant-only samples. (B) Principle Component analysis of microbial

community composition, showing the same tentative clustering. Control treatment is in red, dispersant-only in green, SL samples in yellow, and SW samples in black.

3.3.4 Aqueous Hydrocarbon Concentrations

The concentration of various hydrocarbon groups was measured at all time points in subsurface water given that sufficient sample volume was available for detailed analysis. PAHs had the highest concentration in days 1 and/or 3 in the oil, oil and dispersant (Figure 38), oil sheen and burned oil (Figure 39 bottom) treatments. The oil treatment had highest or measurable PAH concentrations on day 3, however. The burned oil treatment had the lowest concentrations for all hydrocarbons detected. It should be noted that the PAH concentration decreased by day 5, especially PAHs. For the control enclosure, the total PAH background concentration stayed around 50-100 ng/L for both the surface layer and subsurface waters, without a clear trend over the course of the incubation.

In surface layer waters, only the oil sheen and burned oil treatments and the control provided sufficient water sample volume for a full analysis (Figure 39). It should be noted that hydrocarbon concentrations were 2-16 fold higher than in subsurface water. Otherwise, the same patterns can be observed as in subsurface water, i.e., PAHs concentrations decreased with time over the course of the experiment, and the control enclosure had a total PAH background concentration of 50 -100 ng/L.

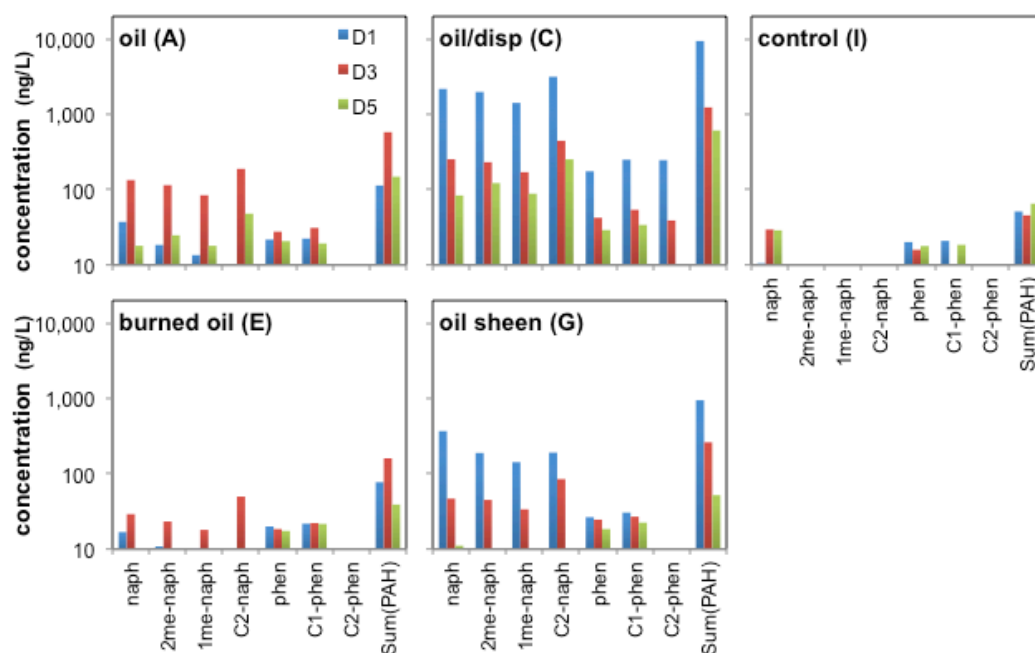


Figure 38 PAH concentration in the subsurface seawater (50 cm depth) treated with oil (treatment A) and a combination of oil+dispersant (C), and control treatment (I) measured on days 1, 3 and 5.

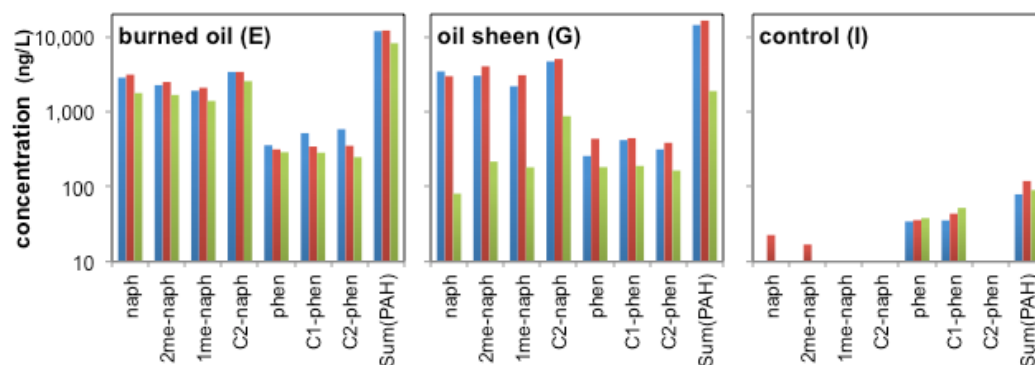


Figure 39 PAH concentrations for surface layer treated with burned oil (treatment E), oil sheen (G) and the control treatment (I), measured on days 1, 3 and 5.

3.3.5 Hydrocarbon Weathering in the Oil Phase

To analyze how the input of the oil into the water changed over the time of the incubation, the oil phase was analyzed for changes in the hydrocarbon composition using comprehensive two-dimensional gas chromatography (GC×GC) (Aeppli et al., 2014). For the oil, the oil/dispersant, and the burned oil treatment, no significant change in the hydrocarbon distribution was observed during the five-day incubation time (Figure 40). However, for the sheen treatment, a slight decrease in volatile compounds was observed.

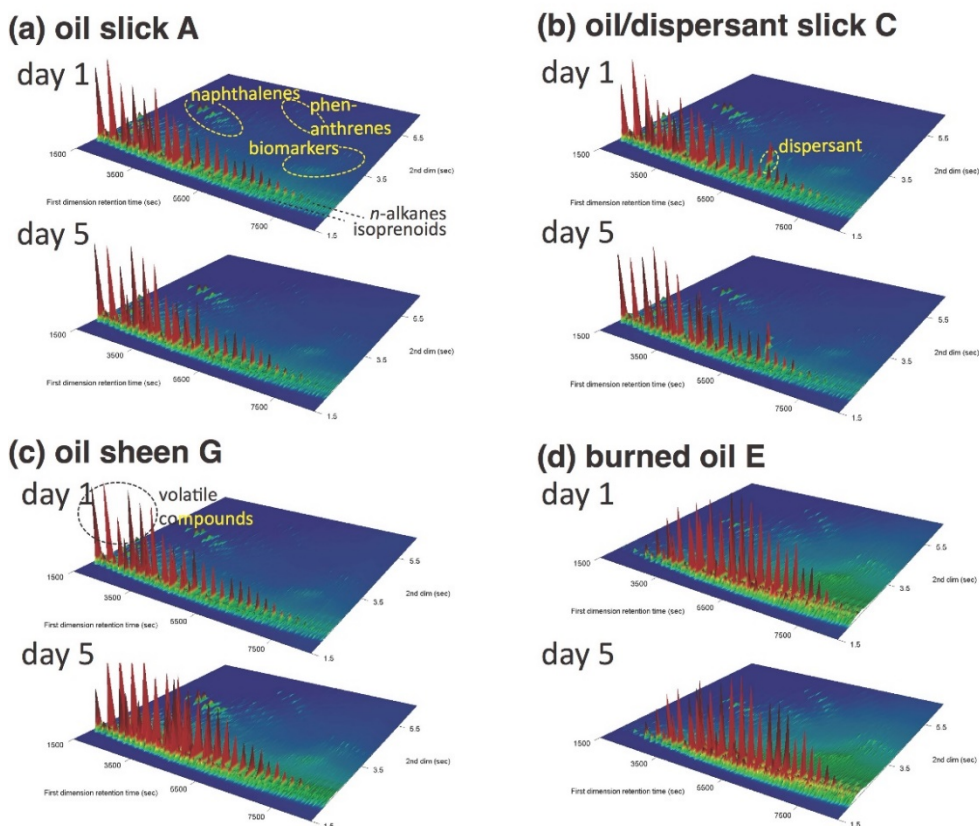


Figure 40 Changes in the hydrocarbon composition in the oil phase during the incubation, as seen by GCxGC-FID chromatograms. Only the oil sheen treatment shows a slight change in composition, with volatile compounds being evaporated during the five days of incubation.

3.4 Polar cod

3.4.1 Water chemistry

The total hydrocarbon content (THC) concentration in water samples from the control treatment was zero throughout the exposure period, and remained relative stable throughout the last 24 h of exposure with values of 0.9 ± 0.5 , 9.2 ± 3.7 , 22.5 ± 3.7 mg/L in BO, MDO and CDO, respectively (Figure 41a). Average $\Sigma 26$ PAH concentrations were highest after 24 h in all treatments and thereafter decreased by ca. 20 % at 48 h (Figure 41b, Table 11). Highest $\Sigma 26$ PAH concentrations were found the CDO treatment (101.5 ± 14.3 $\mu\text{g/L}$) at 24 h followed by the MDO (62.4 ± 20.7 $\mu\text{g/L}$), BO (3.5 ± 1.2 $\mu\text{g/L}$) and Ctrl (1.05 ± 0.0 $\mu\text{g/L}$) treatments. Dominating PAHs (>98 % of $\Sigma 26$ PAH) in all treatments (BO, MDO and CDO) were parent and alkylated naphthalenes, phenanthrene/anthracenes and dibenzothiophenes, whereas only parent and C1, C2-naphthalenes were detected in the Control. In BO treatment, the only high molecular weight PAHs measured above detection limits were benzo(b)fluoranthene (0.03 $\mu\text{g/L}$) and benzo(k)fluoranthene (0.01 $\mu\text{g/L}$), and these concentrations were comparable to measured concentrations in MDO and CDO (0.01 – 0.10 $\mu\text{g/L}$ and 0.01 - 0.013 $\mu\text{g/L}$, respectively; Table

Appendix 2-A). Acenaphthylene was the only PAH with a higher concentration in BO (0.01 µg/L) compared to MDO and CDO (<0.004 – 0.005 µg/L) (Table Appendix 2-A).

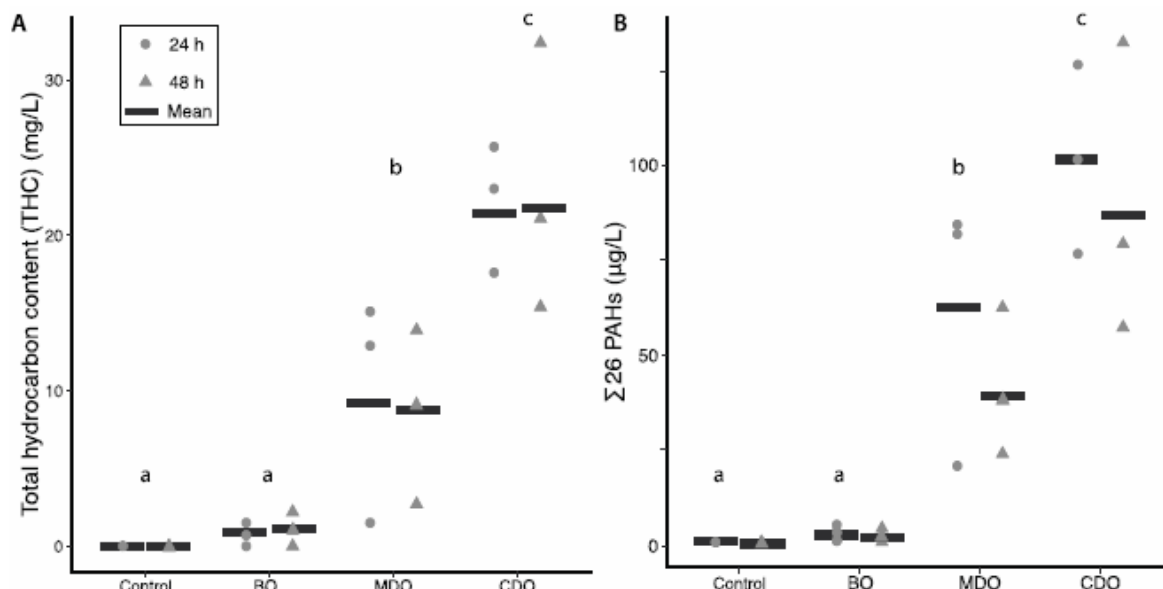


Figure 41 (A) THC and (B) Σ26 PAH concentrations at t24 (circles) and t48 (triangles) for all treatment groups in boxplots. Treatment mean concentrations that do not share a letter are significantly different ($p < 0.01$).

3.4.2 The initial fish population

Fish initially part of the exposure experiment ranged in size from 12.0 – 59.0 g total weight (mean 34.7 ± 0.6 SE), 12.0 – 22.0 cm length (mean 17.3 ± 0.1 SE) and age ranged between 2 and 6 years (mean 4.5 ± 0.1 SE) at T0 (Table 11). Fish used for the exposure experiment were all selected from the intermediate size group of the collected fish (size range 24.0 – 47.5 g) with no significant difference between any of the groups (Ctrl, BO, MDO, CDO). The remaining unexposed polar cod were not included in any of the treatment groups and were classified by size as they exhibited a bimodal size range that was significantly smaller (Unexp1; size range 12-32 g) and bigger (Unexp2; size range 38-59 g) than the exposed fish in the treatment groups.

Table 11 Summary of polar cod sampled in January after a 7-month monitoring period following 48 h exposure to in situ burned oil residues [BO], mechanically dispersed oil [MDO], and chemically dispersed oil [CDO] treatment, and a control group. Unexposed fish have size distributions which fall outside the intermediate range included in the exposure experiment. Age, as determined by otoliths, somatic weight, total length, hepatosomatic index (HSI), and condition factor were calculated for all fish. All values are mean \pm SE.

Treatment	Number of fish sampled			Age	HSI (%)	Condition factor
	Females	Males	Total			
Control	27	20	48	4.7 ± 0.1	9.3 ± 0.3	0.53
BO	26	22	49	4.7 ± 0.1	9.3 ± 0.3	0.53
MDO	20	19	40	4.4 ± 0.1	9.5 ± 0.4	0.53
CDO	25	18	46	4.5 ± 0.1	9.6 ± 0.3	0.54
Unexp. 1	12	18	30	3.8 ± 0.2	8.5 ± 0.3	0.55
Unexp. 2	17	6	23	4.6 ± 0.2	9.4 ± 0.4	0.54

3.4.3 Mortality

Mortality was observed after the first month post collection, and in the period February/March 2015 following the natural spawning period before exposure took place (data not shown), after which mortality stabilized. Fish were otherwise in good condition throughout the acclimation, exposure and post-exposure monitoring period. No mortality was registered in any treatments tanks during the 48h exposure period. Mortality was, however, observed during the post exposure period for all treatments independent of exposure. Mortality was most prevalent in the first month post-exposure (between T1-T2) for all treatments with 8-12% mortality occurring in all oil treatments and control. The mortality rate steadied to between 2-5 % per month until the final sampling in January for all treatments and control with no statistical difference in cumulative mortality (Figure 42). The group of larger unexposed fish (Unexp 2.) exhibited the highest cumulative mortality (32%).

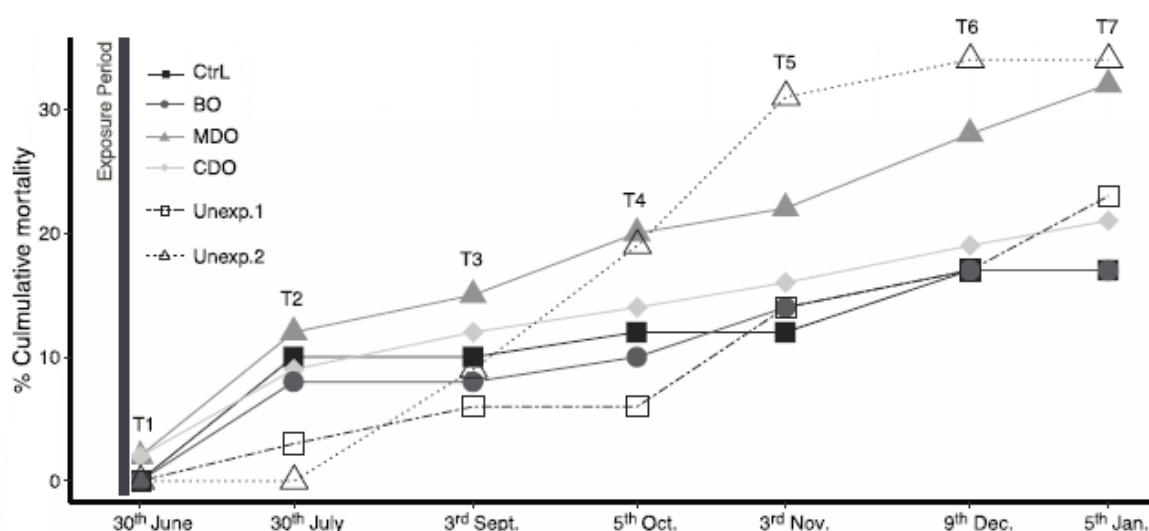


Figure 42 Cumulative mortality (% of overall mortality) of polar cod during the course of the exposure and post exposure period (June 2015 – January 2016) for each treatment group. No significant difference in % mortality was found between treatment groups, control or unexposed groups.

3.4.4 Specific growth rate

In general, there was a great variation in SGR within all treatment groups throughout the experiment ranging from -2.5 to 3.5 % change in body weight per day. Significant treatment effects were observed between the high growth rates in the BO compared to lower growth rates in the MDO ($p < 0.01$) and CDO treatments ($p < 0.01$) in the period from tagging to immediately after exposure (T0-T1[May 19th - June 30th]) (Figure 43). Growth rates in the BO treatment in the following period (June 30th – July 30th) were significantly reduced only when compared to the CDO treatment ($p < 0.01$). Overall, growth rates (mean \pm SE) were lowest immediately following tagging and exposure (0.06 ± 0.0 % increase in body weight per day) and highest in the consecutive time period i.e. July (0.63 ± 0.0 % increase in body weight per day). No significant differences in SGR were seen between any treatment groups or unexposed fish for any other growth periods beyond the first two or for the whole period in total (May 19th – Jan 5th). Female and male SGR were not significantly different at any time period, therefore both sexes were pooled for statistical analysis.

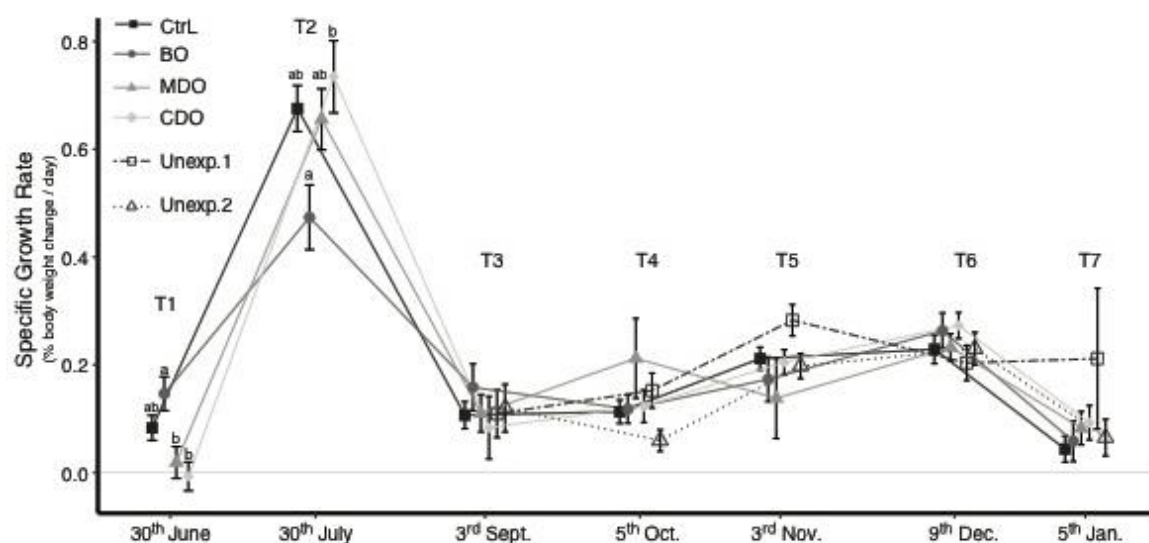


Figure 43 Specific growth rate (SGR; % change in body weight per day) mean ± SE of fish during after exposure to different OSR measures or unexposed (n=40-49 per treatment [Unexp. n is 23-30 fish]). Different letters indicate significant differences between treatment groups.

3.4.5 Condition factor and hepatosomatic index

At T0 (May 19th), males (exposed and unexposed combined) had a significantly higher condition factor compared to females, 0.68 ± 0.0 and 0.64 ± 0.0 , respectively. At T1, the condition factor was significantly higher in female in BO (0.66 ± 0.0) compared to females in the other groups (control [0.62 ± 0.0], MDO [0.62 ± 0.0] and CDO [0.60 ± 0.0]). At no other time point were significant differences found between any of the treatment groups (including control) or sex. Furthermore, no significant difference in age, HSI, or condition factor was seen between any treatment or sex at the end of the experimental period in January (Table 11).

3.4.6 Reproductive development

3.4.6.1 Females

Histological analyses revealed that iteroparity was exhibited by 56% of female fish as determined by presence of residual oocytes, while 22% exhibited first time maturation with no evidence of previous spawning and the remaining specimens were immature (6%) or resting (16%). From the maturing females, 68% revealed a leading oocyte cohort that had reached the vitellogenic stage II (Vtg II) and were categorized as advanced maturing with mean oocyte diameter of $547 \pm 8 \mu\text{m}$, a centrally placed nucleus and the cytoplasm filled with vitellogenin derived oil droplets (Figure 44). In 32 % of maturing females, however, the most advanced oocyte cohort was in an early vitellogenic stage (Vtg I) and was thus categorized as early maturing with an oocyte diameter of $446 \pm 11 \mu\text{m}$ and vitellogenin derived yolk droplets only at the periphery of the cytoplasm and persisting cortical alveolar vesicles, often in combination with atresia (Figure 44).

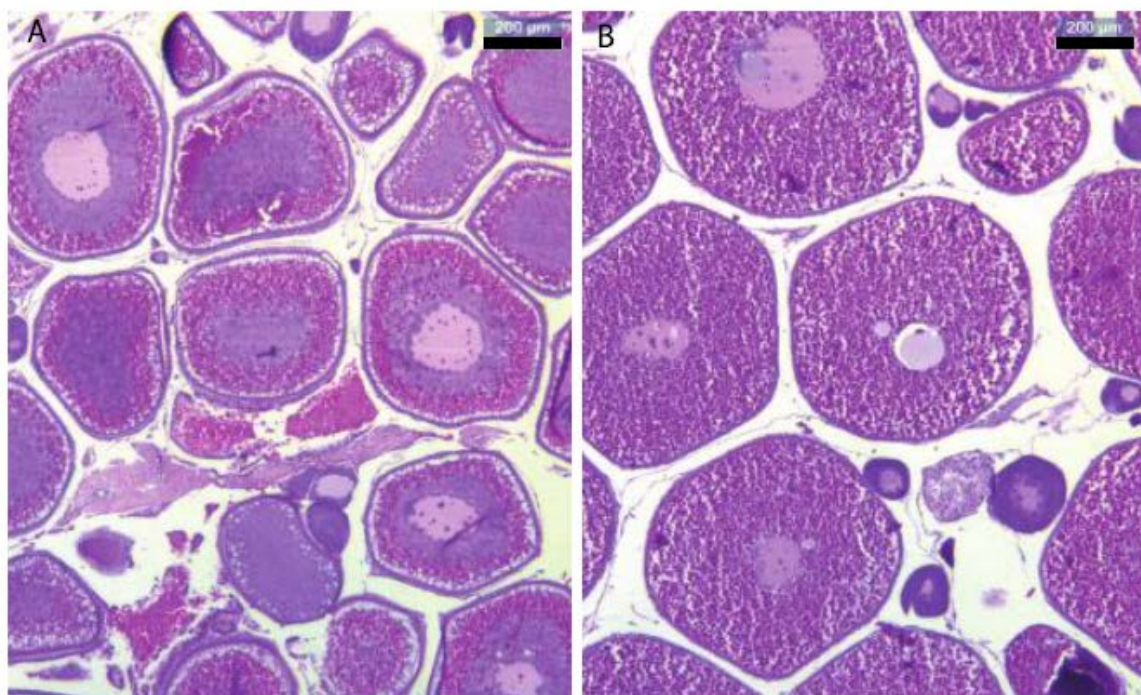


Figure 44 (A) Histological representation of an early maturing female with cortical alveoli vesicles and early signs of vitellogenesis with yolk globules present in oocyte periphery; (B) Histological representation of an advanced maturing female with vitellogenic oocytes. Scale bare is 200 µm in both pictures.

Abnormal oocyte development, characterized by partial inclusion of cortical alveolar vesicles into the cytoplasm, non-radial yolk globule orientation around nucleus, and few oocytes in the most advanced oocyte cohort, was observed in 35 % of early maturing females with no statistical significance of treatment. Significant differences in gonadal maturity stage was observed in the BO exposed females exhibited by a lower percentage of advanced maturing (35%) and higher percentage of early maturing females (38%) compared to other treatment groups (mean percentage in advanced maturing stage is 61%) ($p=0.042$) and when tested against the control group only, the significance increased (X-squared = 7.99, $df = 2$, $p\text{-value} = 0.018$) (Figure 45a). No significant differences were found between treatments in mean oocyte diameter, the relative number of oocytes in the leading cohort, presence of residual oocytes or frequency of atresic oocytes. However, significantly greater variation in oocyte diameter was observed in early maturing females in the BO treatment ($443.5 \pm 42 \mu\text{m}$, $n=7$) compared to the control ($409.0 \pm 10.7 \mu\text{m}$, $p= 0.015$, $n=5$). Gonadosomatic index (GSI) in females ranged between 0.6 and 11.5% with no significant difference between any of the treatments (Figure 45b). GSI (Mean \pm SE) for immature, resting, advanced maturing and early maturing females was (0.9 ± 0.0), (2.6 ± 0.8), (5.7 ± 0.3) and (3.6 ± 0.3), respectively and GSI in the advanced maturing females was significantly higher than all other maturity stages ($p<0.001$).

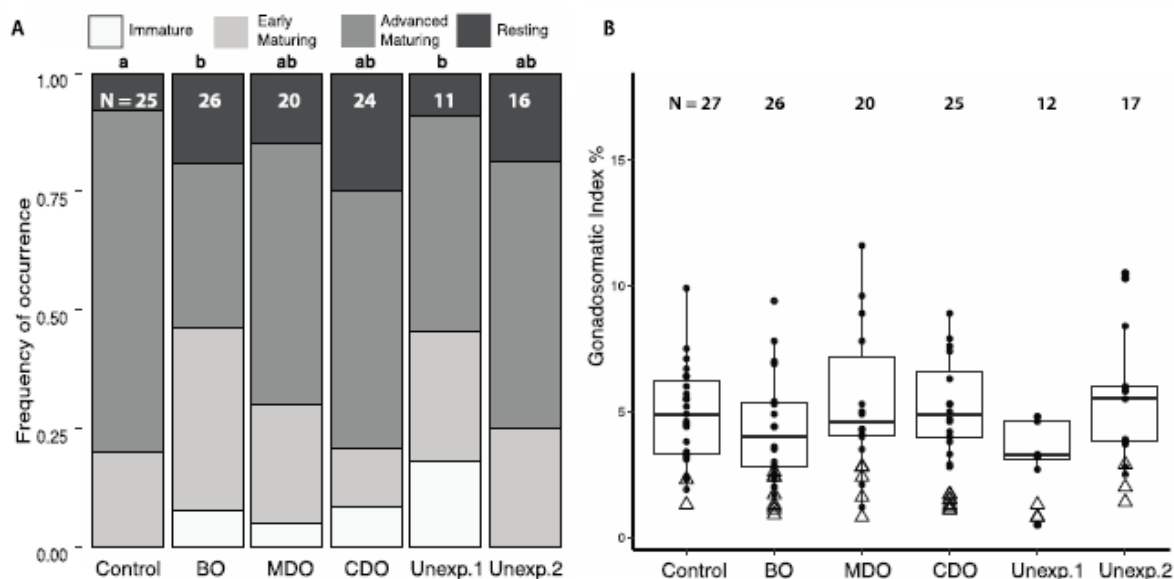


Figure 45 (A) Maturity stage frequency distribution of females from all treatments; (B) boxplots of GSI of female fish in different treatment groups, maturing females are plotted in the boxplots and immature and resting females are indicated at triangles. Different letters indicate significant differences between treatment groups where those groups with no letters in common are significantly different from one another and those sharing a letter are not. The number above each treatment refers to N.

3.4.6.2 Males

Testis development appeared normal for males in all treatments with no significant difference in the frequency of occurrence of different maturity stages among the treatments (Figure 46a). GSI in males at the end of the experiment (T7) ranged between 0.0 and 33.3% with no significant difference between any of the treatments (Figure 46b). Immature and resting fish made up 5.9% and 2.9% of the sampled males respectively while 53.9% of males were in an early stage of maturation (late Sc I) and 37.3% of the males were in a later stage of development (late Sc II). Immature and resting males had a low mean GSI ($2.0 \pm 1.6\%$ and $2.0 \pm 0.9\%$, respectively). Maturing males with late spermatocytes stage I had a lower GSI ($15.8 \pm 0.8\%$) compared to those with more developed late spermatocytes stage II ($22.6 \pm 1.0\%$).

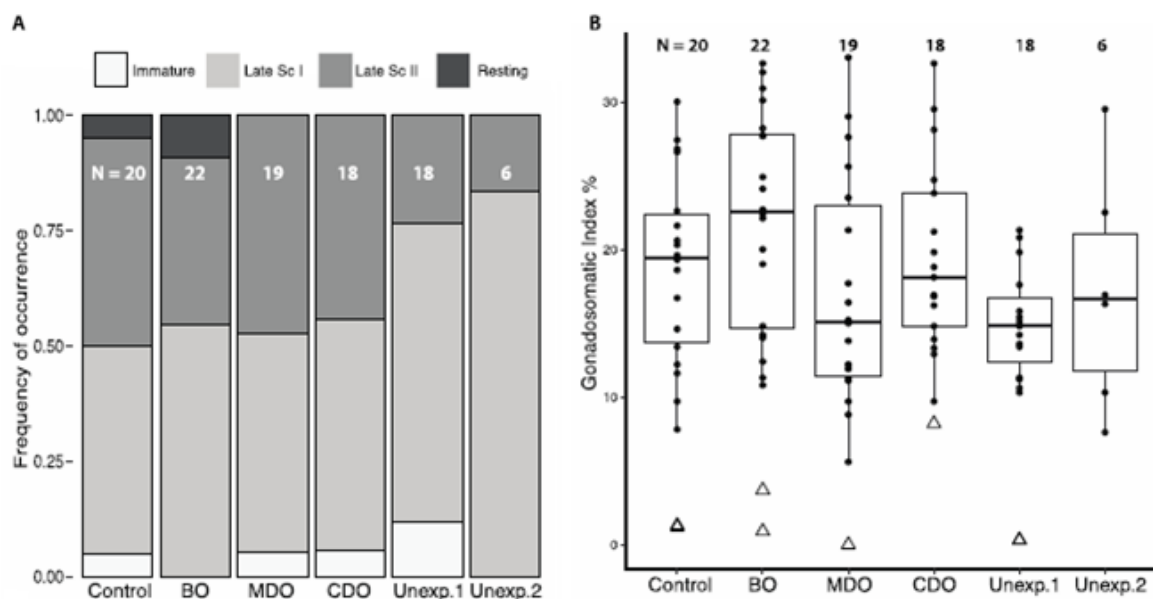


Figure 46 (A) Maturity stage frequency distribution of males from all treatments; (B) boxplot of GSI of male fish in different treatment groups, maturing males are plotted in the boxplots and immature and resting males are indicated at triangles

4 DISCUSSION

4.1 Effects of oil compounds from OSR technologies on plankton

4.1.1 *Microplankton*

In winter, low concentrations of PAH found in the mesocosm water samples indicate that the oil compounds stayed trapped inside the growing ice, and thus only small amounts of pollutants reached the water underneath (also see Petrich et al., 2013 and references therein). Low efficiency of dispersant mixture containing commercial surfactants (Aerosol OT, Brij 92, and Brij 96) under similar temperature conditions was reported in a study by Siron et al., (1993). Even though the concentrations of PAH in the water column were low in oil+dispersant and crude oil treatments, they were still significantly higher (7 times higher) than in the control and burnt oil treatments.

Overall, the nutrient concentrations decreased, and the pH concentrations increased, over the course of experiments in all four treatments (control, crude oil, oil and dispersant and burnt oil), demonstrating comparable microbial activity in the treatment groups as found in Parsons et al., (1984b), Hofslagare et al., (1983), and Siron et al., (1996). In line with this, the biomasses of microzooplankton (dinoflagellates and ciliates) and phytoplankton (pico-, nanophytoplankton, and diatoms) were similar among the treatments, however, some discrepancies in the bacterial and HNF biomasses in the oil treatments were observed compared to the control. The biomass of bacteria was significantly lower in burnt oil and crude oil treatments compared to the control group (and oil+dispersant), and one could speculate that the predation rate on bacteria was probably higher in the former treatments than in the latter ones. However, that was presumably not the case here, as the biomass of HNF was the highest in the control group, and if the same reasoning is followed, then the bacterial population in control should have experienced the highest predation pressure. In addition, the predation rate on HNF was similar in all the treatments, since the biomass of dinoflagellates was not significantly different among the groups. If this assumption is valid, then the pollutants found in the water column in oil treatments may have affected the growth of bacteria and HNF in winter. This conclusion, however, is in contrast to the previous observations where enhanced growth of bacteria (and subsequently HNF) in various oil treatments was observed (Jung et al., 2010; Ortmann et al., 2012; Delille and Siron, 1993).

In spring, increasing air temperatures initiates the brine channel formation in the sea-ice, which consequently lead to the leakage of previously trapped oil chemicals into the water column (Otsuka et al., 2004). The concentrations of PAH in oil+dispersant and crude oil treatments were thus significantly higher than the concentrations in control and burnt oil (100 and 12 times higher) in the water column. The probable reason for the low PAH concentrations measured in burnt oil treatment is the removal of more than 85% of crude oil components via incineration. Significantly higher concentrations of PAH in oil+dispersant and crude oil groups reflected low growth of most of the organisms during the exposure experiments (4/7 and 5/7 groups), which accordingly led to approximately 50% lower biomasses compared to the control group. The in-effective dispersant application scenario negatively affected the growth of microzooplankton as well as pico- and nanophytoplankton, but stimulated the growth of bacteria and HNF. These observations are in agreement with the studies by Parsons et al., (1984b) and Ortmann et al., (2012), who disclosed that oil+dispersant treatment resulted in enhanced growth of bacteria and HNF, but depressed

the growth of other zooplankton phyla (also Almeda et al., 2014). Similarly, we observed that crude oil (natural attenuation) negatively affected the growth of microzooplankton, HNF, pico- and nanophytoplankton, but stimulated the growth of bacteria. In a study by Koshikawa et al., (2007), the authors reported increased bacterial production and decreased abundance of microzooplankton in the water-soluble fraction of diesel fuel oil treatment, and conversely, increased production of HNF. Finally, our results indicate that chemically oil+dispersant and crude oil treatments had no effect on growth of diatoms. González et al., (2009) reported that diatoms smaller than 20 μm were stimulated by the water-soluble fraction of oil, while those larger than 20 μm were negatively affected by high ($\sim 20 \mu\text{g L}^{-1}$ chrysene equivalents) but not by low oil concentrations ($\sim 10 \mu\text{g L}^{-1}$ chrysene equivalents). In our study, the concentration of PAH in the water samples from the crude oil treatment was about 5 times lower ($\sim 2 \mu\text{g L}^{-1}$) than the low oil concentration treatment in González et al., (2009), which may explain why the diatom population was not affected by the crude oil pollutants. Conversely, the concentration of PAH in oil+dispersant treatment was as high as their high oil concentration treatment ($\sim 20 \mu\text{g L}^{-1}$), yet no effect on the growth of diatoms was observed in our study. Burnt oil treatment on the other hand had no effect on the growth of microzooplankton, HNF, and picophytoplankton, but stimulated the growth of bacteria and diatoms. However, the treatment negatively affected the growth of nanophytoplankton. The variances in microbial activity among the treatments were also reflected in the differences in utilized nutrients during the experiments. Overall, the concentration of nutrients decreased in all treatments, but stayed significantly higher in crude oil treatment compared to the control. The concentrations of nitrate and phosphate were significantly higher in oil+dispersant compared to the control; yet, the concentration of silica was comparable to the concentration measured in the control group. The concentrations of nitrate and silicate in burnt oil were similar to those in the control, but the phosphate concentration was significantly lower compared to the control group. Generally, the nutrient concentrations were the lowest in the control group, indicating that the restricted growth of organisms in oil+dispersant and crude oil treatments was not due to the nutrient limitation.

Although the pH concentrations in the treatments decreased during the experiments, the highest pH levels were measured in the control, which is probably a result of the strongest disturbance of CO_2 equilibria due to the highest microbial activity compared to the oil treatments. In line with this, the levels of pH cannot explain the restricted growth of organisms in oil+dispersant and crude oil treatments. Overall, our results show that when dispersant mixed with oil is frozen into ice this most likely affect the structure of the community and the biomass production (net population biomass in oil+dispersant and crude oil treatment is $\sim 50\%$ lower compared to the control and burnt oil treatments) of the Arctic microbial community. Depending on the scale and the duration of the spill, this may potentially affect the functioning of the local microbial food web, and subsequently of the lipid-driven Arctic marine ecosystem. To which extent, it remains to be investigated.

4.1.2 Copepods

In Ice covered arctic areas *Calanus glacialis* is the key secondary producer responsible for transferring energy from the ice biota and up the food web, and if this transfer is disturbed it may have consequences for the higher trophic levels. Having a high lipid content, *C. glacialis*, is a keystone species in the Arctic. When food is particularly abundant during the ice algae peak and the short, but intensive spring phytoplankton bloom, high latitude *Calanus* spp accumulate

essential polyunsaturated fatty acids. They transform low energy carbohydrates and proteins from the algae into high-energy lipids that are accumulated mainly as wax esters in energy reserves (Sargent and Falk-Petersen 1988, Lee 1975, Søreide et al. 2008, Søreide et al., 2010, Leu et al., 2011). The stored energy is utilized when food is scarce, during diapause in winter and in the maturation of gonads and developing oocysts in the following spring (Sargent and Falk-Petersen 1988). Part of the wax esters must be transformed into triacylglycerols and lipovitellins (phospholipids and protein) in the female prior to the transfer of maternal lipid reserves to eggs. In the eggs lipid droplets (wax esters or triacylglycerols) and lipovitellins work as energy reserve and building material during development of the eggs, embryos through hatching and until the first feeding nauplii stage (Sargent and Falk-Petersen 1988, Lee et al., 2006). Polycyclic aromatic hydrocarbons include compounds with environmental effects of the compounds in crude oil). PAH's in ocean water enter copepods passively by diffusion and actively during feeding either through ingestion of oil droplets in the water or by ingesting oil coated algae (Conover 1971, Gyllenberg 1981, Oil in the sea III, pers. comm. Richard Lee). Because of their lipophilic nature, these compounds might be stored in the copepods lipid reserves and may pose a significant risk of bioaccumulation passing these toxic compounds to higher trophic levels. When metabolized, these hydrocarbon compounds can cause both lethal and sublethal effects. Sublethal effects of contaminants in marine organisms include impairment of physiological processes that may alter the energy available for growth and reproduction and other effects on reproductive and developmental processes including direct genetic damage (Capuzzo 1988). On *C. glacialis* toxic responses of exposure to pyrene, a toxic polycyclic aromatic hydrocarbon present in crude oil, have been observed on grazing (Jensen et al., 2008), egg production (Jensen et al., 2008, Hjorth and Nielsen 2011) and nauplii growth and survival (Grenvald et al., 2013). In addition, reduced hatching success was observed in *C. glacialis* exposed to high water soluble fractions of crude oil (Jensen and Carroll 2010). *C. glacialis* seems less sensitive to oil exposure than its smaller relative *C. finmarchicus* dominating the Atlantic water masses (Jensen et al., 2008, Jensen and Carroll 2010, Hjorth and Nielsen 2011, Grenvald et al., 2012). In this study, no clear effects were observed on adult female of *C. glacialis* when exposed to water from the mesocosms treated with three different oil response technologies. Much of this can be explained by total PAH concentrations (sum 21 different PAHs) in the mesocosm water at the time of sampling. Specifically, in burnt oil treatment where only background levels of PAH's were present as indicated by the chemical analysis of the PAH concentrations, we would not expect to see an effect on *C. glacialis*. The concentration of PAH was slightly higher in the crude oil treatment, that might be reflected in hatching success and egg production but not on the other parameters measured in this study. In the oil+dispersant and crude oil treatment, significantly higher PAH levels was measured, this might be reflected in the tendency for increased egg production and hatching success but not on the other response parameters considered in this study. The results of survival, faecal pellet production, egg production and hatching success are discussed in the following subsections followed by an overall discussion of the limitations to the study and suggestions for further investigation. Although there were no observed direct effects of crude oil on the copepod *C. glacialis* in this study, some uncertainties still remain to be further investigated in order to better predict effects of oil spill and oil spill response technologies on Arctic copepods under a broad range of operational conditions (e.g. other oil type, spill rates etc.).

4.1.2.1 Survival

No effect was found in any treatments at any measured concentrations on survival of the copepods after 14 days exposure. This result is in accordance with previous studies on the effects of oil exposure on copepods with a similar range of PAHs exposure concentrations. Hansen et al., (2011) evaluated the survival of *C. glacialis* exposed to water accommodated fractions (WAF) of artificially weathered crude oil from the Troll field in the northern North Sea and found a LC₅₀ of 557 µg THC L⁻¹ after 144 h (Hansen et al., 2011). In this study, a total hydrocarbon concentration of 888 µg THC L⁻¹ was measured in the WAF represented with concentrations of to 11.8 µg PAH +2 rings L⁻¹ and 220.5 µg naphthalenes L⁻¹. At 223 µg THC L⁻¹, the lowest concentration tested, their study showed no effect on survival. Gardiner et al., (2013) conducted a 12-day exposure study with *C. glacialis* exposed to WAF of Alaska North Slope crude oil in a period representing the early ice free season. They found no statistical significant difference in survival between WAF exposure of 67.0 µg TPAH L⁻¹ and the control. A LC₅₀ value was derived of 430 µg TPAH L⁻¹ for chemically enhanced WAF. In the current study, at the 100% mesocosm concentration, the oil+dispersant and oil treatment had the highest concentrations of PAH's observed in all treatments and concentrations with an initial concentration of 16.935 µg PAH's L⁻¹ (including naphthalenes in the PAHs). That is a factor of ten lower than the lowest concentration in Hansen et al., (2011) experiment and a factor of three lower than the TPAH concentration in Gardiner et al., (2013) showing no effect. Even though the duration of the experiment in the current study was 14 days extending the time for effects to occur compared to previous studies, the concentration of PAH's in the water might simply have been too low to induce a lethal effect on *C. glacialis* in the current study.

4.1.2.2 Faecal pellet production

Faecal pellet production was quantified as a measure of grazing activity. Ingested feed is either absorbed or egested. The absorbed fraction is allocated to metabolism or growth. A narcotic effect has been observed in copepods exposed to PAHs. The narcotic effect can increase the exposure to predators and result in decreased feeding activity (Lotufo, 1998; Van Wezel and Opperhuizen, 1995). As the adult copepod does not spend energy on somatic growth, all energy exceeding metabolic needs can be expressed predominantly as egg production (Kjørboe et al., 1985) or storage lipid accumulation (Jónasdóttir, 2015). If the copepod responds to oil exposure by decreasing feed intake, a decrease in growth is expected, which depending on the following allocation of resources presumable result in a decrease in egg production (Klok et al., 2012). This could ultimately yield less input to the next generation and less energy available for higher trophic levels.

We report no statistically significant difference in average cumulative pellet production after the 14 days experiment among treatments and concentrations. This indicates that grazing in *C. glacialis* is insensitive to exposure to TPAH < 2.190 µg L⁻¹ and TPAH < 16.935 µg L⁻¹ from KOBBE crude oil and oil+dispersant, respectively that had been degraded in sea ice for three months. These results are in line with previous studies showing no effect on faecal pellet production of *C. glacialis* exposed to pyrene at the concentration of 20.225 µg L⁻¹ (Hjorth and Nielsen, 2011) and WSF of crude oil at the concentration of TPAH (16-EPA PAHs) of 10.4 µg L⁻¹ (Jensen and Carroll, 2010). Jensen et al., (2008) did find a time dependent reduction in grazing at 20.225 µg L⁻¹ through linear regression, which is comparable to 16.935 µg TPAH's L⁻¹ in the 100% mesocosm water of the dispersant and oil treatment in the current study. Pyrene is several times more toxic to marine

copepods than naphthalene, fluorene and phenanthrene, which has been shown in a study by Barata et al., 2005 comparing the toxicity of several single and mixtures of PAH's on the copepod *Oithona davisae* (Barata et al., 2005). Considering that pyrene accounts for less than 1% and naphthalene for more than 90% of the PAH's in the current study (data not shown), a straightforward comparison with concentrations in pyrene studies is not possible. The current study indicates that the PAH's leaking from three months in ice degraded oil+dispersant might not affect the grazing activity in the same way as pyrene.

4.1.2.3 Egg production

Egg production was quantified as one indicator of population growth. Ingested feed is either absorbed or egested. The absorbed fraction is allocated to metabolism or growth. As the adult copepod does not spend energy on somatic growth, all energy exceeding metabolic needs can be expressed predominantly as egg production (Kiørboe et al., 1985) or storage lipid accumulation (Jónasdóttir, 2015). If the copepod responds to oil exposure by decreasing egg production, it could be a signal of a direct effect of the oil exposure interfering with the different steps in oogenesis or increasing reproduction costs. It could also be an indirect effect of decreased feeding or inhibition of the absorption in the gut of the copepod caused by the oil exposure restricting the resources available for growth (Klok et al., 2012). Decreased egg production due to oil exposure has been observed in several copepod species (Almeda et al., 2014; Bellas and Thor, 2007; Hjorth and Nielsen, 2011; Jensen et al., 2008). A decreased egg production caused by PAH exposure could in the end give less input to the next generation and less energy available for higher trophic levels. At the exposure concentrations in this study such an effect on *C. glacialis* was not observed. In general higher lipid content has been linked to a delay and decreased response to oil exposure (Grenvald et al., 2013; Hjorth and Nielsen, 2011; Lotufo, 1998). In the dispersant and oil treatment, there is a tendency for a higher egg production in the 100 % treatment even though the difference is not statistical significant. Positive responses to low toxic exposure concentrations has been observed in a range of organisms (known as hormesis), where small doses of a toxin activate the repair system of the organism (Calabrese, 2005). It is unclear whether this mechanism is responsible for the higher egg production observed here.

4.1.2.4 Hatching success

Hatching success was also considered as an indicator of population growth. A reduced hatching success from oil exposure to the adult females could give less input to the next generation and less energy available for higher trophic levels. We found a moderate hatching success in all concentrations and treatments. Weydmann et al., 2015 found an average hatching success of *C. glacialis* after 7 days incubation to be 75% and 86% at 0 degrees in 2009 and 2010 respectively (Weydmann et al., 2015). That is much higher than the mean hatching success in this current study even though the experimental temperature was the same. The explanation for the lower hatching success in this study is unknown. In the current study, there has been no clear connection between different oil treatments and the effect on hatching success. This is in line with studies by Jensen et al., (2008) and Hjorth and Nielsen (2011) showing no effect on hatching success of eggs laid by *C. glacialis* to pyrene. Jensen and Carroll (2010) however examined the hatching success of *C. glacialis* after one and two days of exposure to WSF of crude oil. In high WSF concentrations of crude oil (initial TPAH (16-EPA) concentration of $10.4 \mu\text{g L}^{-1}$) the hatching success (12%) was significantly lower than the control (52%). They contribute this lower hatching success to the possible vertical transfer from female to eggs of PAH's bound in lipids (Jensen and Carroll, 2010).

Concentrations of total PAH in the high concentration in the study of Jensen and Carroll (2010) was half of the total initial PAH concentration in the 100% mesocosm water of the oil+dispersant treatment in the current study.

However, we did not see the same reduction in hatching success. Greenvald et al., (2013) found no significant effect on hatching after female *C. glacialis* have been exposed to pyrene in concentrations up to 20.225 $\mu\text{g L}^{-1}$, but reduced growth and survival of nauplii. To be able to evaluate the total reproductive output, it is therefore necessary to determine if there are later implications for the hatched nauplii caused by the exposure of the adult females to the different oil response technologies. Indeed, the hatched nauplii from this experiment showed increased deformation in the nauplii from the 100% chemically oil+dispersant treatment. This finding amplifies the significance to include nauplii and maybe also copepodite development to determine actual reproductive output.

The fact that we see no significant effects on the measured parameters on *C. glacialis* in our study does not eliminate a risk of oil spill and oil spill response technologies on *C. glacialis* copepods in ice covered areas in the Arctic for several reasons. Firstly, a possible indirect effect on copepods can be present if the ice algae and phytoplankton community are affected by the presence of oil. The bulk movement of oil-in-ice is the upward migration of oil through brine channels during melting, due to density differences, solar radiation and heat capacity of the oil (Faksness and Brandvik, 2008; Payne et al., 1991a; Payne et al., 1991b; Word, 2013). Another process is the downward transport of dissolved aromatic hydrocarbons with the dense brine water in brine channels described by Faksness and Brandvik (2008). The major brine-channel growth occurs in the spring when the air temperature increases and the ice warms up towards melting point (Faksness and Brandvik, 2008). At our sampling in the middle of May, brine channel formation had begun, whereas sea ice breakup did not occur until 6 weeks later. The long duration between start of brine channel formation until sea ice breakup indicates that the ice algae living within and on the underside of the sea ice and the phytoplankton in the underlying water might be exposed to low levels of toxic water-soluble components for a prolonged period of time (Faksness and Brandvik, 2008). We would like to address the possible indirect effect on copepods if the algae community is affected by the presence of oil. Females of *C. glacialis* utilize the high-quality ice algae bloom to fuel early maturation and reproduction, whereas the resulting offspring utilize the high quality food during the phytoplankton bloom (Søreide et al., 2010). If the quantity and quality of the food for the copepods change, it could have possible implications for reproduction and growth of *C. glacialis*. Secondly, *C. glacialis* grazing on contaminated ice algae is a pathway of toxins to the copepods that only was indirectly included in the experimental setup of this study. Instead, copepods were fed with a "clean" culture of the diatom *Thalassiosira weissflogii*. At the time of sampling in the middle of May, brine channel formation was visible.

In the experimental setup in this study, female *C. glacialis* were only exposed to the water from underneath the ice, while being fed a clean culture of *T. weissflogii*. The pathway of PAH's from feeding on possibly more contaminated ice algae was not included in the study, except for any oil components which were taken up by the diatom during the exposure study. Based on the arguments *C. glacialis* might in a real oil spill in ice covered waters be directly exposed to higher concentrations of PAH's with an additional effect from contaminated algae that were not included in this study.

Thirdly, we studied the effect of exposure to adult female *C. glacialis* on reproduction considering egg production and hatching success. The state of the hatched eggs and possible effect on the developing nauplii should also be included to give a better idea of the total reproductive output. While accumulated PAH's can be stored in maternal lipid reserves and be metabolized by the female, they might also be extruded with the lipid rich eggs. In a study by Lotufo (1998), 50% of the accumulated fluoranthene was extruded with the eggs (Lotufo, 1998), suggesting that this transfer can have occurred. During oocyte development, lipids are mobilized from the oil sac via the ovaries to the maturing oocytes (Lee et al., 2006; Niehoff, 2007). PAH's accumulated in the maternal lipid stores could be transferred to the oocytes during this process as suggested by Nørregaard et al., (2014). Our data on PAH content in eggs cannot confirm or dismiss the notion, due to low values and incoherent patterns.

In the eggs lipid droplets (wax esters or triacylglycerols) and lipovitellins work as energy reserve and building material during development of the eggs, embryos through hatching and until the first feeding nauplii stage (Lee et al., 2006; Sargent and Falk-Petersen, 1988). Grenvald et al., (2013) found no significant effect on hatching when exposed to pyrene in concentrations up to $20.225 \mu\text{g L}^{-1}$, but reduced growth and survival of nauplii. We followed the hatched nauplii from the 100% concentrations in this experiment and reported an increased deformation in the nauplii from the oil+dispersant treatment. The results could indicate that PAH's from the female had indeed been transferred to the eggs and interferes with the development of the nauplii when these toxicants are metabolized. This study shows the importance of including the examination of early life stages living off internal reserves. The examination of nauplii is equally important as the examination of egg production and hatching success as it contributes to the comprehensive estimation of the total reproductive output. The phenomenon should be investigated further. Finally, the no observed effects of oil spill response technologies in this study may be seasonal specific. As ice grows downward, oil spilled in the Arctic marine environment can rapidly be encapsulated in growing ice. Once the oil becomes fixed within the ice, the oil will be preserved, in the sense that evaporation, dissolution, and degradation will be reduced. This implies that the oil will retain much of its potential toxicity upon release from the ice, either via transport in brine channels, and/or eventual breakup and melting of the ice (Fingas and Hollebone, 2003; Word, 2013). Migration rates within the ice depend not only on oil properties and chemical composition, but also on ice thickness and the air temperature prior to the spill is important, determining the porosity of the ice (Faksness and Brandvik, 2008). At the sampling date in May, the majority of oil was still encapsulated in the ice (visual examination of ice cores). Closer to ice break-up brine channel formation increases and following an expected increase of oil transport in brine channels with the denser brine water. Late in the melting season the salinity in the ice might be so low that downward transport of PAH's decreases. At sea ice break up, oil will be released and mixing with water. Therefore the concentration of oil in the water column will likely increase. Mixing creates oil droplets increasing the availability of oil to the copepods as the oil droplets can be ingested with the food (Conover, 1971; Gyllenberg, 1981; National Research Council, 2003). Sea ice break up coincide in timing with nauplii development (Søreide et al., 2010). Exposure of the early life stages of copepods could impact the survival and development as those early life stages are thought to be more sensitive than the adult stage (Mohammed, 2013).

4.2 Light penetration, nutrients and ice-algal growth

Collectively, the abundance and chlorophyll data are consistent in indicating the extremely low algal biomass that prevailed in all mesocosms. Even the highest cell abundances and chl a concentrations reported here do not exceed what are considered to be winter "background" values in other studies. These studies often report Chl a inventories in areal units (per m²). The highest value we observed in our study was 0.008 mg m⁻² in a control mesocosm on 6th of May. Allowing for the fact that we melted 5-cm cores (instead of 3 or 4-cm cores in some other studies) would only rise our highest value to 0.013 mg m⁻². Maximum Chl a inventories observed at the peak of ice-algal blooms across the Arctic Ocean are at least 2 orders of magnitude higher (Leu et al., 2015), ranging from 1.0 mg m⁻² in very oligotrophic areas (e.g. Young Sound) to 110 mg m⁻² in very productive areas (e.g. Resolute area). The fjords of Svalbard are considered moderately productive. Samples taken at another location in Mijenfjorden on 22 April 2015 yielded chl a inventories of ca. 4.4 mg m⁻² (estimated from different core sections; Janne Søreide, personal communication), roughly 2 orders of magnitude higher than our maximum value in the controls. Under-ice PAR levels at the same location were an order of magnitude higher than the maximum we observed at any time in our controls. The maximum abundance of protists in our study was also extremely low. In the oligotrophic Beaufort Sea, as example, the inventories of pennate diatoms and chl a in early February prior to the onset of the ice-algal growth season were 0.001×10^9 cells m⁻² and 0.01 mg chl a m⁻², respectively (Rozanska et al., 2009), both values corresponding to the maximum ones we observed in May in control mesocosm I. In the Beaufort Sea, these background winter values increased to maxima of 3.58×10^9 cells m⁻² and 28.6 mg chl a m⁻² during the peak of the bloom in May (Rosanska et al., 2009).

The extremely low biomass of ice algae that prevailed during this study could easily have thwarted the experiment because small fluctuations or spatial heterogeneity in "natural" factors (e.g. grazing or passive trapping of planktonic algae in growing ice) might have superseded treatment effects. The positive correlations shown in Figure 7 for several groups of algae are supportive in this respect, especially for the pennate diatoms group that comprised several species that do not grow in the water column. When these algae were abundant, their association with relatively high chl a concentrations and low contributions of phaeophytin to total pigments was consistent with the growth of healthy cells *in situ* within the brine channels of sea ice. In addition, the coincident increase in empty diatom frustules and intact pennate diatoms as well as the lack of consistent differences in the proportion of empty frustules between mesocosms collectively indicate that differential grazing pressure does not account for observed differences between treatments. Thus we surmise that those differences represent an intrinsic response of the protist community to the experimental perturbations.

Overall the "burnt oil" treatment was more similar to the controls than the "oil" and "oil+dispersant" treatments, implying that, within the context of this particular experiment, the addition of burnt oil had a lesser ecological impact on ice algae than a lack of response (oil alone) and oil premixed with Finasol dispersant. It must be pointed out, however, that we have no way of normalizing the treatments in terms of actual dose of contaminating substances. Also the addition of burnt oil residue to surface water before the formation of ice cannot be simply equated to *in situ* burning. With these caveats in mind, our results nevertheless suggest that the inclusion of burnt oil residues may be less detrimental than oil alone or a mixture of oil and dispersants in terms of the amount of light penetrating through the sea ice. This was barely detectable at T1 but, unfortunately, the mesocosms themselves attenuated so much light that

potential differences between the "contaminated" treatments were masked most of the time. A lesser impact of the "burnt" oil treatment on light penetration is intuitive since the clumpy residues exhibit a scattered dispersion in the sea ice, presumably allowing better light penetration through clean interstices. Moreover, it seems that the addition of Finasol did not discernably affect the results with respect to the inclusion of crude oil alone.

Ice is a strongly scattering environment and a large fraction of the light converging on a single point is supplied laterally (e.g. Zhao et al., 2010). The opaque side walls blocked this lateral supply, leading to very low light levels even in the controls, which must therefore be considered as a "perturbed" setting for the biological communities thriving in bottom ice as well as the ice-water interface. While future studies should consider using clear or semi-transparent side walls, which were not available at the time of mesocosm construction, the absorption of laterally supplied photons in this experiment is not completely unrealistic as it contributed to simulate a wider contaminated area. A real oil spill would attenuate light over an area much wider than the diameter of the mesocosms, thereby constraining the lateral light supply to a specific point much more than would have occurred if the mesocosm walls had been perfectly clear. The experimental set up we used can therefore be considered as a compromise toward simulating a realistic light environment for the contaminated treatments, but failed to produce an ecologically-relevant control for the communities living in bottom ice. It is likely that the response of bottom-ice protist communities would have been more contrasted between controls and treatments had the controls experienced higher light levels more typical of unperturbed ice.

The taxonomic analyses provided several additional insights into the response of bottom-ice communities. The absence or relatively low abundance of several algal species in some of the mesocosms suggest that the ecological services that bottom-ice communities provide (i.e. food provision, mitigation of the atmospheric CO₂ burden) may be affected by the presence of crude oil in the ice, with or without dispersant. These treatments favored a greater importance of flagellates relative to pennate diatoms. We interpret this at least partially as a consequence of extremely low light since a similar observation has been made before by comparing locations with a high snow cover (less light and enhanced flagellate contributions) and a low snow cover (more light and enhanced pennate contributions) in the Beaufort Sea (Rozanska et al., 2010). Whether the absence of specific species (especially those of the *Navicula* genus) and the low abundance of cryptophytes in the "oil" and "oil+dispersant" was caused by extremely low light level or toxicity cannot be ascertained with the experimental designed we used here and would warrant further investigation.

One positive aspect of the low light levels in the controls is that the lack of significant biomass accumulation permits a clearer assessment of the impact of treatments on nutrient availability. When large accumulation of algae occur, large and variable amounts of nutrients are stored in their biomass, which may complicate the interpretation of ambient concentrations. This complexity was not present in our experiment so that we can infer from the data presented in Figure 3 that the treatments had no discernible impact on the exchange of nutrients between the brine channels of sea ice and the underlying water. In this context, we can conclude that the experimental responses to treatments in terms of overall algal biomass and cell abundance were primarily caused by the differential attenuation of light, with possible but unconfirmed toxicity effects on some algae.

4.3 Sea Surface Layer Microbial Community

4.3.1 Difference Between Surface Layer and Underlying Water

This study assessed the impact of oil and two oil response treatments (oil+dispersants and in-situ burning) on the density of bacterial and pico/nano-eukaryotes as well as on bacterial community diversity in Arctic Ocean surface layer seawater near to and subsurface seawater below sea ice. No difference in abundance or diversity of bacterial and eukaryotes was observed between surface layer and subsurface waters, regardless of treatment. On the other hand, enrichment was reported in *surface microlayers* with respect to subsurface seawater within leads of the high Arctic Ocean for bacterial density, but not for bacterial production (Matrai et al., 2008), as a measure of bacterial activity. It should be noted that the *surface microlayers* were two orders of magnitude thinner ($<83\mu\text{m}$) than the *surface layers* sampled herein (6-8mm) allowing for the possibility of significant dilution of our concentrations.

4.3.2 Influence of Treatment to Microbial Community

The bacterial abundance was not different among the different treatments and no change was observed as a function of time over the course of the experiment. Similarly, pico and nanoplankton maintained their abundance across the various treatments. There was also no or little change observed in bacterial composition and diversity within and among the various treatments, except for some known oil-degrading bacterial species (i.e., *Colwellia* in subsurface water). Indeed, only the control showed a decrease in bacterial abundance both in surface and subsurface water. The increase of oil-degrading bacteria demonstrates that these organisms are present and have the potential to respond to hydrocarbon input within day.

4.3.3 Influence of Treatment on Hydrocarbon Concentration

The different treatment led to variable PAH concentrations in the surface layer as well as in the underlying water. As can be expected, the presence of dispersants led immediately (Day 1) to the highest concentration in the water sampled at 50 cm depth. This can be explained by formation of small oil droplets that can be transported into the water column. For oil alone, the peak concentration was only reached at Day 3, since the droplet formation was not assisted by the presence of dispersant. For the burnt oil, only low subsurface water PAH concentrations were measured because the burned oil residue is comprised of viscous and relatively water-insoluble compounds.

For all treatments (except the control treatment), there were clear decreases in PAH concentration for last day of the experiment. The reason for this decrease can be due to dilution of the water in our enclosure with uncontaminated seawater (the enclosures were open at the bottom), caused lateral advection within the fjord. Tidal advection would also be possible; however, we measured no change in water height in our experimental enclosures over one tidal cycle. An alternative explanation for the decrease in hydrocarbon concentration would be establishment of an effective oil-degrading microbial community in the water column. The microbial community analysis shows some increases in species such as *Colwellia*, which is a known hydrocarbon degrader. While biodegradation is possible as a cause for decrease in aqueous concentrations, this did not translate into measurable biodegradation-induced changes in the oil phase (Fig 9). Furthermore, a recent study of an experimental oil spill in the North Sea suggest

that physical processes are the main driver of hydrocarbon changes in the first days of an oil spill (Gros et al., 2014).

4.3.4 Comparison of hydrocarbon degradation to mesocosm experiments (section 1)

The fact that no significant biodegradation was observed in the 5-day incubations in the enclosures is not surprising. From the biodegradation study performed with samples from ice and seawater from mesocosms experiments described in section 1, half-lives around 70 days were observed for naphthalene. Given that these bacteria have been in contact with hydrocarbons for several months in the mesocosms before the incubation started, we would only expect slower biodegradation rates in the enclosures, which were not oiled before the experiments started. Even at oil spills such as the *Deepwater Horizon*, biodegradation of compounds larger than hexane was only observed months after the onset of the spill (Aeppli et al., 2012).

4.3.5 Comparison of microbial community to mesocosm experiments (section 1)

Parallels can also be drawn with respect to the microbial community in these results from 5-day incubations in enclosures and in the mesocosm experiments (section 1). In seawater collected under oil-treated oil, a similar microbial community was observed as in the seawater samples at 50 cm depth under the enclosures (dominated by *Colwellia* sp., *Oceanospirillaceae*, *Proteobacteria* and *Flavobacteriaceae*). However, whereas in the mesocosms a distinction between the control (no oil) and the oiled treatment was apparent, the control clustered with the oiled treatment in the enclosures (Figure 7). This seems to suggest that no distinct oil-influenced microbial community formed on a time scale of five days.

4.4 Polar cod

4.4.1 Exposure to dispersed oil and burned oil residue

The present study simulates conditions in which dispersant (CDO treatment) or in situ burning (BO treatment) might be used to combat an oil spill in Arctic waters in comparison to no action (MDO treatment). THC and PAH water concentrations in both MDO and CDO reflected environmentally realistic concentrations reported from experimental field trials and dispersant operations during actual oil spills (i.e. THC concentrations of 30-50 mg/L below the spill just after treatment before decreasing to <1-10 mg/L, and Σ PAH concentrations of 6-115 mg/L the first days or weeks after accidental oil spills) (Humphery et al., 1987; Kingston, 1999; Law, 1978; Lessard and DeMarco, 2000; Lunel et al., 1995; Short and Harris, 1996; Reddy and Quinn, 1999). Reports of hydrocarbon concentration in seawater after in situ burning operations are scarce. PAH and THC levels in the present study are below seawater concentrations measured after experimentally spilled and burned oil in the Newfoundland Oil Burn Experiment (3.78 μ g/L Σ 16 EPA PAHs) (Daykin et al., 1994), and above THC concentration from an oil spill simulation and test burning experiment in the Barents Sea (13 μ g/L) (Brandvik et al., 2010).

The overall THC and Σ 26 PAH concentrations in the Ctrl, MDO and CDO treatments were in agreement with previous experiments using the same nominal oil concentrations and exposure set-up as in the present study (Frantzen et al., 2015, 2016), and confirms that the addition of chemical dispersant increases the efficiency of the dispersion process leading to significantly elevated THC and PAH concentrations in CDO compared to MDO. Measured BO concentrations

were 8 ± 2 % of the measured MDO concentrations, indicating that mechanical dispersion of BO into the water column was equally efficient as for oil. In the present study, an identical exposure protocol was used for all treatments to allow for direct comparison of effects between the oil spill response measures investigated. Energy was added to the seawater to simulate a dynamic exposure with wave energy for the period of 4 tidal systems (48 hours) (Milinkovitch et al., 2011), and the measured concentrations of hydrocarbons represented both the water-soluble fraction as well as BO residue particles/dispersed oil droplets. Adding mixing energy to simulate wave action to the BO residue exposure dispersing it in the water column is, however, novel as previous studies have exposed organisms only to the burned oil WSF (Faksness et al., 2011; Gulec and Holdway, 1999), and reported measurements are taken of seawater hydrocarbon concentrations underneath burned areas in calm conditions (Brandvik et al., 2010).

Forming of short-term temporary oil slicks, variation in oil adherence to equipment and mixing by fish movements between replicate tanks may be a source of the individual variability in THC and PAHs concentrations between replicate water samples, and the increased PAH/THC concentration at T48h compared to T24h observed in two individual tanks (one MDO and one CDO tank, respectively). Inter- and intra-tank variations did however not influence the overall significant difference in THC/PAH concentrations between the OSR actions investigated. Low concentrations of naphthalene measured in the control water may be considered elevated background levels with no potential toxic effects to biota (Molvær et al., 1997) and are evidence of the ubiquity of PAHs, especially naphthalene, one of the most abundant PAHs in the marine environment (Latimer and Zheng, 2003).

4.4.2 *Physiological and reproductive effects*

No relationship was found between treatment and mortality. Sustained mortality rate in all groups (both exposed and unexposed) are most likely due to the post spawning physiological state of the fish as confirmed by the presence of residual oocytes in 56% of females. Handling stress at the beginning of the experiment could have induced higher mortality at this early time point. The mortality rate seen in this experiment (~24%) was lower than the mortality observed (~56%) in a long-term crude oil exposure on adult feral polar cod held in captivity (Bender et al., 2016). Fish were in a good state of health as evidenced by an unanimously high condition factor and HSI in all treatment groups at the final sampling in January, although the HSI values reported for fish in the present study (8.5 - 9.6 %) were lower than for polar cod of a similar size held in captivity at the same time of year (10.9-13.1%) (Bender et al., 2016). Fish in the latter study were fed a natural diet of *Calanus* sp. zooplankton whereas commercial feed was used in the present study and this difference in diet may have influenced the liver weight relative to somatic weight. Higher condition factor in males compared to females at the start of the experiment is most likely due to the difference in the timing of reproductive investment, where males start gonadal investment earlier in the season than females (Hop et al., 1995; Nahrgang et al., 2014).

Growth rates observed in polar cod of the present study were within reported ranges from previous studies (Jensen et al., 1991; Hop et al., 1997). Furthermore, the observed trends in growth rate did not indicate significant long-term effects by any of the OSR actions. The transient decrease in SGR for the MDO and the CDO treatments compared to BO treatment, may however, be due to a transient appetite depression in these two groups in the first days following the exposure. Low feeding activity was visually observed at this time. No effect of crude oil exposure on appetite has been observed in polar cod previously; however, exposure to crude oil

contaminated food did lead to reduced growth in exposed fish (Christiansen and George, 1995). The SGR in July (T1-T2) was highest (0.6 ± 0.0 % body weight change per day) in all treatment groups compared to all other periods (0.1-0.2 % change per day) and may reflect some compensatory growth following handling and fasting during exposure (Ali et al., 2003).

Females likely to spawn in the coming winter season were in the late maturing (Vg II) stage with a GSI around 5.7 ± 0.3 % while it is unclear when or if the females in the early maturing stage would spawn. The timing of spawning from other laboratory polar cod populations in an analogous reproductive stage indicates that the late maturing females would be ready to spawn in March (Bender et al., 2016). The high frequency of early maturing females may be an evidence of stress resulting in reduced investment into reproductive development (Rideout et al., 2005; Kime, 1995). However, with only a single histological sampling point it is not possible to resolve if the females in the early maturation stage initiated vitellogenesis at the same time as females in the late maturing phase and then paused further development or if vitellogenesis was ongoing at a reduced pace. Nevertheless, abnormal oocyte development observed in some early maturing females (i.e. nonconforming yolk globule orientation) may suggest that vitellogenesis was interrupted and that these oocytes may soon be reabsorbed through atresia (Rideout et al., 2005). Reabsorbing vitellogenic oocytes results in a lower fecundity and has been observed in Atlantic cod under environmental stressors like low temperature, poor nutritional, and pollution (Rideout et al., 2005). However, no increased incidence of atresia was observed in early maturing females at sampling. The increased frequency of early maturing females in the BO exposure group could indicate a reduced population fecundity compared to the unexposed and control groups. The large variation in oocyte size of early maturing females exposed to BO treatment may be early signs of reabsorption of vitellogenetic oocytes or of some other disruption of oogenesis. PAHs have endocrine disrupting properties with potential to impair vitellogenesis in fish (Hylland et al., 2006; Aruwke and Goksøyr, 2003). Despite low tissue PAH concentrations, reproductive impairment was seen in Gulf killifish two months after the Deepwater Horizon oil spill (Whitehead et al., 2012). Similarly, depressed plasma 17β -estradiol concentrations were seen in Dolly Varden and Yellowfin sol after the Exxon Valdez oil spill (Sol et al., 2000). Although the overall THC/PAH concentration in BO was an order of magnitude lower than in MDO and CDO, differences in physical characteristics may have caused altered exposure route and thus toxicity of the BO residue compared to MDO and CDO. Burned oil residues have increased viscosity and stickiness compared to crude oils (Fritt-Rasmussen et al., 2015; Fingas, 1995), and, although oil droplet sizes/BO particle sizes were not measured in this experiment, BO particles were most likely significantly larger than MDO and CDO oil droplets as they could be observed by eye as "black dots" in the water column. Mechanically and chemically dispersed oil droplets are generally found to be in the size range ≥ 100 μ m and 10-50 μ m, respectively (Lessard and DeMarco, 2000; Lewis and Daling, 2001), and, in contrast to BO particles, they could not be observed by eye. After an in situ burning action, fish can be exposed to the residue through the WSF in the water column or through direct contact with the residue, which may clog gills, adhere to skin or be ingested. In the present study, exposure to the residue through gill clogging and ingestion may have increased the bioavailability to PAHs and other compounds present in the residue compared to the bioavailable fraction of MDO and CDO. Burned residues are enriched in high molecular weight PAHs, pyrogenic PAHs and metals (Shigenaka et al., 2015; Buist 2004). Indeed, the UCM profiles of burned oil residues from DWH burns have an altered shape compared to unburned fresh oil with enrichment of more volatile n-alkanes (Stout and Payne, 2016). The UCM fraction at environmentally relevant concentrations has been found to exert additional sub-lethal

and lethal effects on marine benthos and increase the bioavailability of PAHs (Du et al., 2011). Other studies investigating acute toxicity of BO residues have found non-toxic or little effects on snails and amphipods at concentrations below 1.46 mg/L THC or 5.83 µg/L total PAHs when exposed for 24 hours (Gulec and Holdway 1999) and no additional effect of the WSF after burning on *Calanus* spp. when exposed for 96 h at concentrations less than 1 mg/L THC compared to the WSF prior to burning (Faksness et al., 2011).

Gonadal investment occurred earlier in males compared to females in accordance with other studies investigating polar cod reproductive development (Bender et al., 2016; Nahrgang et al., 2014). No effect of any treatment on the timing, structure, or investment in male reproductive development indicated the relative resilience of this sex. Male polar cod invest less energy in reproductive development compared to females (Hop et al., 1997), which may allow for greater tolerance to xenobiotic exposure during the reproductive development period. Inclusion of the unexposed fish into the experimental design provided additional information on background physiological change due to size differences. The smaller unexposed fish (Unexp. 1) were generally younger and less likely to mature in the current season, with an increased prevalence of immature individuals and lower HSI compared to their larger unexposed counterparts (Unexp. 2). Maturing individuals in Unexp. 1 had generally lower GSI values than maturing fish in larger size categories emphasising the importance of size in reproductive output (Nahrgang et al., 2014). The Unexp. 2 fish were of a similar age and larger size (both length and weight) than fish included in the exposure experiment but a higher mortality rate and no immature individuals further supporting the hypothesis that mortality is related to previous spawning events.

5 CONCLUSIONS

Overall, the study performed herein with applied oil spill response technologies in the mesocosms show no major effects on sea-ice communities. Among the numerous parameters that were measured, there were some significant effects on microplankton structure and growth. There were some indications of effects on nauplii development of which the population consequences should be further studied. Finally, polar cod reproduction system was significantly affected by the residues of the burnt oil which requires further validation.

5.1 Microplankton

Our results show that when oil gets frozen into ice, mixed with dispersants or without dispersants, this will result in the altered structure and production (net population biomass in oil+dispersant and crude oil treatment ~50% lower compared to the control and burnt oil treatments) of the Arctic microbial community. Depending on the scale and the duration of the spill, this may potentially affect the functioning of the microbial food web, and subsequently of the entire lipid-driven Arctic marine ecosystem. To which extent this is likely, remains to be investigated.

5.2 Copepods

No quantifications of effect concentrations on copepods were derived in this study. Exposure concentrations under the ice were too low to derive effect concentrations. It is suggested that future studies should focus on the consequence of exposure to early life stages, direct exposure of nauplii and copepodites. It would also be interesting to investigate how copepods perform their diapause after the exposure to oil in the sea ice, and also, to follow the maturation and gonad development when lipid reserves are used in the metabolism in the following spring.

5.3 Light penetration, nutrients and ice-algal growth

The experimental responses observed in this study are valid only within the context of the low biological productivity imposed by mesocosm design and the geographical location of the study. The same study conducted in a different productivity zone of the Arctic Ocean could have yielded different results. Our results nevertheless provided novel insights into the sensitivity of bottom-ice protist communities to oil spills and response technologies and point out the need to adjust mesocosms design to increase the realism of light conditions in future experiments.

5.4 Sea Surface Layer Microbial Community

Different oil response treatments were visually very different. Whereas oil as well as the oil/dispersant mixture formed a slick, burned oil residues were oil "junks" that did not form a coherent slick (although a rainbow-colored thing slick formed around these "junks"). This suggests that after burning, the residue has less of a potential to cover large areas than oil slicks. A further visual observation was that the oil/dispersant mixture formed a mousse-like oil slick after three days. This implies that although the dispersant was pre-mixed with oil and then experienced almost no wind or wave energy, it still performed its intended function, dispersing oil and mixing it with water.

The different oil spill response treatment also had a significant influence on the hydrocarbon concentration measured 50 cm below the surface. The oil/dispersant treatment had the highest concentrations, followed by the oil treatment and then the burned oil residue treatment. This signifies that the dispersant seem to perform its intended effect (i.e., brining oil droplets into the water column, where it can be degraded more easily), even though it was applied in a non-realistic manner (oil/dispersant mixture applied as slick, rather than sprayed on the oil), and that the burned oil residue delivers the lowest hydrocarbon input of these three treatments into the seawater.

From a microbial abundance perspective, no significant differences were observed between the treatments—and also the control—in samples from 50cm depth. This signifies that the presence of oil does not translate to an increase or decrease in phytoplankton or bacterial numbers within five days, irrespective of the response option chosen. The same conclusion holds true considering the bacterial community composition at 50 cm depth, which were not significantly different between control and treatments. The only exception was the dispersant-only treatment where, after 72h, bacterial cell abundance clearly decreased in surface layer water. However, application of dispersant without the presence of an oil slick would not be a realistic scenario.

5.5 Polar cod

The transient effect on growth observed in the present study posed no effect on the overall growth and survival of the polar cod, demonstrating the robustness of adult polar cod compared to early life stages (Nahrgang et al., 2016). However, an oil spill in areas/ times of high biological activities, i.e. spring bloom along the ice edge, could pose sufficient risk of exposure for polar cod and other organisms which rely on this high productivity in an Arctic system where primary production is spatially and temporally limited (Leu et al., 2015). The decreased frequency of maturing females exposed to the BO treatment is of importance with regard to potential reductions in population fecundity (Spromberg and Meador, 2004) and may reveal a sensitivity of polar cod when exposed to dispersed residues from this OSR countermeasure. This effect observed on the fitness of female polar cod exposed to BO may not be adequately explained by the relatively low THC and PAH levels measured in the BO treatment, therefore other hydrocarbon compounds, the UCM, and the physical properties of the BO residue should be further investigated.

With increasing anthropogenic activity in the Arctic, polar cod are at risk for exposure to petroleum and OSR actions through accidental spills. The purpose of a NEBA is to aid in the decision making in the event of an OSR where the environmental effects of an action or combination of actions should be evaluated. However, no long-term effects on polar cod survival and growth were observed under acute dynamic exposure conditions to BO, MDO or CDO. Observed effects were overall limited. The physiological effects of BO need further investigation, including experimental method validation. The reduction of overall oil by ~90% with in-situ burning will reduce the oil volume and the potential for organisms to come into contact with the oil and may still be a viable option despite the potential adverse effects observed in this study. The NEBA process will help deciding what response strategy eventually will lead to the least environmental impact and fastest recovery. Overall, this study demonstrates the robustness of the adult life stage of polar cod to a variety of OSR actions. The final endpoints of reproduction, such as fecundity, fertilization success and survival and fitness of offspring of exposed polar cod,

were not included in the present study, however these endpoints would provide valuable information on ecosystem sensitive for the NEBA in the Arctic marine system. This study provides new evidence to aid in OSR decision making on the sensitivities and tradeoffs between growth, mortality, and reproductive development in the Arctic key species polar cod.

6 REFERENCES

- Aeppli C., Carmichael C.A., Nelson R.K., Lemkau K.L., Graham W.M., Redmond M.C., Valentine D.L. and Reddy C.M. (2012). Oil weathering after the Deepwater Horizon disaster led to the formation of oxygenated residues. *Environmental Science & Technology* 46(16): 8799-8807.
- Aeppli C., Nelson R.K., Radović J.R., Carmichael C.A., Valentine D.L. and Reddy C.M. (2014). Recalcitrance and degradation of petroleum biomarkers upon abiotic and biotic natural weathering of Deepwater Horizon oil. *Environmental Science & Technology* 48(12): 6726- 6734.
- Ali, M., Nicieza, A., Wootton, R.J., 2003. Compensatory growth in fishes: a response to growth depression. *Fish. Fish.* 4, 147-190.
- Almeda R, Hyatt C, Buskey EJ (2014) Toxicity of dispersant Corexit 9500A and crude oil to marine microzooplankton. *Ecotoxicology and Environmental Safety* 106, 76–85.
- Andersen, Ø., Frantzen, M., Rosland, M., Timmerhaus, G., Skugor, A., Krasnov, A., 2015. Effects of crude oil exposure and elevated temperature on the liver transcriptome of polar cod (*Boreogadus saida*). *Aquat. Toxicol.* 165, 9–18.
- Arukwe, A., Goksøyr, A., 2003. Eggshell and egg yolk proteins in fish: hepatic proteins for the next generation: oogenetic, population, and evolutionary implications of endocrine disruption. *Comp. Hepatol.* 2, 1–21.
- Balk L, Hylland K, Hansson T, Berntssen MHG, Beyer J, Jonsson G, Melbye A, Grung M, Torstensen BE, Børseth JF, Skarphedinsdottir H, Klungsoyr J (2011) Biomarkers in natural fish populations indicate adverse biological effects of offshore oil production. *PLoS One* 6, e19735. doi:10.1371/journal.pone.0019735.
- Barata C, Calbet A, Saiz E, Ortiz L, Bayona JM (2005) Predicting single and mixture toxicity of petrogenic polycyclic aromatic hydrocarbons to the copepod *Oithona davisae*. *Environ. Toxicol. Chem.* 24, 2992–2999. doi:10.1897/05-189R.
- Bellas J, Thor P (2007) Effects of selected PAHs on reproduction and survival of the calanoid copepod *Acartia tonsa*. *Ecotoxicology* 16, 465–74. doi:10.1007/s10646-007-0152-2
- Bender, M.L., Frantzen, M., Vieweg, I., Falk-petersen, I., Kreutzer, H., Rudolfson, G., Erik, K., Dubourg, P., Nahrgang, J., 2016. Effects of chronic dietary petroleum exposure on reproductive development in polar cod (*Boreogadus saida*). *Aquat. Toxicol.* 180, 196–208. doi:10.1016/j.aquatox.2016.10.005
- Bérard-Therriault L., Poulin M., Bossé L. (1999) Guide d'identification du phytoplancton marin de l'estuaire du Saint-Laurent, incluant également certains protozoaires. *Publ spéc can sci halieut aquat* 128:1–387.
- Bradstreet MSW, Cross WE (1982) Trophic Relationships at High Arctic Ice Edges. *Arctic* 35:1-12
- Brandvik, P.J., Fritt-Rasmussen, J., Reed, M., Bodsberg, N.R., 2010. Predicting ignitability for in situ burning of oil spills as a function of oil type and weathering degree. In: *Proceedings of the 33rd AMOP Seminar on Environmental Contamination and Response*, Environment Canada, Ottawa, ON, pp. 773–786.
- Buist, I., 2004. In Situ Burning for Oil Spills in Ice-Covered Waters, in: *Interspill*. pp. 1–24.
- Buist, I.A., Potter, S.G., Trudel, B.K., Shelnutt, S.R., Walker, A.H., Scholz, D.K., Brandvik, P.J., Fritt-Rasmussen, J., Allen, A.A., Smith, P., 2013. *In Situ Burning in Ice-Affected Waters: State of Knowledge Report, Final report 7.1.1, Report from Joint Industry Programme.*
- Calabrese EJ (2005) Paradigm lost, paradigm found: The re-emergence of hormesis as a fundamental dose response model in the toxicological sciences. *Environ. Pollut.* 138, 379–412. doi:10.1016/j.envpol.2004.10.001.
- Capuzzo JM, Moore MN, Widdows J (1988) Effects of toxic chemicals in the marine environment: predictions of impacts from laboratory studies. *Aquat. Toxicol.* 11, 303–311. doi:10.1016/01669445X(88)90080-X.
- Christiansen, J., George, S., 1995. Contamination of food by crude oil affects food selection and growth performance, but not appetite, in an Arctic fish, the polar cod (*Boreogadus saida*). *Polar Biol.* 15, 277–281.

- Conover R (1971) Some relations between zooplankton and bunker C oil in Chedabucto Bay following the wreck of the tanker Arrow. *J. Fish. Board Canada* 28, 1327–1329.
- Cross W.E., 1982. In situ studies of effects of oil and dispersed oil on primary productivity of ice algae and on under-ice amphipod communities. In: Special studies - 1981 study results, Book Baffin Island Oil Spill Working Report 81-10.
- Cross W.E., 1987. Effects of oil and chemically treated oil on primary productivity of high Arctic ice algae studied in situ. *Arctic* 40, 266-276.
- Cunningham L., Stark J.S., Snape I., McMinn A., Riddle M.J., 2003. Effects of metal and petroleum hydrocarbon contamination on benthic diatom communities near Casey Station, Antarctica: an experimental approach. *J. Phycol* 39: 490–503.
- Daykin, M., Sergy, G., Aurand, D., Shigenaka, G., Wang, Z., Tang, A., 1994. Aquatic toxicity resulting from in-situ burning of oil- on-water. In: Proceedings of the Seventeenth Arctic and Marine Oil Spill Program Technical Seminar, Vancouver, British Columbia, Canada.
- Degnan P.H. and Ochman H. (2012). Illumina-based analysis of microbial community diversity. *Isme J* 6(1): 183-194.
- Delille D, Siron R (1992) Effect of Dispersed Oil on Heterotrophic Bacterial Communities in Cold Marine Waters. *Microb Ecol* 25:263-273.
- Doherty S.J., Grenfell T.C., Forsstrom S., Hegg D.L., Brandt R.E., Warren S.G., 2013. Observed vertical redistribution of black carbon and other insoluble light-absorbing particles in melting snow. *Journal of Geophysical Research-Atmospheres* 118, 5553-5569. doi:10.1002/jgrd.50235.
- Du, J., Tyler Mehler, W., Lydy, M.J., You, J. 2011. Toxicity of sediment-associated unresolved complex mixture and its impact on bioavailability of polycyclic aromatic hydrocarbons. *Journal of Hazardous Materials*.203-204, 169-175. doi:10.1016/j.jhazmat.2011.11.099
- Eni Norge, 2015 "Goliat Crude oil Blend" accessed on May 30th 2017
http://www.eninorge.com/Documents/Goliat_blend.pdf
- Faksness L-G, Brandvik PJ (2008) Distribution of water soluble components from oil encapsulated in Arctic sea ice: Summary of three field seasons. *Cold Reg. Sci. Technol.* 54, 106–114. doi:10.1016/j.coldregions.2008.03.006.
- Fakness, LG., Hansen, B.H., Altin, D., Brandvik, P.J. 2011. Chemical composition and acute toxicity in the water after in situ burning- A laboratory experiment. *Mar Poll. Bull.* 64, 49-55. doi:10.1016/j.marpolbul.2011.10.024
- Fingas, M.F., 1995. Oil Spills and their cleanup. *Chemistry and Industry*, December, pp. 1005-1008.
- Fingas MF, Hollebone BP (2003) Review of behaviour of oil in freezing environments. *Mar. Pollut. Bull.* 47, 333–340. doi:10.1016/S0025-326X(03)00210-8.
- Frantzen, M., Hansen, B.H., Geraudie, P., Palerud, J., Falk-Petersen, I.-B., Olsen, G.H., Camus, L., 2015. Acute and long-term biological effects of mechanically and chemically dispersed oil on lumpsucker (*Cyclopterus lumpus*). *Mar. Environ. Res.* 105, 8-19.
- Frantzen, M., Regoli, F., Nahrgang, J., Ambrose, W., Geraudie, P., Benedetti, M., Locke, W., Camus, L., 2016. Biological effects of mechanically and chemically dispersed oil on the Icelandic scallop (*Clamys islandica*). *Ecotox. Environ. Safe.* 127, 95-107.
- Fritt-Rasmussen, J., Wegeberg, S., Gustavson, K., 2015. Review on Burn Residues from In Situ Burning of Oil Spills in Relation to Arctic Waters. *Water Air Soil Pollut.* 226. doi:10.1007/s11270-015-2593-1.
- Gardiner WW, Word JQ, Word JD, Perkins RA, McFarlin KM, Hester BW, Word LS, Ray CM (2013) The acute toxicity of chemically and physically dispersed crude oil to key arctic species under arctic conditions during the open water season. *Environmental Toxicology and Chemistry / Setac* 32:2284-2300.
- González J, Figueiras FG, Aranguren-Gassis M, Crespo BG, Fernandez E, Moran XAG, Nieto-Cid M. (2009) Effect of a simulated oil spill on natural assemblages of marine phytoplankton enclosed in microcosms. *Estuarine, Coastal and Shelf Science* 83, 265–276.

- Grenvald JC, Nielsen TG, Hjorth M. (2013) Effects of pyrene exposure and temperature on early development of two co-existing Arctic copepods. *Ecotoxicology* 22: 184-198, DOI 10.1007/s10646-012-1016-y.
- Gros J., Nabi D., Würz B., Wick L.Y., Brussaard C.P.D., Huisman J., Van Der Meer J.R., Reddy C.M. and Arey J.S. (2014). First day of an oil spill on the open sea: Early mass transfers of hydrocarbons to air and water. *Environmental Science & Technology* 48(16): 9400-9411.
- Gulec, I., Holdway, D.A., 1999. The Toxicity of Laboratory Burned Oil to the Amphipod *Allorchestes compressa* and the Snail *Polinices conicus*. *Spill Sci. Technol. Bull.* 5, 135–139.
- Gyllenberg G (1981) Ingestion and Turnover of Oil and Petroleum Hydrocarbons by Two Planktonic Copepods in the Gulf of Finland. *Ann. Zool. Fennici* 18, 225–228.
- Hansen PJ (1989) The red tide dinoflagellate *Alexandrium tamarense*: effect on behavior and growth of a tintinnid ciliate. *Marine Ecology Progress Series* 53:105–116.
- Hansen BH, Altin D, Rørvik SF, Øverjordet IB, Olsen AJ, Nordtug T (2011) Comparative study on acute effects of water accommodated fractions of an artificially weathered crude oil on *Calanus finmarchicus* and *Calanus glacialis* (Crustacea: Copepoda). *Sci. Total Environ.* 409, 704–709. doi:10.1016/j.scitotenv.2010.10.035.
- Hjorth M & Nielsen TG (2011) Oil exposure in a warmer Arctic: potential impacts on key zooplankton species. *Marine Biology* 158:1339–1347, DOI 10.1007/s00227-011-1653-3.
- Hofslagare O, Samuelsson G, Sjöberg S, Ingri N (1983) A precise potentiometric method for determination of algal activity in an open CO₂ system. *Plant. Cell and Environment* 6, 195-201.
- Holmes R.M., Aminot A., Kerouel R., Hooker B.A., Peterson B.J., 1999. A simple and precise method for measuring ammonium in marine and freshwater ecosystems. *Canadian Journal of Fisheries and Aquatic Sciences*, 56, 1801-1808.
- Hop H, Tonn WM, Welch HE (1997) Bioenergetics of Arctic cod (*Boreogadus saida*) at low temperatures. *Can J Fish Aquat Sci* 54:1772-1784.
- Hop, H., Graham, M., Wordeau, V.L., 1995. Spawning energetics of Arctic cod (*Boreogadus saida*) in relation to seasonal development of the ovary and Plasma Sex Steroid Levels. *Can. J. Fish. Aquat. Sci.* 52, 541–550.
- Horner R.A. (2002) A taxonomic guide to some common marine phytoplankton. Biopress Limited, Bristol, England. 195p.
- Hsiao S.I.C., Kittle D.W., Foy M.G., 1978. Effects of crude oils and oil dispersant corexit on primary production of arctic marine-phytoplankton and seaweed. *Environmental Pollution* 15, 209-221. doi:10.1016/0013-9327(78)90066-6.
- Hylland, K., 2006. Polycyclic aromatic hydrocarbon (PAH) ecotoxicology in marine ecosystems. *J. Toxicol. Env. Health Part A* 69, 109–123.
- Humphery, B., Green, D.R., Fowler, B.R., Hope, D., Bohem, P.D., 1987. The fate of oil in the water column following experimental oil spills in the arctic Marine Nearshore. *Arctic* 40, 124-132.
- Jensen, T., Ugland, K.I., Anstensrud, M., 1991. Aspects of growth in Arctic cod, *Boreogadus saida* (Lepechin 1773). *Polar Res.* 10, 547–552. doi:10.1111/j.1751-8369.1991.tb00672.x.
- Jensen MH, Nielsen TG, Dahlloef I (2008) Effects of pyrene on grazing and reproduction of *Calanus finmarchicus* and *Calanus glacialis* from Disko Bay, West Greenland. *Aquatic Toxicology* 87: 99-107, DOI 10.1016/j.aquatox.2008.01.005.
- Jensen L, Carroll J (2010) Experimental studies of reproduction and feeding for two Arctic-dwelling *Calanus* species exposed to crude oil. *Aquat. Biol.* 10, 261–271. doi:10.3354/ab00286.
- Jónasdóttir SH (2015) A journey from light into darkness. Fatty acids in the marine ecosystem: From photosynthesis to copepod lipids and sequestration. Technical University of Denmark.
- Jonsson, H., Sundt, R.C., Aas, E., Sanni, S., 2010. The Arctic is no longer put on ice: Evaluation of Polar cod (*Boreogadus saida*) as a monitoring species of oil pollution in cold waters. *Mar. Pollut. Bull.* 60, 390–395.

- Jung SW, Park JS, Kwon OY, Kang J-H, Shim WJ, Kim Y-O (2010) Effects of Crude Oil on Marine Microbial Communities in Short Term Outdoor Microcosms. *The Journal of Microbiology*, Vol. 48, No. 5, pp. 594-600.
- Keith Bigg E., Leck C. and Tranvik L. (2004). Particulates of the surface microlayer of open water in the central Arctic Ocean in summer. *Mar Chem* 91(1-4): 131-141.
- Kime, D.E., 1995. The effects of pollution on reproduction in fish. *Rev. Fish Biol. Fish.* 5, 52–95. doi:10.1007/BF01103366.
- Kingston, P., 1999. Recovery of the marine environment following the Braer Spill, Shetland. In: *Proceedings of the 1999 Oil Spill Conference*. American Petroleum Institute, Washington, DC, pp. 103-109.
- Kjørboe T, Møhlenberg F, Hamburger K (1985) Bioenergetics of the planktonic copepod *Acartia tonsa* : relation between feeding, egg production and respiration, and composition of specific dynamic action. *Mar. Ecol.* 26, 85–97.
- Klok C, Hjorth M, Dahllöf I (2012) Qualitative use of Dynamic Energy Budget theory in ecotoxicology. *J. Sea Res.* 73, 24–31. doi:10.1016/j.seares.2012.06.004.
- Koshikawa H, Xu KQ, Liu ZL, Kohata K, Kawachi M, Maki H, Zhu MY, Watanabe M (2007) Effect of the water-soluble fraction of diesel oil on bacterial and primary production and the trophic transfer to mesozooplankton through a microbial food web in Yangtze estuary, China. *Estuarine, Coastal and Shelf Science* 71 68-80.
- Kuznetsova M., Lee C., Aller J. and Frew N. (2004). Enrichment of amino acids in the sea surface microlayer at coastal and open ocean sites in the North Atlantic Ocean. *Limnol Oceanogr* 49(5): 1605-1619.
- Lacroix, C., Le Cuff, N., Receveur, J., Moraga, D., Auffret, M., Guyomarch, J., 2014. Development of an innovative and green stir bar sorptive extraction–thermal desorption–gas chromatography–tandem mass spectrometry method for quantification of polycyclic aromatic hydrocarbons in marine biota. *J.Chromatogr. A* 1349, 1–10.
- Larsen A, Fonnes Flaten GA, Sandaa R-A, Castberg T, Thyrhaug R, Erga SR, Jacquet S, Bratbak G (2004) Spring Phytoplankton Bloom Dynamics in Norwegian Coastal Waters: Microbial Community Succession and Diversity. *Limnol. Oceanogr.*, 49(1), 180-190.
- Latimer JS, Zheng J (2003) The Sources, Transport, and Fate of PAHs in the Marine Environment. *PAHs: An Ecotoxicological Perspective*. John Wiley & Sons, Ltd
- Law, R.J., 1978. Determination of petroleum hydrocarbons in water, fish and sediments following the Ekofisk blow-out. *Mar. Pollut. Bull.* 9, 321-324.
- Lee RF (1975) Lipids of Arctic zooplankton. *Comp. Biochem. Physiol. B.* 51, 263–6. doi:10.1016/03050491(75)90003-6.
- Lee R, Hagen W, Kattner G (2006) Lipid storage in marine zooplankton. *Mar. Ecol. Prog. Ser.* 307, 273–306. doi:10.3354/meps307273.
- Lessard, R.R., DeMarco, G., 2000. The significance of oil spill dispersants. *Spill Sci. Technol. Bull.* 6, 59- 68.
- Leu E, Søreide JE, Hessen DO, Falk-Petersen S, Berge J (2011) Consequences of changing sea ice cover for primary and secondary producers in the European Arctic shelf seas: Timing, quantity, and quality. *Prog. Oceanogr.* 90, 18–32. doi:10.1016/j.pocean.2011.02.004.
- Leu E., Mundy C.J., Assmy P., Campbell K., Gabrielsen T.M., Gosselin M., Juul-Pedersen T., Gradinger R., 2015. Arctic spring awakening – steering principles behind the phenology of vernal ice algae blooms. *Progr. Oceanogr.* 139: 151-170.
- Lewis, A., Daling, P.S., 2001. Oil Spill Dispersants. Guidelines on the Planning and Effective Use of Oil Spill Dispersants to Minimise the Effects of Oil Spills. *AMOS Report*. SINTEF, Trondheim, pp. 1-113.
- Lewis M., Pryor R., 2013. Toxicities of oils, dispersants and dispersed oils to algae and aquatic plants: Review and database value to resource sustainability. *Environmental Pollution* 180, 345-367. doi:10.1016/j.envpol.2013.05.001.
- Levinsen H, JT Turner, TG Nielsen TG & BW Hansen (2000). On the trophic coupling between protists and copepods in Arctic marine Ecosystems. *Mar. Ecol. Prog. Ser.* 204:65-77.

- Liss P.S. and Duce R. (1997). The Sea Surface and Global Change. Cambridge University Press, Cambridge, 519 pages.
- Lotufo GR (1998) Bioaccumulation of sediment-associated fluoranthene in benthic copepods: Uptake, elimination and biotransformation. *Aquat. Toxicol.* 44, 1–15. doi:10.1016/S0166445X(98)00072-1.
- Lund J.W.G., Kipling C., Le Cren E.D., 1958. The inverted microscope method of estimating algal numbers and the statistical basis of estimations by counting. *Hydrobiologia* 11, 143–170.
- Lunel, T., Swannell, R., Rusin, J., Wood, P., Bailey, N., Halliwell, C., Davies, L., Sommerville, M., Dobie, A., Mitchell, D., McDonagh, M., Lee, K., 1995. Monitoring the effectiveness of response operations during the sea empress incident: a key component of the successful counter-pollution response. *Spill Sci. Technol. Bull.* 2, 99-112.
- Madsen SD, Nielsen TG, Hansen BW (2001) Annual population development and production by *Calanus finmarchicus*, *C. glacialis* and *C. hyperboreus* in Disko Bay, western Greenland. *Marine Biology* 139:75-93, DOI 10.1007/s002270100552.
- Marie D, Brussaard CDP, Thyraug R, Bratbak G, Vaulot D (1999) Enumeration of Marine Viruses in Culture and Natural Samples by Flow Cytometry. *Applied and environmental microbiology*, 65 1, p. 45–52.
- Matrai P.A., Tranvik L., Leck C. and Knulst J.C. (2008). Are high Arctic surface microlayers a potential source of aerosol organic precursors? *Mar Chem* 108(1-2): 109-122.
- Medlin L.K., Hasle G.R. (1990) Some *Nitzschia* and related diatom species from fast ice samples in the Arctic and Antarctic. *Polar Biol* 10:451–479.
- Milinkovitch, T., Ndiaye, A., Sanchez, W., Le Floch, S., Thomas-Guyon, H., 2011. Liver antioxidant and plasma immune responses in juvenile golden grey mullet (*Liza aurata*) exposed to dispersed crude oil. *Aquat. Toxicol.* 101, 155-164.
- Mohammed A (2013) Why are Early Life Stages of Aquatic Organisms more Sensitive to Toxicants than Adults? New Insight into Toxicity and Drug Testing. *InTech*. doi:10.5772/55187.
- Molvær, J., Knutzen, J., Magnusson, J., Rygg, B., Skei, J., Sørensen, J. (1997) Klassifisering av miljøkvalitet i fjorder og kystfarvann. SFT-veiledning nr. 97:03.
- Nahrgang, J., Camus, L., Carls, M.G., Gonzalez, P., Jönsson, M., Taban, I.C., Bechmann, R.K., Christiansen, J.S., Hop, H., 2010. Biomarker responses in polar cod (*Boreogadus saida*) exposed to the water soluble fraction of crude oil. *Aquat. Toxicol.* 97, 234–242. doi:10.1016/j.aquatox.2009.11.003.
- Nahrgang, J., Varpe, Ø., Korshunova, E., Murzina, S., Hallanger, I.G., Vieweg, I., Berge, J., 2014. Gender Specific Reproductive Strategies of an Arctic Key Species (*Boreogadus saida*) and Implications of Climate Change. *PLoS One* 9, e98452. doi:10.1371/journal.pone.0098452.
- Nahrgang, J., Dubourg, P., Frantzen, M., Storch, D., Dahlke, F., Meador, J., 2016. Early life stages of an arctic keystone species (*Boreogadus saida*) show high sensitivity to a water-soluble fraction of crude oil. *Environ. Pollut.* doi:10.1016/j.envpol.2016.07.044.
- Niehoff B (2007) Life history strategies in zooplankton communities: The significance of female gonad morphology and maturation types for the reproductive biology of marine calanoid copepods. *Prog. Oceanogr.* 74, 1–47. doi:10.1016/j.pocean.2006.05.005.
- Nørregaard RD, Nielsen TG, Møller EF, Strand J, Espersen L, Møhl M (2014). Evaluating pyrene toxicity on Arctic key copepod species *Calanus Hyperboreus*. *Ecotoxicology* 23: 163-174, DOI 10.1007/s10646-013-1160-z.
- Ortmann AC, Anders J, Shelton N, Gong L, Moss AG, et al. (2012) Dispersed Oil Disrupts Microbial Pathways in Pelagic Food Webs. *PLoS ONE* 7(7): e42548. doi:10.1371/journal.pone.0042548.
- Otsuka N, Kondo H, Saeki H (2004) Experimental Study on the Characteristics of Oil Ice Sandwich.
- Parsons T.R., Maita Y., Lalli C.M., 1984a. A manual of chemical and biological methods for seawater analysis. Pergamon Press, Toronto.
- Parsons TR, Harrison PJ, Acreman JC, Dovey HM, Thompson PA, Lallit CM, Lee K, Guanguo L, Xiaolin C (1984b) An Experimental Marine Ecosystem Response to Crude Oil and Corexit 9527: Part 2-- Biological Effects. *Marine Environmental Research* 13 (1984) 265-275.

- Payne JR, Hachmeister LE, McNabb GD, Sharpe HE, Smith GS, Menen C a (1991a) Brine induced advection of dissolved aromatic hydrocarbons to Arctic bottom waters. *Environ. Sci. Technol.* 25, 940–951. doi:10.1021/es00017a018.
- Payne JR, McNabb GD, Clayton JR (1991b) Oil-weathering behavior in Arctic environments. *Polar Res.* 10, 631–662. doi:10.3402/polar.v10i2.6774.
- Pelletier MC, Burgess RC, Ho KT, Kuhn A, McKinney RA, Ryba SA (1997) Phototoxicity of Individual Polycyclic Aromatic Hydrocarbons and Petroleum to Marine Invertebrate Larvae and Juveniles. *Environ. Toxicol. Chem.* 16, 2190–2199. doi:10.1897/15551-5028.
- Petrich C, Karlsson J, Eicken H (2013) Porosity of growing sea ice and potential for oil entrainment. *Cold Regions Science and Technology* 87, 27–32.
- Pineault S., Tremblay J.E., Gosselin M., Thomas H., Shadwick E., 2013. The isotopic signature of particulate organic C and N in bottom ice: Key influencing factors and applications for tracing the fate of ice-algae in the Arctic Ocean. *J. Geophys. Res.* 118: 287-300. doi:10.1029/2012jc008331.
- Poulin M. (1991) Sea ice diatoms (Bacillariophyceae) of the Canadian Arctic. 2. A taxonomic, morphological and geographical study of Gyrodinium concilians. *Nord J Bot* 10:681–688.
- Poulin M., Cardinal A. (1982) Sea ice diatoms from Manitousuk Sound, southeastern Hudson Bay (Quebec, Canada). II. Naviculaceae, genus Navicula. *Can J Bot* 60:2825–2845.
- R Development Core Team, 2014. R: A Language and Environment for Statistical Computing. R Foundation for Statistical Computing, Vienna, Austria.
- Reddy, C.M., Quinn, J.G., 1999. GCeMS analysis of total petroleum hydrocarbons and polycyclic aromatic hydrocarbons in seawater samples after the North Cape oil spill. *Mar. Pollut. Bull.* 38, 126-135.
- Rideout, R.M., Rose, G.A., Burton, M.P.M., 2005. Skipped spawning in female iteroparous fishes. *Fish Fish.* 6, 50–72.
- Rozanska M., Gosselin M., Poulin M., Wiktor J.M., Michel C., 2009. Influence of environmental factors on the development of bottom ice protist communities during the winter–spring transition. *Mar. Ecol. Prog. Ser.* 386: 43–59.
- Sargent JR, Falk-Petersen S (1988) The lipid biochemistry of calanoid copepods. *Hydrobiologia* 167- 168, 101–114. doi:10.1007/BF00026297.
- Shannon C.E. and Weaver W. (1949). *The Mathematical Theory of Communication*. Univ of Illinois Press, 114 pages.
- Shigenaka, G., Overton, E., Meyer, B., Gao, H., Miles, S., 2015. Physical and chemical characteristics of in-situ burn residue and other environmental oil samples collected during the Deepwater Horizon spill response. pp. 1–11.
- Short, J.W., Harris, P.M., 1996. Petroleum hydrocarbons in caged mussels deployed in Prince William sound after the Exxon Valdez oil spill. *Am. Fish. Soc. Symposium* 18, 29-39.
- Shrivastava, A. and Gupta, V. B., 2011. Methods for the determination of limit of detection and limit of quantification of the analytical methods. *Chron. of Young Sci.* 2 (1), 21–25.
- Sieracki M., Poulton N. and Crosbie N. (2005). *Automated Isolation Techniques for Microalgae*. In *Algal Culturing Techniques* (Eds.), Elsevier: 101-116.
- Siron R, Pelletier E, Delille D, Roy S (1993) Fate and Effects of Dispersed Crude Oil Under Icy Conditions Simulated in Mesocosms. *Marine Environmental Research* 35, 273-302.
- Siron R, Pelletier E, Roy S (1996) Effects of dispersed and adsorbed crude oil on microalgal and bacterial communities of cold seawater. *Ecotoxicology* 5, 229-251.
- Sol, S.Y., Johnson, L.L., Horness, B.H., Collier, T.K., 2000. Relationship between oil exposure and reproductive parameters in fish collected following the Exxon Valdez oil spill. *Mar. Pollut. Bull.* 40, 1139–1147. doi:10.1016/S0025-326X(00)00074-6.
- Spromberg, J.A., Meador, J.P., 2006. Relating chronic toxicity responses to population- level effects : A comparison of population-level parameters for three salmon species as a function of low-level toxicity three salmon species as a function of low-level toxicity. *Ecol. Modell.* 199, 240–252. doi:10.1016/j.ecolmodel.2006.05.007.

- Stout, S.A., Payne, J.R., 2016. Chemical composition of floating and sunken in-situ burn residues from the Deepwater Horizon oil spill. *Mar Poll Bull.* 108,186-202.
<http://dx.doi.org/10.1016/j.marpolbul.2016.04.031>.
- Swailethorp R, Kjellerup S, Dünweber M, Nielsen TG, Møller EF, Rysgaard S, Hansen BW (2011) Grazing, egg production and biochemical evidence of differences in the life strategies of *Calanus finmarchicus*, *C. glacialis* and *C. hyperboreus* in Disko Bay, western Greenland. *Marine Ecology Progress Series* 429:125-144, DOI 10.3354/meps09065.
- Sørreide J, Falk-Petersen S, Hegseth EN, Hop H, Caroll ML, Hobson KA, Blachowiak-Samolyk K (2008) Seasonal feeding strategies of *Calanus* in the high-Arctic Svalbard region. *Deep-Sea Research II* 55: 2225-2244.
- Sørreide J, Leu E, Berge J, Graeve M, Falk-Petersen S (2010) Timing of blooms, algal food quality and *Calanus glacialis* reproduction and growth in a changing Arctic. *Global Change Biology* 16, 3154–3163, doi: 10.1111/j.1365-2486.2010.02175.x.
- Thrandsen J., Hasle G.R., Tangen K. (2007) *Phytoplankton of Norwegian coastal waters*. Almatier Forlag As, Oslo, Norway. 343p.
- Tomas C.R. (ed.) (1997) *Identifying marine phytoplankton*. Academic Press, San Diego, USA. 858p.
- Vancoppenolle M., Goosse H., de Montety A., Fichet T., Tremblay B., Tison J.L., 2010. Modeling brine and nutrient dynamics in Antarctic sea ice: The case of dissolved silica. *Journal of Geophysical Research-Oceans* 115, doi:10.1029/2009jc005369.
- Van Wezel AP, Opperhuizen A (1995) Narcosis Due to Environmental Pollutants in Aquatic Organisms: Residue-Based Toxicity, Mechanisms, and Membrane Burdens. *Crit. Rev. Toxicol.* 25, 255–279.
- Vaulot D., Courties C. and Partensky F. (1989). A simple method to preserve oceanic phytoplankton for flow cytometric analyses. *Cytometry* 10(5): 629-635.
- von Quillfeldt C.H. (2001) Identification of some easily confused common diatom species in Arctic spring blooms. *Bot. Mar.* 44:375–389.
- Weydmann A, Zwolicki A, Muś K, Kwaśniewski S (2015) The effect of temperature on egg development rate and hatching success in *Calanus glacialis* and *C. finmarchicus*. *Polar Res.* 34, 1–8.
doi:10.3402/polar.v34.23947.
- Whitehead, A., Dubansky, B., Bodinier, C., Garcia, T.I., Miles, S., Pilley, C., Raghunathan, V., Roach, J.L., Walker, N., Ronald, B., Rice, C.D., Galvez, F., 2012. Genomic and physiological footprint of the Deepwater Horizon oil spill on resident marsh fishes. *Proc. Natl. Acad. Sci.* 109, 20298–20302.
doi:10.1073/pnas.1109545108.
- Word, JQ (2013) *Environmental Impacts of Arctic Oil Spills and Arctic Spill Response Technologies Literature Review and Recommendations*. Arctic Oil Spill Response Technology Joint Industry Programme.
- Wurl O., Wurl E., Miller L., Johnson K. and Vagle S. (2011). Formation and global distribution of sea-surface microlayers. *Biogeosciences* 8(1): 121-135.
- Yang G.-P., Levasseur M., Michaud S. and Scarratt M. (2005). Biogeochemistry of dimethylsulfide (DMS) and dimethylsulfoniopropionate (DMSP) in the surface microlayer and subsurface water of the western North Atlantic during spring. *Mar Chem* 96(3-4): 315-329.
- Zhao J.P., Li T., Barber D., Ren, J.P., Pucko M., Li S.J., Li X., 2010. Attenuation of lateral propagating light in sea ice measured with an artificial lamp in winter Arctic. *Cold. Reg. Sci. Tech.* 61: 6-12.
- Zubkov MV, Burkill PH, Topping JN (2007) Flow cytometric enumeration of DNA-stained oceanic planktonic protists. *Journal of Plankton Research*, Vol 29, 1, 79–86.

7 APPENDIX

7.1 1-A List of analysed chemical compounds

For PAHs, all compounds in the list below were analysed (dissolved, i.e. in the sea water and in the ice; and PAHs trapped in the oil droplets).

Benzo(b)thiophene	BT
C1-benzo(b)thiophenes	BT1
C2-benzo(b)thiophenes	BT2
C3-benzo(b)thiophenes	BT3
C4-benzo(b)thiophenes	BT4
Naphtalene	N
C1-Naphtalenes	N1
C2-Naphtalenes	N2
C3-Naphtalenes	N3
C4-Naphtalenes	N4
Biphenyl	B
Acenaphtylene	ANY
Acenaphtene	ANA
Fluorene	F
C1-Fluorenes	F1
C2-Fluorenes	F2
C3-Fluorenes	F3
Phenanthrene	P
Anthracene	A
C1-phenanthrenes/anthracenes	P1
C2-phenanthrenes/anthracenes	P2
C3-phenanthrenes/anthracenes	P3
C4-phenanthrenes/anthracenes	P4
Dibenzothiophene	D
C1-dibenzothiophenes	D1
C2-dibenzothiophenes	D2
C3-dibenzothiophenes	D3
C4-dibenzothiophenes	D4
Fluoranthene	FL
Pyrene	PY
C1-fluoranthenes/pyrenes	FL1
C2-fluoranthenes/pyrenes	FL2
C3-fluoranthenes/pyrenes	FL3
Benzo[a]anthracene	BA
Chrysene	C
C1-chrysenes	C1
C2-chrysenes	C2
C3-chrysenes	C3
Benzo[b+k]fluoranthene	BBF
Benzo[e]pyrene	BEP
Benzo[a]pyrene	BAP
Perylene	PE
Indeno(1,2,3-cd)pyrene	IN
Dibenz(a,h)anthracene	DBA
Benzo(g,h,i)perylene	BPE

For n-alkanes, compounds between nC10 and nC36 were analysed.

Unique Arctic Communities and Oil Spill Response Consequences: "Oil Biodegradation & Persistence" and "Oil Spill Response Consequences Resilience and Sensitivity"

7.2 1-B Tiles experiment

Quantification of n-alkanes in the oil on the tiles

Alkanes concentration in µg/g																	
	FT1	FT2	FT3	FT6	MhT2	MhT3	MhT4	AT1	AT3	AT5	MyT2	MyT4	MyT5	MhT6	MhT7	AT6	AT7
nC10	222	427	63	271	83	78	78	113	24	60	66	18	31	0	0	0	0
nC11	487	771	284	671	214	173	215	390	213	267	110	104	151	0	0	0	0
nC12	807	1229	707	1061	584	403	465	728	647	561	684	442	340	0	0	0	0
nC13	1479	1960	1267	1569	1249	820	781	1309	1388	988	1515	1166	669	0	0	0	0
nC14	1820	2256	1395	1760	1755	1110	957	1549	1519	1250	2263	1970	901	0	0	0	0
nC15	3794	4298	2327	3176	3479	2293	1612	3083	2465	2058	4079	3993	1523	0	0	0	0
nC16	5594	6469	3100	4507	4884	3534	2606	5009	3748	3244	6141	6564	2383	0	0	0	0
nC17	5588	6884	3119	4760	4985	3689	3126	5631	3327	3780	6112	7313	2767	0	0	0	0
pristane	9303	10469	5165	7979	9740	8552	5325	10391	6331	6561	11598	14016	5815	0	0	0	0
nC18	6756	7916	4398	6418	5270	4945	4684	7683	4587	5657	7532	9496	4047	0	0	0	0
phytane	5210	6029	3216	5078	5403	5102	3961	6823	4210	4770	7066	8943	4115	0	0	0	0
nC19	7916	9303	6770	8194	5432	5665	6524	9668	6471	7761	8191	11195	5391	0	0	0	0
nC20	6573	7650	8350	7537	4059	4592	5894	8001	6408	6973	6002	8537	4861	0	0	0	0
nC21	5295	6391	11158	6945	2858	3422	4682	6014	5357	5707	4096	6006	3794	0	0	0	0
nC22	5246	5354	13437	6522	2113	2677	2644	4700	4860	4460	2933	4416	3006	0	0	0	0
nC23	2630	3443	11023	4804	1280	1711	2256	2868	4394	2951	1717	2559	1842	0	0	0	0
nC24	1966	2959	10644	4571	1073	1517	1785	2412	4166	2506	1362	2019	1391	0	0	0	0
nC25	1960	3061	11062	4955	1374	1973	2266	3349	3759	3275	1818	2510	1822	0	0	0	0
nC26	1560	2890	6802	4655	1412	2102	2139	2903	3386	3005	1662	2113	1667	0	0	0	0
nC27	485	1117	2482	3596	668	997	874	1503	1687	1432	620	776	685	0	0	0	0
nC28	152	441	1125	2429	289	423	364	793	1173	601	246	279	294	0	0	0	0
nC29	104	394	790	2007	259	272	313	969	1411	565	211	214	263	0	0	0	0
nC30	67	286	929	1592	218	198	242	794	970	480	154	166	224	0	0	0	0
nC31	50	224	384	780	138	123	160	551	641	274	117	112	158	0	0	0	0
nC32	21	113	529	557	65	75	78	313	275	126	51	37	60	0	0	0	0
nC33	9	74	300	189	44	39	42	214	127	62	18	15	22	0	0	0	0
nC34	12	46	151	113	34	13	30	161	49	44	13	7	18	0	0	0	0
nC35	0	39	107	59	38	9	21	76	0	0	0	0	0	0	0	0	0
nC36	0	0	0	64	0	0	0	0	0	0	0	0	0	0	0	0	0
TOTAL	74 106	92 490	111 186	96 854	59 000	56 505	55 124	87 997	73 992	69 618	76 376	95 185	48 238	0	0	0	0

nC10 - nC14	4815	6642	3715	5332	3885	2585	2495	4089	3791	3127	4638	3700	2092	0	0	0	0
nC15 - nC25	66830	80224	93768	72545	51952	49671	48365	75631	59581	59901	68647	87666	42756	0	0	0	0
nC26 - nC36	2460	5623	13703	15977	3164	4250	4264	8277	9720	6590	3091	3819	3390	0	0	0	0

nC10 - nC14	T0			T1			T2			T3		
	mean	std	n	mean	std	n	mean	std	n	mean	std	n
Polluted	5126	1215	4	2988	778	3	3669	492	3	3476	1288	3
Non Polluted	n.d	n.d	0	0	0	2	0	0	2	0	0	2

nC15 - nC25	T0			T1			T2			T3		
	mean	std	n	mean	std	n	mean	std	n	mean	std	n
Polluted	79092	11249	4	49996	1815	3	65038	9175	3	66357	22542	3
Non Polluted	n.d	n.d	0	0	0	2	0	0	2	0	0	2

nC26 - nC36	T0			T1			T2			T3		
	mean	std	n	mean	std	n	mean	std	n	mean	std	n
Polluted	9441	6434	4	3909	646	3	8195	1567	3	3433	366	3
Non Polluted	n.d	n.d	0	0	0	2	0	0	2	0	0	2

Quantification of PAHs in the oil

PAHs concentration in µg/g																					
		FT1	FT2	FT3	FT6	MhT2	MhT3	MhT4	AT1	AT3	AT5	MyT2	MyT4	MyT5	MhT6	MhT7	AT6	AT7	MyT6	MyT7	
C1-phenanthrenes/anthracenes	Benzofluoranthene	BT	1	0	0	0	1	1	0	0	0	0	3	0	0	0	0	0	0	0	
	C1-benzofluoranthene	BT1	0	0	0	0	0	0	0	0	0	0	0	0	0	0	0	0	0	0	
	C2-phenanthrenes/anthracenes	BT2	0	0	0	0	0	0	0	0	0	0	0	0	0	0	0	0	0	0	0
		C2-benzofluoranthene	BT2	0	0	0	0	0	0	0	0	0	0	0	0	0	0	0	0	0	0
	C3-phenanthrenes/anthracenes	BT3	0	0	0	0	0	0	0	0	0	0	0	0	0	0	0	0	0	0	0
		C3-benzofluoranthene	BT3	0	0	0	0	0	0	0	0	0	0	0	0	0	0	0	0	0	0
	C4-phenanthrenes/anthracenes	BT4	0	0	0	0	0	0	0	0	0	0	0	0	0	0	0	0	0	0	0
		C4-benzofluoranthene	BT4	0	0	0	0	0	0	0	0	0	0	0	0	0	0	0	0	0	0
	Naphthalene	N	19	28	8	21	15	13	10	11	6	10	22	7	7	4	0	0	0	0	0
		C1-Naphthalenes	N1	67	91	41	65	50	37	48	43	49	92	52	23	0	0	0	0	0	0
	C2-Naphthalenes	N2	110	134	56	82	119	82	51	76	69	74	140	103	41	0	0	0	0	0	0
		C2-Naphthalenes	N2	110	134	56	82	119	82	51	76	69	74	140	103	41	0	0	0	0	0
	C3-Naphthalenes	N3	137	165	65	100	157	111	61	102	80	88	170	148	57	0	0	0	0	0	0
		C3-Naphthalenes	N3	137	165	65	100	157	111	61	102	80	88	170	148	57	0	0	0	0	0
	C4-Naphthalenes	N4	119	145	54	79	128	102	56	100	67	79	140	144	53	0	0	0	0	0	0
		C4-Naphthalenes	N4	119	145	54	79	128	102	56	100	67	79	140	144	53	0	0	0	0	0
	Biphenyl	B	12	16	6	10	12	8	6	7	8	13	10	4	0	0	0	0	0	0	0
		Biphenyl	B	12	16	6	10	12	8	6	7	8	13	10	4	0	0	0	0	0	0
	Acenaphthylene	ANY	2	2	2	3	2	2	1	2	2	2	4	0	0	0	0	0	0	0	0
		Acenaphthylene	ANY	2	2	2	3	2	2	1	2	2	4	0	0	0	0	0	0	0	0
Acenaphthene	ANA	12	2	5	1	11	7	4	9	7	5	11	10	4	0	0	0	0	0	0	
	Acenaphthene	ANA	12	2	5	1	11	7	4	9	7	5	11	10	4	0	0	0	0	0	0
Fluorene	F	63	79	26	44	61	42	25	44	32	37	57	62	22	0	0	0	0	0	0	
	Fluorene	F	63	79	26	44	61	42	25	44	32	37	57	62	22	0	0	0	0	0	0
C1-Fluorenes	F1	185	232	81	147	177	151	77	164	110	119	161	227	92	0	0	0	0	0	0	
	C1-Fluorenes	F1	185	232	81	147	177	151	77	164	110	119	161	227	92	0	0	0	0	0	0
C2-Fluorenes	F2	279	342	127	274	267	233	158	278	194	222	254	346	157	0	0	0	0	0	0	
	C2-Fluorenes	F2	279	342	127	274	267	233	158	278	194	222	254	346	157	0	0	0	0	0	0
C3-Fluorenes	F3	192	192	100	185	165	170	133	223	142	176	189	260	150	0	0	0	0	0	0	
	C3-Fluorenes	F3	192	192	100	185	165	170	133	223	142	176	189	260	150	0	0	0	0	0	0
Phenanthrene	P	273	345	153	246	227	188	158	245	160	191	227	298	139	0	0	0	0	0	0	
	Phenanthrene	P	273	345	153	246	227	188	158	245	160	191	227	298	139	0	0	0	0	0	0
A	A	2	2	1	1	1	2	158	1	1	1	12	298	1	0	0	0	0	0	0	
	A	2	2	1	1	1	2	158	1	1	1	12	298	1	0	0	0	0	0	0	
C1-phenanthrenes/anthracenes	P1	402	475	248	391	338	319	271	420	288	336	350	483	280	0	0	0	0	0	0	
	C1-phenanthrenes/anthracenes	P1	402	475	248	391	338	319	271	420	288	336	350	483	280	0	0	0	0	0	0
C2-phenanthrenes/anthracenes	P2	331	366	256	369	275	287	271	444	314	344	327	453	307	0	0	0	0	0	0	
	C2-phenanthrenes/anthracenes	P2	331	366	256	369	275	287	271	444	314	344	327	453	307	0	0	0	0	0	0
C3-phenanthrenes/anthracenes	P3	224	235	192	300	173	196	209	294	257	257	210	288	245	0	0	0	0	0	0	
	C3-phenanthrenes/anthracenes	P3	224	235	192	300	173	196	209	294	257	257	210	288	245	0	0	0	0	0	0
C4-phenanthrenes/anthracenes	P4	125	136	127	170	111	114	125	182	152	156	119	165	143	0	0	0	0	0	0	
	C4-phenanthrenes/anthracenes	P4	125	136	127	170	111	114	125	182	152	156	119	165	143	0	0	0	0	0	0
Dibenzofluoranthene	D	31	37	17	29	26	20	19	27	19	26	26	32	15	0	0	0	0	0	0	
	Dibenzofluoranthene	D	31	37	17	29	26	20	19	27	19	26	26	32	15	0	0	0	0	0	0
C1-dibenzofluoranthenes	D1	83	98	52	78	74	66	59	92	61	67	75	101	58	0	0	0	0	0	0	
	C1-dibenzofluoranthenes	D1	83	98	52	78	74	66	59	92	61	67	75	101	58	0	0	0	0	0	0
C2-dibenzofluoranthenes	D2	75	74	43	74	55	54	49	78	53	64	63	86	52	0	0	0	0	0	0	
	C2-dibenzofluoranthenes	D2	75	74	43	74	55	54	49	78	53	64	63	86	52	0	0	0	0	0	0
C3-dibenzofluoranthenes	D3	45	45	37	57	35	39	38	56	44	41	46	59	42	0	0	0	0	0	0	
	C3-dibenzofluoranthenes	D3	45	45	37	57	35	39	38	56	44	41	46	59	42	0	0	0	0	0	0
C4-dibenzofluoranthenes	D4	0	0	0	0	0	0	0	0	0	0	0	0	0	0	0	0	0	0	0	
	C4-dibenzofluoranthenes	D4	0	0	0	0	0	0	0	0	0	0	0	0	0	0	0	0	0	0	
Fluoranthene	FL	5	7	3	5	2	2	3	4	3	3	3	4	3	0	0	0	0	0	0	
	Fluoranthene	FL	5	7	3	5	2	2	3	4	3	3	4	3	0	0	0	0	0	0	0
Pyrene	PI	6	6	5	6	5	5	5	6	5	5	7	5	0	0	0	0	0	0	0	
	Pyrene	PI	6	6	5	6	5	5	6	5	5	7	5	0	0	0	0	0	0	0	0
C1-fluoranthenes/pyrenes	FL1	61	69	51	77	45	59	46	81	75	59	47	67	52	0	0	0	0	0	0	
	C1-fluoranthenes/pyrenes	FL1	61	69	51	77	45	59	46	81	75	59	47	67	52	0	0	0	0	0	0
C2-fluoranthenes/pyrenes	FL2	53	59	64	88	41	54	52	84	90	56	44	70	54	0	0	0	0	0	0	
	C2-fluoranthenes/pyrenes	FL2	53	59	64	88	41	54	52	84	90	56	44	70	54	0	0	0	0	0	0
C3-fluoranthenes/pyrenes	FL3	34	36	44	63	26	30	30	51	59	42	25	46	36	0	0	0	0	0	0	
	C3-fluoranthenes/pyrenes	FL3	34	36	44	63	26	30	30	51	59	42	25	46	36	0	0	0	0	0	0
Benzofluoranthene	BA	2	2	2	3	2	2	3	4	2	1	2	2	0	0	0	0	0	0	0	
	Benzofluoranthene	BA	2	2	2	3	2	2	3	4	2	1	2	2	0	0	0	0	0	0	0
Chrysene	C	6	7	11	10	6	7	6	12	10	7	7	9	0	0	0	0	0	0	0	
	Chrysene	C	6	7	11	10	6	7	6	12	10	7	7	9	0	0	0	0	0	0	0
C1-chrysenes	C1	8	12	17	18	7	8	11	18	21	13	8	13	12	0	0	0	0	0	0	
	C1-chrysenes	C1	8	12	17	18	7	8	11	18	21	13	8	13	12	0	0	0	0	0	0
C2-chrysenes	C2	9	14	21	22	7	9	19	23	14	9	11	12	0	0	0	0	0	0	0	
	C2-chrysenes	C2	9	14	21	22	7	9	19	23	14	9	11	12	0	0	0	0	0	0	0
C3-chrysenes	C3	0	0	0	0	0	0	0	0	0	0	0	0	0	0	0	0	0	0	0	
	C3-chrysenes	C3	0	0	0	0	0	0	0	0	0	0	0	0	0	0	0	0	0	0	0
Benzofluoranthene	BBF	0	1	3	1	0	0	1	1	1	2	1	1	0	0	0	0	0	0	0	
	Benzofluoranthene	BBF	0	1	3	1	0	0	1	1	1	2	1	1	0	0	0	0	0	0	0
Benzofluoranthene	BEP	1	1	1	1	0	0	0	2	1	1	0	0	1	0	0	0	0	0	0	
	Benzofluoranthene	BEP	1	1	1	1	0	0	0	2	1	1	0	0	1	0	0	0	0	0	0
Benzofluoranthene	BAP	0	0	0	0	0	0	0	0	0	0	0	0	0	0	0	0	0	0	0	
	Benzofluoranthene	BAP	0	0	0	0	0	0	0	0	0	0	0	0	0	0	0	0	0	0	0
Benzofluoranthene	PE	0	0	2	0	0	0	0	1	3	1	0	0	0	0	0	0	0	0	0	
	Benzofluoranthene	PE	0	0	2	0	0	0	0	1	3	1	0	0	0	0	0	0	0	0	0
Indeno[1,2,3-cd]pyrene	IN	0	0	0	0	0	0	0	0	0	0	0	0	0	0	0	0	0	0	0	
	Indeno[1,2,3-cd]pyrene	IN	0	0	0	0	0	0	0	0	0	0	0	0	0	0	0	0	0	0	0
Benzofluoranthene	DBA	0	0	0	0	0	0	0	0	0	0	0	0	0	0	0	0	0	0	0	

N - N4 (µg/g)	T0			T1			T2			T3		
	mean	std	n	mean	std	n	mean	std	n	mean	std	n
Polluted	396	188	4	352	135	3	302	36	3	400	200	3
Non Polluted	n.d	n.d	n.d	0	0	2	0	0	2	0	0	2

BT - C3 (µg/g)	T0			T1			T2			T3		
	mean	std	n	mean	std	n	mean	std	n	mean	std	n
Polluted	2444	525	4	2046	111	3	2409	381	3	2533	782	3
Non Polluted	n.d	n.d	n.d	0	0	2	0	0	2	0	0	2

BBF - BPE (µg/g)	T0			T1			T2			T3		
	mean	std	n	mean	std	n	mean	std	n	mean	std	n
Polluted	3,5	2,2	4,0	1,7	0,1	3,0	5,0	2,5	3,0	1,1	0,5	3,0
Non Polluted	n.d	n.d	n.d	0	0	2	0	0	2	0	0	2

7.3 1-C Mesocosm experiment

7.3.1 PAHs concentration in the sea water

Mesocosm_crude oil

	T1			T2			T3			T4		
	N - N3 (µg/L)			N - N3 (µg/L)			N - N3 (µg/L)			N - N3 (µg/L)		
	0 m	1 m	2m	0 m	1 m	2m	0 m	1 m	2m	0 m	1 m	2m
Oil A	1,4	1,5	1,0	1,8	2,2	1,0	0,8	0,8	0,5	17,4	6,5	6,8
Oil B	3,6	1,7	1,0	3,3	1,0	2,2	0,7	0,6	0,5	6,6	14,3	10,3
	BT - C3 (µg/L)			BT - C3 (µg/L)			BT - C3 (µg/L)			BT - C3 (µg/L)		
	0 m	1 m	2m	0 m	1 m	2m	0 m	1 m	2m	0 m	1 m	2m
Oil A	0,5	0,2	0,2	0,3	0,5	0,3	0,1	0,1	0,1	1,1	0,7	0,9
Oil B	0,7	1,3	1,1	0,7	0,4	0,2	0,2	0,2	0,1	0,8	1,8	1,3
	BBF - BPE (µg/L)			BBF - BPE (µg/L)			BBF - BPE (µg/L)			BBF - BPE (µg/L)		
	0 m	1 m	2m	0 m	1 m	2m	0 m	1 m	2m	0 m	1 m	2m
Oil A	0,1	0,1	0,0	0,1	0,1	0,1	0,1	0,1	0,1	0,0	0,0	0,0
Oil B	0,1	0,1	0,1	0,1	0,1	0,1	0,1	0,1	0,1	0,0	0,0	0,0

Mesocosm_oil+dispersant

	T1			T2			T3			T4		
	N - N3 (µg/L)			N - N3 (µg/L)			N - N3 (µg/L)			N - N3 (µg/L)		
	0 m	1 m	2m	0 m	1 m	2m	0 m	1 m	2m	0 m	1 m	2m
Oil C	18,6	12,3	1,0	1,0	0,3	0,5	0,8	0,8	0,5	62,0	6,5	0,5
Oil D	2,7	2,0	8,8	2,2	1,0	0,8	1,5	0,4	0,8	58,5	14,1	3,3
	BT - C3 (µg/L)			BT - C3 (µg/L)			BT - C3 (µg/L)			BT - C3 (µg/L)		
	0 m	1 m	2m	0 m	1 m	2m	0 m	1 m	2m	0 m	1 m	2m
Oil C	1,5	1,7	0,1	0,2	0,1	0,1	0,2	0,2	0,1	3,5	1,2	0,2
Oil D	0,3	0,3	0,8	0,2	0,2	0,1	0,3	0,1	0,2	3,3	1,7	0,6
	BBF - BPE (µg/L)			BBF - BPE (µg/L)			BBF - BPE (µg/L)			BBF - BPE (µg/L)		
	0 m	1 m	2m	0 m	1 m	2m	0 m	1 m	2m	0 m	1 m	2m
Oil C	0,1	0,1	0,1	0,1	0,1	0,1	0,1	0,1	0,1	0,0	0,0	0,0
Oil D	0,1	0,1	0,1	0,1	0,1	0,1	0,1	0,1	0,1	0,0	0,0	0,0

Mesocosm_burnt oil

	T1			T2			T3			T4		
	N - N3 (µg/L)			N - N3 (µg/L)			N - N3 (µg/L)			N - N3 (µg/L)		
	0 m	1 m	2m	0 m	1 m	2m	0 m	1 m	2m	0 m	1 m	2m
Oil E	0,3	0,9	0,3	0,4	0,8	0,7	0,8	1,3	0,4	0,3	0,1	0,8
Oil F	0,4	0,3	0,8	0,5	0,6	0,5	0,5	0,6	0,4			
	BT - C3 (µg/L)			BT - C3 (µg/L)			BT - C3 (µg/L)			BT - C3 (µg/L)		
	0 m	1 m	2m	0 m	1 m	2m	0 m	1 m	2m	0 m	1 m	2m
Oil E	0,1	0,3	0,1	0,1	0,2	0,2	0,5	0,8	0,1	0,1	0,1	0,2
Oil F	0,1	0,2	0,7	0,1	0,1	0,1	0,2	0,2	0,1			
	BBF - BPE (µg/L)			BBF - BPE (µg/L)			BBF - BPE (µg/L)			BBF - BPE (µg/L)		
	0 m	1 m	2m	0 m	1 m	2m	0 m	1 m	2m	0 m	1 m	2m
Oil E	0,1	0,1	0,1	0,1	0,1	0,1	0,1	0,1	0,1	0,0	0,0	0,0
Oil F	0,1	0,1	0,1	0,1	0,1	0,1	0,1	0,1	0,1			

7.3.2 Oil concentration in the ice cores

SNOW

Sum of alkanes in oil droplets trapped in snow (µg/g)

Sum of alkanes (µg/g)	T1			T2			T3		
	mean	std	n	mean	std	n	mean	std	n
Oil A	88964	13353	4	-	-	-	-	-	-
Oil B	70056	57520	2	58867	-	1	-	-	-
Dispersant C	69276	17703	4	40746	-	1	-	-	-
Dispersant D	70540	8009	3	58388	-	1	-	-	-
ISB E	98879	9916	4	-	-	-	-	-	-
ISB F	69818	13362	7	-	-	-	-	-	-
Control I	-	-	-	-	-	-	-	-	-
Control J	-	-	-	-	-	-	-	-	-
Clean site 1	-	-	-	-	-	-	-	-	-
Clean site 2	-	-	-	-	-	-	-	-	-

Sum of PAHs in oil droplets trapped in snow (µg/g)

Sum of PAHs (µg/g)	T1			T2			T3		
	mean	std	n	mean	std	n	mean	std	n
Oil A	6742	911	4	-	-	-	-	-	-
Oil B	7415	3083	2	13032	-	1	-	-	-
Dispersant C	8795	2896	4	13708	-	1	-	-	-
Dispersant D	10513	447	3	17373	-	1	-	-	-
ISB E	-	-	-	-	-	-	-	-	-
ISB F	-	-	-	-	-	-	-	-	-
Control I	-	-	-	-	-	-	-	-	-
Control J	-	-	-	-	-	-	-	-	-
Clean site 1	-	-	-	-	-	-	-	-	-
Clean site 2	-	-	-	-	-	-	-	-	-

Sum of dissolved PAHs in snow (µg/L)

Sum of Dissolved PAHs (µg/L)	T1			T2			T3		
	mean	std	n	mean	std	n	mean	std	n
Oil A	1203	1505	4	226	189	3	480	383	4
Oil B	641	799	2	207	164	3	346	180	3
Dispersant C	3083	1808	2	908	286	3	1703	1362	4
Dispersant D	4700	1905	2	1170	373	2	1030	470	4
ISB E	-	-	-	3	1	3	-	-	-
ISB F	-	-	-	-	-	-	-	-	-
Control I	-	-	-	-	-	-	-	-	-
Control J	-	-	-	-	-	-	-	-	-
Clean site 1	-	-	-	-	-	-	-	-	-
Clean site 2	-	-	-	-	-	-	-	-	-

TOP ICE / MCL

Sum of alkanes in top ice (µg/g)

Sum of alkanes (µg/g)	T1			T2			T3		
	mean	std	n	mean	std	n	mean	std	n
Oil A	56181	55186	2	83657	5739	3	86579	7295	4
Oil B	91310	5479	3	78591	16755	3	86882	14707	4
Dispersant C	88842	3668	3	98297	718	3	87984	3716	4
Dispersant D	99656	1590	3	116102	33695	3	116771	12899	3
ISB E	33249	1962	3	31967	8699	3	36618	2283	4
ISB F	28400	1592	2	28166	986	3	39478	1910	4
Control I	-	-	-	-	-	-	-	-	-
Control J	-	-	-	-	-	-	-	-	-
Clean site 1	-	-	-	-	-	-	-	-	-
Cleann site 2	-	-	-	-	-	-	-	-	-

Sum of PAHs in top ice (µg/g)

Sum of PAHs (µg/g)	T1			T2			T3		
	mean	std	n	mean	std	n	mean	std	n
Oil A	2688	2550	2	12788	1623	3	11166	6599	4
Oil B	10626	2749	3	12095	966	3	13588	2572	4
Dispersant C	7838	557	3	11874	694	3	10991	803	4
Dispersant D	5874	684	3	13288	2422	3	8746	51	3
ISB E	3297	110	2	4010	1582	3	4704	351	4
ISB F	3821	103	2	4654	416	3	4948	352	4
Control I	-	-	-	-	-	-	-	-	-
Control J	-	-	-	-	-	-	-	-	-
Clean site 1	-	-	-	-	-	-	-	-	-
Clean site 2	-	-	-	-	-	-	-	-	-

Sum of dissolved PAHs in top ice (µg/L)

Sum of Dissolved PAHs (µg/L)	T1			T2			T3		
	mean	std	n	mean	std	n	mean	std	n
Oil A	1043	158	3	717	668	3	678	136	4
Oil B	729	83	3	321	234	3	252	387	4
Dispersant C	1821	1033	3	793	477	3	2474	1672	4
Dispersant D	2794	396	3	1789	2093	3	2032	811	4
ISB E	48	36	3	23	18	3	66	33	3
ISB F	50	4	2	22	9	3	29	40	4
Control I	-	-	-	-	-	-	-	-	-
Control J	-	-	-	-	-	-	-	-	-
Clean site 1	-	-	-	-	-	-	-	-	-
Clean site 2	-	-	-	-	-	-	-	-	-

MIDDLE ICE

Sum of alkanes in middle ice (µg/g)

Sum of alkanes (µg/g)	T1			T2			T3		
	mean	std	n	mean	std	n	mean	std	n
Oil A	-	-	-	-	-	-	-	-	-
Oil B	88374	-	1	-	-	-	-	-	-
Dispersant C	-	-	-	-	-	-	-	-	-
Dispersant D	-	-	-	-	-	-	-	-	-
ISB E	-	-	-	-	-	-	-	-	-
ISB F	-	-	-	-	-	-	-	-	-
Control I	-	-	-	-	-	-	-	-	-
Control J	-	-	-	-	-	-	-	-	-
Clean site 1	-	-	-	-	-	-	-	-	-
Cleann site 2	-	-	-	-	-	-	-	-	-

Sum of PAHs in middle ice (µg/g)

Sum of PAHs (µg/g)	T1			T2			T3		
	mean	std	n	mean	std	n	mean	std	n
Oil A	-	-	-	-	-	-	-	-	-
Oil B	14403	-	1	-	-	-	-	-	-
Dispersant C	-	-	-	-	-	-	-	-	-
Dispersant D	-	-	-	-	-	-	-	-	-
ISB E	-	-	-	-	-	-	-	-	-
ISB F	-	-	-	-	-	-	-	-	-
Control I	-	-	-	-	-	-	-	-	-
Control J	-	-	-	-	-	-	-	-	-
Clean site 1	-	-	-	-	-	-	-	-	-
Clean site 2	-	-	-	-	-	-	-	-	-

Sum of dissolved PAHs in middle ice (µg/L)

Sum of Dissolved PAHs (µg/L)	T1			T2			T3		
	mean	std	n	mean	std	n	mean	std	n
Oil A	542	366	3	208	203	3	46	9	3
Oil B	410	308	3	90	4	3	262	251	4
Dispersant C	2193	1746	3	364	208	3	797	75	3
Dispersant D	1119	900	3	289	193	3	202	52	4
ISB E	5	-	1	4	2	3	7	3	3
ISB F	-	-	-	8	3	3	10	2	4
Control I	-	-	-	1	1	3	1	0	4
Control J	-	-	-	1	0	3	1	0	4
Clean site 1	0	0	3	2	2	4	1	1	4
Clean site 2	1	0	3	2	1	4	1	1	4

BOTTOM ICE

Sum of alkanes in bottom ice (µg/g)

Sum of alkanes (µg/g)	T1			T2			T3		
	mean	std	n	mean	std	n	mean	std	n
Oil A	-	-	-	-	-	-	-	-	-
Oil B	-	-	-	-	-	-	-	-	-
Dispersant C	-	-	-	-	-	-	-	-	-
Dispersant D	-	-	-	-	-	-	-	-	-
ISB E	-	-	-	-	-	-	-	-	-
ISB F	-	-	-	-	-	-	-	-	-
Control I	-	-	-	-	-	-	-	-	-
Control J	-	-	-	-	-	-	-	-	-
Clean site 1	-	-	-	-	-	-	-	-	-
Clean site 2	-	-	-	-	-	-	-	-	-

Sum of PAHs in bottom ice (µg/g)

Sum of PAHs (µg/g)	T1			T2			T3		
	mean	std	n	mean	std	n	mean	std	n
Oil A	-	-	-	-	-	-	-	-	-
Oil B	-	-	-	-	-	-	-	-	-
Dispersant C	-	-	-	-	-	-	-	-	-
Dispersant D	-	-	-	-	-	-	-	-	-
ISB E	-	-	-	-	-	-	-	-	-
ISB F	-	-	-	-	-	-	-	-	-
Control I	-	-	-	-	-	-	-	-	-
Control J	-	-	-	-	-	-	-	-	-
Clean site 1	-	-	-	-	-	-	-	-	-
Clean site 2	-	-	-	-	-	-	-	-	-

Sum of dissolved PAHs in bottom ice (µg/L)

Sum of Dissolved PAHs (µg/L)	T1			T2			T3		
	mean	std	n	mean	std	n	mean	std	n
Oil A	110	65	2	112	22	3	73	22	4
Oil B	52	54	3	118	27	3	152	69	4
Dispersant C	127	65	3	198	139	3	255	107	4
Dispersant D	227	125	3	90	12	3	152	30	3
ISB E	25	8	3	3	1	3	5	3	2
ISB F	16	6	2	13	12	3	11	5	4
Control I	2	1	3	1	0	3	1	0	4
Control J	1	0	3	2	2	3	1	0	4
Clean site 1	1	1	4	1	1	4	1	1	4
Clean site 2	1	1	2	2	1	4	0	0	4

7.4 1-D Microbial community analysis

Full data tables for the sequencing

Relative abundance (%) of bacteria/taxonomic group (> 1%) in pristine ice core samples from February, DNA and RNA approach

Bacterial genus/ taxonomic group	DNA				RNA		
	Top	Middle	Bottom		Top	Middle	Bottom
Colwellia;	61,753	24,324	16,4419	I	70,1364	47,5677	35,8997
Oleispira;	7,712	3,7456	2,8519	I	9,6382	14,3374	3,7601
Chloroplast;	7,5697	27,4011	26,2381	I	3,5884	10,6343	8,684
Balneatrix;	3,045	19,1846	14,5881	I	3,6032	7,8739	28,8272
Polaribacter;	2,7604	4,0202	16,4579	I	2,6394	3,3713	2,3277
Colwelliaceae;uncultured;	2,2197	0,4745	1,6654	I	0,2372	0,181	0,0895
Octadecabacter;	1,1668	0,3193	2,5613	I	0,9045	3,0394	0,8057
Planctomycetes;OM190;	0,8537	0,197	0,2706	I	0,0593	0,0377	0,0895
Nitrospina;	0,8253	0,6297	0,5311	I	0,5042	0,3319	0,5372
Glaciecola;	0,7684	0,2895	0,4429	I	0,9342	0,2791	0,2686
Planktomarina;	0,5692	0,4805	0,4008	I	0,1186	0,0377	0,1791
Magnetospira;	0,5692	0,2179	0,1623	I	0,0593	0,0453	0,1791
Rhodobacteraceae;uncultured;	0,5407	0,5342	0,7215	I	0,1779	0,2036	0,4476
Sulfotobacter;	0,5122	0,1224	0,3247	I	0,1779	0,2036	0
Rhodospirillaceae;uncultured;	0,5122	0,582	0,4129	I	0,1186	0,0528	0,0895
Verrucomicrobiales;DEV007;	0,4838	0,0806	0,1443	I	0,2224	0,1131	0,2686
Flavobacteriaceae;NS5 marine group;	0,4269	0,2238	0,3788	I	0,089	0,0377	0
Acidimicrobiales;Sva0996 marine group;	0,3699	0,2925	0,1443	I	0,1779	0,0905	0,1791
Nostoc;	0,2846	0	0	I	0,1779	0,0075	0
Rhodospirillaceae;OM75 clade;	0,2846	0,1403	0,2024	I	0,1779	0,0528	0,0895
SAR86 clade;	0,2846	0,6208	0,4229	I	0,0445	0,1282	0,0895
Ilumatobacter;	0,2561	0,2537	1,0622	I	0,2669	0,7768	0,2686
Pelagibacter;	0,2561	0	0	I	0	0	0
Roseibacillus;	0,2561	0,0806	0,0962	I	0	0	0
Pseudospirillum;	0,2277	0,5969	0,5111	I	0,0445	0,0905	0
Actinomarina;	0,1992	0,0388	0,0561	I	0	0,0075	0
Mitochondria;	0,1992	0,0597	0,1243	I	0	0,0302	0
Phycisphaeraceae;CL500-3;	0,1707	0,0149	0,022	I	0	0,0075	0
Alphaproteobacteria;OCS116 clade;	0,1707	0,0955	0,1042	I	0	0	0
Bdellovibrionaceae;OM27 clade;	0,1707	0,0657	0,0421	I	0,0148	0,0754	0
Oceanospirillales;ZD0405;	0,1707	0,5641	0,3046	I	0,1483	0,1433	0,0895
Sphingomonas;	0,1423	0,003	0,006	I	0	0,0075	0
NS9 marine group;	0,1138	0,2865	0,3788	I	0,0593	0,1056	0,1791
Blastopirellula;	0,1138	0,0358	0,0361	I	0	0	0
ARKICE-90;	0,1138	0,0806	0,1423	I	0,1928	0,0226	0
Amylibacter;	0,1138	0,1045	0,0842	I	0	0,0075	0,0895
SAR11 clade;Surface 4;	0,1138	0,0388	0,0481	I	0,0148	0	0
Paraglaciecola;	0,1138	0,2835	0,0441	I	0,1186	0,083	1,1638
Psychromonas;	0,1138	0,7163	0,024	I	0,089	0,0603	1,1638
Neptunomonas;	0,1138	0,7581	0,1223	I	0,1483	1,7799	2,1486

Relative abundance (%) of bacteria/taxonomic group (> 1%) in pristine seawater at 5, 10 and 25 m depth, DNA and RNA approach

Bacterial genus/ taxonomic group	DNA				RNA			
	5M	10M	25M		1M	5M	10M	25M
Balneatrix;	13,840 4	16,422 4	11,727 7	I	8,9565	8,2487	11,7826	10,9265
Nitrospina;	2,616	3,4889	2,5078	I	8,247	5,2735	5,6882	7,042
Rhodospirillaceae;uncultured;	1,6698	2,6063	1,5917	I	4,7218	2,4229	3,225	2,8251
Chloroflexi;SAR202 clade;	1,9852	0,8567	1,0858	I	4,7077	8,0349	7,6689	7,2289
Bdellovibrionaceae;OM27 clade;	1,577	1,4244	0,9007	I	3,5505	3,6522	4,1392	3,3236
Rhodobacteraceae;uncultured;	2,0779	3,9069	2,9766	I	3,0465	2,3695	2,3108	3,0951
Planktomarina;	1,2059	3,4837	3,0846	I	3,0437	0,873	1,3459	1,6618
Marinimicrobia (SAR406 clade);	3,2282	1,5793	1,9155	I	2,7565	3,8838	3,3266	3,2405
Magnetospira;	1,0019	1,3161	1,0981	I	2,6157	2,227	1,4728	2,1604
Asciadiaceihabitans;	2,0594	1,7135	1,0457	I	2,5848	1,2471	2,7679	2,285
Oceanospirillales;ZD0405;	1,6883	2,6063	2,699	I	2,2666	2,7614	2,1585	1,7449
Rhodospirillaceae;OM75 clade;	0,4453	0,8671	0,5059	I	2,199	1,2115	1,1427	0,9555
Desulfuromonadales;GR-WP33-58;	1,2801	1,0064	0,6971	I	2,0188	2,4942	2,6409	2,1604
Oceanospirillales;SAR86 clade;	2,1892	3,0708	3,0476	I	1,9822	2,7793	2,5648	2,472
Acidimicrobiales;Sva0996 marine group;	2,7273	2,4618	1,5639	I	1,9287	2,512	2,0315	2,4096
Nitrosococcus;	0,4082	0,48	0,2406	I	1,8837	1,6747	1,9807	2,2642
Pseudospirillum;	1,3173	2,9986	1,8384	I	1,8105	1,3718	1,0665	1,0386
Verrucomicrobia;OPB35 soil group;	0,7792	0,3974	0,3825	I	1,7513	2,4586	1,422	0,9971
Gemmatimonadetes;BD2-11 terrestrial group;	0,2226	0,5109	0,3516	I	1,6978	0,481	0,9142	1,1425
Rickettsiales;SAR116 clade;	0,5566	1,0528	0,9408	I	1,436	0,7126	0,7872	0,7063
SAR11 clade;Surface 1;	0,4267	1,4709	5,2932	I	1,3431	1,9419	1,4728	1,558
Deltaproteobacteria;Sh765B-TzT-29;	1,3729	0,5832	0,6416	I	1,3008	1,4787	1,3713	1,4333
Defluviicoccus;	0,5195	0,6555	0,5491	I	1,2952	0,9442	0,9396	1,0179
Oceanospirillales;OM182 clade;	1,744	1,698	1,0673	I	1,2558	1,0689	1,676	1,7865
Deltaproteobacteria;SAR324 clade(Marine group B);	0,4638	1,0425	0,6509	I	1,2389	0,8195	1,3459	0,6647
Nitrosomonas;	0,2597	0,4697	0,4874	I	1,1995	0,6592	0,5079	0,5401
Porticoccaceae;SAR92 clade;	1,243	1,3419	1,0549	I	1,16	1,1758	1,3713	0,9971
Colwellia;	1,8924	1,0683	1,1629	I	1,1178	0,8373	1,0665	2,2227
Rhodospirillaceae;AEGEAN-169 marine group;	0,6308	0,7225	0,7958	I	0,9967	1,1758	1,0411	0,9971

Relative abundance (%) of bacteria/taxonomic group (> 1%) in seawater from mesocosm treatments, DNA and RNA approach

Bacterial genus/ taxonomic group	RNA					DNA		
	oil	oil+disp	burnt oil	control		oil+disp	burnt oil	control
Colwellia;	31,6485	46,8212	73,8409	0,8708		42,0558	0,8319	3,7323
Balneatrix;	15,1439	14,6564	0,9193	22,2605		14,7002	25,7443	27,1805
Polaribacter;	8,3981	6,12	0,7794	11,5747		13,9679	23,1173	25,8012
Flavobacteriales;NS9 marine group;	6,9401	3,3868	0,2198	9,6335		6,3968	11,4711	10,4665
SAR92 clade;	6,2014	4,2781	0,3997	8,7808		4,1448	7,0053	6,0446
Cyanobacteria	3,0715	1,5449	0,0799	4,1183		0,9947	2,8459	1,0548
Rhodobacteraceae;uncultured;	2,0801	1,5845	0,06	1,9049		0,7599	1,0946	1,3793
SAR86 clade;	1,9051	0,8517	0,1199	2,9209		1,05	2,627	2,1095
Oceanospirillales;ZD0405;	1,283	1,327	0,1998	2,3948		0,677	0,9632	0,568
Pseudospirillum;	1,2247	1,0101	0,0799	2,0864		0,5388	0,9632	1,2576
Flavobacterium;	1,1858	0,3961	0,04	0,2721		0,7461	1,0946	1,4199
Sva0996 marine group;	0,7776	0,515	0	1,5421		0,3868	0,7005	0,8114
Cryomorphaceae;uncultured;	0,7776	0,6734	0,06	0,7257		0,4974	1,4886	0,8925
Oceanospirillales;OM182 clade;	0,7193	1,4458	0,1599	3,0479		0,3454	1,1821	0,8114
PAsciidaehabitans;	0,6804	0,3763	0,02	0,5443		0,1382	0,2627	0,284
Oleispira;	0,661	1,7033	19,9241	0,127		1,05	0,1751	0,6491
SAR11 clade;Surface 1;	0,6026	0,515	0,0799	0,635		0,152	0,1751	0
Methylophilaceae;OM43 clade;	0,486	0,2575	0	1,2881		0,0967	0,1313	0,2434
Flavobacteriaceae;NS4 marine group;	0,4666	0,4753	0	1,2337		0,525	0,6567	0,6897
Sulfitobacter;	0,4666	0,6536	0,04	1,1974		0,7875	1,6637	1,8661
Planktomarina;	0,4277	0,6734	0	1,4151		0,0691	1,4011	1,1765
Defluviicoccus;	0,4082	0,3169	0	1,0704		0,0691	0,5254	0,2028
Magnetospira;	0,4082	0,3961	0	1,143		0,0691	0,4816	0,4057

Relative abundance (%) of bacteria/taxonomic group (> 1%) in ice core samples, different treatments in March, analysis on RNA level

Bacterial genus/ taxonomic group	Top layer					Bottom layer			
	oil	oil+disp	burnt oil	control		oil	oil+disp	burnt oil	control
Colwellia;	63,80	28,64	78,34	89,43		64,84	18,36	81,34	89,80
Oleispira;	29,22	68,10	14,31	2,08		18,32	79,96	4,91	2,44
Balneatrix;	0,12	0,09	0,16	1,24		1,91	0,04	2,33	1,66
Cyanobacteria	0,01	0,05	0,12	0,10		0,46	0,00	0,55	0,41
Polaribacter	0,06	0,04	0,07	0,01		0,75	0,00	0,33	0,26
Oceanospirillaceae;uncultured;	5,81	1,64	5,73	5,38		6,86	0,74	7,71	3,31

Relative abundance (%) of bacteria/taxonomic group (> 1%) in ice core samples, different treatments in April, analysis on RNA level

Bacterial genus/ taxonomic group	Top layer				Bottom layer			
	oil	oil+disp	control		oil	oil+disp	burnt oil	control
Colwellia;	76,02	73,43	95,12		64,52	73,45	71,33	89,43
Oleispira;	21,82	22,87	2,81		14,89	16,35	13,32	2,68
Balneatrix;	0,03	0,56	0,09		6,34	0,07	1,90	1,08
Cyanobacteria	0,00	0,08	0,08		1,76	0,00	0,85	3,57
Polaribacter	0,03	0,08	0,11		1,19	0,09	0,16	0,14
Oceanospirillaceae;uncultured;	0,67	0,13	0,46		1,13	5,05	4,31	0,17

Relative abundance (%) of bacteria/taxonomic group (> 1%) in ice core samples, different treatments in May, analysis on RNA level

Bacterial genus/ taxonomic group	Top layer					Bottom layer			
	oil	oil+disp	burnt oil	control		oil	oil+disp	burnt oil	control
Colwellia;	61,5467	79,6257	67,5301	67,9915		41,0894	74,2255	40,803	49,0432
Oleispira;	28,9379	8,408	19,704	6,3292		39,1593	7,5535	10,8475	1,3685
Balneatrix;	0,9562	0,1581	0,0925	0,2466		2,013	0,1118	9,3001	1,5688
Cyanobacteria	0,0093	0	0	0,0193		0,2605	0,0319	0,4682	0,6008
Polaribacter	0,4571	0,6853	2,4052	13,0838		1,6933	1,0859	1,6823	3,2599
Oceanospirillaceae;uncultured;	0,2099	2,4381	0,8326	0,0387		0,9236	3,2418	0,5475	0,267

Relative abundance (%) of bacteria/taxonomic group (> 1%) in ice core samples, different treatments in March, analysis on DNA level

Bacterial genus/ taxonomic group	Top layer					Bottom layer			
	oil	oil+disp	burnt oil	control		oil	oil+disp	burnt oil	control
Colwellia;	70,4772	44,6989	74,171	80,0593		68,9537	43,4733	76,5515	81,5518
Oleispira;	23,1602	50,5448	13,438	2,7519		18,2731	53,059	2,9759	2,5119
Oceanospirillaceae;uncultured;	5,4848	2,589	9,904	12,433		5,9719	1,8326	12,0233	11,1638
Polaribacter;	0,0132	0,0293	0,1091	0,5363		1,132	0,0276	1,974	0,8094
Balneatrix;	0,1188	0,0527	0,5236	1,1995		1,5766	0,2093	1,6749	1,0885
Arcobacter;	0,0264	0,0059	0	0,0706		0,1512	0	0,1047	0

Relative abundance (%) of bacteria/taxonomic group (> 1%) in ice core samples, different treatments in April, analysis on DNA level

Bacterial genus/ taxonomic group	Top layer					Bottom layer			
	oil	oil+disp	burnt oil	control		oil	oil+disp	burnt oil	control
Colwellia;	78,6321	82,8737	66,6826	71,7367		74,877	74,2453	61,2778	74,4908
Oleispira;	18,2829	14,9985	19,1914	1,7561		17,1117	14,0121	13,0982	3,0434
Oceanospirillaceae;uncultured;	1,5545	0,816	1,7737	1,12		1,9765	6,8915	5,0149	0,3834
Polaribacter;	0,0717	0	0,3516	2,4475		1,5109	0,6038	1,7403	1,9171
Balneatrix;	0,0598	0,0103	0,0959	2,7102		0,7027	0,0416	1,5571	1,7973
Arcobacter;	0,4903	0,1033	0,4954	0,0415		0,3777	1,2284	1,2823	0,0479

Relative abundance (%) of bacteria/taxonomic group (> 1%) in ice core samples, different treatments in May, analysis on DNA level

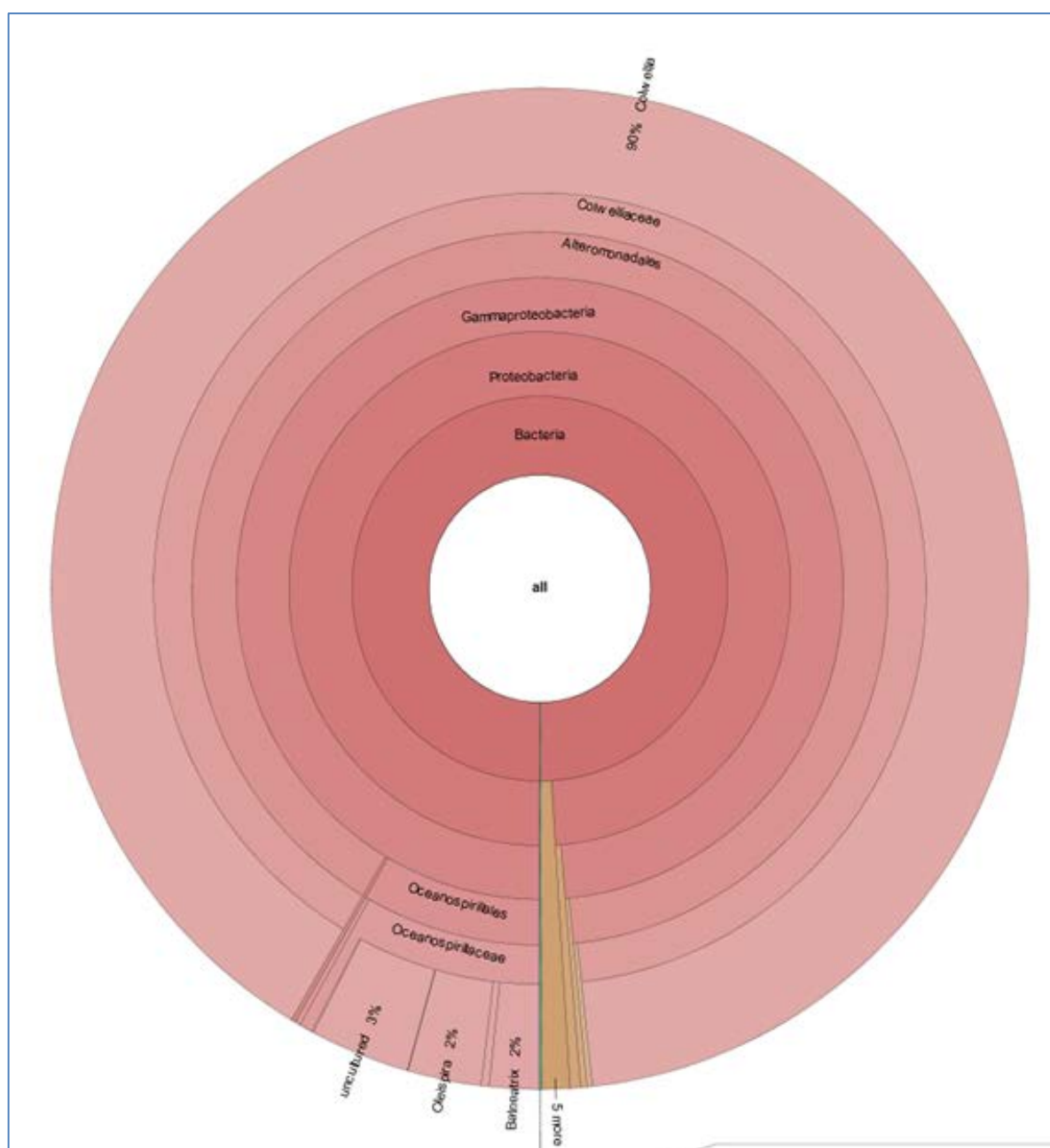
Bacterial genus/ taxonomic group	Top layer					Bottom layer			
	oil	oil+dis p	burnt oil	contro l		oil	oil+dis p	burnt oil	contro l
Colwellia;	54,549 9	85,087 6	64,066	61,662 1		38,801 7	83,208 8	51,3565	50,481 6
Oleispira;	35,190 3	9,9676	22,2348	7,4498		37,644 6	6,0164	13,2751	2,1932
Oceanospirillaceae;uncultured;	0,6045	0,2206	0,3809	0,0339		1,7999	2,0055	0,6007	0,3927
Polaribacter;	1,552	0,1298	2,4549	21,124 7		4,5513	1,0392	4,4898	5,7239
Balneatrix;	0,196	0	0,0847	0,2221		1,8899	0,0365	8,225	2,6675
Arcobacter;	1,8788	0,7268	0,8465	0,0062		2,1857	1,2762	0,2549	0,0037

Relative abundance (%) of bacteria/taxonomic group (> 1%) in the biofilm samples from May, analysis on DNA and RNA level

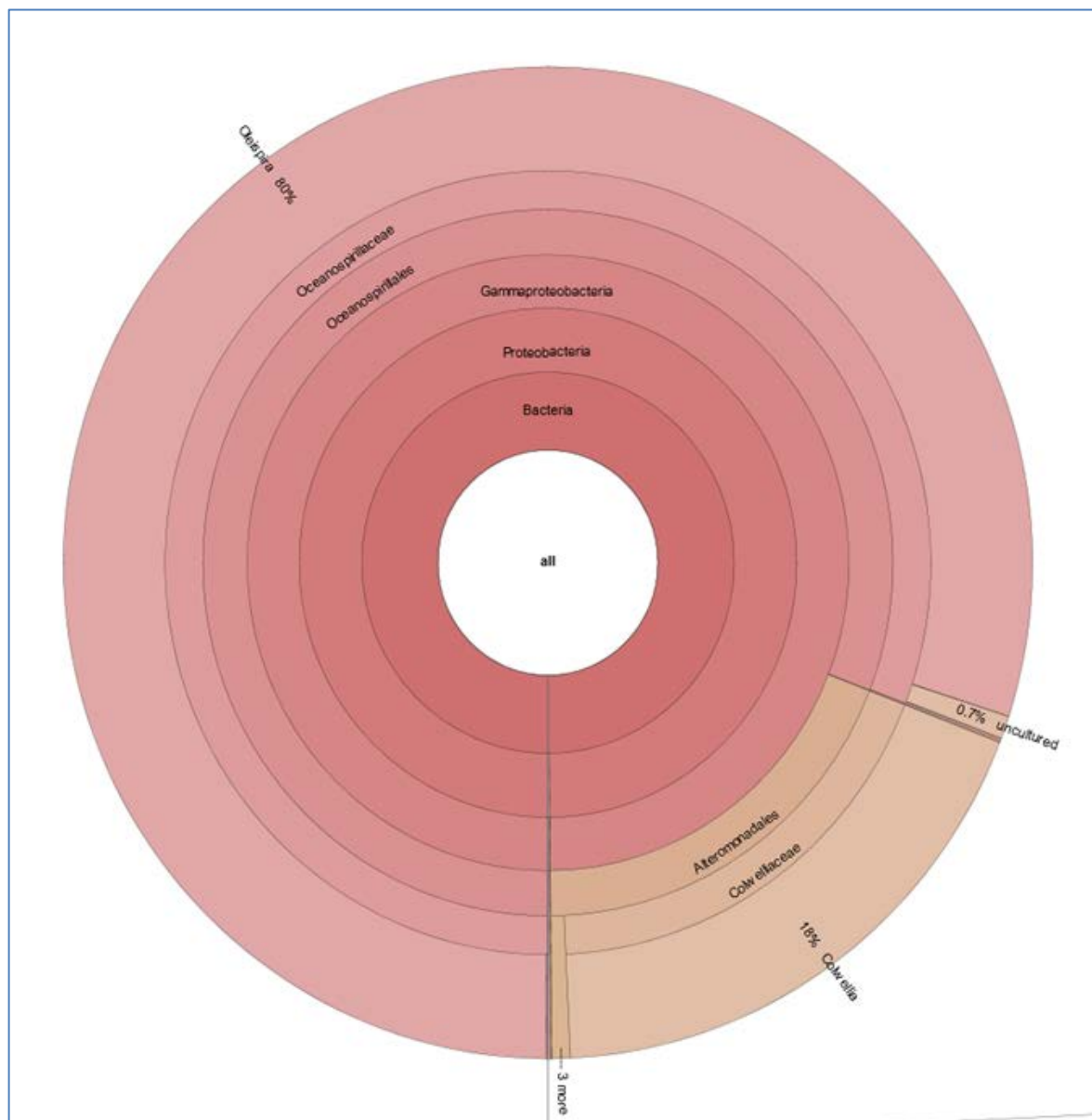
Bacterial genus/ taxonomic group	DNA					RNA			
	oiled 1	oiled 2	contro l1	contro l2		oiled 1	oiled 2	contro l1	contro l2
Oceanospirillales;SS1-B-06-26;	17,201	21,905 7	0,3778	0		25,770 2	25,205 1	2,0114	0,4053
Colwellia;	16,575 7	13,634 6	17,478 6	20,687 3		13,817 6	4,8383	35,338 2	22,124 4
Oleispira;	15,836 7	16,149 3	8,6743	3,7736		11,313 8	18,050 2	6,0343	3,1307
Neptunomonas;	6,1505	7,8094	0,3007	0,1348		6,8418	4,4281	2,2481	0,3774
Pseudofulvibacter;	4,9341	1,8369	1,3164	0,7412		0,9171	0,8205	0,355	0,4333
Cryomorphaceae;uncultured;	4,0359	3,5756	1,0401	0,1348		1,999	3,3301	0,493	0,4472
Oleibacter;	3,7517	3,389	7,5204	0		8,9851	7,348	3,2538	0,2516
Salinirepens;	3,4561	3,2613	0,0163	0		1,6383	2,1839	0,0986	0,0699
Fluviicola;	3,3083	1,8566	0,6826	0,2695		4,0289	2,3769	0,6113	0,3494
Pseudoteredinibacter;	2,3647	1,0806	0,0691	0		0,9067	0,2654	0,0197	0
Crocinitomix;	2,2055	3,2809	2,4784	0,6739		1,154	2,3287	1,2029	1,3277
Gracilibacteria;	1,9554	2,2004	0,2031	0,1348		0,4946	1,2548	0,1183	0,0839
Rickettsiales;SM2D12;	1,3756	1,8762	0,0244	0		2,9985	6,2862	0,1578	0,028
Sufflavibacter;	1,2619	1,336	0,0934	5,1213		0,7831	0,7963	0,0592	3,1586
Polaribacter;	1,2165	0,5501	1,4301	18,059 3		0,3297	0,3016	3,451	4,3746
Arcobacter;	1,0232	2,1611	0,7882	0,6065		0,3297	0,6274	0,7099	0,1677
Paraglaciecola;	1,0232	0,9037	0,3007	1,4825		0,9171	0,3861	0,355	1,9706
Flavobacteriaceae;uncultured;	0,739	0,7859	0,1666	0,4717		0,2473	0,4947	0,0986	0,2096
Cyanobacteria	0,7162	0,7073	9,4503	3,2345		0,0721	0,0362	1,8537	3,6198
Marinicella;	0,6025	0,8939	0,6216	1,4825		0,6388	1,0859	0,2958	3,1307
Cycloclasticus;	0,5571	0,8644	0,2478	0,4717		0,9377	1,472	0,3747	1,761
Tenacibaculum;	0,5343	0,2259	0,1666	8,221		0,2576	0,181	0,0986	2,2781
Rickettsiales	0,523	0,2259	0,2072	0		2,0711	0,3982	0,1972	0,0699
Alphaproteobacteria;OCS116 clade;	0,4434	1,0413	0,0731	0		0,1958	0,6998	0,1972	0,0839
Piscirickettsiaceae;uncultured;	0,3638	0,3733	2,6774	0,8086		0,2473	0,3137	0,7099	1,775
Kangiella;	0,2842	0,2259	0,3291	0,876		0,5976	0,374	0,0592	1,2718

7.5 1-F Bacterial community composition – Silva NGS analysis

The active bacterial compositions (based on RNA) are shown here for the bottom layer of the sea ice samples in March (Control in Figure 1 and Oil+dispersant Figure 2) and May (Control in Figure 3 and Oil+dispersant Figure 4). Also shown are the results from the seawater samples collected just under the sea-ice layer in May (Control in Figure 5 and oil+dispersant Figure 6), and samples from non-contaminated biofilms (Figure 7) and biofilms from oiled tiles (Figure 8), all collected in May 3 months after the start of the exposure.



Appendix Figure 1 Active bacterial community composition (based on total RNA). Bottom layer of sea ice in Control no oil mesocosm in March (1 month after start of exposure). Silva NGS analysis. In blue are non classified organisms.



Appendix Figure 2 Active bacterial community composition (based on total RNA). Bottom layer of sea ice in Oil+dispersant mesocosm in March (1 month after start of exposure). Silva NGS analysis. In blue are non classified organisms.



Appendix Figure 3 Active bacterial community composition (based on total RNA). Bottom layer of sea ice in Control no oil mesocosm in May (3 months after start of exposure). Silva NGS analysis. In green are non-classified organisms.



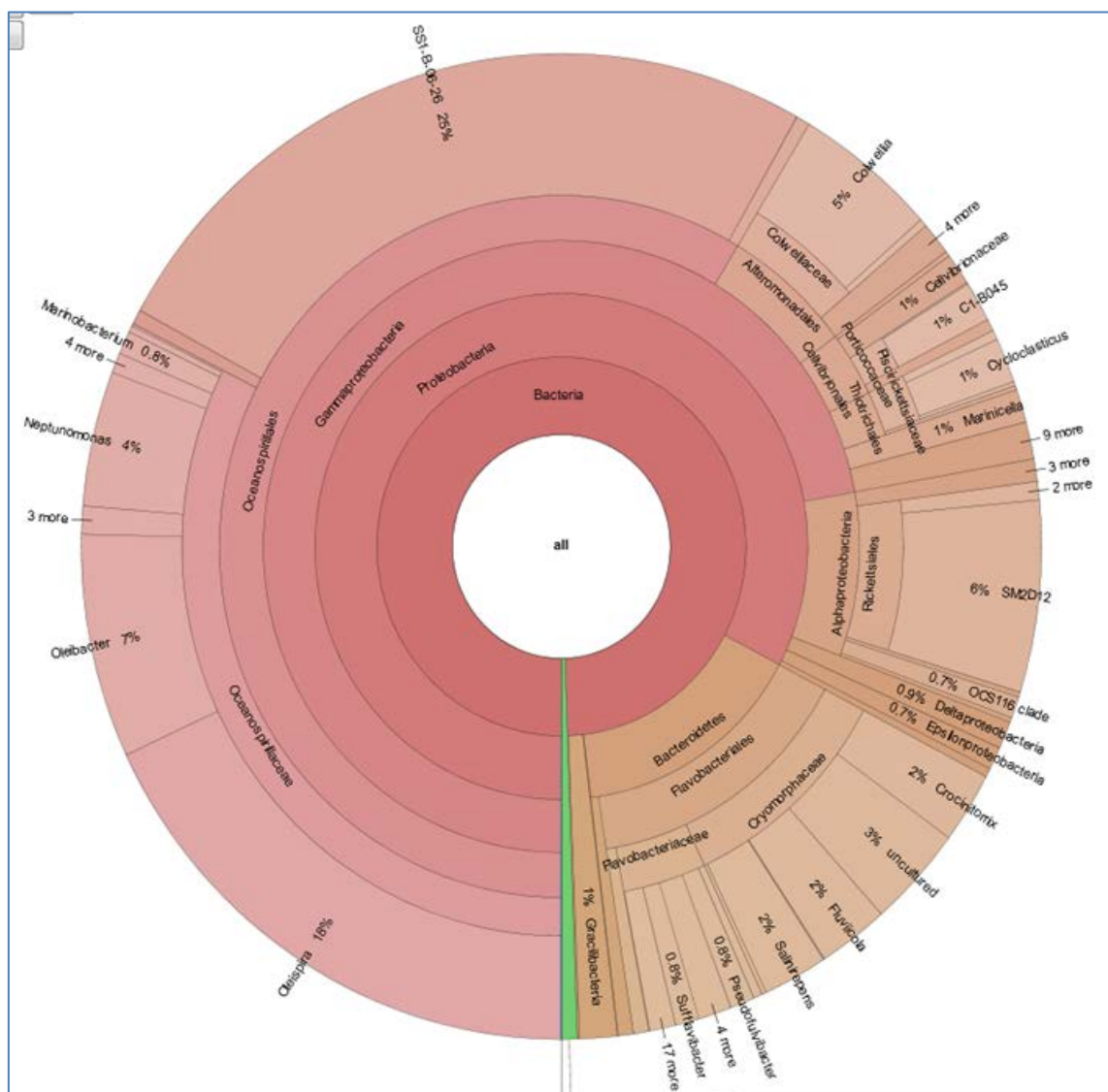
Appendix Figure 4 Active bacterial community composition (based on total RNA). Bottom layer of sea ice in Oil+dispersant mesocosm in May (3 months after start of exposure). Silva NGS analysis. In blue are non classified organisms.



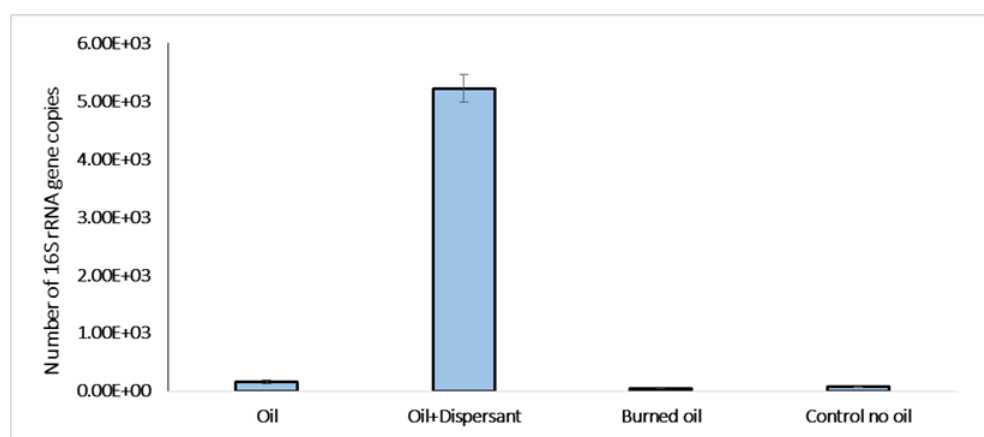
Appendix Figure 5 Active bacterial community composition (based on total RNA). Seawater collected from just under the ice layer in the Control no oil mesocosm in May (3 months after start of exposure). Silva NGS analysis. In green are non classified organisms.



Appendix Figure 7 Active bacterial community composition (based on total RNA). Biofilm collected from control non-contaminated tiles in May (3 months after start of exposure). Silva NGS analysis. In green are non classified organisms.



Appendix Figure 8 Active bacterial community composition (based on total RNA). Biofilm collected from oiled tiles in May (3 months after start of exposure). Silva NGS analysis. In green are non classified organisms.



Appendix Figure 9 Quantification of *Oleispira* (total number of bacterial 16S rRNA gene copies per 1ml seawater) under the sea-ice layer, Samples from May, 3 months after exposure in the control, oil, oil+dispersant and burned oil mesocosms

Microbial activity tables

Bacterial abundance of the ice and water samples before filtration and preparation for incubation.

Mesocosm	ice/water	section	T2 (April)		T3 (May)	
			measured (cells/mL)	corrected ^(a) (cells/mL)	measured (cells/mL)	corrected ^(a) (cells/mL)
A-oil	ice	middle	4.51E+05	9.51E+05	6.59E+05	1.21E+06
A-oil	ice	bottom	n.d.	n.d.	5.08E+05	5.08E+05
B-oil	ice	middle	2.32E+05	4.51E+05	2.89E+05	5.29E+05
B-oil	ice	bottom	n.d.	n.d.	3.74E+05	3.74E+05
C-oil/disp	ice	middle	1.56E+06	3.12E+06	7.74E+05	1.33E+06
D-oil/disp	ice	middle	1.63E+06	2.98E+06	8.28E+05	1.66E+06
E-burned	ice	middle	6.30E+05	1.16E+06	5.91E+05	9.75E+05
F-burned	ice	middle	1.55E+05	2.71E+05	2.42E+05	4.29E+05
I-control	ice	middle	1.39E+05	2.42E+05	3.83E+05	6.22E+05
J-control	ice	middle	2.14E+05	3.39E+05	4.68E+05	7.27E+05
A-oil	water	1m depth	2.84E+05	2.84E+05	9.02E+05	9.02E+05
B-oil	water	1m depth	3.41E+05	3.41E+05	7.37E+05	7.37E+05
C-oil/disp	water	1m depth	2.81E+05	2.81E+05	7.67E+05	7.67E+05
D-oil/disp	water	1m depth	2.49E+05	2.49E+05	7.45E+05	7.45E+05
E-burned	water	1m depth	2.96E+05	2.96E+05	7.20E+05	7.20E+05
F-burned	water	1m depth	2.75E+05	2.75E+05	7.61E+05	7.61E+05
I-control	water	1m depth	2.83E+05	2.83E+05	9.38E+05	9.38E+05
J-control	water	1m depth	2.88E+05	2.88E+05	7.42E+05	7.42E+05

(a) Bacterial abundance corrected for added sterile seawater during melting

Bacterial abundance and corresponding calculated cell growth rates.

Mesocosm	ice/ water	section	field campaign	Bacterial Abundance				interval ^(a) type	Calculated Exponential Growth Rate				
				reactor ^(b)	F1	F2	F3		F1-F2	F1-F2-F3	F1-F2-F3	F1-NO	
				unit	(cells/mL)	(cells/mL)	(cells/mL)		rate unit	rate (day ⁻¹)	±SE (day ⁻¹)	rate (day ⁻¹)	
ice				sampling ^(c)	D0	D9	D20	D20					
A-oil	ice	middle	T2 (April)		1.46E+05	7.10E+05	6.61E+05	9.74E+05		1.8E-01	7.2E-02	5.2E-02	9.5E-02
A-oil	ice	bottom	T2 (April)		n.d.	n.d.	n.d.	n.d.		n.a.	n.a.	n.a.	n.a.
B-oil	ice	middle	T2 (April)		1.11E+05	1.16E+06	1.58E+06	1.70E+06		2.6E-01	1.3E-01	6.6E-02	1.4E-01
B-oil	ice	bottom	T2 (April)		n.d.	n.d.	n.d.	n.d.		n.a.	n.a.	n.a.	n.a.
C-oil/disp	ice	middle	T2 (April)		4.76E+05	3.21E+05	3.22E+05	4.95E+05		-4.4E-02	-1.9E-02	1.2E-02	2.0E-03
D-oil/disp	ice	middle	T2 (April)		4.08E+05	3.08E+05	3.70E+05	6.90E+05		-3.1E-02	-4.1E-03	1.4E-02	2.6E-02
E-burned	ice	middle	T2 (April)		2.25E+05	4.34E+05	4.76E+05	7.03E+05		7.3E-02	3.6E-02	1.8E-02	5.7E-02
F-burned	ice	middle	T2 (April)		8.57E+04	7.27E+05	9.38E+05	1.01E+06		2.4E-01	1.2E-01	6.1E-02	1.2E-01
I-control	ice	middle	T2 (April)		7.59E+04	9.03E+05	1.15E+06	1.37E+06		2.8E-01	1.3E-01	7.2E-02	1.4E-01
J-control	ice	middle	T2 (April)		1.45E+05	5.81E+05	7.08E+05	8.91E+05		1.5E-01	7.7E-02	3.9E-02	9.1E-02
water				sampling ^(c)	D0	D10	D20	D20					
A-oil	water	1m depth	T2 (April)		2.37E+05	2.24E+05	3.30E+06	2.98E+06		-6.1E-03	1.4E-01	7.1E-02	1.3E-01
B-oil	water	1m depth	T2 (April)		2.12E+05	2.05E+05	2.68E+06	2.40E+06		-3.9E-03	1.3E-01	6.8E-02	1.2E-01
C-oil/disp	water	1m depth	T2 (April)		1.93E+05	2.48E+05	2.32E+06	3.36E+06		2.8E-02	1.3E-01	5.0E-02	1.4E-01
D-oil/disp	water	1m depth	T2 (April)		2.01E+05	3.64E+05	2.78E+06	3.88E+06		6.6E-02	1.3E-01	3.4E-02	1.5E-01
E-burned	water	1m depth	T2 (April)		1.78E+05	2.27E+05	3.65E+06	3.83E+06		2.7E-02	1.5E-01	6.4E-02	1.5E-01
F-burned	water	1m depth	T2 (April)		1.76E+05	1.72E+05	3.20E+06	3.75E+06		-2.6E-03	1.5E-01	7.6E-02	1.5E-01
I-control	water	1m depth	T2 (April)		2.21E+05	3.16E+05	2.80E+06	2.38E+06		3.9E-02	1.3E-01	4.5E-02	1.2E-01
J-control	water	1m depth	T2 (April)		2.15E+05	1.96E+05	3.12E+06	3.93E+06		-1.0E-02	1.4E-01	7.5E-02	1.5E-01
ice				sampling ^(c)	D0	D4	D7	D7					
A-oil	ice	middle	T3 (May)		1.69E+05	1.03E+06	9.19E+05	1.20E+06		4.5E-01	2.5E-01	1.4E-01	2.8E-01
A-oil	ice	bottom	T3 (May)		1.15E+05	5.52E+05	5.50E+05	7.82E+05		3.9E-01	2.3E-01	1.1E-01	2.7E-01
B-oil	ice	middle	T3 (May)		1.45E+05	5.02E+05	5.97E+05	1.02E+06		3.1E-01	2.1E-01	7.1E-02	2.8E-01
B-oil	ice	bottom	T3 (May)		1.39E+05	4.58E+05	5.20E+05	5.85E+05		3.0E-01	1.9E-01	7.2E-02	2.1E-01
C-oil/disp	ice	middle	T3 (May)		1.33E+05	7.08E+05	1.20E+06	1.31E+06		4.2E-01	3.2E-01	6.8E-02	3.3E-01
D-oil/disp	ice	middle	T3 (May)		1.35E+05	9.30E+05	1.53E+06	9.77E+05		4.8E-01	3.5E-01	8.9E-02	2.8E-01
E-burned	ice	middle	T3 (May)		2.07E+05	5.98E+05	9.97E+05	4.90E+05		2.7E-01	2.3E-01	2.7E-02	1.2E-01
F-burned	ice	middle	T3 (May)		7.50E+04	2.79E+05	1.33E+06	9.87E+05		3.3E-01	4.1E-01	5.4E-02	3.7E-01
I-control	ice	middle	T3 (May)		1.76E+05	9.83E+05	1.57E+06	1.00E+06		4.3E-01	3.2E-01	7.7E-02	2.5E-01
J-control	ice	middle	T3 (May)		1.94E+05	1.53E+06	2.10E+06	1.03E+06		5.2E-01	3.5E-01	1.2E-01	2.4E-01
water				sampling ^(c)	D0	D7	D10	D10					
A-oil	water	1m depth	T3 (May)		6.71E+05	8.54E+05	1.33E+06	1.33E+06		6.0E-02	9.6E-02	2.5E-02	9.8E-02
B-oil	water	1m depth	T3 (May)		5.65E+05	5.82E+05	1.10E+06	1.53E+06		7.0E-03	9.1E-02	5.8E-02	1.4E-01
C-oil/disp	water	1m depth	T3 (May)		4.87E+05	9.48E+05	1.61E+06	2.35E+06		1.7E-01	1.7E-01	2.9E-03	2.2E-01
D-oil/disp	water	1m depth	T3 (May)		3.57E+05	6.36E+05	1.23E+06	1.24E+06		1.4E-01	1.7E-01	2.1E-02	1.8E-01
E-burned	water	1m depth	T3 (May)		5.71E+05	5.10E+05	1.62E+06	1.50E+06		-2.8E-02	1.4E-01	1.2E-01	1.4E-01
F-burned	water	1m depth	T3 (May)		6.16E+05	7.18E+05	1.18E+06	1.05E+06		3.8E-02	8.9E-02	3.5E-02	7.7E-02
I-control	water	1m depth	T3 (May)		6.34E+05	6.54E+05	9.52E+05	9.91E+05		7.5E-03	5.5E-02	3.3E-02	6.4E-02
J-control	water	1m depth	T3 (May)		5.39E+05	5.80E+05	1.32E+06	7.42E+05		1.8E-02	1.2E-01	7.1E-02	4.6E-02

(a) Reactors F1, F2, and F3 were amended with oil, reactor "NO" contained no added oil. (b) Day of the incubation the reactor was sampled for bacterial abundance. (c) Interval for which an exponential growth rate constant was determined.

Calculated zero-order oxygen consumption rates for reactors incubated with (F2, F3) and without (NO) oil. The rates were normalized to the number of cell present at time of sampling.

Mesocosm	ice/ water	section	field campaign	Rate for reactor F2		Rate for reactor F3		Rate for reactor NO		Average Rate	
				rate	±SE ^(a)	rate	±SE ^(a)	rate	±SE ^(a)	rate	±StDev
				pmol/cells/day		pmol/cells/day		pmol/cells/day		pmol/cells/day	
T2 - ice				interval ^(b)		D0 - D9		D0 - D20		D0 - D20	
A-oil	ice	middle	T2 (April)	1.21	0.15	1.20	0.20	1.55	0.30	1.32	0.20
A-oil	ice	bottom	T2 (April)	n.d.	n.a.	n.d.	n.a.	n.d.	n.a.	n.d.	n.a.
B-oil	ice	middle	T2 (April)	0.61	0.08	0.81	0.12	0.74	0.09	0.72	0.10
B-oil	ice	bottom	T2 (April)	n.d.	n.a.	n.d.	n.a.	n.d.	n.a.	n.d.	n.a.
C-oil/disp	ice	middle	T2 (April)	2.96	0.49	2.39	0.38	2.34	0.33	2.56	0.35
D-oil/disp	ice	middle	T2 (April)	2.45	0.35	2.90	0.39	3.61	0.70	2.99	0.59
E-burned	ice	middle	T2 (April)	1.41	0.25	1.73	0.18	1.72	0.24	1.62	0.18
F-burned	ice	middle	T2 (April)	1.07	0.12	1.53	0.34	1.14	0.14	1.25	0.25
I-control	ice	middle	T2 (April)	0.91	0.11	1.51	0.49	0.87	0.51	1.10	0.36
J-control	ice	middle	T2 (April)	2.19	0.81	1.20	0.16	1.08	0.24	1.49	0.61
T3 - water				interval ^(b)		D0 - D10		D0 - D20		D0 - D20	
A-oil	water	1m depth	T2 (April)	3.35	0.35	3.50	0.34	2.82	0.32	3.22	0.36
B-oil	water	1m depth	T2 (April)	3.60	0.35	3.66	0.38	3.04	0.32	3.43	0.34
C-oil/disp	water	1m depth	T2 (April)	2.73	0.38	2.85	0.25	2.72	0.31	2.77	0.07
D-oil/disp	water	1m depth	T2 (April)	2.04	0.21	2.38	0.22	1.95	0.23	2.13	0.23
E-burned	water	1m depth	T2 (April)	3.40	0.38	3.50	0.37	2.98	0.37	3.30	0.28
F-burned	water	1m depth	T2 (April)	4.71	0.53	4.65	0.46	4.45	0.47	4.60	0.13
I-control	water	1m depth	T2 (April)	2.91	0.30	2.71	0.27	2.15	0.24	2.59	0.39
J-control	water	1m depth	T2 (April)	3.54	0.49	4.08	0.42	4.03	0.41	3.88	0.30
T3 - ice				interval ^(b)		D0 - D4		D0 - D7		D0 - D7	
A-oil	ice	middle	T3 (May)	0.93	n.a.	0.54	n.a.	0.34	n.a.	0.44	0.30
A-oil	ice	bottom	T3 (May)	0.58	n.a.	0.58	n.a.	0.47	n.a.	0.52	0.06
B-oil	ice	middle	T3 (May)	1.71	n.a.	0.85	n.a.	0.50	n.a.	0.68	0.62
B-oil	ice	bottom	T3 (May)	n.d.	n.a.	0.77	n.a.	0.64	n.a.	0.70	0.10
C-oil/disp	ice	middle	T3 (May)	0.87	n.a.	0.38	n.a.	0.29	n.a.	0.34	0.31
D-oil/disp	ice	middle	T3 (May)	0.91	n.a.	0.30	n.a.	0.57	n.a.	0.44	0.30
E-burned	ice	middle	T3 (May)	1.08	n.a.	0.58	n.a.	1.16	n.a.	0.87	0.31
F-burned	ice	middle	T3 (May)	2.66	n.a.	0.30	n.a.	0.26	n.a.	0.28	1.37
I-control	ice	middle	T3 (May)	0.74	n.a.	0.38	n.a.	0.52	n.a.	0.45	0.18
J-control	ice	middle	T3 (May)	0.44	n.a.	0.12	n.a.	0.42	n.a.	0.27	0.18
T3 - water				interval ^(b)		D0 - D7		D0 - D10		D0 - D10	
A-oil	water	1m depth	T3 (May)	0.52	n.a.	0.29	n.a.	0.23	n.a.	0.26	0.15
B-oil	water	1m depth	T3 (May)	0.71	n.a.	0.34	n.a.	0.23	n.a.	0.29	0.25
C-oil/disp	water	1m depth	T3 (May)	0.56	n.a.	0.34	n.a.	0.19	n.a.	0.27	0.18
D-oil/disp	water	1m depth	T3 (May)	0.98	n.a.	0.25	n.a.	0.17	n.a.	0.21	0.45
E-burned	water	1m depth	T3 (May)	0.60	n.a.	0.18	n.a.	0.16	n.a.	0.17	0.25
F-burned	water	1m depth	T3 (May)	0.63	n.a.	0.13	n.a.	0.15	n.a.	0.14	0.28
I-control	water	1m depth	T3 (May)	0.72	n.a.	0.19	n.a.	0.23	n.a.	0.21	0.29
J-control	water	1m depth	T3 (May)	0.82	n.a.	0.18	n.a.	0.33	n.a.	0.25	0.33

(a) Standard error of linear regression. Since the oxygen saturation was only measured at the beginning and end of each incubation during field campaign T4, no standard error is available for these samples. (b) Beginning and end day of the incubation (e.g., D0 = beginning of incubation, D7 = day 7 of the incubation). Different incubation times were used for the two matrices as well as for the two field campaigns.

Remaining naphthalene fractions in reactors during the incubation experiments, and corresponding calculated first-order degradation rate constants.

Mesocosm	ice/ water	section	field campaign	Remaining naphthalene fraction			Calculated degradation rate constant			
				Reactor F1	Reactor F2	Reactor F3	individual mesocosms		combined mesocosms	
				unit	{-}	{-}	rate	±SE	rate	±Diff
							{day-1}	{day-1}	{day-1}	{day-1}
ice - T2				sampling ^(a)	D0	D9	D20			
A-oil	ice	middle	T2 (April)	100%	100%	99%	4.9E-04	9.0E-06	9.5E-04	4.5E-04
A-oil	ice	bottom	T2 (April)	n.a.	n.a.	n.a.	n.a.	n.a.	n.a.	n.a.
B-oil	ice	middle	T2 (April)	100%	99%	n.a.	1.4E-03	n.a.		
B-oil	ice	bottom	T2 (April)	n.a.	n.a.	n.a.	n.a.	n.a.		
C-oil/disp	ice	middle	T2 (April)	100%	98%	92%	4.0E-03	6.4E-04	5.0E-03	1.0E-03
D-oil/disp	ice	middle	T2 (April)	100%	93%	89%	6.0E-03	6.3E-04		
E-burned	ice	middle	T2 (April)	100%	91%	86%	8.1E-03	6.9E-04	5.1E-03	2.9E-03
F-burned	ice	middle	T2 (April)	100%	98%	n.a.	2.2E-03	3.9E-19		
I-control	ice	middle	T2 (April)	100%	88%	n.a.	1.4E-02	n.a.	8.1E-03	5.8E-03
J-control	ice	middle	T2 (April)	100%	100%	95%	2.2E-03	8.8E-04		
water - T2				sampling ^(a)	D0	D10	D20			
A-oil	water	1m depth	T2 (April)	100%	98%	n.a.	1.8E-03	n.a.	1.8E-03	n.a.
B-oil	water	1m depth	T2 (April)	100%	n.a.	n.a.	n.a.	n.a.		
C-oil/disp	water	1m depth	T2 (April)	100%	99%	99%	6.7E-04	6.4E-07	2.2E-03	1.5E-03
D-oil/disp	water	1m depth	T2 (April)	100%	90%	96%	3.8E-03	2.4E-03		
E-burned	water	1m depth	T2 (April)	100%	96%	n.a.	4.1E-03	n.a.	2.9E-03	1.2E-03
F-burned	water	1m depth	T2 (April)	100%	99%	96%	1.7E-03	2.7E-04		
I-control	water	1m depth	T2 (April)	100%	n.a.	n.a.	n.a.	n.a.	4.6E-03	1.3E-03
J-control	water	1m depth	T2 (April)	100%	99%	90%	4.6E-03	1.3E-03		
ice - T3				sampling ^(a)	D0	D4	D7			
A-oil	ice	middle	T3 (May)	100%	92%	n.a.	2.0E-02	n.a.	1.6E-02	3.6E-03
A-oil	ice	bottom	T3 (May)	100%	100%	93%	8.4E-03	3.4E-03	1.0E-02	1.6E-03
B-oil	ice	middle	T3 (May)	100%	95%	n.a.	1.2E-02	n.a.		
B-oil	ice	bottom	T3 (May)	100%	98%	91%	1.2E-02	2.2E-03		
C-oil/disp	ice	middle	T3 (May)	100%	n.a.	n.a.	n.a.	n.a.	1.1E-03	2.2E-03
D-oil/disp	ice	middle	T3 (May)	100%	102%	98%	1.1E-03	2.2E-03		
E-burned	ice	middle	T3 (May)	100%	100%	92%	9.0E-03	3.6E-03	9.0E-03	3.6E-03
F-burned	ice	middle	T3 (May)	100%	n.a.	n.a.	n.a.	n.a.		
I-control	ice	middle	T3 (May)	100%	96%	94%	9.3E-03	9.2E-05	1.1E-02	4.7E-03
J-control	ice	middle	T3 (May)	100%	96%	91%	1.3E-02	1.5E-03		
water - T3				sampling ^(a)	D0	D7	D10			
A-oil	water	1m depth	T3 (May)	100%	100%	n.a.	-4.2E-04	0.0E+00	-4.2E-04	2.1E-04
B-oil	water	1m depth	T3 (May)	100%	n.a.	n.a.	n.a.	n.a.		
C-oil/disp	water	1m depth	T3 (May)	100%	102%	n.a.	-2.1E-03	2.5E-19	-8.1E-03	1.1E-03
D-oil/disp	water	1m depth	T3 (May)	100%	113%	113%	-1.4E-02	1.7E-03		
E-burned	water	1m depth	T3 (May)	100%	104%	n.a.	-6.2E-03	n.a.	-5.5E-03	3.1E-03
F-burned	water	1m depth	T3 (May)	100%	103%	n.a.	-4.7E-03	n.a.		
I-control	water	1m depth	T3 (May)	100%	101%	97%	2.0E-03	1.4E-03	2.0E-03	9.8E-04
J-control	water	1m depth	T3 (May)	100%	n.a.	n.a.	n.a.	n.a.		

(a) Day of the incubation the reactor was sampled for naphthalene abundance (e.g., D0 = beginning of incubation, D7 = day 7 of incubation).

7.6 2-A Mean concentrations of PAHs and total hydrocarbon concentration in polar cod experiment

Mean concentrations of 26 PAHs, $\Sigma 16$ EPA PAHs and $\Sigma 26$ PAHs ($\mu\text{g/L}$ water \pm SEM), and total hydrocarbon concentration (THC, mg/L water \pm SEM) in water at 24 hours and 48 hours into exposure for each treatment (control, In situ burned oil residues [BO], mechanically dispersed oil [MDO], and chemically dispersed oil [CDO] treatment). Three replicates were analyzed for each treatment group. Values under limit of detection (LOD) are not included in $\Sigma 26$ PAH calculations. Values with no SE are singular replicates that exceeded the LOD.

PAH Composition	24 hour				48 hour			
	Control	BO	MDO	CDO	Control	BO	MDO	CDO
Naphthalene	0.28 ± 0.01	0.31	1.26 ± 0.30	1.11 ± 0.16	0.21 ± 0.005	0.25 ± 0.01	0.89 ± 0.31	0.74 ± 0.16
C1-Naphthalene	0.45 ± 0.02	0.54 ± 0.01	3.18 ± 0.13	3.15 ± 0.45	0.37 ± 0.02	0.43 ± 0.02	2.36 ± 0.46	2.41 ± 0.43
C2-Naphthalene	0.32 ± 0.02	0.50 ± 0.03	9.46 ± 2.46	12.36 ± 2.16	0.29 ± 0.02	0.44 ± 0.04	5.23 ± 0.82	9.09 ± 2.43
C3-Naphthalene	< 0.572	0.63 ± 0.04	22.85 ± 8.70	34.99 ± 5.11	< 0.572	< 0.572	13.03 ± 4.17	27.94 ± 7.66
Phenanthrene	< 0.090	0.10 ± 0.00	2.01 ± 0.68	2.92 ± 0.42	< 0.090	< 0.090	1.13 ± 0.28	2.19 ± 0.53
Antracene	< 0.009	< 0.009	0.03 ± 0.01	0.02 ± 0.00	< 0.009	< 0.009	0.015 ± 0.001	0.14 ± 0.12
C1-Phenanthrene/anthracene	< 0.146	0.26 ± 0.04	4.02 ± 1.59	6.68 ± 0.88	< 0.146	0.18	2.77 ± 0.96	6.05 ± 1.53
C2-Phenanthrene/anthracene	< 0.257	0.75 ± 0.30	7.24 ± 2.90	14.36 ± 2.10	< 0.257	0.59 ± 0.25	5.82 ± 2.06	13.89 ± 3.11
C3-Phenanthrene/anthracene	< 0.169	0.90 ± 0.32	6.42 ± 2.53	13.56 ± 1.80	< 0.169	1.08 ± 0.40	5.59 ± 1.96	15.17 ± 3.61
Dibenzothiophene	< 0.007	< 0.007	< 0.007	0.01 ± 0.00	< 0.007	0.01 ± 0.001	0.20 ± 0.05	0.36 ± 0.08
C1-Dibenzothiophene	< 0.025	0.41 ± 0.01	0.63 ± 0.25	1.14 ± 0.11	< 0.025	0.04 ± 0.01	0.45 ± 0.14	1.03 ± 0.27
C2-dibenzothiophene	< 0.051	0.21 ± 0.08	2.12 ± 0.83	4.82 ± 0.36	< 0.051	0.19 ± 0.08	1.76 ± 0.62	4.56 ± 1.12
C3-dibenzothiophene	< 0.041	0.29 ± 0.11	2.17 ± 0.86	4.64 ± 0.60	< 0.041	0.34 ± 0.14	1.90 ± 0.70	4.91 ± 1.09
Acenaphthylene	< 0.004	0.01 ± 0.00	0.004 ± 0.00	< 0.004	< 0.004	0.009 ± 0.001	< 0.004	0.004 ± 0.00
Acenaphthene	< 0.013	< 0.013	0.05 ± 0.01	0.06 ± 0.01	< 0.013	< 0.013	0.038 ± 0.006	0.05 ± 0.01
Fluorine	< 0.044	< 0.044	0.28 ± 0.07	0.37 ± 0.05	< 0.044	< 0.044	0.172 ± 0.22	0.27 ± 0.05
Fluoranthene	< 0.040	< 0.040	0.18 ± 0.00	0.25 ± 0.02	< 0.040	< 0.040	0.10 ± 0.03	0.22 ± 0.04
Pyrene	< 0.200	< 0.200	< 0.200	0.28 ± 0.06	< 0.200	< 0.200	< 0.200	0.34
Benzo(a)anthracene	< 0.025	< 0.025	0.05 ± 0.00	0.07 ± 0.01	< 0.025	< 0.025	0.044 ± 0.01	0.08 ± 0.01
Chrysene	< 0.053	< 0.053	0.16 ± 0.00	0.22 ± 0.03	< 0.053	< 0.053	0.13 ± 0.03	0.23 ± 0.05
Benzo(b)fluoranthene	< 0.018	0.03	0.06 ± 0.00	0.01 ± 0.01	< 0.018	0.028	0.04 ± 0.01	0.10 ± 0.01
Benzo(k)fluoranthene	< 0.007	0.01	0.01 ± 0.00	0.001 ± 0.00	< 0.007	< 0.007	0.01	0.013 ± 0.002
Benzo(a)pyrene	< 0.034	< 0.034	< 0.034	0.04	< 0.034	< 0.034	< 0.034	0.045
Indeno(1,2,3-cd)pyrene	< 0.011	< 0.011	< 0.011	< 0.011	< 0.011	< 0.011	< 0.011	< 0.011
Benzo(ghi)perylene	< 0.029	< 0.029	< 0.029	< 0.029	< 0.029	< 0.029	< 0.029	0.037
Σ 16 EPA, µg/L:	0.28 ± 0.01	0.4 ± 0.05	3.95 ± 0.62	5.32 ± 0.80	0.21 ± 0.01	0.27 ± 0.01	2.69 ± 0.28	4.50 ± 1.04
Σ26 PAHs, µg/L:	1.05 ± 0.02	3.49 ± 1.23	62.36 ± 20.71	101.45 ± 14.33	0.88 ± 0.03	2.71 ± 0.56	41.60 ± 11.21	89.56 ± 22.19
THC, mg/ kg water	0 ± 0	0.73 ± 0.43	9.82 ± 4.22	22.1 ± 2.37	0 ± 0	1.05 ± 0.63	8.55 ± 3.23	22.98 ± 4.99

Unique Arctic Communities and Oil Spill Response Consequences: "Oil Biodegradation & Persistence" and "Oil Spill Response Consequences Resilience and Sensitivity"

